Journal of
Composites Science

MDPI

Review

Calcium Orthophosphate ($CaPO_4$) Containing Composites for Biomedical Applications: Formulations, Properties, and Applications

Sergey V. Dorozhkin

Faculty of Physics, M.V. Lomonosov Moscow State University, Leninskie Gory 1-2, Moscow 119991, Russia; sedorozhkin@yandex.ru

Abstract: The goal of this review is to present a wide range of hybrid formulations and composites containing calcium orthophosphates (abbreviated as $CaPO_4$) that are suitable for use in biomedical applications and currently on the market. The bioactive, biocompatible, and osteoconductive properties of various $CaPO_4$-based formulations make them valuable in the rapidly developing field of biomedical research, both in vitro and in vivo. Due to the brittleness of $CaPO_4$, it is essential to combine the desired osteologic properties of ceramic $CaPO_4$ with those of other compounds to create novel, multifunctional bone graft biomaterials. Consequently, this analysis offers a thorough overview of the hybrid formulations and $CaPO_4$-based composites that are currently known. To do this, a comprehensive search of the literature on the subject was carried out in all significant databases to extract pertinent papers. There have been many formulations found with different material compositions, production methods, structural and bioactive features, and in vitro and in vivo properties. When these formulations contain additional biofunctional ingredients, such as drugs, proteins, enzymes, or antibacterial agents, they offer improved biomedical applications. Moreover, a lot of these formulations allow cell loading and promote the development of smart formulations based on $CaPO_4$. This evaluation also discusses basic problems and scientific difficulties that call for more investigation and advancements. It also indicates perspectives for the future.

Keywords: calcium orthophosphates; hydroxyapatite; biocomposites; hybrid biomaterials; bone grafts; biomedical applications; tissue engineering

check for updates

Citation: Dorozhkin, S.V. Calcium Orthophosphate ($CaPO_4$) Containing Composites for Biomedical Applications: Formulations, Properties, and Applications. *J. Compos. Sci.* **2024**, *8*, 218. https://doi.org/10.3390/jcs8060218

Academic Editors: Patrizia Bocchetta and Meenal Gupta

Received: 18 April 2024
Revised: 10 May 2024
Accepted: 4 June 2024
Published: 8 June 2024

Copyright: © 2024 by the author. Licensee MDPI, Basel, Switzerland. This article is an open access article distributed under the terms and conditions of the Creative Commons Attribution (CC BY) license (https://creativecommons.org/licenses/by/4.0/).

1. Introduction

Bone fractures resulting from traumatic injury or age-related conditions are a common form of tissue damage. Orthopedic surgeons face significant challenges in surgically treating such fractures, particularly when dealing with large bone defects that require the implantation of temporary or permanent prostheses. The rapid aging of the population and the limitations of natural bone grafts only exacerbate the situation, leading to a high demand for bone replacement materials. However, the use of xenografts in medicine, such as bovine bone, can increase the risk of viral infection. Additionally, xenografts have a lower potential for bone formation, are highly immunogenic, and generally resorb more quickly than autogenous bone. Similar limitations exist for human allogeneic grafts, which are tissue transplants between individuals who are homologous but not genetically identical. The concerns about the risk of tumor cells and bacterial and viral infections, as well as potential immunological and blood group incompatibility, are even greater. Additionally, the collection and preservation of allogeneic grafts (exogenous bone) present additional limiting factors [1–3]. Autologous bone (also known as endogenous bone) remains the preferred choice among all other alternatives, owing to its exquisite osteoconductive, osteogenic, osteoinductive, and biocompatible features, as well as its non-allergic and non-toxic characteristics. Furthermore, it has bone matrix proteins and live osteogenic cells that encourage osteogenesis. The body generally accepts autografts and they quickly

integrate with the adjacent bone tissue. Therefore, these devices are regularly utilized for prolonged periods of time, yielding favorable clinical results [2–5]. However, it is worth noting that there have been frequent instances of complications in the past [6]. Furthermore, the availability of autografts from the iliac crest or other areas of the patient's body is regrettably restricted due to the limited number of donor sites. This may necessitate further healing of the donor site and may cause prolonged post-operative pain. Moreover, the utilization of biological transplantation in medicine results in additional trauma and scarring due to the removal of donor tissue during extra surgical procedures. Additionally, the limited amount of donor tissue, morbidity of the donor site, and potential risk of immunological incompatibility and disease transfer make biological transplantation an imperfect solution [7–9]. In this context, engineered materials (synthetic or alloplastic bone grafts) are a viable option due to their widespread availability and ability to be processed and tailored to meet specific needs. Furthermore, they are not associated with concerns such as infection, immunologic incompatibility, sterility, or donor-site morbidity. The research on developing engineered materials for bone tissue repair is a crucial challenge in the field of clinical biomaterials [10,11].

Several categories of synthetic bone graft biomaterials are suitable for in vivo use. They can be classified according to their source (biological, non-biological), materials (metals, ceramics, polymers, composites), material consistency (implantable solids, injectables, adhesives), and the presence or absence of porosity, living cells, nanoparticles, and other factors [12]. Natural corals, coral-derived materials, bovine porous demineralized bones, human demineralized bone matrix, bioactive glass, glass ceramics, and calcium orthophosphates (abbreviated as $CaPO_4$) are all materials used in bone regeneration [13]. Porous bioceramics composed of $CaPO_4$ are especially prominent due to their excellent biocompatibility and ability to bind to biological bones because $CaPO_4$ is a key component of mammalian calcified tissues, including teeth and bones [14,15]. A variety of $CaPO_4$-based biomaterials with diverse chemical structures are currently available for purchase on the market [16,17]. However, $CaPO_4$ alone does not possess the mechanical or elastic properties of natural calcified tissues. In other words, $CaPO_4$ scaffolds pose several concerns for mechanical performance after implantation due to their low elasticity, high brittleness, poor tensile strength, low reliability, and fracture toughness. Additionally, molding $CaPO_4$ into the desired shape proves difficult in many instances [16,17].

Partial flexibility coupled with the superior strength of natural biomineralized tissues (bones and teeth) are attributed to the presence of bioorganic polymers (predominantly collagen type I fibers) coupled with the natural ceramic (largely a poorly crystalline ion-substituted calcium-deficient hydroxyapatite (CDHA) phase, referred to as 'bioapatite')—refer to Table 1 [18–22]. In bones, elastic collagen fibers align with the primary direction of tension. Demineralized bone has high flexibility and is easily bent, whereas collagen-free bone is highly brittle. This is due to inorganic nanoscale bioapatite crystals that confer stiffness and rigidity, whereas bioorganic fibers provide elasticity and toughness. In bones, the integration of both types of materials occurs at the nanometer scale, with the size of the crystallites, the orientation of the fibers, and the order within the components determining the nanostructure and, consequently, the function and mechanical features of the entire composite. From a mechanical standpoint, bone is highly sturdy at low strain rates, but exhibits brittleness at high strain rates. Additionally, bone is an anisotropic material due to the directional dependence of its properties [18–21].

Table 1. The biochemical composition * of bones [22].

Inorganic Phases	wt%	Bioorganic Phases	wt%
$CaPO_4$ (biological apatite)	~60	collagen type I	~20
water	~9	non-collagenous proteins: osteocalcin, osteonectin, osteopontin, thrombospondin, morphogenetic proteins, sialoprotein, serum proteins	~3
carbonates	~4	other traces: polysaccharides, lipids, cytokines	balance
citrates	~0.9	primary bone cells: osteoblasts, osteocytes, osteoclasts	balance
sodium	~0.7		
magnesium	~0.5		
other traces: Cl^-, F^-, K^+ Sr^{2+}, Pb^{2+}, Zn^{2+}, Cu^{2+}, Fe^{2+}	balance		

* The composition is varied from species to species and from bone to bone.

Designing an optimal bone graft that mimics the structure and function of natural bone is a significant obstacle. Understanding bone structure is crucial before attempting to create a bone graft. According to conventional expectations, ideal bone grafts must possess certain characteristics. They should be benign, available in varied shapes and sizes, and possess adequate mechanical properties for use in load-bearing regions. They should be capable of forming chemical bonds at the bone–implant interface, while also being osteogenic, osteoinductive, osteoconductive, biocompatible, and fully biodegradable, to favor bone growth and moldable for filling and repairing bone defects [23,24]. Furthermore, ideal implants should have a chemical composition similar to bone, wherein the presence of $CaPO_4$ is essential. They should also exhibit continuous porosity, facilitating penetration of living host tissues, and have viscoelastic and semi-brittle behavior similar to bone [25–27]. Additionally, the desirable degradation rate of implants needs to match the healing rate of human tissues and be free from chemical and biological irritation and toxicity resulting from corrosion and degradation. Ideally, the mechanical strength of the implant and the transplanted bone should remain constant during the regeneration process [28]. Some argue that the mechanical properties of implants should exceed those of bones; therefore, in cases of severe trauma, it may be necessary to destroy the bone rather than the implant [23]. To enable clinical applications, grafts must be sterile, easily preservable, processable, and cost-effective. Unfortunately, there are currently no engineered biomaterials that fully meet these requirements and it seems unlikely that such materials will be developed in the near future. Most of the available bone grafting biomaterials are either osteogenic, osteoinductive, or osteoconductive [1].

The design of bone replacement materials necessitates thoughtful contemplation of the bone type and its mechanical properties. Specifically, bones that are highly loaded, such as the femur, require an implant with sufficient stiffness to provide stability, yet not so rigid as to cause strain retention. On the other hand, in applications with relatively low loads, like skull repair, having the appropriate three-dimensional shape is crucial for stability and aesthetic purposes. One promising option is to utilize materials with a composition and nanostructure similar to that of bone tissues. Organic–inorganic hybrid biomaterials development, which imitates the structure of calcified tissue and combats the limitations of individual materials, has great potential for enhancing conventional bone implants. Biologically important $CaPO_4$ and bioabsorbable polymers can be combined to create biocomposites with unique physical, biological, and mechanical properties and predictable degradation behavior [29]. The general characteristics of these biocomposites depend on the nature, structure, and relative content of the components, while other factors such as

preparation conditions also play a role in determining the properties of the final material. Currently, $CaPO_4$ is applied as fillers or coatings, either in the form of particles or fibers, incorporated into or applied on top of biodegradable polymer matrices. Due to its improved physical, biological, and mechanical properties, it is slowly being considered as a scaffold for bone tissue engineering [30–33]. Furthermore, these biocomposites meet the overall criteria for next-generation biomaterials by combining bioactivity and bioabsorbability, activating in vivo tissue regeneration mechanisms, stimulating the body's self-healing capacity, and resulting in implant replacement with regenerated tissue. Thus, an optimal material can be designed by effectively combining a ductile polymer matrix with a tough, bioactive particulate bioceramic filler. Ideally, this approach will yield superior structures suitable for use as implants and posterior dental restorations [29,34].

In clinical orthopedic practice, the initial composite materials were lint-reinforced plasters utilized by Mathijsen as external fixatives (bandages) in fracture treatment back in 1852 [35], followed by Dreesman in 1892 [36]. Subsequently, considerable advancements have been made in the clinical usage of dissimilar types of composite materials. It is possible to create and use a variety of composite materials with distinct mechanical and biological properties to satisfy a range of clinical needs [37]. Therefore, the purpose of this review is to outline the wide range of hybrid formulations and $CaPO_4$-based composites that are now available and appropriate for use in biomedical applications.

2. General Knowledge and Experience

According to Wikipedia, "A *composite material* (also called a *composition material* or shortened to *composite*, which is the common name) is a material which is produced from two or more constituent materials. These constituent materials have notably dissimilar chemical or physical properties and are merged to create a material with properties unlike those of the individual elements. Within the finished structure, the individual elements remain separate and distinct, distinguishing composites from mixtures and solid solutions" [38]. Composite materials are inherently heterogeneous, with each phase retaining its unique identity and properties while being bonded to maintain an interface. This results in enhanced specific or synergistic properties that cannot be achieved from the original phase alone [39]. In line with previous research, we also explore the following: "for the purpose of this review, composites are defined as those having a distinct phase distributed through their bulk, as opposed to modular or coated components" ([40], p. 1329). Therefore, with a few exceptions, we did not consider $CaPO_4$ deposits produced on different materials by various deposition techniques [41–46] or $CaPO_4$ coated with other compounds [47–51]. However, we did include composite coatings. Structures such as porous $CaPO_4$ scaffolds with cells filling the pores [52–54] and $CaPO_4$ impregnated with bioactive substances [55,56] can also be described as composites or hybrids, but we did not consider them in this study. Finally, biohybrids are also defined as "the functional combination of proteins, viable cells or microorganisms with non-biological materials" [57]; such compositions are also excluded.

Composite materials consist of two primary components: a matrix (also referred to as the continuous phase) and dispersed phase(s). The presence of at least one component from each category is essential to form a composite material. Typically, the matrix is considered to be the component constituting the major and continuous phase (making up >50% by volume, often exhibiting relatively low stiffness and strength), whereas the reinforcement is the one present as a minor, discontinuous, and/or dispersed phase (comprising <50% by volume, frequently showcasing relatively high stiffness and strength). An interface serves as a boundary between the constituents, typically located in a small area where the chemical composition significantly changes and forms a bond with one another, thereby playing a vital role in load transfer. The advantage of composites lies in their customizable properties, achieved by modifying ratios and placement of constituents, as well as adjusting interfaces. The literature contains a comprehensive overview of the primary manufacturing and processing techniques [40,58]. The matrix not only occupies the space but also upholds the dispersed phase by enveloping it and preserving its respective positions. One or several

dispersed phases are usually responsible for augmenting one or several matrix properties. The main goal of the majority of composite materials is to improve the matrix's mechanical properties, like strength and stiffness. To achieve the intended results, however, additional characteristics including biocompatibility, radiopacity, density, transport qualities (thermal or electrical), and erosion stability are also essential. This combined effect generates properties that are inexistent in individual component materials [58,59]. Control of the volume fraction and arrangement of dispersed phases allows for modification and adaptation of the properties and design of composite materials to meet specific conditions. For instance, in ceramics, the dispersed phase functions as a crack inhibitor and reinforcing material. To do this, techniques include bridging the crack face, deflecting the crack tip, absorbing energy during shrinkage, and producing stress redistribution in the vicinity of the crack tip [60]. The dispersed phase's volume proportion, size, form, and orientation; the condition of the reinforcement/matrix contact; and the homogeneity of the composite material as a whole are additional variables to take into account with composites. A higher volume fraction of the reinforcement phase enhances the mechanical properties of composite materials. Continuous and aligned fibers are effective in preventing crack propagation by having an anisotropic behavior. Composites are structurally anisotropic, and their mechanical properties vary with orientation. Furthermore, in addition to functionally graded materials, a uniform distribution of dispersed phases is also desirable in order to provide composite materials with consistent properties [38,58,59].

Composites can be classified into four types: simple, complex, graded, and hierarchical. A simple composite contains one dispersed phase that is homogeneously distributed throughout the matrix. A complex composite, on the other hand, contains multiple dispersed phases that are homogeneously distributed within a matrix. A graded composite is intentionally structured in a heterogeneous manner by distributing one or more dispersed phases throughout the matrix. Hierarchical composites are structures whereby fine entities from a simple or complex composite combine to create coarse particles or granules. These particles are subsequently dispersed within another matrix, generating composite structures at a second hierarchical scale. Another classification categorizes composites into four groups: (i) fiber-reinforced composites, where fibers are embedded in the matrix; (ii) layered composites, where layers of different materials are incorporated to form a structure; (iii) particulate composites, where particles or flakes are dispersed in the matrix; and (iv) hybrid composites, which are combinations of any of the above types. Particulate composites typically employ micro- or nanoscale reinforcements made up of particles. In contrast, fibrous composites may consist of long, continuous fibers that are either aligned or woven and short fibers that are either aligned or randomly oriented. Another means of classifying composites is based on the matrix material. For example, there are ceramic, polymer, and metal composites [37].

In the design of composite materials, three interdependent factors must typically be taken into account: (i) the selection of suitable matrix and dispersion materials; (ii) the selection of appropriate manufacturing and processing methods; and (iii) the internal and external device design [40]. Additionally, all composite materials require shaping, which may involve adding a matrix material before or after placing the dispersion material on the mold surface or in the mold cavity. Matrix materials go through melting processes that can happen in various ways, like chemical polymerization, curing, or solidification from the molten state. The particular melting mechanism depends on the nature of the matrix material. Because of the overall heterogeneity, many composite materials exhibit orthotropic physical properties, meaning that different strengths or properties exist in different orthogonal directions [38,58,59].

Since composites require the mixing of two or more materials, the process of phase-mixing is essential [61,62]. Moreover, interfacial strength between the phases is crucial since inadequate adhesion between them can cause early degradation of the interface, leading to lower mechanical properties, particularly the tensile strength. From a chemical standpoint, various types of interactions exist among composite materials. These include materials

with strong interactions (covalent, coordination, and ionic bonds), those with weak interactions (van der Waals forces, hydrogen bonds, hydrophilic–hydrophobic equilibrium), and materials with no chemical interactions between the components [63]. Furthermore, wetting plays a significant role in the bonding and adhesion of materials. The result is determined by the polar groups in the matrix and the hydrophilicity or polarity of the filler.

Biocomposites have two definitions. Firstly, they refer to a composite material that is safe and contains one or more components that can interact favorably with the human body in vivo, thus promoting healing processes and implant uptake [64]. Secondly, they are a type of biomaterial with composite properties. The most recent definition of a biomaterial is as follows: 'A biomaterial is a material designed to take a form that can guide the process of treatment or diagnosis through its interaction with a living system' [65]. In any case, the biocompatibility of biocomposites appears to be more crucial than other forms of compatibility [37,66,67].

Historically, according to the Scopus database, the earliest article featuring the term 'biocomposite' in the title was published in 1987 [68], while an article combining 'biocomposite' and $CaPO_4$ (it was hydroxyapatite, HA) in the title was published in 1991 [69]. However, a study published in 1976 [70] marks the earliest paper that combines the terms "composite" and HA in its title without the prefix "bio". As of May 2024, Scopus reports 7633 articles with titles featuring the combination of "composite" and "apatite" and 2160 articles featuring "composite" and "calcium phosphate". These numbers indicate an active field of research.

The most common properties of bio-organic and inorganic domains formulated into biocomposites are summarized in Table 2 [24], while, for an overview of the general advantages of modern $CaPO_4$-based biocomposites compared to $CaPO_4$ bioceramics and bioabsorbable polymers, readers are referred to "Composite materials strategy" section of Ref. [29].

Table 2. General respective properties from the bioorganic and inorganic domains to be combined in various composites and hybrid materials [24].

Inorganic	Bioorganic
hardness, brittleness	elasticity, plasticity
high density	low density
thermal stability	permeability
hydrophilicity	hydrophobicity
high refractive index	selective complexation
mixed valence slate (red-ox)	chemical reactivity
strength	bioactivity

3. Main Components of Bone Graft Biocomposites and Hybrid Biomaterials

3.1. $CaPO_4$

$CaPO_4$ was first identified as a significant constituent of bone in 1769 and has become the subject of constant study ever since [71,72]. One of $CaPO_4$'s primary applications as a material for bone replacement is its chemical resemblance to the mineral elements of mammalian teeth and bones [14–16]. $CaPO_4$ is biocompatible and non-toxic and exhibits bioactive behavior while assimilating into biological tissue via the same processes present in healthy bone remodeling. This results in a close physico-chemical bond between the $CaPO_4$ implant and bone, referred to as osteointegration. Moreover, $CaPO_4$ promotes osteoblast adhesion and proliferation, making it an essential component in various orthopedic applications. However, the mechanical properties of using $CaPO_4$ alone as a load-bearing biomaterial, such as brittleness, zero elasticity, and low fatigue resistance [23], limit its effectiveness. In porous ceramics and scaffolds, this poor mechanical behavior is more prominent, as voids larger than 100 μm are crucial for proper vascularization and osteocyte colony formation [73,74]. Therefore, in biomedical applications, $CaPO_4$ alone is used mainly as a filler or coating [16].

Table 3 provides a comprehensive list of all known forms of $CaPO_4$, together with standard abbreviations and important features. Books and monographs on the subject can provide further in-depth information on $CaPO_4$ [16,75–78].

Table 3. Existing forms of $CaPO_4$ and their major properties [16].

Ca/P Molar Ratio	Compound	Formula	Solubility at 25 °C, −log(K_s)	Solubility at 25 °C, g/L	pH Stability Range in Aqueous Solutions at 25 °C
0.5	Monocalcium phosphate monohydrate (MCPM)	$Ca(H_2PO_4)_2·H_2O$	1.14	~18	0.0–2.0
0.5	Monocalcium phosphate anhydrous (MCPA or MCP)	$Ca(H_2PO_4)_2$	1.14	~17	[c]
1.0	Dicalcium phosphate dihydrate (DCPD), mineral brushite	$CaHPO_4·2H_2O$	6.59	~0.088	2.0–6.0
1.0	Dicalcium phosphate anhydrous (DCPA or DCP), mineral monetite	$CaHPO_4$	6.90	~0.048	[c]
1.33	Octacalcium phosphate (OCP)	$Ca_8(HPO_4)_2(PO_4)_4·5H_2O$	96.6	~0.0081	5.5–7.0
1.5	α-Tricalcium phosphate (α-TCP)	α-$Ca_3(PO_4)_2$	25.5	~0.0025	[a]
1.5	β-Tricalcium phosphate (β-TCP)	β-$Ca_3(PO_4)_2$	28.9	~0.0005	[a]
1.2–2.2	Amorphous calcium phosphates (ACP)	$Ca_xH_y(PO_4)_z·nH_2O$, n = 3–4.5; 15–20% H_2O	[b]	[b]	~5–12 [d]
1.5–1.67	Calcium-deficient hydroxyapatite (CDHA or Ca-def HA) [e]	$Ca_{10-x}(HPO_4)_x(PO_4)_{6-x}(OH)_{2-x}$ ($0 < x < 1$)	~85	~0.0094	6.5–9.5
1.67	Hydroxyapatite (HA, HAp or OHAp)	$Ca_{10}(PO_4)_6(OH)_2$	116.8	~0.0003	9.5–12
1.67	Fluorapatite (FA or FAp)	$Ca_{10}(PO_4)_6F_2$	120.0	~0.0002	7–12
1.67	Oxyapatite (OA, OAp or OXA) [f], mineral voelckerite	$Ca_{10}(PO_4)_6O$	~69	~0.087	[a]
2.0	Tetracalcium phosphate (TTCP or TetCP), mineral hilgenstockite	$Ca_4(PO_4)_2O$	38–44	~0.0007	[a]

[a] These compounds cannot be precipitated from aqueous solutions. [b] Cannot be measured precisely. However, the following values were found: 25.7 ± 0.1 (pH = 7.40), 29.9 ± 0.1 (pH = 6.00), and 32.7 ± 0.1 (pH = 5.28). The comparative extent of dissolution in an acidic buffer is ACP >> α-TCP >> β-TCP > CDHA >> HA > FA. [c] Stable at temperatures above 100 °C. [d] Always metastable. [e] Occasionally it is called "precipitated HA (PHA)". [f] Existence of OA remains questionable.

3.2. Polymers

Polymers are (bio)organic compounds consisting of big molecules covalently bound to thousands of smaller units (monomers) to form lengthy chains, resulting in highly malleable materials. In this regard, synthetic polymers can be likened to natural ones (lipids, proteins, and polysaccharides), which are the primary functional constituents of the biological environment. Polymers vary from one another in terms of their chemical composition, molecular weight, polydispersity, crystallinity, hydrophobicity, solubility, and thermal transition. Furthermore, through the copolymerization or blending of two or more polymers, as well as by adjusting the polymer type and chain length, their properties can be precisely altered throughout a wide range [79,80]. Due to their strong viscoelastic characteristics, polymers can be easily shaped into intricate porous networks and channels, spongy sheets, and gels [81]. Non-magnetic and X-ray transparent polymeric materials are completely interoperable with modern diagnostic techniques such as magnetic resonance imaging and computed tomography. Regrettably, the in vivo physiological environment

presents stringent requirements, which many of these materials fail to meet. The primary criteria for polymers that are appropriate for biomedical applications are biocompatibility, lack of excessive or chronic inflammatory reactions after implantation, and degradation into non-toxic products. However, for load-bearing applications, most polymers lack the necessary stiffness, ductility, and ultimate mechanical properties. Thus, in the case of good biocompatibility, most polymeric materials are primarily employed for soft tissue replacement (e.g., skin, vascular, cartilage, and ligament replacements). Moreover, the characteristics of polymers can be impacted by sterilizing procedures, such as autoclaving, ethylene oxide, and ^{60}Co irradiation [82].

Several biocompatible polymers are suitable for biomedical applications [83–85]. For instance, researchers have investigated polyacrylates, poly(acrylonitrile-*co*-vinyl chloride), and polylysine for cell encapsulation and immunoseparation [86,87]. Additionally, researchers have examined polyorthoesters and PCL as drug delivery devices, with the latter's slow degradation rate enabling long-term sustained release [88]. PCL is a semi-crystalline aliphatic linear polyester polymer with a low degradation rate of more than 2 years. It is both bioabsorbable and biocompatible, with an adequate absorption time and non-toxic by-products generated upon degradation and release. As a result, it finds extensive use in pharmaceuticals and wound dressings [89,90]. Likewise, PU is employed in hard and soft tissue engineering as well as nanomedicine [91]. Polyanhydrides are utilized as polymers for orthopedic purposes and can undergo photopolymerization in situ. Additionally, they are currently being researched as delivery devices for bone replacement and augmentation due to their rapid and clear surface erosion properties [88,92,93]. To counteract their suboptimal mechanical properties, researchers have either copolymerized the materials with imides or formulated them to be cross-linkable in situ [93]. Other polymers, such as polyphosphazene, are potential materials for regenerating skeletal tissue due to their modifiable properties (e.g., degradation rate) through changes in their side chain structure and their demonstrated ability to enhance osteoblast adhesion [93]. PPF exhibits outstanding mechanical properties (comparable to trabecular bone), can cross-link in vivo through C=C bonds, and has risen to prominence as a replacement material for bones due to its hydrolyzability. It is also considered a material for drug delivery devices [88,92–99]. Polycarbonate has been suggested as an appropriate material for bone replacement scaffolds and has been altered with tyrosine-derived amino acids to make it biodegradable. Polydioxanone has been tested for biomedical applications, while PMMA is commonly used in orthopedic surgery as bone cement for implant fixation and to repair fractures and bone defects such as osteoporotic vertebrae. However, the polymerization of toxic monomers to form PMMA generates significant heat that can harm tissues. Moreover, PMMA is non-degradable and bio-inactive, and it does not chemically bind to bone, resulting in fragmented debris that may cause inflammatory foreign body reactions [92,100]. Other non-degradable polymers commonly used in orthopedic procedures include low-density PE, HDPE, and ultra-high molecular weight PE (commonly utilized as the surface of artificial hip implants [101,102]). Additionally, PU, polyethylene terephthalate, and PP are employed for knee ligament repair [103]. Polyactive™, which is a block copolymer of PEG and PBT, has also undergone research for biomedical applications [104–106]. Cellulose [107,108] and its derivatives [109,110] are commonly used in biomedical applications. Furthermore, polyethylene oxide, PHB, and their blends have undergone testing for biomedical purposes [29].

Linear aliphatic poly(α-hydroxyesters), like PLA [111], PGA [112], and their copolymers, are the most commonly used synthetic polymers in medical practice. Manipulation of mechanical properties can be achieved through the polymerization of D-lactide, L-lactide, D,L-lactide, or meso-lactide due to the chiral nature of lactide monomers. Additionally, PLA/PGA copolymers, known as PLGAs, can be tailored to exhibit specific properties, like crystallinity and degradation rate, by altering their composition. These thermoplastic polyesters are fully biodegradable and derived from renewable sources like starch, corn, and sugar cane. They currently rank second in global bioplastic consumption, find-

ing extensive use in both general and specialized applications. Notably, these synthetic polymers have received FDA approval and are the only known biodegradable ones with this distinction [29,93,111,112]. They are biocompatible, primarily non-inflammatory, and degraded in vivo through hydrolysis and enzymatic action, resulting in the excretion of products from the body via normal metabolic pathways [88,93,113]. Additionally, they have potential for drug delivery [114]. Poly(α-hydroxyesters) have been studied as medication and protein delivery systems, including for growth factors, and as scaffolds for tissue regeneration and replacement. They have also been studied as cell carriers. Additionally, they have been used in the production of membranes and films, as well as screws, pins, and plates for orthopedic applications [88,93,115,116]. Among the resorbable polyesters, PGA exhibits a more rapid degradation rate compared to others (less than 12 months) [112]. Therefore, the degradation rate of PLGA can be modified by adjusting the amounts of two-component monomers. In orthopedic applications, this can enable the creation of materials that degrade in sync with bone growth [117]. The varying degradation timeframes present a range of possibilities for biomedical applications. Furthermore, PLGA has been shown to stimulate osteoblast migration and proliferation, which is vital for bone tissue regeneration [93,118]. However, PLGA alone may decrease the impact of stress shielding and is too weak to support a load-bearing environment, making it suitable for specific clinical indications such as ankle and elbow fractures [113]. Additionally, it facilitates self-degradation, resulting in decreased mechanical properties and lowered solution pH, which subsequently leads to extensive degradation. The extensive amount of implant degradation products overwhelm the body and can lead to inflammatory foreign reactions. Ultimately, poly(α-hydroxyesters) lack both bioactivity and osteoconductivity [93,119].

Biomedically relevant polymers can be categorized into synthetic and biogenic types. Synthetic polymers, including PE, PMMA, PLA, PGA, and PCL, are one type. Conversely, biogenic polymers are made up of different kinds of polysaccharides, including cellulose, starch, alginate, chitin/chitosan [120,121], pectin, gellan gum, hyaluronic acid, and their derivatives. Proteins like collagen, fibrin, soy, gelatin, silk, and various bio-fibers [122,123], such as lignocellulosic natural fibers, fall under this category. It is worth noting that natural polymers tend to have a highly organized structure. Extracellular substances named ligands are also possible components of polymers, with the purpose of cell receptor binding. However, natural polymers come with various impurities that must be eliminated prior to use. Synthetic polymers, on the other hand, can be created under controlled circumstances, possessing predictable and reproducible mechanical and physical traits, such as tensile strength, modulus of elasticity, and degradation rate. Synthetic polymers have the potential for chemical and molecular modification, allowing for easy customization to meet specific application requirements while also providing control over impurities. Certain researchers distinguish between non-resorbable polymers, like PE, PP, PMMA, and cellulose, and resorbable or biodegradable polymers, like proteins, poly(α-hydroxyester), and polysaccharides [123]. Synthetic polymers can be categorized as thermoplastics or thermosets. Examples of thermoplastics include HDPE and PEEK, while polydimethylsiloxane and PMMA are examples of thermosets [82]. Table 1 in reference [123] provides a list of synthetic biodegradable polymers utilized as scaffolding materials in biomedical applications. Additional information on polymers suitable for biomedical applications can be found in other sources [82,116,124–129]. Excellent literature reviews on the synthesis of diverse biodegradable polymers [130] and current trends in polymer composites [131] are available.

3.3. Inorganic Materials, Substances and Compounds

3.3.1. Metals

Metals are typically assessed for their mechanical performance in bone tissue engineering, despite the potential for increased stress shielding. Titanium and its alloys are among the most biocompatible metals and are widely utilized for bone graft fabrication. Additionally, a range of other metals and their alloys, including zirconium, hafnium, vana-

dium, niobium, tantalum, chromium, iron, cobalt, nickel, copper, silver, magnesium, zinc, and stainless steel, are employed in the human body [132–136]. Recent research has shown that porous metals have significant biomedical potential [137–139]. Metal implants exhibit the necessary strength and toughness to support load-bearing body parts and will continue to play a crucial role as orthopedic biomaterials despite the potential risks of poor wear resistance, as well as the potential release of certain ions and corrosion products from metal implants. Elemental metals do not exist in the human body, thus, neither metals nor their alloys can be considered biomimetic in terms of chemical composition. The term 'biomimetic' refers to a processing technique that imitates or is inspired by biological mechanisms [140]. Though biocompatible metals are tolerated by the body and not rejected, they do not actively interact with surrounding tissues. Metal implants frequently exhibit poor attachment to host tissue, thereby limiting their integration with bone. However, in certain scenarios (particularly when coated with $CaPO_4$ [47]), metallic implants can exhibit acceptable biocompatibility [141]. Traditionally, permanent implants were exclusively made of stable, inert metals or alloys, resistant to degradation and corrosion. However, the paradigm has recently shifted to propose biodegradable implants consisting of Mg, Zn, Fe, and their alloys, allowing for bone ingrowth [142,143].

3.3.2. Glasses and Glass–Ceramics

Special glasses [144,145], glass ceramics [146,147], and pure silica (SiO_2) are suitable materials for biomedical applications. It is recommended to focus on the bioactive ones, which have compositions belonging to the $CaO–P_2O_5–SiO_2–MgO–Na_2O$ system and may have small amounts of CaF_2, MgF_2, K_2O, and SrO [148]. The specific $Na_2O–CaO–SiO_2–P_2O_5$ formulation known as Bioglass® [149,150] is the most well-known among them. They are manufactured through standard glassmaking techniques and necessitate pure raw materials. Bioglass® and other bioactive glasses, which are biocompatible and osteoconductive biomaterials, bind to bones through fibrous connective tissue interfaces, making them extensively employed in bone defect fillings owing to their characteristics. The primary drawbacks of bioactive glasses are their mechanical fragility and low fracture durability accounted for by the amorphous 2D glass network. The flexural strength of most bioactive glass formulations falls within the 40–60 MPa range, rendering them unsuitable for high-load applications. Porous Bioglass® scaffolds, however, exhibit improved bioactivity and resorption properties [149,150].

Through the process of heat treatment, glasses can be transformed into glass–crystal composites. These composites consist of crystalline phases that are precisely controlled in size and composition. The mechanical properties of the resulting glass–ceramics can often be better than those of the parent glass or sintered crystalline ceramics [146,147]. Bioactive A-W glass–ceramics are produced by a conventional melt quenching process and are made from parent glasses of the pseudo-$3CaO·P_2O_5–CaO·SiO_2–MgO·CaO·2SiO_2$ system. The bioactivity of A-W glass–ceramics surpasses that of sintered HA. Moreover, their exceptional mechanical properties make them suitable for clinical implementation as prosthetics for iliac and vertebral joints, as well as intervertebral spacers [151,152]. These ceramics serve as a valuable alternative to conventional biomaterials.

3.3.3. Ceramics

Metal oxide ceramics are a category of inorganic biomaterials that have played a significant role in bone tissue engineering. There are a number of factors that support their prominence as biomaterials for bone tissue engineering. Alumina (Al_2O_3), zirconia (ZrO_2), and titania (TiO_2) are among them and have been extensively researched due to their exceptional tribological qualities, bioinertness, high wear resistance, fracture toughness and strength, and comparatively low friction [153,154]. The cooling of pure zirconia from tetragonal to monoclinic phase results in a volume change that creates cracks in zirconia ceramics [155]. To stabilize the material in the tetragonal or cubic phase, it is necessary to mix zirconia with additives such as magnesia (MgO), calcia (CaO), and yttria (Y_2O_3).

These materials are commonly known as PSZ [156,157]. However, the clinical application of all ceramics is limited by their brittle nature, necessitating further research to enhance their properties.

3.3.4. Carbon

Elemental carbon has served as a biomaterial since 1972 because of its strength, bioinertness, superior tribological qualities, fracture toughness, and low friction [158]. Its uses include bone bridges, prosthetic hip joints, structural skeletal extensions, glassy carbon roots for artificial teeth, and orthopedic prostheses. Researchers have also studied the biomedical properties of amorphous carbon [159]. However, current research trends focus on biomedical applications of nanotubes and other allotropes of nanodimensional carbons [160,161].

Nanodimensional allotropes of carbon, namely nanotubes, fullerenes, and graphene, exhibit promising potential for biomedical applications because of their small dimensions, high aspect ratios (length/diameter or surface/thickness), large surface area, and excellent mechanical properties. These properties include extreme flexibility and strength, high elasticity, great resistance to bending (in the case of nanotubes), and an ability to undo tube buckling (in the case of nanotubes). Research indicates that non-functionalized nanodimensional carbon tends to aggregate and form bundles while having some biological activities [162,163]. Although these forms are insoluble in water and organic solvents, chemical functionalization [164] allows for better dispersion of carbon nanotubes and improves interfacial bonding within the composite [165]. Technical abbreviations will be explained when first used. Consistent citation and footnote styles will be used throughout the paper. Furthermore, it has been found that the surface functionalization of carbon nanotubes with carboxyl groups can cause calcification, much like in woven bone [166]. CDHA can be deposited in situ on the surface of carbon nanotubes to functionalize them [167]. Surface functionalization is also widely used to enhance the characteristics of other types of nanodimensional carbon, such as fullerenes [168] and graphene [169].

4. A Brief Information on Preparation Techniques

In general, the preparation of composite materials involves wetting, mixing, saturating, and compressing the reinforcement and matrix. The matrices are then bonded together (through heat or chemical reaction) to form a rigid structure. Typically, these processes are performed in open or closed molding dies and involve melting. Different materials require different processing conditions, such as temperature and type of solvent, as well as the order and method of adding components vary greatly. Depending on the constituents, composites can be produced in a variety of ways, including fiber placement, filament winding, souring, tufting, z-pinning, various types of casting and molding, braiding (into formers), filament winding, and slip molding [38]. However, before mixing, the particle size dimensions of the mixed components need to be considered. $CaPO_4$, carbon, and metal oxide ceramics are almost always fine powders that can be mixed immediately, but this is not the common case for other materials. For example, polymers are often supplied as pellets, granules, or coarse powders and often require an additional grinding step, and, for low-melting polymers such as PCL, cryogenic milling can be effective. Similarly, glasses and metals may also require a grinding process.

With regard to $CaPO_4$-based formulations, various methods have been realized to combine matrix and dispersion components to form biocomposites. For example, mechanical blending or mixing, ball milling, compounding, compression, and casting into a polymer–solvent solution followed by solvent evaporation, e.g., by freeze-drying, dispersion of $CaPO_4$ particles, or whisking into a liquid monomer, followed by polymerization, a melt extrusion of $CaPO_4$/polymer mixtures, and co-precipitation or co-deposition, as well as a rapid prototyping, selective laser sintering, and 3D printing [22,37,170–173]. Four-dimensional printing, in which the resulting 3D shape is able to morph into different forms in response to environmental stimulus, with the fourth dimension being the

time-dependent shape change after the printing, is used as well [174]. There has been a comparison of three techniques for creating homogenous blends of PLLA and HA [170]. Prior to compression molding, polymer pellets and ceramic powder were combined using a dry technique. The second technique involved distributing the ceramic filler into a solution of polymer and solvent. The third technique used combined powders of ceramic and polymer via melt extrusion. A network of ceramic particles surrounds the polymer pellets when a dry powder is combined, but the solvent and melt procedures also produce a uniform distribution of HA in the matrix. The possibility of hazardous organic solvent remains is the primary drawback of the solvent casting technique. It has been demonstrated that the melt extrusion approach is appropriate for creating homogenous ceramic/polymer blends [170]. However, it should be noted that non-melt-based routes often lead to the development of composites with poor mechanical performance and often require the use of toxic solvents and intensive manual labor [125].

Other options include in situ formation, where the reinforcement is synthesized within a pre-formed matrix, or synthesizing the matrix around the reinforcement [37,175–178]. One of the most appealing approaches is this one since it prevents large-scale particle aggregation. For instance, a number of studies have described in situ creation methods for creating different composite materials with carbon nanotubes and $CaPO_4$ [179–182]. The same is true for $CaPO_4$/graphene composites [177,178]. Other examples include biomimetic synthesis [177,178,183,184], the use of amino acid-coated gold nanosized particles as scaffolds to grow CDHA [185], and the preparation of nanosized HA/PA biocomposites [186,187]. In some cases, mechanochemical routes [188,189], emulsions [190–195], lyophilization [171,196,197] and freeze–thaw techniques [198], and gel templating mineralization [198,199], as well as vat photopolymerization [200], can be applied to produce $CaPO_4$-based biocomposites. Various techniques, such as in situ preparation, spark plasma synthesis, hydrothermal treatment, biomimetic mineralization, hot isostatic pressing, electrochemical deposition, and ball milling, have been used to prepare graphene/HA nanocomposites [178]. In the case of $CaPO_4$ biocomposites with metals, a powder metallurgy approach [201,202] combining direct ink writing with liquid pressure infiltration [203], as well as various types of additive manufacturing [204,205], can be used. The details of various production methods are well described in other publications [22,37,117,170,171]. Furthermore, additional types of preparation techniques are briefly mentioned below when describing the individual $CaPO_4$-based formulations.

After the desired formulations of $CaPO_4$-based composites and hybrid formulations have been prepared, it frequently becomes necessary to create 3D constructs from them, which might be either the standard geometric shapes (cubes, rectangular blocks, cylinders, filaments, etc., as well as various types of screws and dowels) or complicated shapes of the specific bones or bone fragments. The detailed description of the forming and shaping techniques is beyond the scope of this review but, briefly, one can mention the following. Depending on the nature of the second phase of the biocomposites ($CaPO_4$ is considered as the first one), the standard geometric shapes might be created by common ceramic processing techniques [206,207], metal processing techniques [208–210], and/or polymer processing ones [123,211], while the complicated shapes are commonly created by various types of additive manufacturing techniques, such as 3D printing [173,212–215].

Commonly it is necessary to impart porosity to $CaPO_4$-based composites and hybrid formulations, which is advantageous for most applications as a bone replacement material because porosity facilitates the migration of osteoblasts from the surrounding bone to the implant site. Various material processing strategies to prepare composite scaffolds with interconnected porosity include thermally induced phase separation, solvent casting, particle leaching, solid free-form fabrication techniques, microsphere sintering, and coating [123,216–219]. Supercritical gas foaming techniques can also be used [170,220–222]. Finally, different types of additive manufacturing techniques can also be used [212–215]. Most of those porosity-forming techniques have been adapted from (bio)ceramics [223,224]. Regarding $CaPO_4$-based biocomposites with polymers, the most common technique to

produce porous scaffolds appears to be fused deposition modeling (64%), followed by low-temperature deposition manufacturing (19%), selective laser sintering (12%), and stereolithography (5%) [225]. Further details on porosity creation are available in the topical reviews [218,223].

5. $CaPO_4$-Based Biocomposites and Hybrid Biomaterials

There are multiple (partially overlapping) major categories into which $CaPO_4$-containing composites and hybrid formulations appropriate for biological applications can be classified:

- Biocomposites with polymers;
- Self-hardening biocomposites;
- Nanosized $CaPO_4$-based formulations and nanosized biocomposites;
- Collagen-containing biocomposites;
- Biocomposites with other bio-organic compounds;
- Injectable bone substitutes (IBS);
- Biocomposites with glasses, inorganic compounds, carbon, and metals;
- Biocomposites from $CaPO_4$ only;
- Inks for 3D printing;
- Functionally graded biocomposites;
- Biosensors.

The majority of these have been developed using bone-like concepts to mimic natural bone. Details on each of these areas are as follows.

5.1. Biocomposites with Polymers

5.1.1. History and General Part

Since natural bones represent a biocomposite of ion-substituted CDHA with a bioorganic polymer collagen [18,19], it is plausible to believe that an appropriate biocomposite with mechanical, chemical, and physical properties similar to those of human bones would be made of $CaPO_4$ (such as CDHA) and a bioorganic polymer (such as collagen). Therefore, $CaPO_4$/polymer composites and hybrid formulations have been widely investigated to improve the properties of the constituents with the final purpose of bone regeneration applications. In such biocomposites, hard and rigid $CaPO_4$ bioceramics provide the basic building blocks for both mechanical strength and biomineralization, while flexible and soft polymeric components provide a necessary level of elasticity. Depending on the amounts of the constituents, such formulations can be broadly classified into two categories: $CaPO_4$-reinforced polymers and polymer-reinforced $CaPO_4$ bioceramics. Therefore, the formation of $CaPO_4$/polymer composites and hybrid formulations takes advantage of the advantages of both materials and minimizes their disadvantages. In general, the elastic modulus of polymers is lower (up to 2–7 GPa) than that of bone (3–30 GPa), which means that $CaPO_4$ bioceramics must be loaded at high weight ratios to mimic the latter. General knowledge of composite mechanics also shows that particles with high aspect ratios, such as whiskers and fibers, significantly increase the modulus at low loads. Therefore, some attempts have been made to prepare biocomposites containing whisker- [226–230] or needle-shaped [231–234] $CaPO_4$ and $CaPO_4$ fibers [235].

Implantable $CaPO_4$/polymer biocomposites have a history that dates back to 1981 (while the subject of "ceramic-plastic materials as bone substitutes" is at least 18 years older [236]), with pioneering research on HA/PE blends initiated by Professor William Bonfield and colleagues at the Queen Mary and Westfield College, University of London, UK [237,238]. That early work introduced the concept of bone resemblance, where the proposed biocomposite was composed of a polymeric ductile matrix of PE and a ceramic rigid phase of HA. Of them, HA stiffened the polyethylene, while PE toughened the composite. That approach was significantly extended and developed in further research by the same group [66,239–245]. Further studies investigated the effect of the surface topography of HA/PE composites on cell proliferation and attachment [246–249]. The material consisted of a specific combination of volume-loaded 40% HA particles homo-

geneously dispersed in an HDPE matrix. The idea was to mimic bone by reinforcing the polymer matrix, which can develop significant anisotropy with appropriate orientation techniques, with bone-like bioceramics that guarantee both mechanical reinforcement and bioactive properties of the composite material. Following FDA approval in 1994, a HA/PE formulation with 40 vol.% HA was given a trade name HAPEX™, became commercially available in 1995 [243–245,247] (Smith and Nephew Richards, Bartlett, TN, USA), and has been successfully implanted in more than 300,000 patients to date. It represents a major step forward in the bone grafting field because it was the first commercial product of the 'second-generation' also called surface-active biomaterials [250] that have been developed to be bioactive rather than bioinert [251]. The three primary steps in the production of HAPEX™ include blending, compounding, and centrifugal milling. Bulk materials and devices are then made from this powder through compression and injection molding [37]. In addition, HA/HDPE biocomposites can be prepared by hot rolling techniques that facilitate homogeneous dispersion and mixing of the reinforcement within the matrix [252]. Additionally, PP can be used instead of PE [253–256].

Mechanical interlocking between the two phases of HAPEX™ is formed by the shrinkage of HDPE on HA particles during cooling [66,67,257] and both HA particle size and its distribution in the HDPE matrix have been identified as important parameters affecting the mechanical behavior of HAPEX™. Namely, smaller HA particles were found to result in stiffer composites due to an overall increase in the interface between the polymer and the ceramic. Furthermore, the stiffness of HAPEX™ was found to be proportional to the HA volume fraction [242]. The use of coupling agents, such as 3-trimethoxysilylpropyl methacrylate, for HA and acrylic acid for HDPE can improve the bonding (through both chemical and mechanical adhesion) between HA and HDPE [258,259]. Naturally, in biocomposites including PE, alternative $CaPO_4$ compounds can be employed in place of HA [260]. Additionally, in an effort to enhance the mechanical qualities, efforts have been made to incorporate other bioceramic phases into the HDPE matrix of HAPEX™, such as PSZ [261] and alumina [262]. For example, replacing a portion of the HA filler particles with PSZ ones was found to increase the strength and fracture toughness of HA/HDPE biocomposites: The compressive stresses generated by the volume expansion associated with the transformation of PSZ from tetragonal to monoclinic phase inhibit or delay crack propagation in the composite. As a result, the fracture toughness of HA/ZrO_2/HDPE biocomposites is increased [261].

Numerous investigations have demonstrated that HAPEX™ adheres to bone directly via chemical bonding (biological fixation) as opposed to fibrous encapsulation (morphological fixation); orbital reconstruction was the initial clinical application of HAPEX™ [263], but, since 1995, the biocomposite's primary use has been in the sound transmission shafts of middle ear implants (Figure 1 [264]) for the purpose of treating hearing loss [265,266]. The advantage of HAPEX™ in both applications is its ability to be molded in situ, which gives surgeons the opportunity to make final adjustments to optimize the prosthesis' fit to the patient's bone. This means that there is minimal risk of failure due to insufficient tensile strength for subsequent activities, and only limited mechanical loading is needed [66,67,149]. When HA concentrations are less than 40%, HA/PE composites have superior fracture toughness compared to cortical bone, while concentrations between 45 and 50% show comparable fracture toughness. The Young's modulus result is in the range of 1–8 GPa, which is very close to that of bone. Observation of the fracture surface shows that only a mechanical bond is formed between HA and PE. Unfortunately, HA/PE composites are not biodegradable, the available surface area of HA is low, and the presence of bio-inert PE reduces its ability to bond to bones. Furthermore, HAPEX™ is designed at maximum density to increase strength, which results in a lack of void space limiting osteoblast viability when the implant is placed in the body [23,150]. More information about HAPEX™ can be found in the literature [66,67]. In addition, other types of HA/PE biocomposites have been developed [267–273].

Figure 1. Middle ear implants with HA heads and HAPEX™ shafts. Reprinted from Ref. [264] with permission.

PE has been utilized in both linear and branching forms as the matrix; biocomposites made with the former have higher moduli [270]. There is currently no compelling explanation for the mechanisms of reinforcement in $CaPO_4$/polymer compositions. Generally speaking, if the filler is selected poorly, the polymer matrix will be impacted by it. This can be seen in the forms of inert polymer shell formation around the particles (surface-induced crystallization, transcrystallization, and epitaxial growth), a decrease in molecular weight during composite processing, and conformational changes in the polymer caused by the interparticle space and particle surface [66,67]. On the other hand, the molding method may have an impact on the reinforcing effect of the $CaPO_4$ particles. It has been discovered that the composite's mechanical performance increases with the orientation of the polymer matrix [267,268].

It is also possible to create a wide range of alternative $CaPO_4$ mixes with other polymers [274], including very uncommon formulations that comprise dendrimers [275]. Moreover, $CaPO_4$/polymer compositions with light curing are known [276]. Table 3 provides a list of acceptable $CaPO_4$ products (MCPM and MCPA are both highly acidic and hence not biocompatible [16]; however, this drawback can be addressed by combining them with basic compounds such as TTCP, HA, CaO, and $CaCO_3$). There are two purposes of combining $CaPO_4$ with polymers to make biocomposites: the desirable mechanical properties of the polymer compensate for the poor mechanical behavior of $CaPO_4$ bioceramics and, conversely, the desirable bioactive properties of $CaPO_4$ enhance those of the polymer, expanding the possible uses of each material in the body [277–280]. Namely, the addition of polymers to $CaPO_4$ increased its mechanical strength [277] and the addition of $CaPO_4$ filler to polymers increased their compressive strength and modulus and osteoconductive properties [119,281–284]. As $CaPO_4$ content increased in biocomposites, Young's modulus and bioactivity generally increased, and ductility decreased [23]. Subsequent research has revealed that the mechanical characteristics of $CaPO_4$/polymer biocomposites are more complex. It was discovered that the strength of these biocomposites decreased as the $CaPO_4$ level increased [285]. However, the biocompatibility of such biocomposites increases as the $CaPO_4$ filler causes an increased initial flash spread of serum proteins compared to more hydrophobic polymer surfaces [286]. Furthermore, experimental results of those biocomposites showed enhanced cellular activity and good cell–material interactions compared to the corresponding polymers alone [279]. Moreover, these compositions have the ability to release calcium and orthophosphate ions into myeloma in a sustainable manner, both of which are critical for the regeneration of mineralized tissue [278]. In fact, the combination of two different materials can produce better biocomposites than the materials alone, taking

advantage of the strengths of each. However, in some cases, the incorporation of $CaPO_4$ into biocompatible, mechanically stable, and 3D printable polymers does not improve bone formation in vitro or in vivo [287].

5.1.2. Apatite-Based Formulations

It is recognized that the primary inorganic phase of mammalian calcifying tissues is biological apatite [14,15]. Therefore, CDHA, HA, carbonate apatite, and sometimes FA (all of which can be both pure and contain dopants) have been applied in the preparation of biocomposites with other polymers, often with the aim of improving their biological activity. For example, polysulfone composed of HA can be used as a starting material for long-term implants [288–290]. In in vivo experiments, HA/polysulfone biocomposite-coated specimens from the distal femur of a rabbit showed direct bone attachment to the coating compared to the fibrous encapsulation that occurs when using uncoated specimens [288]. The bioresorption time of such biocomposites is a very important factor that depends on the microstructure of the polymer and the presence of modified phases [289].

Various apatite-containing biocomposites have been developed using PVA [198,291–294], PVAP [295], and other polymers [296–306]. Namely, PVA/CDHA biocomposite blocks were prepared by precipitating CDHA in an aqueous solution of PVA [198]. An artificial cornea consisting of a porous skirt of nanoscale HA/PVA hydrogel and a transparent center of PVA hydrogel was also created. The results showed good biocompatibility and docking between the artificial cornea and the host tissue [291,292]. PVAP was chosen as the polymer matrix due to its phosphate groups acting as binding/anchoring agents and its high affinity for the HA surface [295]. HA/Ca poly(vinyl phosphonate) biocomposites were also created [299,300], while a high-affinity integration of CDHA with PHEMA hydrogel scaffolds was studied by template-guided nucleation and mineral growth processes [305].

Biocomposites including HA have also been created using PEEK [226,227,307–312] and a high-impact polystyrene [313,314], which may find therapeutic application in load-bearing applications. Mechanical properties increased monotonically with reinforcement concentration in tests where PEEK was reinforced with thermally sprayed HA particles; the highest values were obtained in studies where the volume fraction of HA particles was less than 40% [307,308]. The stated strength range of 45.5–69 MPa and hardness range of 2.8–16.0 GPa surpass the lower values for human bone, which are 7–30 GPa and 50–150 MPa, respectively [308]. Since the tensile strength of conventional PEEK/HA biocomposites fell sharply with increasing HA loading, nanodimensional HA rods and carbon nanofibers were used to reinforce PEEK. In that case, the tensile properties of a PEEK/15 vol% HA/1.9 vol% carbon nanofibers biocomposite were found to compare favorably with those of human cortical bones [310]. Modeling of the mechanical behavior of HA/PEEK biocomposites is available elsewhere [309].

Biodegradable poly(α-hydroxyesters) are well known in clinical medicine. Currently, these materials offer good options when looking for suitable polymer fillers. For example, cytocompatible HA/PLGA formulations have been developed for bone tissue regeneration [315–319], while highly porous PLLA foam was seeded with HA particles to enhance the osteoconductivity of polymer scaffolds for bone tissue engineering [281]. Since hydration increases the quantity of COOH and OH groups on the polymer surface, which serve as apatite nucleation sites, the foam's amount of carbonized CDHA material rose before it was incubated in simulated bodily fluid. More information about the mechanical characteristics of PLA/$CaPO_4$ biocomposites made using various methods, as well as the outcomes of in vitro and in vivo tests, is available elsewhere [316].

Poly(α-hydroxyesters), such as PGA and PLA, are known to spontaneously decompose into acidic monomers (glycolic acid and lactic acid, respectively), which catalyze further degradation and cause inflammatory reactions in surrounding tissues [320]. Therefore, in $CaPO_4$ biocomposites with poly(α-hydroxyesters), the presence of slightly basic compounds (HA, TTCP) neutralizes the acid molecules to some extent, leading to a weak pH buffering effect on the polymer surface, thus partially compensating for these disadvan-

tages [119,317,321–323]. However, the addition of more basic chemicals (e.g., CaO, $CaCO_3$) may become necessary [123,323–325]. Extensive cell culture experiments on pH-stabilized PGA and carbonate apatite composites have been reported and subsequently supported by extensive in vitro pH studies [326], which resulted in the design of functionally graded composite cranial implants composed of PLA, carbonate apatite, and $CaCO_3$ [327]. Except for the pH buffering effect, the addition of $CaPO_4$ also increases the hydrophilicity and water absorption of the polymer matrix, thereby modifying the degradation kinetics of the scaffold. For instance, when water enters the interface region, it has been observed that polymer biocomposites containing HA particles hydrolyze uniformly [328].

Poly(α-hydroxyester) and $CaPO_4$ biocomposites are mainly prepared by incorporating the inorganic phase into a polymer solution followed by drying under a vacuum. The resulting solid biocomposites can be molded using various processing techniques. These biocomposites can be made by combining L-lactide and HA particles prior to polymerization [321] or by combining slip casting and hot pressing [329], while other methods of production are also known [316,318,330,331]. The addition of surface active agents (surfactants) may be useful to maintain the homogeneity of the suspension [332]. It is also possible to create HA/PLA [191,192] and HA/PLGA [193] microspheres using microemulsion technology. There are other known more intricate formulations, such as carbonated-FA/PLA [333] and PLGA/carbon nanotube/HA [334]. Durucan and Brown have released a collection of interesting references pertaining to various ways of manufacturing HA/poly(α-hydroxyester) biodegradable composites [335–337]. The authors prepared CDHA/PLA and CDHA/PLGA biocomposites by solvent casting method, followed by hydrolysis of α-TCP to CDHA in aqueous solution. It was found that the presence of both polymers inhibited the hydrolysis of α-TCP compared to single-phase α-TCP and the inhibitory effect of PLA exceeded that of PLGA [335–337]. The physical interactions between poly(α-hydroxyester) and $CaPO_4$ are shown in Figure 2 [337]. Another good illustration is available in the literature [51].

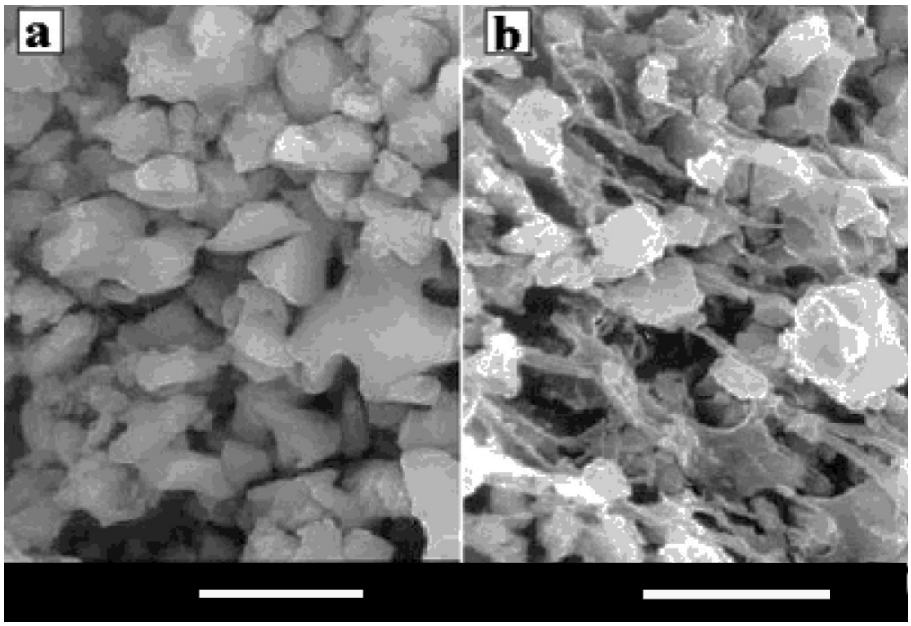

Figure 2. SEM micrographs of (**a**) α-TCP compact; (**b**) α-TCP/PLGA biocomposite (bars = 5 μm). Reprinted from Ref. [337] with permission.

$CaPO_4$ addition has the potential to greatly improve the mechanical characteristics of poly(α-hydroxyesters) [338,339]. Therefore, fixations (screws and plates) built from those composites have been created and evaluated, and CDHA/PLLA biocomposites with extremely high mechanical properties have been developed [119]. The fixations have demonstrated easy handling and molding to the shape of the implant site, complete

absorbability, excellent ability to bond directly to bone tissue without fiber tissue, osteoconductivity, biocompatibility, and high stiffness that can be maintained for the time required for bone union [328,330]. Elastic modulus can reach 12 GPa, and the initial flexural strength of 280 MPa is more than that of cortical bone (120–210 MPa) [119]. In phosphate-buffered saline, this strength could be sustained above 200 MPa for a maximum of 25 weeks. These biocomposites were made by precipitating PLLA/dichloromethane solutions that contained scattered tiny $CaPO_4$ particles [118,340]. PDLLA + HA [221,341,342] and PLGA + HA [343], along with the multicomponent compositions PLA/ethylcellulose/HA [344] and PLA/Fe_3O_4/BCP (HA + β-TCP) [345], were used to fabricate biocompatible porous scaffolds. Compared to single-phase HA bioceramics, biodegradation was markedly accelerated, and freshly generated bone was seen when implanted in rabbit femurs. This could be because HA dissolves when lactic acid is released locally. PLA and PGA fibers were attached to porous HA scaffolds in additional research. The fact that the reinforcement did not prevent bone from penetrating the implant encourages the development of these biocomposites further for usage as alternatives to bone grafts [29,316,317]. Recent data on using of 3D-printed PLA/$CaPO_4$ composite scaffolds for bone tissue engineering in preclinical in vivo studies are available in the literature [346].

Biocomposites, termed SEVA-C, were produced by combining EVOH-starch blends with 10–30 wt% HA fillers. The samples that contained 30 wt% HA had moduli up to 7 GPa, as reported in [347–351]. The purpose of adding bioactive HA fillers in SEVA-C was to create composites that exhibit bioactivity and possess the necessary stiffness similar to those found in human cortical bone. Results indicated that these biocomposites exhibited significant bioactivity in vitro, which was supported by the polymer's water uptake capacity [352]. However, the addition of HA particles to SEVA-C was determined to impact the rheological properties of the blends. A degradation model was subsequently constructed for these mixtures [353].

The homologs poly(3-hydroxybutyrate) and poly(3-hydroxyvalerate) are not very biodegradable. However, biocomposites of these polymers with $CaPO_4$ have shown good biocompatibility both in vitro and in vivo [354–358]. The bioactivity and mechanical properties of these biocomposites can be tuned by changing the volume fraction of $CaPO_4$. Similarly, biocomposites of PHBHV with HA and amorphous carbonate apatite (almost ACP) have been shown to have promising potential for repair and replacement of damaged bone [359–362].

In this framework, a less biodegradable but biocompatible polymer, PCL, has been employed, and PCL/HA and PCL/CDHA biocomposites have been considered viable options for bone tissue regeneration and repair [216,363–369]. For example, biocomposites were obtained by infiltrating porous apatite blocks with ε-caprolactone monomers and polymerizing them in situ [364]. The composite was found to be biodegradable and potentially applicable as a bone replacement and cartilage regeneration material for cancellous bone and trabeculae; the addition of HA strongly enhanced both the mechanical performance and biocompatibility of PCL in osteoblast cultures [370]. For the preparation of PCL/HA biocomposites, various techniques are known [216,366]. For example, to make PCL and nanosized HA biocomposite fibers, the desired amount of nanosized HA powder was dispersed in a solvent using a magnetic stirrer followed by sonication for 30 min. PCL was then dissolved in this suspension and the solvent was evaporated [371]. The reverse preparation sequence is also possible: PCL was dissolved in chloroform at room temperature (7–10 wt%/volume), HA (~10 μm particle size) was suspended in this solution, sonicated for 60 s, and then the solvent was evaporated [372] or immersed in salt [373]. The mechanical properties obtained with this technique are approximately one-third of those of cancellous bone. In a comparative study, PCL and bio-apatite were mixed in an extruder in a 19:1 ratio [374]. After preparation was complete, the mixture was cooled in a nitrogen atmosphere. The authors observed that the presence of bio-apatite increased the modulus of elasticity and also increased the hydrophilicity of the polymeric substrate. Furthermore, increasing the apatite concentration was found to im-

prove both the elastic modulus and yield stress, indicating a good interfacial interaction between biological apatite and PCL. The presence of biological apatite was also found to stimulate osteoblast attachment to the biomaterial and cell proliferation [374]. In another study, PCL/HA biocomposites were prepared by melt stirring at 120 °C in a rheometer connected to a stirrer until the torque reached equilibrium [375]. The samples were then compression molded and cut into specimens of suitable size for testing. The results showed that composites containing 20 wt% HA had the highest strength [375]. However, grafting PCL directly onto the surface of HA particles seems to be the most interesting preparation method [363]. In one more study, HA porous scaffolds were coated with a PCL/HA composite coating [376]. In that system, PCL as a coating component improved the brittleness and low strength of the HA scaffold, while the particles in the coating improved the osteoconductivity and bioactivity of the coating layer. In addition, there are multicomponent biocomposites, including PDLLA/PCL/HA [377], PLLA/PCL/HA [378], FA-HA/PCL [379], chitosan/PCL/PVA/HA [380], magnetic PCL/Fe-doped HA [381], supramolecular PCL/functionalized HA [382,383], Cu_2O@$CuFeS_2$/HA/chitosan [384], etc. In November 2023, results of the first clinical case of the Ilizarov method of bone reconstruction by means of a bioactive and degradable intramedullary HA/PCL biocomposite implant were published [385]. More details on PCL/HA biocomposites and processing methods can be found elsewhere [216,366,368].

At the end of this section, HA biocomposites with other polymers need to be mentioned [386–396]. Among them, PTMC/HA biocomposites have been suggested to be suitable for stereolithographic fabrication of patient-specific flexible implants [393]. Moreover, some of them exhibit interesting properties. Namely, polymers with shape memory properties are worth mentioning [397]. Consequently, it is also thought that composites based on $CaPO_4$ and these polymers exhibit shape memory qualities [389–391]. More complex formulations are also known. Namely, biopolymer/CHDA biocomposites encapsulating magnetic nanoparticles [398], as well as many other magnetic formulations [399], have been prepared. More details on HA/polymer composites and hybrid formulations can be found in other reviews [400–403].

To conclude, currently (May 2024), according to Scopus, there are 900 articles with a combination of "polymer" and "apatite" in the title.

5.1.3. TCP-Based Formulations

Compared to HA, both α-TCP and β-TCP are more soluble in water (Table 3). This is the reason for their faster bioresorption in vivo (although there have been reports of not biodegrading TCP after implantation in calvarial bone defects [404]). Therefore, both types of TCP are widely used to create fully biodegradable biocomposites [405–420]. For instance, β-TCP particles and gelatin have been combined to create a biodegradable and osteoconductive biocomposite [409]. When this substance was evaluated in vivo, positive outcomes were seen. The material was found to be biocompatible, osteoconductive, and biodegradable, and did not require another surgical procedure to remove the device after healing. To that composition, one may add K_2HPO_4 [411] and botanical extracts [410]. After creating a biocomposite using cross-linked gelatin and β-TCP, another research team implanted it subcutaneously in rats and saw good biocompatibility as well as bone development [412]. Later, this was extended to a porous (porosity ~75%) β-TCP/gelatin composite material containing BMP-4 [415]. Furthermore, porous β-TCP/alginate/gelatin scaffolds with cytocompatibility and osteoinductive properties were fabricated and successfully tested in vitro [413]. In addition, multicomponent formulations, such as a phytoconstituents-filled β-TCP biocomposite with gelatin and pectin polymers incorporating *Cissus quadrangularis* L. extract [421], as well as another biocomposite of microporous β-TCP filled with alginate-gelatin crosslinked hydrogel, clindamycin, and bone morphogenetic protein (BMP-2) [422] were prepared. Both formulations appeared to be suitable for drug delivery. In such formulations, $CaPO_4$ filler was found to have a reinforcing effect [423]. In other studies, β-TCP biocomposites with PLLA [340,405–407] and PLGC [408] were prepared. β-TCP was

able to resist the acidic degradation of polyesters to some extent, but could not prevent the pH from dropping to ~6. However, the biocomposite was successfully implanted into the mandible of a beagle [408]. Similarly, α-TCP/gelatin biocomposites are also known [409].

Based on the concept of self-reinforcement, TCP and polylactic acid biocomposites were prepared and studied using conventional mechanical tests [424]. Resorbable scaffolds were prepared from those biocomposites [425]. Chitosan was also used as a matrix to incorporate β-TCP through solid–liquid phase separation of the polymer solution followed by sublimation of the solvent. Due to the complexation of the functional groups of chitosan with the calcium ions of β-TCP, those biocomposites had high compressive modulus and strength [426]. PCL/β-TCP biocomposites were also developed in other studies [368,369,427–431], and an immersion in simulated body fluids at 37 °C allowed for systematic monitoring of their in vitro degradation behavior [429]. Loading of drugs into PCL/β-TCP biocomposites is a further development of this subject [368,430].

In vitro studies using primary rat cervical osteoblasts have shown increased cellular activity in BMP-loaded β-TCP/gelatin biocomposites [415]. Other researchers investigated BMP-2 loaded porous formulations (porosity ~95%, average pore size 180–200 μm) [432] and confirmed the results. Good results were obtained after 12 months from long-term implantation research with PDLLA/α-TCP biocomposites in a sheep implant loading model; however, after 24 months, a severe osteolytic response was detected. This resulted from the residual PDLLA and the nearly total disintegration of α-TCP by this point [433].

There exist more intricate $CaPO_4$-based biocomposites. As an illustration, certain formulations comprise TCP, CDHA, and PLGA, three interpenetrating networks [434]. Firstly, a hydrolyzable α-TCP slurry was applied to PU foam to create a porous TCP network. Second, a self-hardening $CaPO_4$ formulation inserted into the porous TCP network yielded the CDHA network. Lastly, the remaining open porous network of the CDHA/α-TCP complex was compromised by PLGA infiltration. There were three phases to the biocomposite, and each phase had a distinct degrading tendency. It is thought that bone forms on the PLGA network, which deteriorates the quickest, while the remaining $CaPO_4$ phase holds its structure and capacity to support weight [434]. Furthermore, PCL/TCP/boron nitride biocomposites were prepared in a similar manner [435].

5.1.4. Biocomposites with Remaining $CaPO_4$

The number of publications on composites and hybrid formulations containing the remaining $CaPO_4$ compounds and polymers is considerably smaller than the ones with apatite and TCP. Biphasic calcium phosphate (BCP), a solid blend of HA with β-TCP (similar formulations of HA + α-TCP and α-TCP + β-TCP are also known [436]) seems to be the most popular among the remaining $CaPO_4$ compounds. Namely, hydrophilic PEG/vancomycin complexes were coated on porous PDLLA/BCP scaffolds to modify their surface and distribute drugs [437]. More specifically, both PLGA/BCP [438,439] and PLLA/BCP [440] biocomposites have been produced and found acceptable for repairing, filling, and growing native bone tissue due to their cytotoxic and fibroblastic properties [441,442]. In addition, PCL/BCP [443,444], PTMC/BCP [445], PMMA/BCP [446], gelatin/BCP [447,448], and gelatin/PVA/BCP [449] biocomposites are known as well.

DCPD-based biocomposites composed of DCPD, albumin, and duplex DNA were prepared by water/oil/water interfacial reaction method [190]. Wet spinning was used in a different work to create core-shell DCPD/chitosan biocomposite fibers [450]. P atoms were found in trace numbers inside the composite fibers, whereas Ca and P atoms were mostly found in the outer layer, according to energy-dispersive X-ray spectroscopy. This showed that the chitosan core and $CaPO_4$ shell of the composite fibers created a distinctive core-shell structure [450]. For use in self-hardening biocomposites, similar formulations have been produced [451]. Moreover, BSA and DCPA nanoparticles were co-precipitated in ethanol to create DCPA/BSA biocomposites [452], DCPA/ethylcellulose ones were prepared using the sol-gel method [453], while those of DCPA/PVA were produced by freeze-drying [454]. Nanosized particles of DCPA were synthesized and incorporated

into dental resin to form dental biocomposites [455–458], while DCPA/dextran/CMC nanocomposite porous scaffolds were prepared by freeze-drying in a lyophilizer [459]. Interestingly, certain DCPD/polymer composites have the potential to be employed in battery devices as proton conductors [460,461]. Although biocompatibility has not been reported, perhaps in the future better formulations will be used to provide biocompatible batteries for electronic devices that are implanted.

To address the effects of dental caries, a number of hybrid and ACP-based biocomposite formulations have been developed for dental applications [462,463]. Among them, there are rechargeable ones with sustained ion release and re-release, which were introduced in 2016 [464–467]. Furthermore, various ACP-based formulations have been investigated as potential biocomposites for bone grafting [362,468–470] and drug delivery [471,472]. Namely, ACP/PPF biocomposites have been prepared by in situ deposition [469], and PHB/carbonated ACP and PHBHV/carbonated ACP biocomposites appear to be suitable as slow biodegradable bone replacement materials [362].

OCP-based biocomposites with polymers are also known. For example, OCP granules were combined with gelatin and the prepared composites were spread on rat calvaria. Those composites were found to promote bone growth due to the balanced cellular activity of osteoblasts and osteoclasts [473]. There is also an excellent review on OCP/polymer biocomposites with a controlled hierarchical structure from the macro to the nanoscale [474]. The following topical overview contains more details about OCP-based formulations that are relevant to biomedicine [475].

Finally, just a few publications on TTCP-based biocomposites with polymers have been published [476,477].

To conclude, currently (May 2024), according to Scopus, there are 404 articles with a combination of "polymer" and "calcium phosphate" in the title.

5.2. Self-Hardening Biocomposites

The early 1980s saw the introduction of inorganic self-hardening $CaPO_4$ formulations (cements) that were set in vivo [478]. They have been the subject of in-depth research and numerous formulations since then. These mixtures solidify by a variety of chemical reactions among $CaPO_4$ and eventually form a monolithic body composed of CDHA or DCPD, with other phases possible to mix. Unfortunately, self-hardening $CaPO_4$ formulations with ceramic properties become brittle after setting, while the hardening time may not be suitable for clinical procedures [478]. Therefore, several attempts have been made to transform them into biocomposites to improve their properties, for example, by adding PEG [479,480], polylactide [481], PLGA [482], gelatin [414,483–486], osteocalcin/collagen [487], alginic acid [488], chitin [489], chitosan [451,490], fibrin glue [491], silk fibroin [492,493], silanized HPMC [494], CMC [495], PVA fibers with CMC [496] and without CMC [497], CMC/gelatin/fullerenol [498], bioactive glass [499–502], bioactive glass functionalized with hypoxia conditioned medium [503], calcium silicate [504–506], cockle shell powders [507], metals [508], magnetic nanoparticles [509], and so on. Light-curing formulations have also been prepared [510,511]. Furthermore, a wide range of reinforcing additives with varying forms and characteristics are frequently employed to enhance the mechanical characteristics of $CaPO_4$ compositions that self-harden [512,513]. For this, carbon nanotubes have even been employed [514,515]. Furthermore, the addition of a carbonate apatite type B powder into a self-hardening α-TCP formulation was also found to improve the mechanical properties of the final product [516]. An important part of the reinforced formulations can be named $CaPO_4$-based concretes [517,518], although this term is rarely used in the field of biomaterials [478]. The idea with concrete is simple: the presence of a strong filler in the matrix can stop the proliferation of cracks. Most of the aforementioned compounds were added to the self-hardening $CaPO_4$ formulations with the main purpose of improving either the rheological properties of the liquid formulations or the mechanical properties of the hardened ones; however, other aims are also known. For example, the addition of magnetic nanoparticles was found to increase cell adhesion [509].

Various apatite-containing formulations have been developed using PMMA [446,519–525] and polyethylmethacrylate [526,527]. Such biocomposites are prepared by dispersing apatite powder in a polymeric viscous liquid [528] and can be used for drug delivery purposes [529]. The mechanical properties of concretes composed of PMMA matrix and HA particles of various sizes were tested and tensile results showed that the strength was independent of particle size. The tensile strength did not change after immersion in Ringer's solution, but the fatigue properties were significantly reduced. In vivo, tests for PMMA/HA blends' biocompatibility have validated the implants' enhanced osteogenic qualities over single-phase PMMA [520–523]. Not only were the properties improved, but the addition of HA also enhanced the osteoblastic response of PMMA [521]. Thus, the addition of $CaPO_4$ made the non-biodegradable PMMA more bioactive and osteoconductive, resulting in biocomposites with good workability. On the other hand, PMMA/HA biocomposites have low flexural, compressive, and tensile strengths. More complicated formulations, such as PMMA-based HA/$ZnFe_2O_4$/ZnO biocomposites with antibacterial performance and low toxicity, were prepared as well [530].

It is believed that biocomposites composed of $CaPO_4$ and different kinds of resins have mechanical and biological characteristics similar to those of ordinary PMMA cement and can be used for implant fixation [228,229,531–533]. To enhance the mechanical characteristics of self-hardening $CaPO_4$-based formulations and maintain stability at the implant site, numerous researchers have turned to in situ curing formulations, mostly via polymer matrix crosslinking processes [511,534–537]. For instance, crosslinked CDHA/calcium polyacrylate biocomposites were created when TTCP and PAA interacted [534]. TTCP hydrolyzes to CDHA in aqueous solution [16], and the calcium cations that are liberated then combine with PAA to form a crosslinked network [534]. In another study, dicarboxy polyphosphazene crosslinkable with calcium cations was used as the polymeric component, and CDHA/polyphosphazene biocomposites possessing a porosity of around 65% and a compressive strength of approximately 10 MPa were created [535]. To mimic the properties of PMMA cements, PPF/β-TCP biocomposites were prepared by adding vinyl monomers to crosslink PPF. As a result, fast hardening and degradable biocomposites with low heat generation and compressive strength in the range of 1–12 MPa were prepared by varying the molecular weight of PPF, monomer, β-TCP, initiator, and NaCl as porogen [536,537]. Injectable polydimethylsiloxane/HA biocomposites [538], acrylic formulations with Sr-containing HA as filler [100], and formulations with PLGA microspheres and self-hardening $CaPO_4$ [539,540], along with hybrid chitosan oligosaccharide/gelatin/$CaPO_4$ biocomposites [541], have also been investigated.

Numerous researchers used different polymers in self-hardening $CaPO_4$ compositions to increase their mechanical capabilities. To stabilize the $CaPO_4$ paste in an aqueous solution before it sufficiently hardens and then to boost its compressive strength, for instance, gelatin was added [414,483,542]. The addition of rod-shaped fillers also improved the mechanical properties [542]. For instance, the mechanical characteristics of self-hardening TTCP + DCPD formulations were successfully enhanced by PAA and PVA, but, unfortunately, both processability and hardening time were inevitably reduced [543,544]. Similar results have been reported after the addition of sodium alginate and sodium polyacrylate [545]. Other polymers such as polyphosphazene can also be used [546–548]. Other examples of polymer/$CaPO_4$ self-hardening biocomposites can be found elsewhere [549,550]. In addition to polymers, metal wires can also be used as reinforcement to create biocomposites from the self-hardening $CaPO_4$ formulations [551].

Porous $CaPO_4$ scaffolds were created by covering PU foam with a self-hardening TTCP + DCPA formulation and calcining it at 1200 °C. Those scaffolds had interconnected macropores (~1 mm), micropores (~5 μm), and substantial porosity (~80%). To improve their mechanical properties, PLGA solution was infiltrated into the open micropores of the struts to obtain a composite construction made of biodegradable polymers and bioactive ceramics. An additional coating of 58S bioactive glass/PLGA composite was applied to the PLGA-filled struts. The resultant porous biocomposites are suitable for low-load

tissue engineering scaffolds [552]. There are also more complex structures in which the PLGA macroporous phase is reinforced with a self-hardening TTCP + DCPA formulation and the entire structure is surface-coated with a CDHA layer [553]. Furthermore, a moldable $CaPO_4$-based self-setting composite was successfully constructed by infiltrating a wollastonite/$CaPO_4$ paste into a 3D plotted PLGA network. After being heated to 50 °C, the PLGA/wollastonite/$CaPO_4$ composite appeared to be sufficiently plastic for successful adaptation to the complex-shaped bone defects [554]. In another study, PLGA microparticles coated with α-TCP and poly(ethylene phosphate) sodium salt were mixed with castor oil and water to form oil-in-water emulsions. The resulting emulsions solidified spontaneously at room temperature in a humidified atmosphere. The PLGA particles included in the set formulation underwent hydrolysis, leading to the formation of interconnected microporosity [555].

The addition of water-soluble mannitol imparted 42–80% porosity to the self-hardening $CaPO_4$/chitosan biocomposites [556]. Chitosan significantly increased the mechanical strength of the overall formulations [557]. A similar approach was used by other researchers who studied the effect of adding PLGA microparticles [558–561] (which can also be filled with drugs or growth factors [562–564]) to self-hardening $CaPO_4$ formulations. Those biocomposites were implanted into cranial defects in rats and the best results were obtained with a particle content of around 30 wt% [558]. On the other hand, after 2 weeks, the biocomposites containing growth factors greatly enhanced bone contact and, after eight weeks, encouraged the creation of new bone [563]. In an in vivo rabbit femoral implant study, the self-hardening PLGA/$CaPO_4$ formulation showed compatibility and bioactivity as well as better osteoconductivity and degradability than the self-setting formulation consisting of $CaPO_4$ alone [559]. In 2018, researchers succeeded in producing bionic biocomposites with the Harvarsin microstructure from a self-setting TTCP + DCPD formulation combined with small intestinal submucosa [565]. Further details on this topic are available in the literature [566]. In addition, several types of self-hardening $CaPO_4$-containing biocomposites were successfully tested as inks for the 3D printing of scaffolds [486,567] (see Section 5.9 below).

Finally, the addition of $CaPO_4$ to self-hardening calcium sulfate (plaster of Paris) [568,569], or vice versa [570], or to calcium silicate (Portland bone cement) [571] formulations can improve their osteoconductive properties. More complex formulations, such as calcium sulfate/β-TCP/PVA/polyvinylpyrrolidone [572], are also known.

5.3. Nanosized $CaPO_4$-Based Formulations and Nanosized Biocomposites

Nanosized and nanophase materials are materials with particle, crystal, or grain sizes of less than 100 nm. However, before continuing, a clear distinction needs to be made between nanosized composite materials and composite materials containing nanosized particles. The former, which can be any type of composite material, is fragmented into particles with sizes smaller than 100 nm. The second consists of two or more materials, at least one of which is on the nanometer scale. Nevertheless, both possibilities combine the advantages of the two parts to offer more usefulness than just the individual materials.

When compared to large-grained materials with the same chemical composition, materials that are nanosized and nanophase have distinct mechanical and optical properties [573]. Furthermore, as compared to traditional micron-sized materials, they have different surface characteristics including more atoms, flaws, and grain boundaries on the surface, a larger surface area, and a different electrical structure. Regarding $CaPO_4$, the surface roughness of nanosized HA (size ~67 nm) is as high as 17 nm, compared to 10 nm for conventional submicron-sized HA (~180 nm), and the contact angle (a quantitative wetting indicator of solids by liquids) is significantly lower, at 6.1 for nanosized HA compared to conventional HA (11.51). Furthermore, the pore diameters of nanosized HA compacts are approximately 6.6 Å, which is 3–5 times smaller than the pore diameters of normal particle-sized HA compacts, which range from 19.8 to 31.0 Å [574]. Moreover, compared to microcrystalline $CaPO_4$, nanosized ones accelerate the production of new bone tissue by

promoting osteoblast adhesion, differentiation, proliferation, osteointegration, and surface mineral deposition [575–577]. Finally, nanosized HA was found to induce apoptosis of leukemic P388 cells [578].

Biogenic hierarchical biocomposites based on nanosized materials make up natural bones and teeth, as nanosized plate-shaped crystals of biogenic apatite with dimensions of 50 nm × 25 nm × 1–4 nm, growing in close contact with a bioorganic fiber-rich organic matrix; thus, they generate a significant organic/inorganic interface due to the nanoscale dimensions and are arranged in a complex hierarchical structure. When calculating the interface area between the biological apatite and the organic phase based on the crystal dimensions, it becomes ~210 m^2/g. This interface is believed to absorb externally applied forces to dissipate mechanical energy to thermal energy [579]. Given that the main bio-organic phase of bone is collagen, i.e., a natural polymer (Table 1), bio-composites of nanosized $CaPO_4$ and biodegradable polymers are clearly advantageous as bone graft materials. As mentioned before, the polymeric phase offers elasticity, whilst the $CaPO_4$ phase is in charge of biological activity and mechanical strength (hardness). Moreover, $CaPO_4$'s solubility is influenced by its carbonate content and crystal size. The more carbonate present, the more soluble the compound is. The smaller the crystals, the more soluble the compound is. To the best of the author's knowledge, only the apatites (HA, FA, and CDHA) listed in Table 3 were accessible in nanoscale form until recently. However, in an effort to treat dental caries, nanosized MCPM [580] and DCPA [455–457] have recently been synthesized and used to construct biocomposites with potent ion-releasing capabilities. Probably, all known types of $CaPO_4$ from Table 3 can be produced in nanosized and/or nanocrystalline states, but not all of them have been prepared yet [577].

The mineralization, biocompatibility, and mechanical characteristics of biocomposites based on different (bio)polymers and nanosized $CaPO_4$ have all been the subject of recent studies (especially HA). Unfortunately, in most of the published papers, it remains unclear whether 'nanosized HA' actually represents nanosized stoichiometric HA or nanosized non-stoichiometric CDHA, and thus the two cannot be distinguished. Those studies include biocomposites of HA or CDHA with PGA [581], PLA [221,233,582–587] and its copolymers with PGA [588–590] and PCL [591,592], PCL [593], collagen [594–602], collagen + PLA [603–607], collagen + PVA [608], collagen + alginic acid [609,610], alginic acid [394], gelatin [611–615], hyaluronic acid + alkaline gelatin [616], PPF [617,618], PA [186,187,619–624], PVA [291,292,625–627], PVAP [295], BSA [628], poly(ethylene-acrylic) acid [629,630], chitosan [631–638] and derivatives [639], konjac glucomannan + chitosan [640,641], chitosan + gelatin [642–644], xanthan [645], PHEMA + PCL [646], PCL [332,371,647–649], PU [650–652], PLA + PU [653], DNA [654,655], cellulose [41,42,656–659], Ti [660–662], SiC [663,664], ZrO_2 [665–667], glass [668,669], metals and alloys [670,671], carbon quantum dots [672,673], clay [674,675], and many other biocompatible hybrid formulations [199,219,272,290,360,676–689]. A schematic drawing of DNA incorporation inside the HA structure and a TEM micrograph showing CDHA nanoparticles incorporating DNA are shown in Figure 3 [654,655].

Furthermore, any formulation can be coated with a nanosized $CaPO_4$ layer. In other words, nanosized HA rods + gelatin biocomposites are coated with nanosized HA [690]. Certain kinds of nanosized biocomposites seemed to be useful as carriers for the transport of drugs and growth factors [669,691–693], as well as potential vectors with extremely high gene loading and transfection effectiveness [694]. There is information available regarding those biocomposites' exceptional biocompatibility [599]. The state of dispersion of nanosized particles seems to be an important parameter in regulating the mechanical characteristics of nanosized biocomposites since their high surface energy invariably causes them to agglomerate [360]. The mechanical characteristics of biocomposites comprised of PA and nano- and micron-sized HA were compared. The findings demonstrated that, as the amount of nanosized HA in the biocomposites increased, their flexural and tensile strength increased as well, but, as the amount of micron-sized HA content increased, it dropped [186]. Figure 4 displays SEM images of the mineralized collagen fibers, highlighting the intimate

connection between the mineral phase and the restructured collagen fibers as well as the homogeneity of the nanosized biocomposites [695].

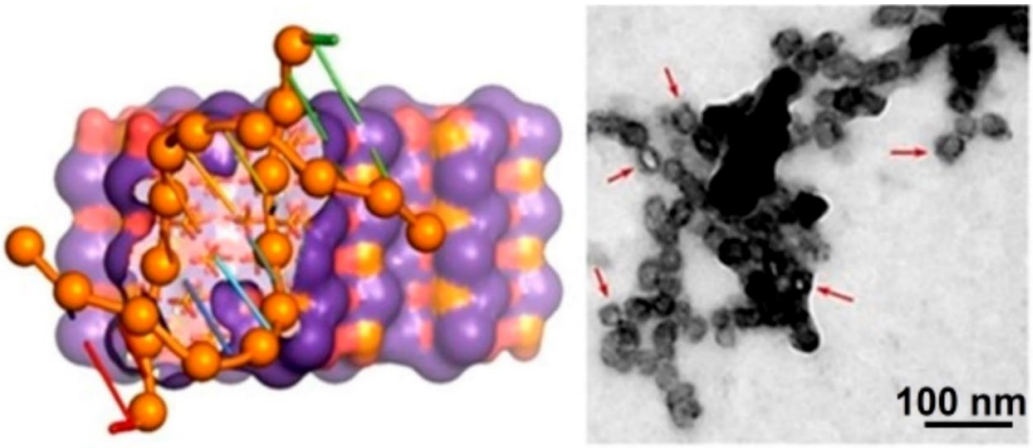

Figure 3. A schematic drawing of DNA incorporation inside the HA structure (**left**) and a TEM micrograph showing CDHA nanoparticles (red arrows) incorporating DNA (**right**). Reprinted from Refs. [654,655] with permission.

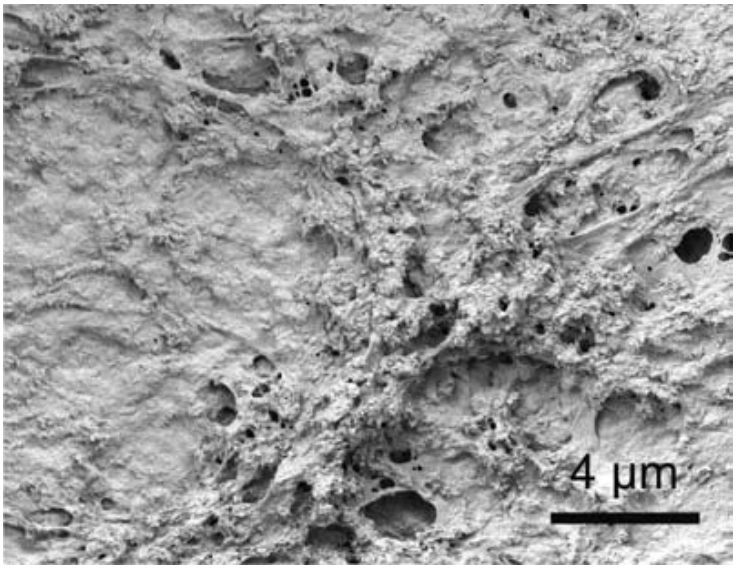

Figure 4. Mineralized collagen I fibrils that have been reconstituted captured in a scanning electron microscope image. An illustration of an organic-inorganic nanostructural composite that, at the nanoscale, resembles the extracellular matrix of bone tissue. Reprinted with permission from Ref. [695].

By means of precipitation and lyophilization, nanosized HA and porous (porosity ~85%) biocomposites consisting of collagen were created. Those biocomposites showed no pH decrease in in vitro degradation [603–605]. They were implanted in rabbit radii, showed high biocompatibility, and were partially resorbed after 12 weeks. From HA/chitosan nanosized rods, nanosized HA/chitosan biocomposites with enhanced mechanical stability were created [696]. Using heat-induced phase separation, nanosized HA/PLLA biocomposites with high porosity (~90%) were created [697]. Additionally, nanosized HA was utilized to create biocomposites with PAA, and the resulting nanosized crystals' nanostructure revealed a core–shell configuration [698,699]. Other researchers discovered that the self-organization of nanodimensional HA with PAA led to the formation of liquid–crystalline nanorod hybrids that formed aligned films and showed stimuli-responsive properties [700].

Nanosized crystals of HA were found to be suitable for endosteal implantation and offered the possibility of creating advanced biocomposites for clinical applications [701]. Thus, the biocompatibility of chitosan in osteoblast cultures was significantly improved by the addition of nanosized HA [702]. Similar findings apply to nanosized HA/PA biocomposites [620]. Additional information about nanoscale biocomposites can be found in the outstanding reviews [22,703]. More specifically, there is also a review of the application of nanosized biomaterials in orthopedic surgery [704] and a review of composites and hybrid formulations containing functional $CaPO_4$ in nanomedicine [705]. More information on this topic can be found in other reviews [218,706–709].

To conclude, currently (May 2024), according to Scopus, there are 3110 articles with a combination of "composite", "apatite", and "nano" in the title, and 422 articles with "composite", "calcium phosphate", and "nano" in the title.

5.4. Collagen-Containing Biocomposites

A characteristic feature of bone is the nanoscale spatial orientation of bioapatite crystals and collagen macromolecules [18,19]; the crystals (about 50 nm long) are aligned parallel to collagen fibers (Figure 5a) [710] and are thought to be the source of bone's mechanical strength. Collagen refers to a family of fibrillary proteins with a triple-helix structure of polyproline-II type. There are many types of collagens that differ in their ratios of helical to nonhelical domains, but all of them share a characteristic triple α-helix supramolecular structure that results from repeating glycine-X-Y sequences, where X and Y are typically proline and hydroxyproline, interspersed with alanine residues. Significantly, collagen type I represents 90% of the collagen present in the human body, mainly in skin, bones, tendons, and organs [711].

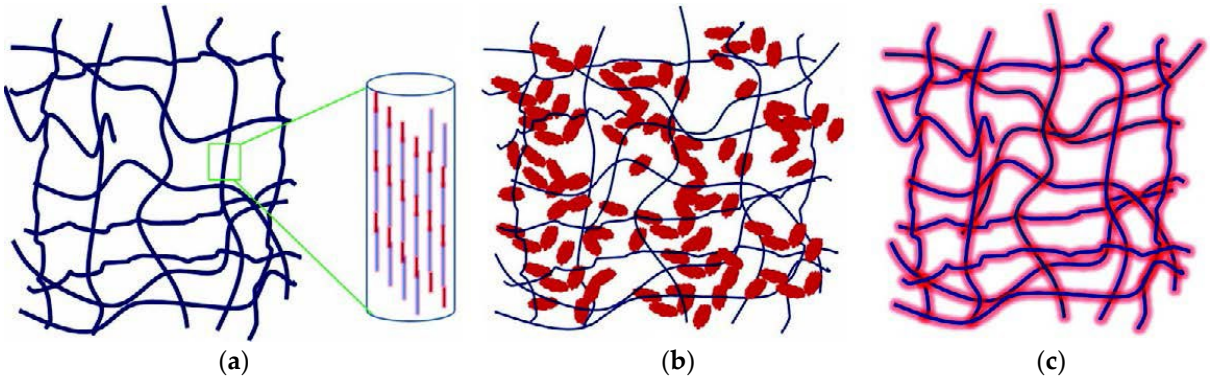

Figure 5. Diagrams showing the collagen/$CaPO_4$ nanocomposites. The structure of bone is composed of (**a**) nanodimensional crystals of biological apatite aligned with collagen fibrils; linking happens between polar groups on collagen chains in bone and apatite; (**b**) nanodimensional $CaPO_4$ crystals physically "trapped" within the collagen matrix; and (**c**) nanodimensional $CaPO_4$ crystals deposited on and covering the surface of the collagen fibrils. Reprinted with permission from Ref. [710].

The mineralized fibers, composed of collagen molecules and biological apatite crystals, are approximately 300 nm long and 6 nm in diameter. The strengthening impact of nanosized bioapatite crystals in calcified tissues can be described by load transfer to inherently rigid inorganic crystals, because the collagen matrix functions as a load transfer medium, even though all of the mechanisms behind the osteogenic approach are yet unknown [14,15,19–21]. Furthermore, the bioapatite crystals present between the entangled fibers cross-link the fibers through mechanical interlocking or by forming bridges of calcium ions and increase the deformation resistance of the collagen fiber network [712].

Since biological apatite and collagen are the major constituents of calcified tissues of mammals, many attempts have been made to combine these two substances in biocomposites in attempts to mimic both the structure and composition of bones. The authors of a recent publication created a plot, showing that, in each passing year since 1990, the

number of published works has increased exponentially (Figure 6) [713]. As seen from this figure, HA/collagen biocomposites are widely explored in the literature. Their physical forms include fibrous matrices, powders, dense materials, films, and gels. The details and references to preparation techniques of all these forms are well described in a recent review [713].

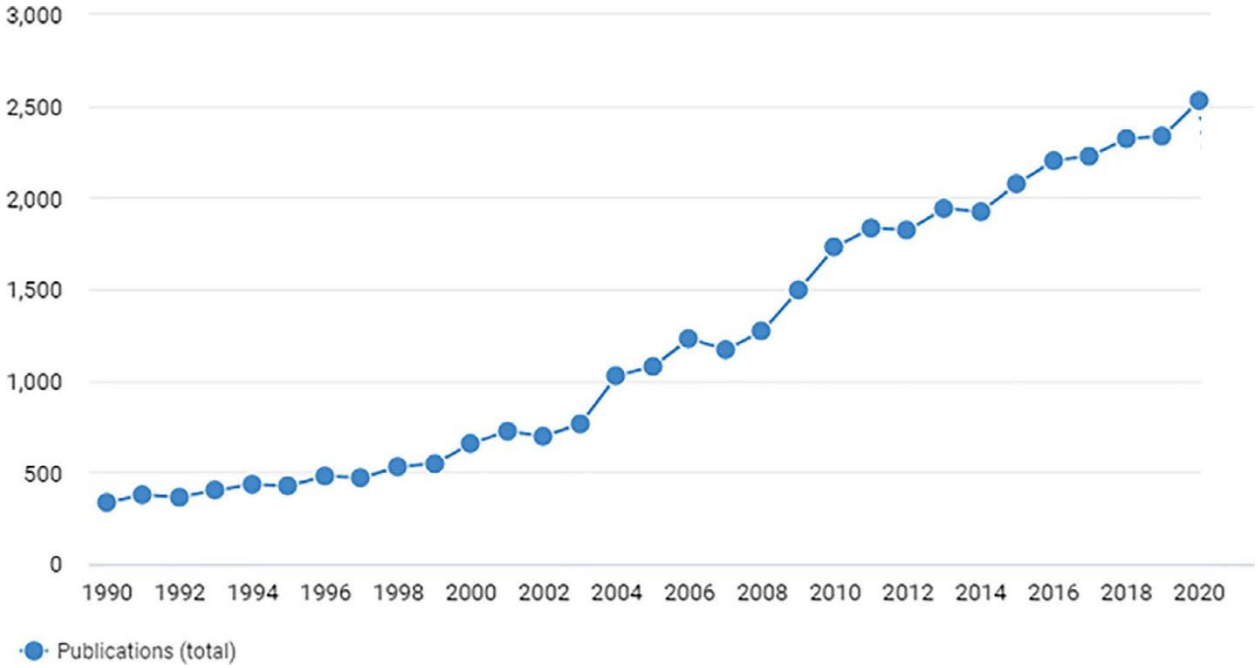

Figure 6. The amounts of publications issued each year with the following keywords: hydroxyapatite and collagen. Reprinted from Ref. [713] with permission.

When combining $CaPO_4$ and collagen in the laboratory, the goal should be to create a material that closely resembles the chemical composition, microstructure, and porosity of bone, but, unfortunately, the prepared biocomposites are very different from bone (Figure 5). The introduction of an organic matrix initially, followed by the development of an inorganic reinforcement phase inside this organic matrix, is the primary characteristic of the process by which mineralized hard tissue is created in vivo [14,15,20,21]. Thus, the best technique to simulate bone is to simulate its formation. This means nucleating and growing nanosized CDHA crystals on and within collagen fibers from supersaturated solutions. Such a synthesis is called 'biologically inspired' [714–716], meaning it produces an order and environment very close to those of nature. There is a long history of using collagen and $CaPO_4$ (mostly apatite) in biologically inspired biocomposites for bone replacement [717–729], starting with the pioneering work of Banks et al. growing CDHA on reconstituted calf collagen bands in 1977 [730], followed by the first medical applications by other researchers in 1982 [731,732]. Such combinations appeared to be bioactive, osteoconductive, and osteoinductive [602,733–735] and, in general, artificial grafts produced from such biocomposites behaved similarly to bone and were found to be more useful in surgery than those prepared from other materials. Certainly, the data showed that $CaPO_4$/collagen biocomposite scaffolds were superior to artificial polymer scaffolds and $CaPO_4$ bioceramic scaffolds separately [736]. In addition, multi-scale simulations of apatite/collagen composites were performed [737].

$CaPO_4$ has been found to successfully precipitate on collagen substrates regardless of their shape or source [594,730,738,739]. Sometimes precipitation can be performed under the presence of external forces, such as an electric field [740]. However, the binding of $CaPO_4$ crystals to collagen depends on the degree to which collagen is denatured; the more fibrillar the collagen, the greater the binding. The first report on biocomposites produced by

precipitating DCPD on collagen matrices with the help of phosphorylated amino acids was published in 1993 [717]. Moreover, CDHA crystals were shown to nucleate on the collagen fiber network when self-hardening CDHA-forming preparations (DCPD + TTCP) were combined with a collagen solution, hydrated, and hardened. This resulted in a material with worse mechanical properties than those documented for bone. Unfortunately, the prepared biocomposites did not have a bone-like nanostructure [718,741]. Using an experimental setup where Ca^{2+} and PO_4^{3-} ions diffused into collagen disks from opposite orientations, the directed development of OCP crystals on collagen was obtained [742,743]. However, those tests did not examine the mechanical properties of the biocomposites; rather, they were merely intended to mimic the in vivo apatite precipitation mechanism [744].

Traditionally, collagen/$CaPO_4$ biocomposites have been produced by blending or mixing $CaPO_4$ with collagen by means of various techniques, as well as by biomimetic precipitation [594,602,604,692,714–718,727,738,742–754]. For example, apatite/collagen bone-like biocomposites were prepared by two different methodologies: (1) dispersion of apatite in collagen aqueous suspension followed by lyophilization and (2) direct nucleation of the apatite phase on collagen fiber aggregates [716]. The biocomposites obtained by the first method resembled uncalcified natural collagen. It is evident from Figure 5b that there was no genuine contact between the apatite and collagen fibers since the crystallite size was not uniform, frequently aggregated, and dispersed randomly in the matrix. The second method allowed nanosized apatite crystals to nucleate directly on the self-assembling collagen fibers. In the latter case, CDHA and collagen showed a strong interaction (Figure 5c), which was highlighted by various analytical techniques showing that the biocomposites completely resembled the calcified natural tissue [716]. Other fabrication techniques are known as well. For example, collagen/apatite biocomposites mimicking the nanostructure of bone have been prepared using a polymer-guided liquid precursor process, in which nanosized apatite crystals are embedded into collagen fibers [750]. Much better results were obtained by other researchers, who produced multilevel hierarchical HA/collagen biocomposite scaffolds with a biomimetic bone Haversian microstructure by a combination of electrospinning, biomimetic mineralization, and rolling techniques for a bottom-up synthesis from nano-level to micro-level and then to macro-level. MicroCT scanning and scanning electron microscopy confirmed the successful preparation of the HA/collagen scaffolds composed of fully assembled microscopic fibers, while the mechanical properties of the scaffolds were double-reinforced by many newborn HA nanoparticles and chemical bonds [753]. Freeze-drying can be used as well [754]. More complex biocomposites, such as magnetite-enriched HA/collagen [755], HA/osteocalcin/collagen [487], HA/collagen/PLA [603–607], HA/collagen/alginic acid [609,610], HA/collagen/PVA [608,756], HA/collagen/chitosan [757], HA/collagen/acidic gelatin/basic fibroblast growth factor (b-FGF) [758], and calcium silicate/β-TCP/collagen [759], have also been developed. Recent research has shown that $CaPO_4$/collagen formulations have the potential to be printed by 3D printers [760].

Collagen can also be added to different self-hardening $CaPO_4$ formulations [718,741,761–765]. In order to facilitate mineral deposition, type I collagen sponges are usually soaked in a highly basic water solution containing PO_4^{3-} ions and then submerged in a solution containing Ca^{2+} ions. An alternative method involves dissolving collagen I fibers in acetic acid and mixing it with phosphoric acid. Next, neutralizing synthesis is carried out at 25 °C, with a pH of 9–10 solution, between an aqueous suspension of $Ca(OH)_2$ and H_3PO_4/collagen solution [714,715]. The Ca/P ratio in the reaction solution needs to be regulated in order to guarantee the quality of the finished product. Dissolving commercially available $CaPO_4$ in the acid is one method for doing this; another one is to add the proper ratio of Ca^{2+} and PO_4^{3-} ions to the solution and then initiate a reaction [766]. Biomimetically, CDHA crystals can be oriented and grown on dissolved collagen fibers in aqueous solution by a self-assembly mechanism [748]. Furthermore, crystallization of CDHA from aqueous solution can occur in the presence of pre-dispersed collagen [594]. More precisely, dispersing collagen in an acidic solution and then adding Ca^{2+} and PO_4^{3-} ions can cause the co-precipitation of collagen and CDHA, followed by either the pH

of the solution increasing or the addition of a mixing agent. In addition, to prepare biocomposites, apatite/collagen blends were kept pressed at 40 °C and 200 MPa for several days, but biocomposites with low mechanical properties were produced [767]. Attempts have also been made to computer simulate the formation process of apatite/collagen composites [768]. It is interesting to note that apatite/collagen biocomposites appear to have some piezoelectric properties [769].

The majority of collagen/HA biocomposites are typically made by fusing HA particles, which are much smaller than microns, into the collagen matrix. This process makes it extremely challenging to create homogeneous and consistent composite grafts. Furthermore, such biocomposites have insufficient mechanical properties and, on top of that, adequate pore size cannot be achieved. In addition, unlike nanocrystalline bone apatite, microcrystalline HA may take a long time to transform into new bone tissue after implantation. Additionally, some biocomposites showed very low mechanical properties, probably due to the lack of strong interfacial bonds between the components. More to the point, in all the blend composites, the crystal size of $CaPO_4$ was not uniform and the crystals were frequently aggregated and dispersed randomly inside the collagen's fibrous matrix. Therefore, only compositional similarity rather than structural similarity to genuine bone was attained. The data clearly show that bone-like chemical composition is insufficient to produce suitable grafts and that both mechanical properties and bone nanostructure need to be mimicked to function as bone at the recipient site. A grain size reduction of HA crystals to an ultrafine apatite matrix can improve its growth and osteointegration. This may improve mechanical properties, enhance biological and biochemical affinity with host bone, and facilitate osteointegration. Furthermore, it has been discovered that porosity enhances the ability of surrounding tissues to enter the pores of collagen/HA biocomposites [770,771].

Biocomposites made from bovine collagen mixed with $CaPO_4$ are commercially available as an alternative to bone grafts. Moreover, they might be mixed with bone marrow extracted from the iliac crest of the fracture site. Bioimplant®, Bio-Oss Collagen®, Boneject®, Collagraft®, CollapAn®, Healos®, Integra Mozaik®, and LitAr® are some examples of commercially available $CaPO_4$/collagen grafts that can be used in clinical practice (Table 4). When treating acute fractures of long bones with defects stabilized by internal or external fixation, such materials have been compared with autografts [772,773]. The biocomposites were discovered to be osteogenic, osteoinductive, and osteoconductive; nevertheless, they are not structurally strong and necessitate the extraction of bone marrow from the patient. OCP/collagen biocomposites have undergone investigation [774] and clinical testing [775], as well.

Table 4. A list of known commercially produced $CaPO_4$-containing biocomposites and hybrid biomaterials.

Calcium Orthophosphate	Trade Name and Producer (When Available)
HA embedded or suspended in a gel	Bio-Gel HT hydroxyapatite (Bio-Rad, Hercules, CA, USA)
	Coaptite (Boston Scientific, Marlborough, MA, USA)
	Facetem (Daewoong, Seoul, Republic of Korea)
	NanoBone (Artoss, Rostock, Germany)
	Nanogel (Teknimed, L'Union, France)
	Radiesse (Merz Aesthetics, Frankfurt, Germany)
	Renú Calcium Hydroxylapatite Implant (Cytophil, East Troy, WI, USA)

Table 4. *Cont.*

Calcium Orthophosphate	Trade Name and Producer (When Available)
HA/collagen, CDHA/collagen and/or carbonate apatite/collagen	AUGMATRIX (Wright Medical Technology, Memphis, TN, USA)
	Bioimplant (Connectbiopharm, Vienna, Austria)
	Bio-Oss Collagen (Geitslich, Wolhusen, Switzerland)
	Boneject (Koken, Tokyo, Japan)
	COL.HAP-91 (JHS Biomateriais, Sabará, Brazil)
	Collagraft (Zimmer and Collagen Corporation, Miami, FL, USA)
	CollaOss (SK Bioland, Cheonan, Korea)
	CollapAn (Intermedapatite, Moscow, Russia)
	COLLAPAT (Symatese, Vourles, France)
	DualPor collagen (OssGen, Seoul, Republic of Korea)
	G-Graft (Surgiwear, Uttar Pradesh, India)
	HAPCOL (Polystom, Moscow, Russia)
	Healos (DePuy Spine, Raynham, MA, USA)
	LitAr (LitAr, Moscow, Russia)
	nanOss Bioactive (Pioneer Surgical Technology, Marquette, MI, USA)
	Ossbone Collagen (SK Bioland, Cheonan, Korea)
	OssFill (Sewon Cellontech, Seoul, Republic of Korea)
	OssiMend (Collagen Matrix, Oakland, NJ, USA)
	OSSIX Bone (Dentsply Sirona, Charlotte, NC, USA)
	Osteomatrix (Connectbiopharm, Russia)
	OsteoTape (Impladent, Queens, NY, USA)
	ReFit (HOYA Technosurgical, Tochigi, Japan)
	RegenOss (JRI Orthopaedics, Sheffield, UK)
	RegenerOss Synthetic (Zimmer Dental, Carlsbad, CA, USA)
	SmartBone (IBI, Mezzovico, Switzerland)
	Straumann XenoFlex (Straumann, Basel, Switzerland)
	SwissBone (IBI, Mezzovico, Switzerland)
HA/sodium alginate	Bialgin (Biomed, Moscow, Russia)
rhBMP-2 + HA carrier	NOVOSIS (CGBIO, Seoul, Republic of Korea)
HA/poly-L-lactic acid	Biosteon (Biocomposites, Keele, UK)
	Fisiograft HA pasta (Ghimas, Casalecchio di Reno, Italy)
	ReOss (ReOss, Filderstadt, Germany)
	OSTEOTRANS MX (Teijin Medical Technologies, Osaka, Japan)
	SuperFIXSORB30 (Takiron, Osaka, Japan)
HA/hyaluronic acid	HArmonyCa (Allergan Aesthetics, an AbbVie Company, Dublin, UK)
HA/polyethylene	HAPEX (Gyrus, Memphis, TN, USA)
HA/glucan polysaccharide	FlexiOss (Medical Inventi, Lublin, Poland)
HA/$CaSO_4$	BioWrist Bone Void Filler (Skeletal Kinetics, Cupertino, CA, USA)
	Bond Apatite (Augma Biomaterials, Spotswood, NJ, USA)
	Hapset (LifeCore, Chaska, MN, USA)
	PerOssal (aap Implantate, Berlin, Germany)

Table 4. *Cont.*

Calcium Orthophosphate	Trade Name and Producer (When Available)
HA/$CaSO_4$ powders suspended in a liquid	CERAMENT (BONESUPPORT, Lund, Sweden)
HA/glass	Bonelike (unknwn producer)
bovine bone (unsintered)	Unilab Surgibone (Unilab, Hillside, NJ, USA)
bovine bone (unsintered) + polymer	Alpha-Bio's Graft (Alpha-Bio Tec, Petah Tikva, Israel)
	C-Graft Putty (unknwn producer)
human bone allograft	ALLOPURE (Wright Medical Technology, Memphis, TN, USA)
	AlloOss (ACE Surgical Supply, Brockton, MA, USA)
	Allosorb (Curasan, Frankfurt, Germany)
	CancellOss (Impladent, Queens, NY, USA)
	CurOss (Impladent, Queens, NY, USA)
	J Bone Block (Impladent, Queens, NY, USA)
	Maxgraft (botiss, Berlin, Germany)
	Mega-Oss (Megagen Implant, Daegu, Korea)
	NonDemin (Impladent, Queens, NY, USA)
	Osnatal (aap Implantate, Berlin, Germany)
	OsteoDemin (Impladent, Queens, NY, USA)
	Osteopure (O.S.T Laboratories, Saint-Beauzire, France)
	OsteoWrap (Curasan, Frankfurt, Germany)
	OVIS ALLO (DENTIS, Seoul, Republic of Korea)
	PentOS OI (Citagenix, Laval, QC, Canada)
	Puros (Zimmer Biomet, Stamford, CT, USA)
	RAPTOS (Citagenix, Laval, QC, Canada)
	Straumann AlloGraft (Straumann, Basel, Switzerland)
	TenFUSE (Wright Medical Technology, Memphis, TN, USA)
β-TCP/$CaSO_4$	Fortoss vital (Biocomposites, Keele, UK)
	Genex (Biocomposites, Keele, UK)
β-TCP/poly-lactic acid	Bilok (Biocomposites, Keele, UK)
	Duosorb (SBM, Lourdes, France)
	Matryx Interference Screws (Conmed, Largo, FL, USA)
β-TCP/poly-lactic-*co*-glycolic acid	Evolvemer TCP30PLGA (Arctic Biomaterials, Tampere, Finland)
β-TCP/polymer	AttraX putty (NuVasive, San Diego, CA, USA)
	ExcelOs-inject (CGBIO, Seoul, Republic of Korea)
	Therigraft (Therics, Akron, OH, USA)
β-TCP/bone marrow aspirate	Induce (Skeletal Kinetics, Cupertino, CA, USA)
β-TCP/collagen	Integra Mozaik (Integra Orthobiologics, Carlsbad, CA, USA)
β-TCP/growth-factor	GEM 21S (Lynch Biologics, Franklin, TN, USA)
β-TCP/rhPDGF-BB solution	AUGMENT Bone Graft (Wright Medical Group, Memphis, TN, USA)

Table 4. *Cont.*

Calcium Orthophosphate	Trade Name and Producer (When Available)
BCP (HA + β-TCP)/collagen	Allograft (Zimmer, Warsaw, IN, USA)
	BestAid (Maxigen Biotech, Taipei, Taiwan)
	collacone max (botiss, Berlin, Germany)
	Collagraft (Zimmer, Warsaw, IN, USA)
	Cross.Bone Matrix (Biotech Dental, Salon-de-Provence, France)
	FormaGraft (Maxigen Biotech, Taipei, Taiwan)
	Indost (Polystom, Moscow, Russia)
	MasterGraft (Medtronic Sofamor Danek, Memphis, TN, USA)
	MATRI BONE (Biom'Up, Saint-Pries, France)
	Osteon III collagen (GENOSS, Suwon, Korea)
	SynergOss (Nobil Bio Ricerche, Portacomaro, Italy)
	without trade name (MedicalGroup, Lyon, France)
BCP (HA + β-TCP)/hydrogel	4MATRIX+ (MIS Implants, Misgav, Israel)
	Eclipse (Citagenix, QC, Laval, Canada)
BCP (HA + β-TCP)/polymer	In'Oss (Biomatlante, Vigneux-de-Bretagne, France)
	Hydros (Biomatlante, Vigneux-de-Bretagne, France)
	Octane HyperPEEK (Octane, Toronto, ON, Canada)
	Osteocaf (Texas Innovative Medical Devices, Fort Worth, TX, USA)
	Osteotwin (Biomatlante, Vigneux-de-Bretagne, France)
BCP (HA + β-TCP)/chitosan	k-IBS (Bioceramed, Lisboa, Portugal)
BCP (HA + β-TCP)/fibrin	TricOS (Baxter BioScience, Maurepas, France)
BCP (HA + β-TCP)/silicon	FlexHA (Xomed, Jacksonville, FL, USA)
BCP (HA + β-TCP)/bioglass	SIGNAFUSE (Bioventus, Durham, NC, USA)
bioglass + α-TCP + β-TCP + HA + polymers	OsteoFlo NanoPutty (SurGenTec, FL, USA)
FA + BCP (HA + β-TCP)	FtAP (Polystom, Moscow, Russia)
DCPA + $MgHPO_4 \cdot 3H_2O$ + SiO_2 + carboxymethyl cellulose	Novogro (OsteoNovus, Toledo, OH, USA)
DCPD/collagen	CopiOs Bone Void Filler (Zimmer, Warsaw, IN, USA)
DCPD + β-TCP/$CaSO_4$	PRO-DENSE (Wright Medical Group, Memphis, TN, USA)
DCPD + β-TCP/$CaSO_4$ + collagen	PRO-STIM (Wright Medical Group, Memphis, TN, USA)
OCP/fibrin	FibroFor (BioNova, Moscow, Russia)
OCP/collagen	Bonarc (Toyobo, Tokyo, Japan)
undisclosed $CaPO_4$ + biologics	i-FACTOR (Cerapedics, Broomfield, CO, USA)
3D-printed Ti mesh embedded in MCPM + β-TCP + Ca pyrophosphate	OssDsign (OssDsign AB, Uppsala, Sweden)

Lyophilization was used to create open-pore (30–100 μm) collagen sponges, which were then coated with a 10 μm layer of biomimetic apatite that was precipitated from artificial bodily fluids [776]. When using fibroblast culture in vitro, researchers discovered good results. There are several possible preparation methods [777]. Injectable bone fillers have been created using collagen/HA microspheres and gel beads [778–780], while a bone structure was mimicked by blending carbonated apatite and collagen [781,782]. When a similar material (mineralized collagen) was implanted into rat femurs, excellent clinical

results were observed after 12 weeks [783]. Collagen/HA biocomposites were prepared and mechanical performance was improved by crosslinking collagen fibers with glutaraldehyde [595–597]. Those biocomposites were tested in rabbits and showed good biological performance, osteoconductivity, and biodegradability. In a similar approach, HA/collagen microspheres (diameter ~5 μm) were prepared by water-in-oil emulsification and their surfaces were crosslinked with glutaraldehyde [779]. The material performed well in vitro with osteoblast culture. Porous bone graft substitutes were created by lyophilization of nanosized HA/collagen biocomposites and PLA. It was discovered that the resultant material resembled real bone at various hierarchical levels [604]. Further in vitro tests verified that osteoblasts adhered, proliferated, and migrated to this composite with acceptable quality [603]. Dopants can be added to increase biocompatibility even further. For example, Si-substituted HA/collagen biocomposites with silicon preferentially incorporated into the collagen phase have been developed to enhance bone replacement [596]. Porous (porosity ~95%, 50–100 μm interconnected pores) biocomposites of collagen (cross-linked with glutaraldehyde) and β-TCP were prepared by freeze-drying techniques followed by the sublimation of solvents. The biocomposite showed good biocompatibility when implanted in the rabbit jaw [783].

Since biocomposites of $CaPO_4$ with collagen were found to be able to form bioconjugates (bioconjugation is a chemical strategy to form a stable covalent link between two molecules, at least one of which is a biomolecule [784]), they are beneficial for the delivery of drugs, growth factors, and other biomolecules [610,720,765,785–787]. Namely, 5 weeks after implantation, HA/collagen-alginate (20 μL) supplemented with rhBMP-2 (100 μg/mL, 15 μL) demonstrated osteogenesis along the implant without the material deforming much [610]. The results of another study showed that HA/collagen biocomposites coupled with rhBMP-2 could significantly improve the formation of new bone and angiogenesis within the scaffolds as well as the proliferation and differentiation of osteoblasts [784]. Furthermore, a bilayer collagen/β-TCP implant supplemented with cartilage-inducing growth factors was developed for the repair of osteochondral defects in the trochlear groove in miniature pigs [785]. More details on this topic can be found in a recent review [786].

Although biocomposites of apatites with collagen appear to be a very hot topic of research (Figure 6 and Table 4), not many papers are devoted to biocomposites of other $CaPO_4$ with collagen [745–747,774,775,785,788–792]. Among them, there are ones with a very complicated composition. For example, a collagen hydrogel incorporating platelet-derived growth factor-loaded photopolymerizable zinc-based zeolitic-imidazolate-frameworks-polydopamine nanoparticles (PDGF@ZIF-8-PDA@COL hydrogel) was prepared and then perfused into PLGA-TCP scaffolds. The resulting PDGF@ZIF-8-PDA@COL/PLGA-TCP biocomposite scaffolds sustainably released PDGF and showed an excellent antibacterial activity against both the Gram-negative bacterium *E. coli* and the Gram-positive bacterium *S. aureus*. Further, the scaffolds exhibited excellent osteoinductive and osteoconductive capacity in vitro and accelerated bone formation in vivo in a rat model of a cranial defect [792].

In conclusion, currently known $CaPO_4$ and collagen biocomposites mimic natural bone to some extent and subsequent biological evaluations show that they do not act as permanent implants but are readily involved in bone metabolism in the form of bone remodeling [604,732]. However, the performance of such biocomposites depends on the source of the processed collagen. In an effort to enhance the mechanical characteristics of these biocomposites, numerous attempts have been made to mimic the collagen-HA interfacial behavior in actual bone using crosslinking agents such glutaraldehyde [595,597,598,738,779,783]. Unfortunately, the progress in this direction has been limited by high costs, difficulties in controlling cross-infection, poorly defined commercial sources of collagen, and a lack of suitable techniques to produce bone-like microstructures. However, since collagen is a protein that makes up the bulk of the organic bone matrix,

the synthesis of $CaPO_4$/collagen biocomposites has been extensively studied for decades. Additional information on this hot topic can be found in the literature [602,710,713,723,793].

Finally, currently (May 2024), according to Scopus, there are 1360 articles with a combination of "collagen" and "apatite" in the title and 438 articles with "collagen" and "calcium phosphate".

5.5. Biocomposites with Other Bio-Organic Compounds

Because the commercial sources of collagen type I are not clearly defined, the two main practical issues with this material are its expense and the challenge of adhering to a well-controlled processing method. Therefore, different substances can be used in place of collagen type I. It should be highlighted that, in addition to collagen, the bodies of humans and other mammals contain a wide variety of bio-organic substances, proteins, and biological macromolecules, all of which have substantial quantities that may be used to create biocomposites with $CaPO_4$ [709]. That is why this topic appears to be broad. For example, the biologically strong adhesion between teeth and the surrounding epithelial tissue (preventing bacterial invasion) is associated with the cell adhesion protein laminin [794]. To mimic this property, a biomimetic approach has been used to create laminin/apatite biocomposite layers on both titanium [795] and EVOH [796,797] surfaces. It was discovered that the more intricate laminin/DNA/apatite biocomposite layer was a successful gene delivery mechanism [798]. More details on this topic can be found in the special review [799].

Let me begin with gelatin (this is a water-soluble protein with a molecular weight from 20 to 100 kDa derived from hydrolysis of collagen type I), which is extensively used in the food industry. $CaPO_4$/gelatin biocomposites have been widely investigated as potential bone replacement biomaterials [196,409–415,432,483–485,611–615,800–803]. For example, gelatin foams have been successfully mechanically reinforced with HA and then crosslinked with carbodiimide derivatives [196]. Such foams have been shown to be good carriers for the antibiotic tetracycline [801]. In addition, electrospun gelatin methacryloyl fibrous scaffold incorporating β-TCP was developed for vital pulp therapy [804].

Since the organic–mineral interface in bones is predominantly polysaccharides [805], various biocomposites of $CaPO_4$ and polysaccharides, such as alginates [413,609,610,612,715,806–809], as well as chitosan [426,450,468,490,519,556,631–644,678,696,702,810–821] and chitin [416,489,822–826], are also very popular. For example, hydrogel-based porous HA/alginate composites have been prepared biomimetrically [715] and by lyophilization [806]. Furthermore, solution-based methods have been developed to combine chitin with HA powder homogeneously dispersed with ceramic particles [822,823]. Unfortunately, it has been difficult to achieve a homogeneous dispersion. The mechanical properties of the final biocomposites were not very good. Both tensile strength and modulus were shown to decrease with increased HA levels, likely due to poor adhesion between the filler and matrix. Microscopy showed that HA particles penetrated between the polymer chains, weakening the interaction and reducing the overall strength [822,823]. Other fabrication techniques can be found in the references, but an interesting approach is the production of HA/chitosan biocomposites from the natural $CaCO_3$/chitosan of crab shells by a hydrothermal process [812]. Similarly, pre-produced DCPD/chitosan biocomposites were converted into HA/chitosan biocomposites by hydrothermal procedures [813]. It was discovered that natural HA and chitosan biocomposites have outstanding osteoconductivity and good hard tissue biocompatibility, which qualifies them as framework materials for tissue engineering and artificial bone implants [811]. Research indicates that, when $CaPO_4$ is added to chitosan instead of chitosan alone, the result is enhanced cell adhesion, high cell proliferation, and well-diffused morphology [633,814]. More complex biocomposites, such as HA/chitosan reinforced with silk fibers [827], HA/collagen/chitosan [828], CDHA/chitosan filled with ciprofloxacin [818], chitosan/silk fibroin/nitrogen-doped carbon quantum dots/α-TCP [829], and others [830–833], have also been investigated. Besides biomedical applications, nanosized HA and chitin/chitosan biocomposites can be used

for the removal of Fe(III) [834] and fluoride [835,836] ions from aqueous solutions. Further details on this topic are available in recent reviews [837,838].

Biocomposites with soluble proteins, such as CDHA/BSA, can be prepared by precipitation methods [549,839–842]. In such biocomposites, BSA does not bind strongly to solid CDHA, which is beneficial for sustained release. However, this is not the case when using the water/oil/water interfacial reaction route [190]. More recently, DNA has been incorporated into CDHA/BSA biocomposites [190,843–845]. In addition, unspecified $CaPO_4$/DNA [846,847] and biomimetic apatite/C_{60} fullerene/Au-DNA nanosized particles [848] biocomposites have been prepared.

Additionally, $CaPO_4$-based biocomposites were produced by immersing hydrogels into supersaturated solutions of Ca^{2+} and PO_4^{3-} ions to precipitate CDHA (up to 70 wt% CDHA can be incorporated) [849]. Chitosan underwent a similar process, with the form of the initial chitosan hydrogel determining the 3D shape of the final biocomposites [850]. A different research team created biocomposites using self-assembled supramolecular hydrogels that underwent in situ $CaPO_4$ mineralization [851]. In addition, there are further experimental strategies that could be used [852,853].

There are numerous CDHA biocomposites that have been made utilizing glutamic and aspartic acids, as well as polyglutamic and polyaspartic acids [296,297,854–857]. By quantitatively incorporating these (poly)amino acids into CDHA crystals, both the coherent length of the crystal domains and the crystal dimensions were reduced. The relative amount of (poly)amino acid content in the solid phase increased with concentration in solution, reaching the maximum value of approximately 7.8 wt% for CDHA/aspartic acid and 4.3 wt% for CDHA/glutamic acid biocomposites, respectively. Small crystal sizes and large surface area due to the presence of (poly)amino acids revealed the potential of these biocomposites for hard tissue replacement [296,297,854–857]. A schematic diagram of biocomposite formation from ACP and amino acids is shown in Figure 7 [858].

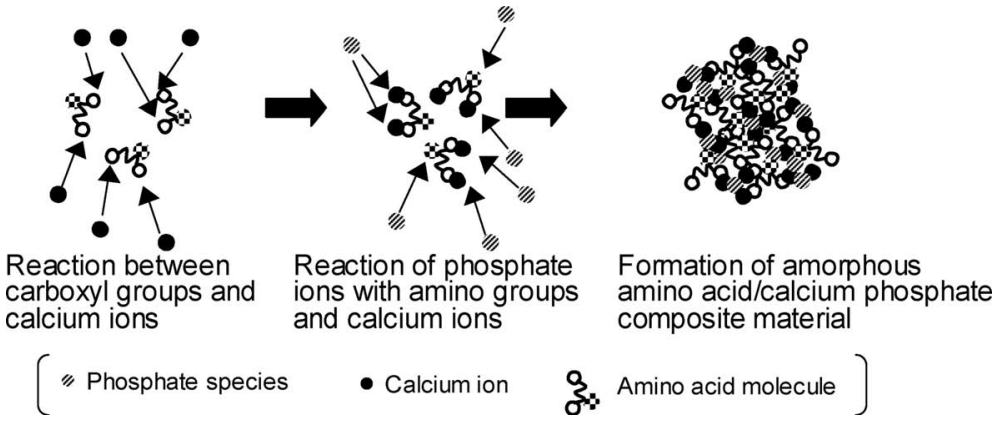

Figure 7. An explanation of how ACP/amino acid biocomposites are formed in aqueous solutions is suggested. Reprinted with permission from Ref. [858].

Macroporous scaffolds of BCP (HA + β-TCP)/agarose with controlled complete interconnections, high porosity, fully open pores, and tailored pore size have been prepared for tissue engineering applications [859,860]. The biodegradable polymer agarose was chosen as the organic matrix as it is a biocompatible hydrogel and acts as a gelling agent, resulting in a strong gel and rapid room-temperature polymerization. A combination of cryoforming, stereolithography, and two different drying techniques produced porous scaffolds with an engineered structure. The biocompatibility of that BCP/agarose system was tested using mouse L929 fibroblasts and human SAOS-2 osteoblasts at different colony formation times [861].

Fibrin sealant is a non-cytotoxic, fully absorbable biomatrix that forms fibrin clots structured like physiological thrombi, mimicking the final stage of the natural coagulation cascade [862]. Clinical use of bone substitutes may be advanced by $CaPO_4$ biocompos-

ites with fibrin sealant. The macro- and microporous structures of $CaPO_4$ ceramics are interwoven with a 3D network of fibrin sealant; as a result, the physical, chemical, and biological characteristics of $CaPO_4$ bioceramics and fibrin sealant were combined to create a biocomposite that may be used to prepare advanced bone grafts [491,863–865].

There are also biocomposites composed of $CaPO_4$ and bisphosphonates [866], silk fibroin [188,679,680,867–872], cellulose [873,874], chitosan + silk fibroin [875], chitosan + zein [876], chitosan derivatives [877], fibronectin [878], triazintrione [879], chondroitin sulfate [734,880], casein phosphopeptide [881], okra hydrocolloid [882], keratin [883], gellan gum [884] and graphene oxide/chitosan [885] hydrogels, amyloid fibrils [886], agarose [887], glycine [888], and vitamins [889]. More complicated formulations, such as sodium alginate/N,O-carboxymethyl chitosan/aldehyde hyaluronic acid/BCP, in which the amount of BCP was varied from 40% to 60% of the hydrogel mass to mimic the composition of the native bone tissues [890], are also known. Photopolymerizable formulations have also been developed [891,892]. Namely, experimental composite resins composed of 75 wt% bisphenol a-glycidyl methacrylate and 25 wt% triethylene glycol dimethacrylate were produced. Some 1 mol% trimethyl benzoyl-diphenylphosphine oxide was used as a photoinitiator and butylated hydroxytoluene was added as a polymerization inhibitor. Silica (1.5 wt%) and barium glass (65 wt%) particles were added as inorganic fillers. For remineralizing and antibacterial effects, α-TCP (10 wt%) and myristyltrimethylammonium bromide (5 wt%) were added, respectively. The authors concluded that the addition of α-TCP and myristyltrimethylammonium bromide promoted remineralizing and antibacterial properties of the resins [892].

The reader is also introduced to an intriguing method of crystallizing CDHA in poly(arylamine)/poly(styrenesulfonic acid) polymer capsules to produce empty biocomposite spheres that are micron in size. The thickness of the shell of the biocomposite spheres can range from 25 to 150 nm, contingent upon the quantity of CDHA that precipitates. Biocomposite capsules can be used as catalyst microreactors for bone mending or as medicinal agents [893].

An interesting phenomenon of fractal growth of FA/gelatin composite crystals (Figure 8) was obtained when two solutions containing Ca^{2+} and $PO_4^{3-} + F^-$ ions were diffused from the opposite sides into a tube filled with gelatin gel [894–898]. The reasons for this phenomenon are not yet fully understood. Other types of $CaPO_4$-based composites based on DCPD and OCP have been similarly grown in iota carrageenan gels [899]. Nothing has been reported so far about potential biomedical applications of those unusual structural composites.

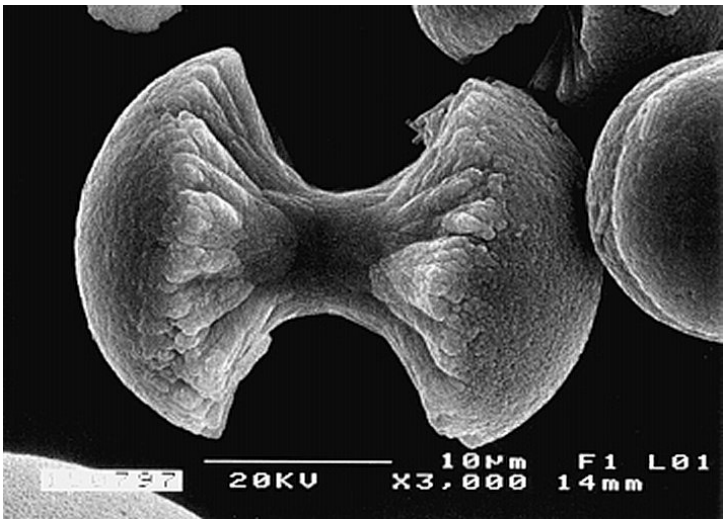

Figure 8. A biomimetically grown aggregate of FA that was crystallized in a gelatin matrix. A fractal development mechanism explains and simulates its shape. Scale bar: 10 µm. Reprinted from Ref. [894] with permission.

5.6. Injectable Bone Substitutes (IBSs)

IBSs are a promising option in bone regenerative medicine due to their ability to optimally fill complex bone defects in a minimally invasive manner. Thus, IBSs are considered a viable alternative to solid bone replacement materials representing a ready-to-use suspension of $CaPO_4$ microspheres [900,901], nanodimensional rods [902], or powders mixed with a viscous polymer solution acting as a liquid carrier phase. However, the addition of other compounds, such as calcium sulfate [903], is also thinkable. In general, IBSs appear as an opaque viscous paste with sufficient rheological properties to be injected into a bone defect using a surgical syringe with a needle. Sometimes, the IBS components may need to be mixed in an operating room and, in that case, it may be possible to produce or combine IBSs with blood, bone marrow, or platelet-rich plasma. Furthermore, IBSs can be easily produced under aseptic conditions. Their mechanical characteristics and consistent composition make them appropriate for biomedical applications [904,905]. All forms of IBSs can be separated into two primary categories: those that self-harden (Section 5.2 above) and those that do not cure. The latter are discussed here.

All types of IBSs require appropriate rheological properties to ensure in situ mineral phase bonding and cohesion combined with good cell permeability. The required viscosity level is usually created by the addition of suitable water-soluble polymers [92,194,614,615,906–916]. However, hydrogel-based IBSs are also known [917–920]. Some of them have the property of self-gelation [920]. Therefore, most of non-hardening $CaPO_4$-based IBS formulations can be considered as a viscous fluid subgroup of the $CaPO_4$/polymer biocomposites. Namely, IBSs containing a silanized hydroxyethylcellulose carrier and BCP (HA + β-TCP) have been described. This suspension is liquid in the pH 10–12 range, but rapidly gels at pH < 9 [907]. β-TCP can also be utilized to create injectable composites that enhance mechanical integrity [536]. Similarly, depending on the situation, polydioxanone-*co*-glycolide-based biocomposites reinforced with HA or β-TCP can be employed as moldable pastes or injectable viscous liquids [908]. The creation of linked pores is made possible by the emission of carbon dioxide during the post-injection crosslinking reaction. Moreover, Pickering emulsification has been used to create HA/poly(L-lactide-*co*-ε-caprolactone) biocomposite microparticles that can be injected without the need for molecular surfactants. Using water-dispersed HA nanosized crystals as particle emulsifiers and poly(L-lactide-*co*-ε-caprolactone) dichloromethane solution as the oil phase, stable injectable oil-in-water emulsions were produced [194]. $CaPO_4$-containing IBSs based on other (bio)organic compounds, such as gelatin [614,615], PVA [909], CMC [911], PAA [916], oligo(poly(ethylene glycol) fumarate) [910], chitosan + collagen [912], and silk fibroin + methylcellulose [913], have also been developed. Furthermore, photo-crosslinkable IBS compositions are also known [914].

Viscous IBS formulations based on BCP (60% HA + 40% β-TCP) suspended in a 2% aqueous solution of HPMC, which appeared to be fully biocompatible, resorbable, and easily adaptable to bone defects (due to initial plasticity), were developed [906,921–925]. It was discovered that the ideal BCP/HPMC aqueous solution ratio was 65/35 w/w. Expanding on this subject, IBSs can be loaded with cells [926,927], radiopaque components [928], microparticles [929] or functionalized with nucleic acids [930]. Self-curing formulations based on Si-HPMC hydrogels are also known [926]. A list of commercially produced $CaPO_4$-containing IBS formulations is given in Table 5 [930].

Table 5. A list of several commercial non-setting $CaPO_4$-based IBS and pastes with indication of producer, product name, composition (when available), and form [930].

Producer	Product Name	Composition	Form
Allergan Aesthetics	HArmonyCa™	HA, hyaluronic acid, 0.3% lidocaine	pre-mixed
ApaTech (Borehamwood, UK)	Actifuse™	HA, polymer and aqueous solution	pre-mixed
	Actifuse™ Shape Actifuse™ ABX	Si-substituted $CaPO_4$ and a polymer	pre-mixed
Baxter (Deerfield, IL, USA)	TricOs T TricOs	BCP (60% HA, 40% β-TCP) granules and Tissucol (fibrin glue)	to be mixed
Berkeley Advanced Biomaterials (Berkeley, CA, USA)	Bi-Ostetic Putty	not disclosed	not disclosed
BioForm (San Diego, CA, USA)	Calcium hydroxylapatite implant	HA powder embedded in a mixture of glycerine, water and CMC	pre-mixed
Biomatlante (Vigneux-de-Bretagne, France)	In'Oss™	BCP granules (60% HA, 40% β-TCP; 0.08–0.2 mm) and 2% HPMC	pre-mixed
	MBCP Gel®	BCP granules (60% HA, 40% β-TCP; 0.08–0.2 mm) and 2% HPMC	pre-mixed
	Hydr'Os	BCP granules (60% HA, 40% β-TCP; micro- and nanosized particles) and saline solution	pre-mixed
Bioceramed (PT)	k-IBS®	BCP granules (75% HA, 25% β-TCP; 0.125–0.355 mm) and chitosan dissolved in PEG	pre-mixed
	n-IBS®	Aqueous suspension of HA powders	pre-mixed
Degradable solutions (Shanghai, China)	Easy graft™	β-TCP or BCP granules (0.45–l.0 mm) coated with 10 µm PLGA, *N*-methyl-2-pyrrolydone	to be mixed
Dentsply (USA)	Pepgen P-15® flow	HA (0.25–0.42 mm), P-15 peptide and aqueous Na hyaluronate solution	to be mixed
DePuy Spine (USA)	Healos® Fx	HA (20–30%) and collagen	to be mixed
Fluidinova (Maia, Portugal)	nanoXIM TCP	β-TCP (5 or 15%) and water	pre-mixed
	nanoXIM HA	HA (5, 15, 30 or 40%) and water	pre-mixed
Integra LifeSciences (Princeton, NJ, USA)	Mozaik Osteoconductive Scaffold	β-TCP (80%) and type 1 collagen (20%)	to be mixed
Mathys Ltd. (Bettlach, Switzerland)	Ceros® Putty/cyclOS® Putty	β-TCP granules (0.125–0.71 mm; 94%) and recombinant Na hyaluronate powder (6%)	to be mixed
Medtronic (USA)	Mastergraft®	BCP (85% HA, 15% β-TCP) and bovine collagen	to be mixed
Merz Aesthetics (GER)	RADIESSE®	HA particles suspended in a gel	pre-mixed
NuVasive (USA)	AttraX® putty	β-TCP and alkylene oxide copolymer	pre-mixed
Osartis/AAP (Münster, Germany)	Ostim®	Nanocrystalline HA (35%) and water (65%)	pre-mixed
Smith & Nephew (Memphis, TN, USA)	JAXTCP	β-TCP granules and an aqueous solution of 1.75% CMC and 10% glycerol	to be mixed
Stryker (Portage, MI, USA)	Calstrux™	β-TCP granules and CMC	to be mixed
Teknimed (FR)	Nanogel	HA (100–200 nm) (30%) and water (70%)	pre-mixed
Therics (USA)	Therigraft™ Putty	β-TCP granules and polymer	pre-mixed
Zimmer (USA)	Collagraft	BCP granules (65% HA, 35% β-TCP; 0.5–1.0 mm), bovine collagen and bone marrow aspirate	to be mixed

IBSs have better qualities because of their easy tissue regeneration, biocompatibility, and good rheological characteristics. The process of creating IBS biocomposites primarily enhances the system's mechanical characteristics and gives the material resistance to fluid penetration; however, the amount of polymer that can be added to the paste limits these outcomes. Namely, depending on the kind and molecular weight of the polymer, there is a reported critical concentration (usually around 10%) above which the polymer begins to form a thick coating on the crystal clusters, preventing their bonding, causing plastic flow, and lowering the mechanical properties [549]. Moreover, a decrease in mechanical properties with increasing gel content was reported, and this was attributed to pore formation due to the dissolution of gelatin in the solution [542]. Therefore, although mechanical properties can be improved by the addition of water-soluble polymers, there still seems to be a limit to the application of $CaPO_4$-based IBS formulations to load-bearing zones [125]. More details on IBSs are available in the literature [567,823,904].

To conclude, currently (May 2024), according to Scopus, there are 232 articles with a combination of "injectable" and "apatite" in the title and 370 articles with "injectable" and "calcium phosphate".

5.7. Biocomposites with Glasses, Inorganic Compounds, Metals, and Carbon

To overcome the problem of low mechanical properties of $CaPO_4$ bioceramics on the one side and induce a positive tissue response of various inorganic materials, glasses, and metals on the other side, suitable biocomposites have also been developed. Such biocomposites can be prepared by common ceramic processing techniques, such as post-mixing heat treatment [931–933], powder slurry coating [934] and metal-sol mixing [935]. For example, HA has been combined with Bioglass® (Novabone Products, Alachua, FL, USA) [936,937] and other glasses [938,939] to form glass–ceramic biocomposites. The same is valid for TCP [940]. Regarding shape, the reinforcing materials for $CaPO_4$ include particles [941,942], platelets [943,944], whiskers [580,664,945–947], and fibers [948–952], regarding their sizes, they can be of nano- (Section 5.3 above), micro-, and macro-dimensions, and certainly they can be of diverse chemical composition. Namely, zirconia and PSZ [931–934,945,953–961], magnesia [962], alumina [941,944,963–966], alumina + magnesia [967], titania [968–971], alumina + titania [972], iron oxides [973–976] (Figure 9), other oxides and mixtures thereof [947,977–982], silica and/or glass [983–994], titania + bioactive glass [995], wollastonite [996–998], mullite [999–1002], natural aluminosilicates [1003,1004], nitrates [1005], various metals and alloys [185,203–205,551,670,671,950,1006–1041], calcium sulfate [1042–1047], calcium carbonate [1048,1049], silicon carbide [663,664,946], barium titanate [1050–1052], zeolites [1053], boron nitride [1054,1055], zirconium nitride [1056], carbon [1057,1058], strontium hexaferrite [1059], and some other materials [1060–1062] have been added to $CaPO_4$ to create biocomposites and improve reliability. Among them, Fe_3O_4/HA formulations have both photocatalytic [973,974] and magnetic properties [399,975,976]. Other magnetic additives to $CaPO_4$-containing formulations comprise ferrites $CoFe_2O_4$, $NiFe_2O_4$, $CuFe_2O_4$, oxides CoO, NiO, and Gd_2O_3, as well as metallic Nd, Gd, and Sm [1063]. The magnetic properties of $CaPO_4$-containing composites and hybrid formulations are widely used for anticancer treatments [1064,1065]. Some formulations can possess important electrical properties [1066]. More complex biocomposites, such as HA/Al_2O_3/carbon nanotubes [1067], PMMA/HA/$ZnFe_2O_4$/ZnO [530], cellulose acetate/HA/bioglass/ZrO_2 [1068], and anorthite/β-TCP/$CaMgP_2O_7$ [1069] formulations, have also been developed. The ability of biocomposites to form a stable interface with bone is lower than that of $CaPO_4$ bioceramics alone because many inorganic materials are either not bioresorbable, not bioinert, or significantly less bioactive than $CaPO_4$. Typically, a significant amount of reinforcing phase is required to achieve the desired properties. These formulations are sometimes called bioinert/bioactive composites because they contain bioinert components [985]. The ideal reinforcement is one that provides mechanical integrity at low loads without reducing the bioactivity of $CaPO_4$. $CaPO_4$/zirconia biocomposites (over 420 publications according to

Scopus) seem to be the most popular research topic. The main drawback of PSZ-reinforced HA is the degradation of zirconia in wet environments [945,954,955,957].

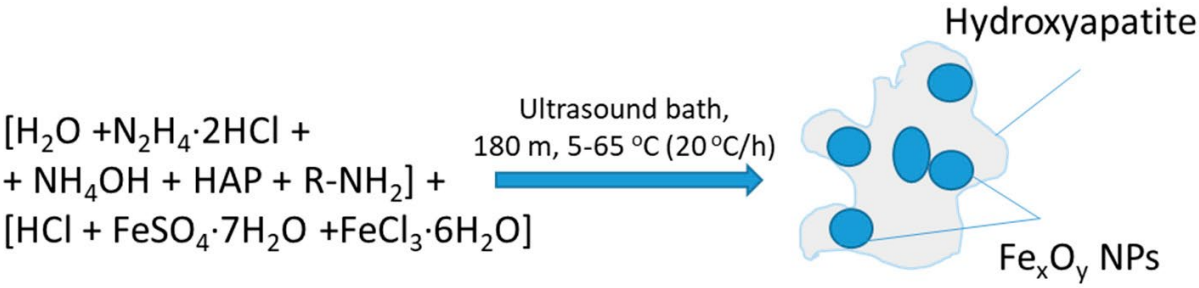

Figure 9. A schematic illustration of composite formation scheme of hydroxyapatite-magnetite HA/Fe_xO_y. NPs = nanodimensional particles. Reprinted from Ref. [975] with permission.

There are various varieties of $CaPO_4$/glass biocomposites. The first, also called bioactive glass–ceramics, represent parent glasses composed of ~34% by weight of 50–100 nm sized oxy-FAP ($Ca_{10}(PO_4)_6(O,F)_2$) and β-wollastonite ($CaO{\cdot}SiO_2$) crystals in a heat-treated MgO-CaO-SiO_2 glassy matrix, resulting in dense and homogeneous biocomposites [995–998]. In addition, there are A-W glass–ceramics that appear to be aggregates of small apatite particles effectively reinforced with wollastonite. A-W glass–ceramics have the highest flexural strength, fracture toughness, and Young's modulus among bioactive glasses and glass–ceramics, making them ideal for applications involving significant compressive loads, such as iliac crest replacement and artificial vertebrae. A-W glass–ceramics combines high bioactivity with favorable mechanical properties [1070]. β-TCP/wollastonite [1071–1073], β-TCP/wollastonite/diopside [1074], and OCP/silica [1075] biocomposites are also known. More complex formulations have also been developed. For example, A-W/HA/silk fibroin biocomposites are designed to match the mechanical strength of human cortical bone, provide good biological activity, and can be used for many orthopedic applications [1076]. Other examples include wollastonite-reinforced HA/Ca polycarboxylate [1077], glass-reinforced HA/polyacrylate [1078], and photocurable 3D-printed mesoporous bioactive glass/TCP [1079] biocomposites, as well as calcium phosphate silicate/wollastonite formulations containing collagen [1080] and gelatin [1081].

$CaPO_4$/glass biocomposites can be prepared by simple sintering of suitable $CaPO_4$/glass powder mixtures [1082–1088]. If sintering is performed below 1000 °C, $CaPO_4$ does not react with bioactive glass [1083], or this reaction is limited [1084]. In a different method, $CaPO_4$ bioceramics were treated with tiny amounts of bioactive glass to enhance densification and/or mechanical characteristics [23]. Furthermore, biocomposites can be sintered from HA and silica powders [985]. On the one hand, the synergistic combination of two bioactive phases can modulate the dissolution of the final system and enhance its biological response, while, on the other hand, the glass acts as a sintering aid aimed at densifying the composite and increasing its mechanical strength [1085]. Under both in vitro and in vivo settings, bioactive glass–ceramics often retain more strength than HA bioceramics for an extended period of time [987]. Additionally, the creation of biocomposites by the addition of bioactive glasses to $CaPO_4$ has positive effects on cell adhesion, viability, and proliferation if compared to pure $CaPO_4$ bioceramics [1086]. More details on this topic can be found in the following reviews [1085,1086].

Regarding biocomposites of $CaPO_4$ with carbon, there are two major directions: bone char [1089,1090] and those with nanodimensional carbon [1091–1112]. Bone char is produced by high-temperature pyrolysis of bones (by-products of the agrifood industry) in an inert atmosphere, which converts the bioorganic compounds (mainly, collagen) into an inorganic graphitic carbon. Differently from standard biochar of plant origin, bone char also contains $CaPO_4$ (commonly HA). The combination of $CaPO_4$ and graphitic carbon makes bone char a unique material, with different possible uses; however, up until now, it has been without biomedical applications [1089,1090].

It is very difficult to prepare homogeneous mixtures of $CaPO_4$ and carbon nanotubes because their shapes are very different: "one can imagine something similar to achieving a homogeneous mixture of peas and spaghetti" ([1091], p. 7). Similar shape incompatibility problems are valid for $CaPO_4$/graphene mixtures. Nevertheless, different strategies can be used to prepare such biocomposites [1092]. For example, apatite can be chemically synthesized using carbon nanotubes with carboxyl functional groups as a matrix [179–182,1093–1097]. The physicochemical properties of those biocomposites have shown that CDHA nucleation is initiated via carboxyl groups [179]. Hot pressing [1098], compression [1099], plasma spraying [1100], laser surface alloying [1101–1103], spark plasma sintering [1104], shear mixing [1105], sol-gel [1106], and deposition [1107] techniques can also be applied. It is recommended that carbon nanotube/$CaPO_4$ biocomposites be sintered in a deoxidizing environment because carbon oxidizes at high temperatures [1108]. Biocomposites of $CaPO_4$ with carbon nanotube oxides [1109] and/or carbon nanotubes with oxygen-containing functional groups [1110] are also known. Regarding the mechanical properties, nanoindentation tests on carbon nanotube-reinforced HA composite coatings were performed to get the numerical values for hardness and Young's modulus [1111]. The results revealed that the higher the nanotube loading, the better the mechanical properties. That is, at 20 wt% loading, hardness and Young's modulus increased by 43% and 21%, respectively, compared to single-phase HA coating. Scratch tests showed that alloyed HA biocomposite coatings exhibited improved wear resistance and lower coefficients of friction when the number of carbon nanotubes in the precursor material powder was increased [1102]. Additionally, examinations of the biocomposite coatings' elastic modulus and hardness revealed that the quantity of carbon nanotubes also had an impact on the mechanical properties [1101]. Compression tests on bulk HA/carbon nanotube biocomposites were conducted by another research group, which reported an improvement in strength compared to single-phase HA [1093]. The maximum compressive strength of any material, however, was only 102 MPa, which is considerably less than the usual values for high-density HA but comparable to cortical bone [1091]. Hybrid biocomposites with more intricate formulations, including poly-L-lysine/HA/carbon nanotube [1111] and multi-walled carbon nanotube/HA/carbon fiber/PEEK [1112], have also been created. Carbon nanotubes, on the other hand, are an extremely stable substance that cannot be biodegraded or reabsorbed. As a result, the nanotubes may enter the human body through the biocomposite matrix during in vivo bioresorption and result in unknown health issues. This issue needs to be resolved.

To conclude the carbon issue, carbon fibers of very small sizes [1113–1115], as well as diamonds [1116,1117], graphene and graphene oxide [171,177,178,197,689,885,1118,1119], fullerenes [848] and their derivatives [498,1120], carbon quantum dots [672,673], and other allotropes of the nanosized carbons were used to reinforce the $CaPO_4$ bioceramics [1092]. More complicated multicomponent formulations, such as HA nanobelts/carbon nanotubes constructed into carbon fiber/DCPA/epoxy biocomposites, have been developed as well [1121]. Additional details on $CaPO_4$/carbon biocomposites and hybrid formulations are available in the excellent recent review [1092].

Additionally, many $CaPO_4$ biocomposites containing metals and alloys have been created [183,203–205,551,670,671,725,1006–1041]. Numerous fabrication techniques have been used to produce them. For example, HA-based biocomposites reinforced with 20% volume Ti particles were produced by hot pressing [1008]. A combination of cold pressing followed by sintering has also been used [1033]. Furthermore, $CaPO_4$ and metal biocomposites can be prepared by a powder metallurgical process [1009,1011,1021,1022], combinations of direct ink writing with a liquid pressure infiltration [203], mechanical compaction and sintering [671,1017,1019], and upward friction stir processing [1032], as well as by additive manufacturing [204,205]. Silver ions integrated into HA particles can be reduced by γ-irradiation to create Ag nanoparticle/HA biocomposites [670]. More complicated formulations, such as Ag/Ag_3PO_4/BCP (HA + β-TCP) [1035], Ti6Al4V/HA/TiB_2 [1030], HA/*i*-$Al_{64}Cu_{23}Fe_{13}$ quasicrystals [1029], and $CaSiO_3$/HA reinforced with a Ti6Al4V alloy [1039], were prepared as well.

In the case of metals and alloys as the matrixes, Mg–3Zn–Ca/1% β-TCP biocomposites were produced by a melt shearing technology combined with a high-pressure die-casting process. The results showed that mechanical properties were not satisfactory, probably due to the poor interfacial bonding between the phases. The authors suggested that hot extrusion and heat treatment might improve the mechanical properties [1016]. More to the point, metal matrix composite with pure Zn as a matrix and HA powder as reinforcement were prepared by a spark plasma sintering [1028], while those with pure Mg as a matrix and HA-Al_2O_3 HA-TiO_2@Al_2O_3 as reinforcements were prepared by a stir casting [1031] techniques. Additive manufacturing based on 3D printing with different content levels of powder and polymer parts, followed by washing in acetone and further sintering, was used to produce Fe-Cu-HA biocomposites [1037]. A friction stir processing technique was used as well [1020,1024]. Regarding metals and alloys with relatively low melting points, $CaPO_4$-containing composites and hybrid formulations with them can be prepared by infiltration of those molten metals through $CaPO_4$ scaffolds [203,1015,1018,1023]. A melt extrusion approach was also tested [1014].

It has been observed that, at high temperatures, the presence of Ti metallic phase accelerates both the dehydration and breakdown of HA to mixes of β-TCP and TTCP [1008, 1009,1019,1122] or β-TCP and calcium titanates [661,1011,1022,1122]. Compared to pure HA bioceramics produced under the same conditions, HA/Ti biocomposites have better fracture toughness, flexural strength, and fracture work, making them suitable for biomedical applications [1017]. However, their mechanical properties did not seem sufficient for the use of HA/Ti biocomposites in load-bearing applications. Fortunately, histological evaluation revealed that HA/Ti biocomposites were partially integrated with new bone tissue after 3 weeks, and fully osteointegrated in vivo after 12 weeks [1008]. Similar findings were previously obtained for HA bioceramics reinforced by the addition of Ag particles (5–30% volume) followed by sintering of HA/Ag powder compacts [1006,1007]. Furthermore, the addition of Ag imparts antimicrobial activity [670,1013,1035]. Other studies on $CaPO_4$/Ti biocomposites are available elsewhere [1010,1012,1022]. In all aforementioned studies, $CaPO_4$ was used as the matrix, but the reverse is also possible: to investigate the effect of 100 nm sized β-TCP spherical particles on the microstructure of the alloy, biocomposites were prepared using an Mg3Zn0.8Zr alloy as a matrix and β-TCP particles as reinforcement [1123].

To conclude, $CaPO_4$/metal biocomposites are commercially produced, for example, OssDsign (Table 4).

5.8. Biocomposites from $CaPO_4$ Only

Now, biocomposites composed only of $CaPO_4$ should be discussed. The earliest paper on this sub-topic was published in 1976 [70]. First, all types of biphasic (BCP), triphasic, and polyphasic $CaPO_4$ formulations should be mentioned [436]. For example, in the 1980s, BCPs were called "TCP ceramics complexed with HA" [1124]. Even today, such multiphasic formulations are sometimes referred to as nanocomposites [1125,1126] or simply composites [1127]. Furthermore, fluorinated HA (chemical formula $Ca_{10}(PO_4)_6(OH)_{2-x}F_x$, where $0 < x < 2$) can also be listed as a composite material [1128], although it is debatable whether the term 'composite' can be applied to such a system. Biocomposites of 70% HA-powder + 30% HA-whiskers should be mentioned and discussed instead. They were made using hot pressing, hot isostatic pressing, and pressureless sintering. Without sacrificing bioactivity or biocompatibility, those biocomposites were shown to have increased toughness, reaching the lower bound of bone fracture toughness [1129,1130]. Another illustration is a dual HA biocomposite, which combines two different porosity HA materials: one with 0% porosity for load carrying and the other with 75% porosity for bone ingrowth. The dual HA biocomposite was discovered to be a viable substitute for iliac bone grafting when used as an implant material for interspinous fusion, eliminating the disadvantages associated with autograft harvesting [1131]. In addition, two-component suspensions of HA nanoparticles with spherical (S-HA, as a matrix) and fiber (F-HA, as a reinforcement) morphologies were

prepared and deposited. The results revealed that long crystalline F-HA particles efficiently reinforced the microstructure of the composite coatings; however, coarse pores were formed by the stacking of F-HA particles. Nevertheless, finer particles of poorly crystalline S-HA efficiently filled these coarse pores, providing the desired corrosion resistance [1132]. Additionally, HA-whisker-strengthened HA scaffolds have been prepared by 3D printing, followed by BCP (HA + β-TCP) coating [1133]. Furthermore, self-setting DCPD forming formulations were reinforced by the addition of CDHA/DCPA fibers [495].

A biodegradable biocomposite porous scaffold composed of a β-TCP matrix and nanosized HA fibers was developed and investigated for load-bearing bone tissue engineering; nanosized HA fibers were prepared by biomimetic deposition method and their incorporation significantly improved the mechanical properties of the scaffold, achieving a compressive strength of 9.87 MPa, comparable to the high-end value (2–10 MPa) of cancellous bone [1134]. Furthermore, HA and β-TCP powders were wet mixed, the powder combination was compacted, and the mixture was calcined to create HA/β-TCP biocomposites with varying β-TCP contents (10, 20 and 30 wt%) [1135]. Additionally, a CDHA/α-TCP biocomposite was prepared by α-TCP addition into a self-setting apatite-forming cement [1136]. Similarly, DCPA/ACP biocomposites were prepared by mixing DCPA and ACP powders followed by setting [1137]; however, it was not the case when carbonate apatite was added into a self-setting α-TCP [516]. Finally, it is interesting to mention the successful reinforcement of carbonate apatite porous blocks with newly prepared carbonate apatite crystals (i.e., the same compound) [1138]. First, calcium salts were added to the micropores of the carbonate apatite blocks. Then, in the second step, the calcium salts were carbonized by exposure to carbon dioxide gas to form calcite in the micropores of the carbonate apatite blocks. In the third step, the blocks were immersed in a Na_2HPO_4 solution. This converted calcite in the micropores of the carbonate apatite block into carbonate apatite and the newly formed carbonate apatite crystals became entangled with the crystals of the existing carbonate apatite block. The bonding of the newly formed carbonate apatite crystals with the crystals of the existing carbonate apatite block increased the mechanical strength of the block by 1.5 times compared to pre-treatment [1138].

5.9. Inks for 3D Printing

According to Wikipedia, "*3D printing* or *additive manufacturing* is the construction of a three-dimensional object from a CAD model or a digital 3D model. It can be done in a variety of processes in which material is deposited, joined or solidified under computer control, with the material being added together (such as plastics, liquids or powder grains being fused), typically layer by layer" [1139]. For the bone grafting cases, 3D printing is used to produce bioresorbable porous grafts of the patient-specific shape and dimensions according to the bones being replaced wholly or partially. This resulted in the development of $CaPO_4$-containing composites and hybrid formulations, which could be used as inks for 3D printing. In most cases, such formulations represent viscous liquids or pastes, which can be both self-hardened and produce solid constructs by either drying or after treatment. The latter procedure can be performed by using both physical treatments (such as light for light-crosslinking formulations), temperature treatments (freezing or sintering), and additional chemical reagents. Therefore, $CaPO_4$-containing inks for 3D printing could also be considered as formulations belonging to either self-hardening biocomposites (Section 5.2) or injectable bone substitutes (Section 5.6); however, since the viscous inks are not designed for in vivo injections, biologically incompatible compounds (such as organic solvents) might be used in their composition because they will be eliminated afterward during either drying or later treatments. Several examples of typical $CaPO_4$-containing formulations are described below [1133,1140–1146].

For example, HA/PCL inks were prepared by PCL dissolving in a ternary solvent prepared by mixing dichloromethane with the surfactant 2-butoxyethanol and plasticizer dibutyl phthalate in a volumetric ratio of 5:3:1, followed by addition of a HA powder through a 30-micron mesh sieve [1140]. The influence of important variables, such as

the polymer type, concentration, solvent, additives, and ceramic particle characteristics, on the printability, shape fidelity, and mechanical properties of the 3D printed scaffolds was investigated. By systematically varying the composition of HA:PCL inks, the authors demonstrated their non-Newtonian flow behavior and identified printable ink formulations based on their rheological properties. The weight ratio of HA in the PCL polymer was found to impact the compressive moduli and toughness of the prepared scaffolds [1140]. Similar results were obtained in another study, in which HA/PCL/polyethylene oxide inks both with and without adding vancomycin were prepared by a similar technique [1141]. To prepare inks, aqueous PVA solutions might be used instead of PCL solutions in organic solvents [1133].

In another study, light-curable gelatin methacrylate/HA inks were prepared by mixing 1% w/v spray-dried fine HA powders with 10% w/v gelatin methacrylate. To do this, photo-crosslinking photoinitiator Irgacure 2959 powder was dissolved in phosphate buffer saline at 70 °C for 60 min (the final concentration was 0.3% (w/v)). Then, the desired amount of gelatin methacrylate was dissolved in the Irgacure 2959 solution at 37 °C. Finally, to produce inks for 3D printing, a suspension of HA in phosphate buffer saline was prepared and applied to the gelatin methacrylate and Irgacure 2959 solution [1142].

In one more study, silk fibroin (0%, 6%, 8%, 10%, 12%), gelatin (10%), and nanodimensional HA powders (3%) were weighed according to different mass fractions and dissolved in deionized water to prepare five formulations of composite hydrogel precursors, which were used as 3D printing inks and stored in a refrigerator at 4 °C. The printing was performed at 5 °C. Subsequently, the samples were frozen for 12 h in a cryogenic storage tank at −20 °C, then taken out and thawed at room temperature for 2 h, repeating the above process 3–4 times. Finally, the samples were soaked in absolute ethanol for storage [1143].

Additionally, several formulations of HA-reinforced alginate–chitosan-based printable hydrogel inks were developed in one more study [1144]. To do this, the authors prepared an aqueous suspension of fine HA powders of different concentrations (0.1, 0.2, and 0.4 w/v %). Then, a fixed concentration of 5 w/v % alginate was dissolved in the HA suspensions through magnetic stirring. Afterward, chitosan (1 and 2 w/v %) was mixed and stirred for a few hours to swell into the alginate solution. Acetic acid was added dropwise (12–14 drops per 10 mL) in the solution with constant stirring. After printing the hydrogel inks, a 10% aqueous solution of $CaCl_2$ was used to cross-link the hydrogel. Afterward, the printed constructs were washed thoroughly with deionized water, followed by drying at 40 °C and storage in a vacuum desiccator [1144].

Finally, HA/PEG diacrylate hydrogel inks should be mentioned [1145]. These inks were prepared by dispersing three different concentrations of HA (1, 2, and 5 wt%) and 20 w% PEG diacrylate hydrogel (700 kDa) in distilled water. The maximum concentration of HA was set at 5 wt% because it did not block the dispensing nozzle. Then, 0.1 wt% of a radical photoinitiator for the UV curing Irgacure 2959 was added and stirred to make homogenous solutions. Afterward, 25 wt% of a non-ionic copolymer surfactant Pluronic F127 was added, and the hydrogel inks were stored in the fridge for two days for the complete dissolution of Pluronic F127. Finally, the inks were loaded into 10 mL cartridges and allowed to equilibrate to room temperature for one hour before printing to initiate the physical gelation of Pluronic F127 [1145].

It is also possible to produce porous bioceramic scaffolds from the $CaPO_4$-containing biocomposite inks. For example, different ink formulations consisting of Mg- and Na-doped carbonated CDHA, β-TCP, and a non-ionic copolymer surfactant Pluronic F127 were prepared and used to print porous scaffolds. Afterward, the scaffolds were first placed at room temperature for 24 h to dry, followed by sintering at 1100 °C for 2 h and cooling [1146].

To finalize this section, one should note that due to the rapid development of additive manufacturing techniques, presumably, by means of the subsequent modifications, any type of $CaPO_4$-containing biocomposite and hybrid formulation might be 3D printed [1147].

5.10. Functionally Graded Biocomposites

In numerous instances, a homogeneous filler distribution within the matrix is necessary [365], but there are certain formulations where this criterion is not applicable. For instance, functionally graded materials (FGMs) denote materials where the structure and/or composition gradually change in one or more directions, leading to correlated changes in the material properties. The primary characteristic of compositional FGMs is an almost continuously graded composition, which yields two distinct properties at either end of the structure. These composite materials can be tailored for particular functions and applications. Various methods, such as bulk (particle processing), pre-mold, additive, and melt processing, are employed for the production of FGMs.

Bone is a biologically created composite that exhibits varying degrees of density: from very dense and hard cortical bone to porous and foamy trabecular bone structures. Typically, cortical bone forms the outer part of long bones, and its density decreases towards the center where the trabecular bone is situated. Trabecular bone is porous, and its spaces are filled with marrow [14,15]. Therefore, bone is a naturally occurring functionally graded composite.

The concept of FGM is becoming increasingly important in the field of biomaterial design and research. Numerous studies have been conducted, for instance, on the synthesis of porous $CaPO_4$ bioceramics to imitate the natural porosity of bones [1148–1150]. This serves as a structural approach to the development of FGMs, in addition to compositional approaches. For instance, functionally graded composite cranial implants have been produced that are made of polylactic acid, carbonate apatite, and $CaCO_3$ [326,327]. Additionally, HA/Ti biocomposite implants, which are functionally graded, have been prepared utilizing powder metallurgy. These implants provide biocompatible HA on the tissue side and mechanically robust Ti on the outer side [201,202,1151,1152]. The longitudinally-graded structure includes more Ti in the upper part and more HA in the lower part. In the Section 5.9, Ti bears direct occlusal forces and provides necessary mechanical performance, whereas, in the Section 5.11 embedded in bone, HA imparts bioactivity and osteoconductivity to the material [1151]. The optimal sintering conditions for Ti and HA differ significantly, creating complications in producing HA/Ti functionally graded biocomposites. Therefore, sintering conditions for the HA/Ti mixtures must be balanced. The anticipated characteristics of the implant are illustrated in Figure 10 [1152]. These biocomposites can either be symmetric [1153] or asymmetric [1154].

Functionally graded $CaPO_4$ coatings with different concentrations of silver were applied on Ti substrates using ion beam-assisted deposition. Cross-sectional analysis revealed a reduction in crystallinity and the dispersion of nanosized silver particles (10–50 nm) from the coating/substrate interface toward the top surface [1155]. Plasma spraying was employed to prepare compositionally graded HA/Ti biocomposite coatings [1156]. Furthermore, laser cladding [1157] and combinatorial matrix-assisted pulsed laser evaporation techniques [1158] have been utilized to deposit graded carbon nanotubes/HA, Sr-substituted HA, and zoledronate-modified HA deposits, respectively. Additionally, functionally graded HA/PMMA biocomposites were developed by dispersing precipitable HA in PMMA viscous liquids using centrifugation to prevent stress convergence at the interface. Technical term abbreviations were explained upon first use. The stress–strain curve of this biocomposite indicates sufficient strength for utilization in biomedical applications, alongside decreased brittleness and fragility [528]. Compositionally graded biocomposite scaffolds made of collagen and nanoscale hydroxyapatite can be produced through in situ diffusion techniques. Chemical and microstructural analyses showed that there is a Ca/P ratio gradient throughout the scaffold template's width, leading to the development of Ca-rich and Ca-deficient sides of the scaffold. The Ca-rich side has low porosity and nanosized HA crystal aggregates, while the Ca-deficient side has high porosity and nanosized HA crystals integrated with collagen fibers to create a porous network structure [1159]. A biocomposite membrane with a gradient structure was created using a layer-by-layer casting method [606]. The three-layer structure consists of a porous

membrane containing 8% nanosized carbonate apatite/collagen/PLGA on one side, a nonporous membrane made of pure PLGA on the opposite side, and a middle layer with a transition zone containing 4% nanosized carbonate apatite/collagen/PLGA. A similarly graded biocomposite made of PLGA/nano-HA/lauric acid was also manufactured [1160]. Functionally graded nonwoven fabrics made of PCL and containing nanosized particles of β-TCP were produced using a hybrid twin-screw extrusion/electrospinning method [1161]. Biocomposites containing functionally graded HA/silk fibroin were developed through pulsed current sintering [1162]. Additionally, HA/glass FGM layers were applied onto a Ti6Al4V substrate with the aim of creating a strong bond between the FGM laminate and the substrate [1163,1164].

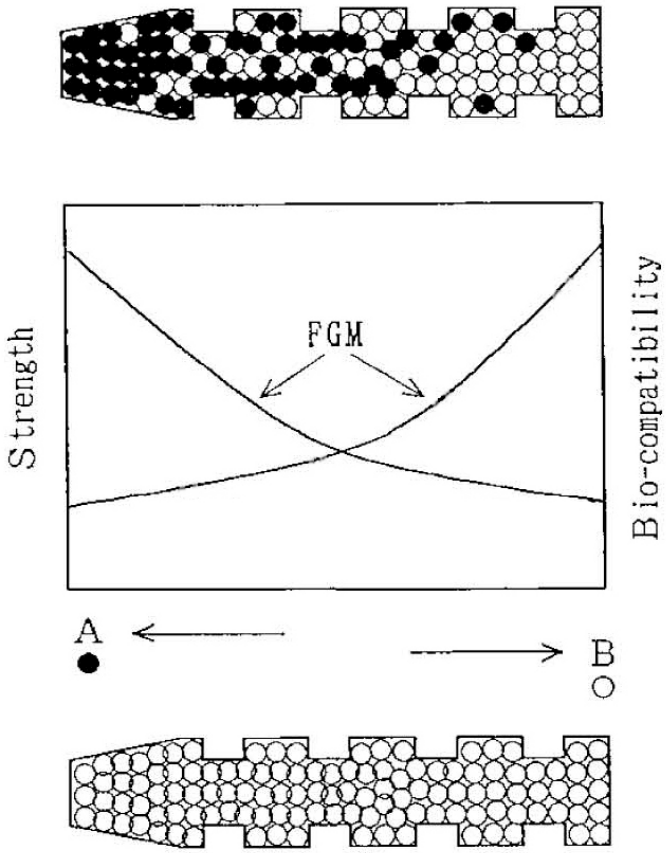

Figure 10. Properties of a functionally graded biocomposite dental implant that are anticipated. In contrast, an implant that is functionally graded is depicted in the upper figure, while a traditional, uniform implant is shown in the lower drawing. In the center are the properties. Due to the formation of discrete boundaries, the implant's composition changed from a biocompatible metal (Ti) at one end (shown on the left in the figure) to an increase in the concentration of bioceramics (HA) toward 100% HA at the other end (shown on the right). This allowed the implant to control both mechanical properties and biocompatibility without experiencing an abrupt change. More titanium was used in the construction of this FGM biocomposite for the upper portion, which is directly subjected to occlusal force, and more HA for the lower portion, which is implanted into the mandible. Reprinted with permission from Ref. [1152].

Functionally graded β-TCP/FA biocomposites combine the biostability of FA with the bioresorbable properties of β-TCP. A multilayered structure, each layer being 1 mm thick, of β-TCP/FA biocomposites with varying molar ratios was produced resulting in the formation of an FGM (Figure 11). After implantation, functionally gradient porosity allowing for bone ingrowth would result from preferential dissolution of the β-TCP phase [1165]. Additionally, the same multilayered technique was used to produce HA/alumina/zirconia biocomposites with a composition gradient [1166] and 316L stainless steel/β-TCP [1167].

Two additional materials were synthesized—fluoridated HA with a fluoride gradient [1168] and carbonated HA with a carbonate gradient [1169]. Furthermore, HA/zirconia-graded biocomposites were developed to enhance HA mechanical characteristics while preserving its ability to attach to bone [958]. Titania and HA were identified as a suitable combination for FGM due to their ability to provide both a gradient of bioactivity and robust mechanical strength [1170]. Additionally, researchers have developed graded biocomposite structures of HA/$CaCO_3$ for improved bone ingrowth [1171]. Furthermore, functionally graded biocomposite skull implants made of polylactides, carbonateapatite, and $CaCO_3$ have been developed [326,327]. The research in this field shows promise, but the mechanical properties of functionally graded biocomposites do not yet match those of bones [1172].

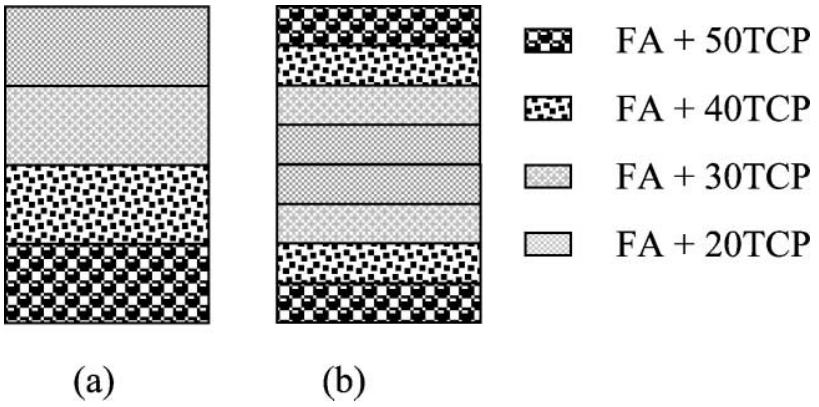

Figure 11. A schematic diagram showing how the layers of the FA/β-TCP biocomposite are arranged for FGM in (**a**) non-symmetric form; (**b**) symmetric form. Reprinted with permission from Ref. [1165].

5.11. Biosensors

Biosensors detect analytes by combining biological and physicochemical detection elements. They are made up of three parts: a biological element that is sensitive, a transducer or detector element that transforms the signal from the interaction of the analyte and the biological element into an electrical signal (current or voltage), and related electronics that present the results in an easy-to-read manner [1173].

$CaPO_4$ surfaces have an excellent adsorption capacity for functional biomolecules such as proteins, albumins, DNAs, and other chemical species. Therefore, $CaPO_4$-based composites and hybrid formulations can be applied to biosensor fabrication [1111,1174–1184]. For instance, the synthesis of hybrid nanoscale particles including poly-L-lysine, HA, and carbon nanotubes was explained, and a generic immunosensing platform design method was suggested, predicated on the adsorption of antibodies onto those biocomposites [1111]. In another paper, a hybrid material consisting of gold nanosized particles mounted on nanosized HA was used to design an interface for antibody-bound piezoelectric immunosensors. The developed sensing interface appears to have advantages over the use of nanosized HA or gold alone, such as immobilization without activation and higher antigen-binding activity of the antibody [1175]. For the detection of phenolic compounds, a novel tyrosinase biosensor based on nanosized HA/chitosan composites has been developed [1178]. A $Bi_2Zr_2O_7$/HA composite sensor showed outstanding selectivity and performance toward sensing lead nitrate and dextrose [1183]. Due to the recent coronavirus disease-19 (COVID-19) pandemic caused by the SARS-CoV-2 virus, it is important to stress that a HA–lanthanum strontium cobalt ferrite (HA–LSCF) composite showed a good response on a screen-printed carbon electrode electrochemical aptasensor to detect the SARS-CoV-2 spike RBD protein. The authors concluded that the developed HA–LSCF-based biosensor could be used as an alternative method for detecting the COVID-19 pandemic [1184]. Finally, it may also become possible to harness the power generated by DCPD/polymer composite-based battery devices [460,461]. More details on $CaPO_4$-based

composites and hybrid formulations as components of various biosensors can be found elsewhere [1111,1174–1184].

To conclude, currently (May 2024), according to Scopus, there are 85 articles with a combination of "sensor" and "apatite" in the title and 46 articles with "sensor" and "calcium phosphate".

6. Interactions among the Phases in $CaPO_4$-Based Biocomposites

One important factor that needs to be carefully examined is whether $CaPO_4$ interacts with other phases in composites and hybrid formulations. This interaction arises exclusively at the interface, a small region where significant alterations in the chemical composition of the constituent materials culminate in their bonding and potential load transfer. In general, interactions between phases in composites can occur through mechanical means, such as the radially compressive forces that the matrix exerts on the filler particles (for example, during cooling due to thermal shrinkage), or chemical means, where the reactivity of the filler with the matrix is of vital importance. In the latter case, it is crucial to differentiate between physical interactions and chemical bonds [268]. According to Wypych, physical interactions are typically temporary and involve hydrogen bonds and van der Waals forces. In contrast, chemical bonds are stronger and more durable as they involve the formation of covalent bonds [1185]. Consequently, composite materials' strength is increased by preferred chemical interfacial bonding between phases. The interfacial bond's size between the phases determines the degree of stress transferred from the weaker matrix to the stronger fibers. However, although a bond between the matrix and reinforcement is necessary for stress transfer, it is insufficient to prevent hardening mechanisms, such as phase segregation and fiber withdrawal [1091].

The precise modes of binding between the bone mineral (bioapatite) and bioorganic material (collagen)—which have a significant influence on the mechanical properties of bone—are still a contentious topic. Bone minerals do not bind directly to collagen; instead, they bind through non-collagen proteins, constituting approximately 3% of bone (Table 1), which offer active sites for biomineralization and cell adhesion [22]. The interfacial binding forces in bones are primarily ionic and hydrogen bonds, along with hydrophobic interactions which are responsible for its complex behavior [337]. In contrast, some argue that, in conventional $CaPO_4$/collagen biocomposites, there is no chemical bonding between phases, possibly due to inadequate interfacial bonding during mixing [766]. Nevertheless, this is not the case with phosphorylated collagen [749]. Experts in computer modeling refer to density functional theory studies of HA surfaces and collagen peptides [1186]. They also look to molecular dynamics simulations of HA surface interactions with three polymers (PE, PA, and PLA) [1187] and an additional three polymers (polyvinylpyrrolidone, polyacrylamide, and PVA) [1188].

Researchers gathered Fourier transform infrared (FTIR) spectra of several $CaPO_4$-based biocomposites and collagen films in order to investigate possible phase interactions [748]. The Kramers–Kronig equation was then used to convert those spectra into absorption ones, which showed energy shifts in residues at the apatite/collagen boundary. Through a thorough comparison of the biocomposite and collagen FTIR spectra, we observed red shifts in the C–O bond absorption bands within the biocomposite spectrum. The red shifts observed were explained by a decrease in the binding energy of C–O bonds and were suggested to be a result of their interaction with Ca^{2+} ions found on the surface of apatite nanosized crystals, as demonstrated in Figure 12 [748]. Another indication of the chemical interaction between apatite and collagen was evaluated in the FTIR spectra of CDHA/collagen biocomposites, whereby the bands associated with the –COO– stretching displayed a shift from 1340 to 1337 cm^{-1} [714,715]. According to earlier research, the carboxylate groups of the collagen macromolecule interacted chemically to generate apatite crystals on collagen [1189–1191].

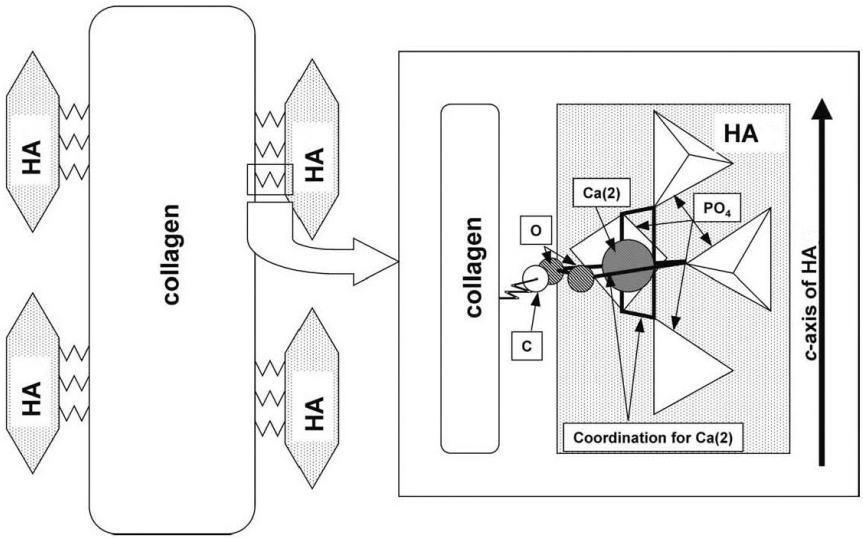

Figure 12. An illustration showing the connection between interfacial interaction in biocomposites and self-organization, or the directed deposition of HA on collagen. The covalent link between COO and Ca(2) limits the direction of contact between HA and collagen in order to preserve the normal coordination number of seven. Reprinted with permission from Ref. [748].

FTIR spectroscopy appears to be a very useful technique for examining possible chemical bonding between phases in hybrid formulations and composites based on $CaPO_4$ [186,269,295,301,302,405,469,597,608,619,621,623,626,630,640,676,677,680,685,715,749,802,803,821,848,875,919,1192–1201]. For example, in HA/PE biocomposites, the characteristic bands of the hydrocarbon backbone of PE at 2918, 2850, and 1472 cm^{-1} show zero shift, while, in HA/PA, bands at 3304, 1273, and 692 cm^{-1} derived from N-H stretching, C–N–H stretching, and N–H vibrations are observed in HA/PA, which move to 3306, 1275, and 690 cm^{-1} in biocomposites. Moreover, the stretching (3568 cm^{-1}) and vibrational (692 cm^{-1}) modes of HA hydroxide shifted to 3570 and 690 cm^{-1} in HA/PA biocomposite, indicating the formation of hydrogen bonds. Furthermore, the bands at 1094 and 1031 cm^{-1} in the PO_4 mode are also shifted to 1093 and 1033 cm^{-1} in the HA/PA biocomposite. The bands' shift in the fingerprint region suggested that hydroxides and orthophosphate on the HA surface can interact by nucleophilic addition with the plentiful carboxyl and amino groups of PA [269]. Similar conclusions were drawn for many other $CaPO_4$-containing composites and hybrid formulations, namely: HA/PVA [626], CDHA/alginate [715], ACP/PPF [469], HA/maleic anhydride [302], HA/carboxylated PU [1198], HA/chitosan [821,1200,1201], and β-TCP/PLLA [405] biocomposites. It has been shown that weak chemical bonds are formed between Ca^{2+} ions on the surfaces of HA, CDHA, ACP, or β-TCP, respectively, and the slightly polarized O atoms of C=O bonds in the surrounding bio-organic compounds. The data obtained showed that the crystallization of $CaPO_4$ in solutions containing chitosan is largely regulated by the chemical interactions of the components. Clearly, part of the calcium was retained by chitosan and was not involved in the formation of the main mineral phase [1197]. Such chemical interactions are schematically illustrated in Figure 13 [715].

Other measuring methods can also demonstrate proof of phase-to-phase chemical interactions in $CaPO_4$-based composites and hybrid formulations [295,405,621,622,626,1193–1203]. For example, such evidence has been observed in nanosized crystals of CDHA/alendronate by thermogravimetric analysis: the DTG plots of the crystals appear quite different from those obtained from a mechanical mixture of CDHA and calcium alendronate of similar composition [1202]. Similar DTG results were obtained for nanosized HA/PVA biocomposites [626]. In the case of nanosized HA and PA biocomposites, hydrogen bonding between the phases was detected by differential scanning calorimetry [621]. Similar results were obtained in another study [1194]. Another example is the application of dynamic mechanical analysis to investigate the softening mechanism of β-TCP/PLLA biocomposites [405]. For

nanosized HA and PVAP biocomposites, X-ray diffraction and thermogravimetric analysis found some indirect evidence of chemical bonding between phases [295]. The orientation of FA crystallites and gelatin within the FA/gelatin composite spheres was shown to have a strong structural link, which suggested a significant remodeling of the macromolecular matrix in the vicinity of growing aggregates [894]. It was found that reverse gas chromatography at infinite dilution can provide some data on the thermodynamic interactions between $CaPO_4$ and PLLA [1203]. Furthermore, using ab initio techniques, the chemical interactions between HA and organic compounds have been clarified [1204].

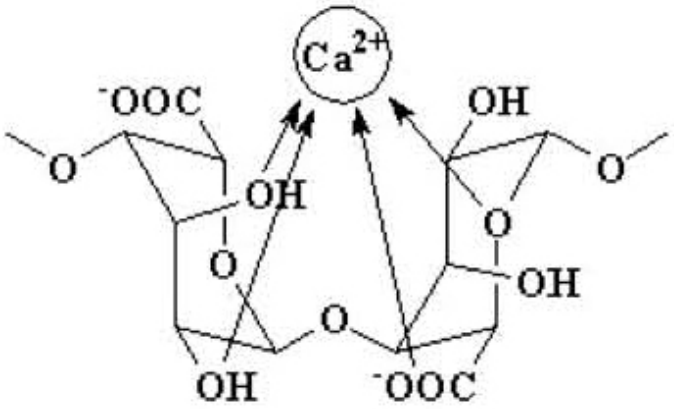

Figure 13. A schematic representation of the binding of Ca^{2+} ions with alginate chains. Reprinted with permission from Ref. [715].

X-ray photoelectron spectroscopy (XPS) revealed that the binding energies of Ca, P, and O atoms were slightly different in nanosized HA (Ca: 350.5 and 345.5; O: 530.2; P: 132.5 eV) and nanosized HA/conjac-glucomannan/chitosan biocomposite (Ca: 352.1 and 347.4; O: 531.2; P: 133.4 eV), respectively [640]. Further measurements by FTIR and X-ray diffraction showed that the nanosized HA was bound to the conjugated glucomannan and chitosan mainly by hydrogen bonds between the OH^- and PO_4^{3-} ions of HA and the –C=O and –NH groups of the conjugated glucomannan and chitosan copolymers, forming a stable interface between the three phases of the biocomposite. On the other hand, coordinate bonds can form between Ca^{2+} and –NH. The three phases of the biocomposite form a stable interface [640]. In a different investigation, XPS revealed hydrogen connections between the surface P–OH groups of HA and the C=O groups of PDLLA [1194]. XPS was used to quantify the Ca^{2+} ions of HA and the $RCOO^-$ groups of collagen molecules in HA/collagen biocomposites in order to generate a covalent link [598]. Several other $CaPO_4$-based composites and hybrid formulations have shown comparable XPS observations [619,676,677]. Figure 14 depicts conceivable types of chemical interaction that could occur between HA crystals and bioorganic molecules in HA/chitosan-gelatin network films [1196].

The possible interaction of BCP and HPMC was investigated in IBS composites [922, 923,1205]. After mixing, a reduction in the average diameter of BCP granules was noted, which affected the viscosity of the paste. During the interaction, the dissolution of the grain boundaries of β-TCP crystals and accumulation of CDHA on the HA crystal surface were observed. These two phenomena are responsible for the observed particle size changes [922,923]. However, the chemical bonding of BCP to HPMC was not found within the sensitivity of the measurement technique used [1205].

CDHA/chitosan biocomposites were prepared using the co-precipitation method [810]. Organic acids with two or more carboxyl groups that were firmly bonded to the CDHA surface via COO–Ca linkages hindered the formation of CDHA crystals. Transmission electron microscopy images revealed that, while nanosized CDHA crystals were aligned along the chitosan molecules with amino groups as nucleation sites, CDHA formed elliptical aggregates due to chemical interactions (possibly coordination bonds) between Ca on the surface and amino groups of chitosan [810]. During the setting of self-hardened (TTCP +

DCPA)/polyphosphazane biocomposites, calcium cross-linked polymer carboxylates were proposed to be formed; based on the pH monitoring results, the chemical participation of the polymer in the setting process was concluded [546–548].

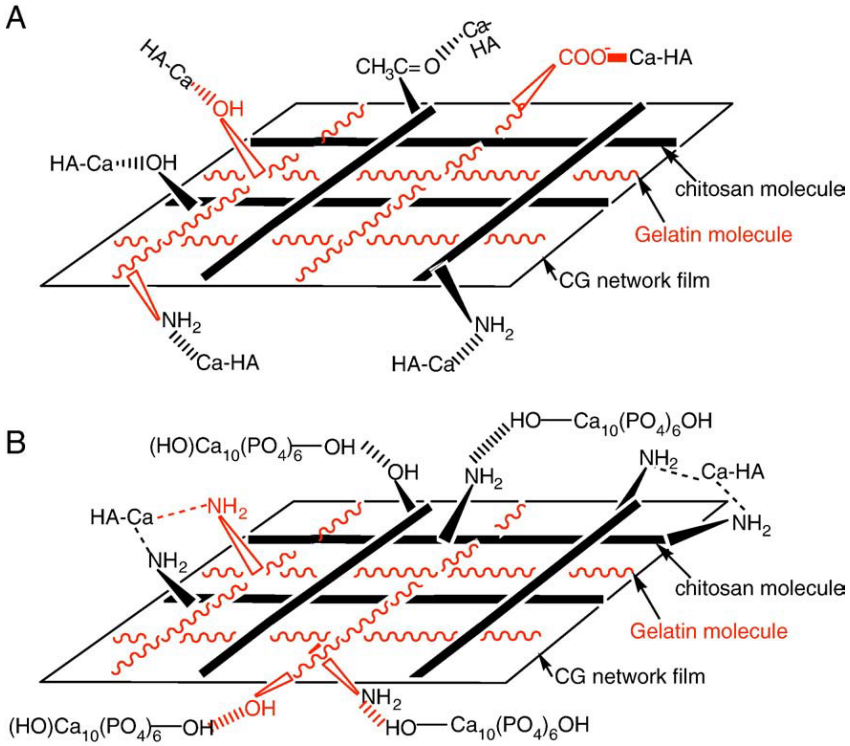

Figure 14. Potential interactions in HA/chitosan-gelatin (CG) biocomposites between HA crystals and a CG network: (**A**) and (**B**), respectively, represent a nano-dimensional HA (nHA) and a micro-dimensional HA (mHA). According to the authors: "When nHA formed on the surface of CG network via biomineralization, the corresponding ion interaction is the main drive force. However, as the mHA crystals depositing on the surface of the CG network, the hydrogen bonds between COOH, OH, $–NH_2$ of CG films and OH groups of HA crystals take the important role." (p. 1215). Reprinted from Ref. [1196] with permission.

For PCL/HA biocomposites prepared by the grafting method, the presence of chemical bonding between the phases was concluded [363], but, unfortunately, strong experimental evidence was not provided. In another study, CDHA/poly(α-hydroxyester) biocomposites were prepared by a chemical route at low temperatures [335]. In that study, α-TCP was combined with PLA, PLGA, and their copolymers to prepare pre-composite structures. Solvent cast or pressed pre-composites were subjected to in situ hydrolysis of α-TCP to CDHA at 56 °C, resulting in the final biocomposite. FTIR spectroscopy showed that there was no chemical reaction between the polymer and $CaPO_4$ during this transition [335].

In $CaPO_4$-based biocomposites capable of sustaining sintering at high temperatures (useful for formulations solely consisting of inorganic components), interdiffusion of chemical elements between phases may occur. Such an effect was detected by energy-dispersive X-ray spectroscopy in the partial formation of calcium titanate in HA/TiO_2 biocomposite particles. This process was found to be advantageous in increasing the cohesion of the particles in the composite coating [1206]; similar high-temperature interactions were detected between HA and zirconia [931,956], as well as between HA and Ti [661,1008,1009,1011,1019,1022]. Namely, composites with low Ti content sintered at 1200 °C exhibited the main crystalline phases of $CaTiO_3$, CaO, and Ti_xP_y, while Ti_2O and residual α-Ti appeared as additional phases as the Ti content increased to 50 vol%. Therefore, the chemical interaction between HA and Ti is represented by the following non-equilibrated chemical scheme [1009]:

$$Ti + Ca_{10}(PO_4)_6(OH)_2 \rightarrow CaTiO_3 + CaO + Ti_xP_y + (Ti_2O) + (Ca_4P_2O_9) + H_2O \quad (1)$$

Such undesirable interactions between Ti and HA will be minimized if Ti particles are coated with silica [1025].

Furthermore, for HA/Al_2O_3 biocomposites, partial HA degradation and the production of different calcium aluminates were observed following sintering at 1200–1300 °C. This is believed to be caused by the diffusion of Ca^{2+} from HA into the alumina matrix and the depletion of Ca^{2+} ions from HA, which transforms HA to β-TCP. The biocomposite mechanical strength is impacted by each of these processes [964–966,1206].

To conclude this section, one should admit that, for many $CaPO_4$-containing biocomposites, the presence of some chemical bonding among the phases was found. Nevertheless, there are formulations, such as biocomposites with PE and PP, in which no chemical bonding was detected.

7. Ways to Create a Chemical Bonding among the Constituents of Biocomposites

The interaction and adhesion at the interface among the constituents have a significant impact on the properties of the composites and are essential for the transmission of loads among the phases because poor adhesion reduces the mechanical properties [301]. Therefore, an interface among the phases appears to be a very important issue in any type of composite and hybrid material. Due to this reason, sometimes, an interface is called "one of the three elements of composite material" ([1207], p. 5). When two or more materials form a composite, there are certain physical and chemical interactions among them at the interface. If they do not have compatibility to form a composite material interface, there is no bonding among them. Possible interconnections between nanosized particles and polymer chains have been classified by Kickelbick into four types (Figure 15): (1) inorganic particles embedded in inorganic polymer, (2) particle association by bonding to the polymer backbone, (3) interpenetrating networks by chemical bonding, and (4) inorganic–organic hybrid polymers [1208].

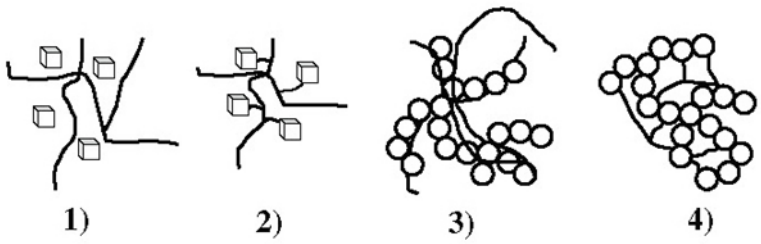

Figure 15. There are four different ways that nanosized particles can be mutually arranged to form a polymer chain: (**1**) inorganic particles embedded in an inorganic polymer; (**2**) particles incorporated by bonding to the polymer backbone; (**3**) chemical linkages forming an interpenetrating network; and (**4**) inorganic–organic hybrid polymers. Reprinted with permission from Ref. [1208].

Nevertheless, the interactions between phases are mechanical in character in a large portion of the above-mentioned formulations. This is due to the fact that the matrix is typically made up of substances devoid of unsaturated bonds or functional groups that could allow $CaPO_4$ components to form ionic complexes. It is evident that the non-polar polymer and the $CaPO_4$ ceramic particles have little in common. Thus, more promising in this regard are polymers having functional groups suspended on the polymer backbone that serve as bridges to $CaPO_4$ [337].

Various approaches have been proposed to solve this problem. Namely, researchers pressed blends with varying PLLA and HA concentrations at varying temperatures and pressures in order to optimize the filler's adherence to the matrix [1209]. About 15 weight percent of PLLA provided the maximum compressive strength; however, by using blends containing 20 wt% PLLA, the authors observed that the mechanical properties were improved with increasing pressing temperature and pressure. The first finding was attributed

to the increased wettability of HA particles due to the decrease in the viscosity of PLLA with increasing temperature. The second one was explained by the increased fluidity of the polymer at higher temperatures and increased compression and pore penetration at higher pressures. The combination of high pressure and high temperature has been found to reduce porosity, guarantee particle-polymer adhesion, and increase the compressive strength [277] and fracture energy [1210] of $CaPO_4$-containing biocomposites. Interestingly, to improve an interfacial bonding between PLLA and HA by stereocomplexation, PDLA was initially grafted onto the surface of HA particles, and then the PDLA-grafted HA particles were incorporated into a PLLA matrix [1211]. In addition, various polymer crosslinking methods have been established to tailor the chemistry of the organic and $CaPO_4$ components and keep the mechanical properties of the biocomposites constant [401].

However, using auxiliary reagents that can positively influence the interaction between the phases appears to be the most common practice. Such additives are called coupling agents [1207,1212]. All coupling agents contain two special functional groups that can be connected with two different types of materials and promote adhesion among the phases. Frequently, the effect is non-specific and can affect, for example, the rheology of the composite [268]. For example, diisocyanate coupling agents [282,1213] and other polymers [1192] were used to bind PEG/PBT (Polyactive^{TM}) block copolymers to HA filler particles. Other researchers modified a surface of nanodimensional HA with dopamine and hexamethylenediamine and grafted PLLA onto it by an aminolysis reaction. Afterward, the PLLA-grafted HA particles were blended with PLLA to fabricate PLLA/HA scaffolds by 3D printing. The results showed that the coating of the polydopamine layer introduced amino groups onto the surface of HA, which acted as active sites for grafting PLLA chains by aminolysis reaction and enhanced interfacial bonding between HAP and PLLA [1214]. Similar results with other coupling agents were obtained in other studies [1215–1217].

Thus, surface modification of the grafted HA filler significantly increased the modulus and strength of polymers compared to polymers filled with ungrafted HA [282,1213–1216]. The polymers were chemically attached to the HA particles via isocyanate groups, as demonstrated by thermogravimetric and infrared studies. This is an appropriate strategy to increase adhesion [1192]. Other researchers have used glutaraldehyde as a crosslinking reagent [415,595,597,598,613,738,779,783,1218]. Silanes [258,259,282,351,625,1219–1224], zirconates [268,351,353,1225–1227], titanates [268,351,1226,1228], phosphoric acid [629], alkaline pretreatment [867,868], PAA [1229], hexamethylene diisocyanate [1230], and other chemicals [1230] were found to have the ability to promote the interfacial bonding between $CaPO_4$ and other components. Additionally, some polymers can be grafted onto the surface of $CaPO_4$ particles [648,1230]. Namely, HA particles were modified by hexamethylene diisocyanate and cross-linked with PVA in situ to prepare a hydrogel suitable for a potential application as a calcified cartilage layer [1230].

Structural modification of the polymer matrix by, for example, adding acrylic acid [258, 259,282], has also been found to be an effective method. In HA/Polyactive^{TM} composites, for instance, the use of polyacids as binding agents produced surface-modified HA particles with enhanced mechanical qualities and greater interaction with the polymer during fracture [282]. It was discovered that the molding technique had a significant impact on the employment of titanate and zirconate binding agents [268]. Prior to being used as fillers in biodegradable composites, silane-bonded HA powders underwent testing. This process allowed HA to withstand aqueous attack without compromising its overall biological activity [1220–1224]. Furthermore, chemically modified reinforced phase–matrix interfaces were found to improve the mechanical properties of biocomposites. Examples include chemically bonded HA/PE [258,259], chemically formed HA/Ca poly(vinyl phosphonate) [299], and PLA/HA fibers [235]. Those biocomposites can consume large amounts of energy in the fracture.

The effect of some binding agents was found to combine two different mechanisms: (i) cross-linking of the polymer matrix (effective with zirconate and titanate binding agents) and (ii) enhanced interfacial interaction between the main phases of the biocomposite.

This enhanced interfacial adhesion was found to be highly dependent on the chemistry of the binding agent (pH and type of metal center) [351]. Several studies have claimed that silanes interact with HA [258,289,1220–1222], suggesting the presence of a silicon-containing interfacial phase between HA and PE that facilitates chemical adhesion between HA particles and polymers. Additionally, silane coupling agents encouraged PE to enter the spaces between individual HA particles, which strengthened the mechanical interlocking at the matrix–supporter contact [258,259].

Therefore, optimizing the properties of biocomposites with binding agents is now an important area of research. It has been suggested that controlling and enhancing the coupling between polymers and $CaPO_4$ at the molecular level is important for the resulting mechanical response of biocomposites. The fundamental molecular understanding of interfacial behavior in biocomposites appears to be an under-addressed area in the literature. Various experimental characterization techniques using electron microscopy, vibrational spectroscopy, X-ray diffraction, and scanning probe microscopy are routinely used to characterize such materials beyond mechanical characterization. In addition, atomic-scale models to simulate phase interactions and predict responses in novel material systems, including nanostructures and nanointerfaces, are important for understanding and predicting load-deformation behavior [1172].

Moreover, the $CaPO_4$ surface itself can be modified in a similar way [648,1225–1240]. This process is also known as $CaPO_4$ surface functionalization [1238]. A fascinating method for modifying the HA surface has been reported [1236]. First, during the hydrothermal synthesis of HA, 3-mercaptopropionic acid was used to achieve in situ synthesis of surface thiol-functionalized HA (HA-SH) (A in Figure 16). This was followed by the generation of sulfur-centered radicals on the HA surface by radical chain transfer (B in Figure 16) initiating surface graft polymerization of ethylene glycol methacrylate phosphate (C in Figure 16) [1236]. In one case, surface functionalization of $CaPO_4$ particles was found to reduce bacterial adhesion to their surface [1237]. Other examples can be found in the literature [648,1225–1240]. In general, the aim of surface modification is to prevent or delay the exfoliation process of $CaPO_4$ particles from the matrix and at the same time ensure homogeneous distribution of $CaPO_4$ particles in the matrix at high loading levels. Naturally, all surface modifiers must meet various biomedical requirements, such as non-toxicity, good biocompatibility, and no alteration of the biological or physicochemical properties of the filler [1238].

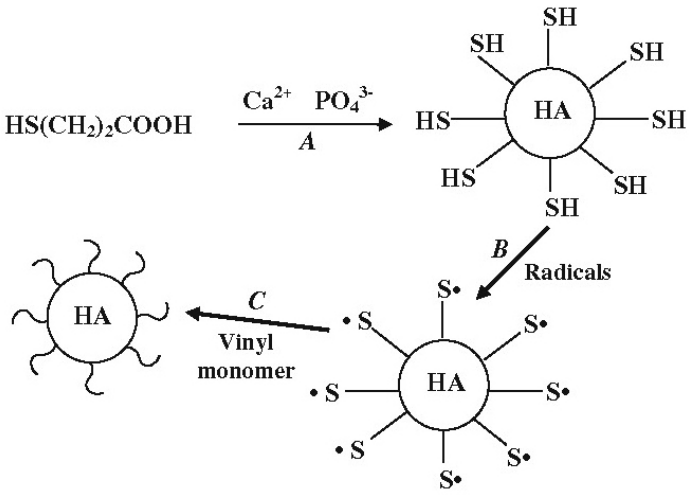

Figure 16. Grafting-induced surface alteration of HA particles: A is sulfur-centered radical on the surface of HA, B is surface thiol functionalized HA, and C is surface grafting polymerization of ethylene glycol methacrylate phosphate. Reprinted with permission from Ref. [1236].

The addition of adhesion promoters may become an alternative way to improve the interaction between the filler and matrix. For example, 4-methacryloyloxyethyl trimellitate

anhydride was added to promote polymer adhesion to HA [1241]. In another study, phosphate esters were added to the liquid component of the formulation [1242]. Both the strength and the affinity index of the biocomposite were found to increase, probably due to copolymerization.

In almost all studies on HA/carbon nanotube biocomposites, the nanotubes have been functionalized before incorporation into HA. Most researchers have achieved this via oxidation [180–182,1093,1094], but non-covalent functionalization with sodium dodecyl sulfate [1093] and coating the nanotubes with a polymer prior to incorporation into HA [1243] have also been reported. Several transmission electron microscopy studies have shown that functionalization enhances the interaction between carbon nanotubes and HA [1093,1094,1244].

To conclude, there are several ways to either improve or create chemical bonding among the constituents of $CaPO_4$-containing composites and hybrid formulations, but using coupling agents currently seems to be the most common way to solve the problem. However, the reactive sites on the $CaPO_4$ surface are so many that the content of the coupling agent is very difficult to control. According to the topical publication: "Too much coupling agent may condense with adjacent silanols to form a siloxane layer or remain partly uncondensed at the surface, which thereby decreasing the mechanical properties. Therefore, the content of the coupling agent should be controlled carefully to maximize the efficiency of interfacial reinforcement. Additionally, the coupling agent is a chemical agent, which must be studied widely in vitro and in vivo for its biocompatibility before being used in the human body" ([1207], p. 13).

8. Bioactivity and Biodegradability of $CaPO_4$-Containing Biocomposites

All types of biodegradable formulations begin to decompose and resorb in vivo by surrounding fluids and cells after implantation. The biodegradation process is accompanied by loss of mass and changes in shape and size. In general, biodegradation of implants occurs in two ways: surface erosion and bulk degradation. Surface erosion occurs mainly in the outermost layer and at the interface between the implant and the surrounding tissue, while bulk degradation occurs simultaneously in the entire volume of the implant. Therefore, biodegradation appears to be a combination of these two processes with different weights, but the underlying mechanisms depend on the type of material [1245].

The bioactivity and biodegradability of composites and hybrid formulations are therefore determined by the same properties of the components. These two processes are highly multifactorial, as the surface of the graft encounters biological fluids after implantation and is colonized by cells shortly afterward. This highly complex process involves much more biology than chemistry and materials science [1246], and many specific details are not yet known. In addition, biodegradation of all components of a biocomposite can occur simultaneously and the resulting by-products can affect both the overall process and the biodegradation of individual components. For example, in biocomposites prepared from polyesters and TCP, hydrolysis reactions of ester bonds, acid decomposition of carboxyl end groups, dissolution of TCP, and buffering reactions due to dissolved phosphate ions occur simultaneously [1247–1251]. Swelling was also detected [1246]. In those formulations, autocatalysis is inhibited, and polymer degradation is postponed by basic TCP buffering the polyester's acidic breakdown products. As a result, the pure polymer sample experiences a reduction in pH and mass at an earlier stage of degradation than the matching composite. This is not always the case, though. Namely, there have been studies showing that the presence of $CaPO_4$ does not affect the degradation rate of polymer matrices [1252–1254]. Therefore, to simplify the learning, the biodegradation of individual components needs to be considered independently. In other words, the chemical dissolution of physiologically significant $CaPO_4$ in weakly acidic media (they are nearly insoluble in alkaline solutions [74,75]) can account for the in vitro biodegradation of the compound. In the case of CDHA, this can be expressed as four successive chemical Equations (2)–(5) [1255,1256]:

$$Ca_{10-x}(HPO_4)_x(PO_4)_{6-x}(OH)_{2-x} + (2-x)H^+ = Ca_{10-x}(HPO_4)_x(PO_4)_{6-x}(H_2O)_{2-x}{}^{(2-x)+} \quad (2)$$

$$Ca_{10-x}(HPO_4)_x(PO_4)_{6-x}(H_2O)_{2-x}{}^{(2-x)+} = 3Ca_3(PO_4)_2 + (1-x)Ca^{2+} + (2-x)H_2O \quad (3)$$

$$Ca_3(PO_4)_2 + 2H^+ = Ca^{2+} + 2CaHPO_4 \quad (4)$$

$$CaHPO_4 + H^+ = Ca^{2+} + H_2PO_4{}^- \quad (5)$$

The degradation process of polymers is a chain scission process in which oligomers, monomers, and/or other low molecular weight species are formed by breaking atomic bonds, while the cleavage of polymeric bonds can be hydrolytic, enzymatic, or stimuli-associated. Therefore, the biodegradability of polymers is determined by the presence of cleavable bonds that can be broken by hydrolysis, oxidation, cellular activities, and/or enzymes, as well as under the influence of various stimuli [1245,1257]. All these types of biodegradation mechanisms of polymers are described in detail in a recent review [1258], to which the interested readers are referred. Furthermore, the biodegradability of polymers is contingent upon the subsequent factors: (1) the hydrophobicity of the monomer; (2) the chemical stability of the polymer backbone; (3) polymer morphology; (4) initial molecular weight; (5) manufacturing procedures; (6) implant geometry; and (7) porosity and pore diameter [1245,1257,1258]. The literature has a synopsis of the degradation of PLA, PGA, and SEVA-C (Ref. [125], pp. 798 and 803, in that order).

The biodegradation of HA/PLLA and CDHA/PLLA biocomposite rods in rabbit subcutaneous and medullary cavities was investigated using mechanical and histological techniques in in vivo investigations. It was found that degradation was faster when unsintered CDHA was used instead of sintered HA [1259]. Two weeks following implantation, neoplastic bone growth was seen in a more thorough investigation, particularly in preparations with a higher concentration of HA [1260]. Notably, in that instance, direct contact between these composites and bone was found, with no fiber tissue in between [1260,1261]. After 12 weeks of subcutaneous implantation, an in vivo investigation on the biodegradation of PLGA, gelatin, and PTMC microspheres/$CaPO_4$ biocomposites revealed that the microspheres broke down and their compressive strength decreased [1262]. Interestingly, the amount of $CaPO_4$ in the biocomposite was found to have a greater effect on the early stages of osteoblast behavior (cell attachment and proliferation) rather than the immediate and late stages (proliferation and differentiation) [1263]. A degradation model was also proposed for SEVA-C/HA biocomposites. It consists of three successive periods of time and, in fact, is determined by the leaching of plasticizers and low molecular weight polymeric chains with a minor HA dissolution [353].

The biodegradation of nanosized HA/collagen/PLA biocomposites was studied in 1% trypsin/phosphate-buffered saline at 37 °C for in vitro testing and the samples were implanted in the posterolateral lumbar spine of rabbits for in vivo testing [605]. The findings indicated that weight loss increased steadily in vitro, reaching a mass loss of approximately 20% after 4 weeks. The relative rates of reduction of the three components in this material varied significantly during the experimental period in vitro: collagen decreased the fastest, going from 40% by weight to about 20% in the composite; the HA content increased from 45 to approximately 60%; and the amount of PLA changed slightly. It was discovered that, in vivo, the collagen/HA ratio was marginally greater closer to the transverse processes than it was in the space between them [605]. High-strength HA/PLLA biocomposite rods were used for internal fixation of fractures in a 5–7-year in vivo study for internal fixation of fractures [1264]. In that study, both unsintered CDHA and sintered HA were used as reinforcing phases within a PLLA matrix. The prepared biocomposites were implanted into the femurs of 25 rabbits. The results showed that the implanted material resorbed six years after implantation. Bone remodeling and the presence of trabecular bone union were significant results [1264]. Data on the release kinetics of monomers from dental composites containing fluoride-doped $CaPO_4$-containing biocomposites are also available [1265].

To conclude this part, one should mention an outstanding Ph.D. thesis defended by Dr. Ismael Moreno-Gomez in 2019 at Cambridge University devoted to the mathematical modeling of the degradation of bioresorbable composites [1266], in which chapters 4 and 5 are devoted to the degradation of the TCP- and HA-containing biocomposites, respectively.

9. Biomedical and Non-Biomedical Applications

First, one should remember that the goal of this review is to inform readers of a wide variety of known $CaPO_4$-containing composites and hybrid formulations. Even cataloging them and providing a brief description of their composition and properties coupled with the key processing parameters appears to be rather long. Therefore, let me limit myself to just brief descriptions of the most important applications.

Due to the fact that $CaPO_4$ represents the major inorganic constituent of calcified tissues of mammals, most $CaPO_4$-based composites and hybrid materials have been developed for potential applications as artificial bone grafts. That is why they are called *bio*composites and *bio*materials. In addition to all that has been previously mentioned, the examples of biomedical applications of $CaPO_4$-containing formulations comprise regeneration of critical-sized mandibular defects [1267], orthopedic applications [401], bone revascularization [1268], bone tissue engineering [1269,1270], anti-cancer treatments [1064,1065], etc. Additionally, composite fillers composed of HA and CMC gel possess biostimulatory and skin-tightening properties that have been applied not just to the face but also to the body to boost rejuvenation [900,901].

Non-biomedical applications of $CaPO_4$-based composites and hybrid formulations are also known, and their amount rapidly increases [460,461,834–836,874,980,1089,1090,1271–1285]. For example, battery devices employ DCPD/polymer composites as proton conductors [460,461], an HA-contained porous gel polymer electrolyte was developed for a quasi-solid-state sodium ion battery [1280], and HA/carbon nanotube was found to be an anode modifying material [1284], while CuO/HA composites appeared to be excellent dielectric materials [1283]. Other formulations composed from $CaPO_4$ and wood processing residues, agricultural fibers (such as dried crushed sugarcane bagasse), pulp mill sludge, or waste-paper were found to meet the requirements for Portland-cement-bonded particleboards [1271]. In addition, nano-fibrillated cellulose/HA composites appeared to possess excellent fire [1273] and water [874] resistances, while both HA/calcium silicate [1274] and HA/manganese dioxide [980] were found to be effective adsorbents for Pb removal from aqueous solutions. All-weather flexible electrically conductive paper [1272] and another recyclable, fire-resistant, superhydrophobic, and magnetic paper [1278] were produced using nanodimensional HA wires, while a heat-insulating and fire-retardant inorganic paper was produced by employing ultralong HA nanowires as scaffolds for silica aerogels particles [1277]. HA/gold composites appear to preserve some wooden artifacts [1276]. Furthermore, PEG/HA composites appeared to be a suitable phase change material, which was useful for thermal energy storage [1275], while a full-daytime sub-ambient cooling TCP/acrylic paint was found to be effective for energy saving [1281]. In addition, $CaPO_4$/chitosan composites could be used as a plant growth promoter [1282], while HA/gelatin ones appeared to resemble a synthetic ivory suitable to produce piano keys [1279]. Finally, there are different fields of application for bone char, starting from environmental remediation to sustainable agriculture and catalysis [1089,1090].

However, the most unusual application of $CaPO_4$-based composites and hybrid formulations lies at the interface between biomedical and non-biomedical applications. Namely, there is a recent study in which simple, translucent, highly stretchable, and high-performance HA/polydimethylsiloxane bionanocomposite film-based triboelectric nanogenerators were developed to synergistically capture external mechanical energy from biomechanical sources, such as wearable devices, into electricity [1286]. A triboelectric nanogenerator (2×2 cm^2) with a pushing force of 2 N and different amounts of HA in polydimethylsiloxane produced a highly stable output voltage, current, surface charge density, and power density values of 300 V, 22.4 μA, 90.36 $\mu C/m^2$, and 27.34 W/m^2, which were 6-, 9-, and 10-times higher than those without HA, respectively. The HA/polydimethylsiloxane bionanocomposites were found to exhibit a remarkable stretchability of more than 290%. The authors attached these nanogenerators to cloth, skin, an insole, and a person's lap. Effectively harvesting energy from body movements, the triboelectric nanogenerators may be used to charge multiple commercial capacitors, drive up to 100 LEDs, and power a

low-power electronic device, such as a commercial calculator. Therefore, self-powered sensing and wearable devices are made possible by HA/polydimethylsiloxane biocomposite nanogenerators, which allow their large-scale preparation and deployment [1286].

10. Some Issues and Key Challenges

The objective of this review is to summarize scientific information on various fabrication approaches that have been used to produce a broad range of $CaPO_4$-based composites and hybrid formulations. These materials aim to enhance the weak properties of $CaPO_4$ bioceramics, specifically mechanical ones, without compromising their biological performances. However, reasonable compromises are often necessary. Nevertheless, these biocomposites, particularly if enhanced by biologically active biocompounds like osteoconductive and osteoinductive factors, as well as osteogenic cells, are already of significant interest as a novel group of adaptable biomaterials and are acknowledged for their usefulness in numerous bone grafting applications [22,1287]. Regrettably, despite the significant development and testing of $CaPO_4$-based composites and hybrid formulations in numerous biomedical applications, their commercial distribution and industrial production fall short of expectations. Presumably, this stems from the fact that each formulation and fabrication technique has specific advantages and disadvantages. As a result, there are still disputes that need to be explored further in bone tissue engineering to obtain suitable $CaPO_4$-based biocomposite scaffolds with tunable properties. Therefore, better comprehension of their performance and limitations is necessary for their biomedical applications, which require further in vivo investigations. The main issues are summarized as follows [251]:

- When compared to traditional monolithic materials, the long-term performance of biocomposites is not well-supported by sufficient credible experimental and clinical data.
- The number of design variables that must be taken into account makes the design of hybrid and composite formulations significantly more challenging than the design of classic single-phase ones.
- Manufacturing techniques might be costly, time-consuming, dependent on cutting-edge technology, and restricted to certain reinforcing configurations. They might also call for certain cleaning and sterilizing procedures.
- There are currently no adequate guidelines for biocompatibility testing of biocomposite implants since it is unclear how the components of biocomposites interact with biological tissues.
- The fatigue behavior of biocomposites is much more complex and less predictable than conventional single-phase materials and there are not enough criteria to evaluate the fatigue performance of the biocomposites.

Significant research remains to be conducted regarding the analysis of cells and their various behaviors in relation to interacting with $CaPO_4$-containing biocomposites. Crucial unresolved questions include the following: (1) What mechanisms underlie the promotion of cellular growth and differentiation by these biocomposites? (2) How can these pathways be determined? In the future, biocomposite surfaces will be functionalized with molecules of various properties and sizes that can selectively interact with biomolecules, such as proteins and peptides, by binding to cells [218].

Although processing techniques for biocomposites have advanced significantly, there is still a need for more sophisticated technological advances to produce bone-like hierarchical structures at various length scales to achieve the desired properties. The development of new implantable materials relies on advances in research on natural bone structure. One of the primary obstacles is to comprehend the basis of biomineralization and then effectively apply this knowledge to develop superior synthetic methods for producing bone graft materials. Unfortunately, the production of biocomposites that mimic natural bone at nanometer to micrometer levels presents numerous poorly understood issues, such as morphological regulation, the addition of foreign ions, interactions with proteins, and the construction of organic and inorganic phases. The gap in processing between lower-grade constituent units and higher-grade architectures may considerably restrict the practical

applications of existing $CaPO_4$-based composites and hybrid formulations. Thus, important additional research endeavors are outlined to tackle the ensuing crucial challenges [22]:

- Optimization of processing conditions for biocomposites.
- Enhancement of interfacial adhesion and strength similar to that of genuine bone.
- To facilitate bone formation, both surface characteristics and pore size should be optimized.
- Maintaining sufficient in vivo structure volume for osteogenesis to occur.
- Resistance to load-bearing conditions.
- Matching the bioabsorbability and biomechanical properties of the graft when creating new bone.
- Understanding the molecular processes by which cells and biocomposite matrices interact in vivo to support bone regeneration is necessary.
- Promoting angiogenesis and vascularization for healthy bone cell growth and subsequent tissue formation and remodeling.

To widely commercialize $CaPO_4$-based composites and hybrid formulations in surgery and medicine, these important difficulties must be resolved.

11. Conclusions

The calcified tissues in mammals contain poorly crystalline ion-substituted $CaPO_4$ with an apatitic structure (CDHA) and have a complex hierarchical assembly, making them complicated bioorganic/inorganic composites. Their mechanical properties are remarkable, considering the weak components they consist of, surpassing what can be achieved by currently available synthetic materials. This is due to the fact that organisms produce biocomposites that are hierarchically ordered at the nano, micro, and meso levels and comprise brittle $CaPO_4$ and ductile bio-organic components. These biocomposites are organized in both composition and structure. Furthermore, calcified tissues always have multiple functions, therefore necessitating multifunctional $CaPO_4$-containing composites and hybrid formulations [1288]. Bone provides structural support for the body and is responsible for hematopoiesis. Additionally, in contrast to current synthetic systems, biological systems possess the capacity for self-repair, which is almost universal in nature. These intricate structures, developed over millions of years of evolution, have motivated materials scientists to create novel biomaterials [1289].

The present review highlights a wide range of $CaPO_4$-containing composites and hybrid formulations currently available for biomedical applications. By synergizing the favorable biocompatible properties of $CaPO_4$ with the mechanical ones of other compounds, a significant potential arises for the advancement of bone substitute materials with markedly improved microstructure and properties. Therefore, it is essential to develop multiphase biocomposites that offer a multistage design approach and consequently offer more control over their material and biological properties than the individual constituents alone. As a result, the addition of $CaPO_4$ to polymers was conceived, leading to the development of bioactive biodegradable biocomposites from the originally bioinert monolithic materials used in the 1970s and 1980s. These materials are now utilized as elasticity-matched biomaterials and recently as scaffolds for tissue engineering [1290]. The application of traditional composite manufacturing techniques to the biomaterials field has resulted in this approach. The review's summary of several studies shows that there are several benefits to using a brittle, tough, bioactive $CaPO_4$ filler in combination with a ductile matrix for biomedical applications. The favorable characteristics of each component can offset the inadequate mechanical performance of $CaPO_4$ bioceramics. Furthermore, the beneficial bioactive features of $CaPO_4$ can improve the qualities of the other phase, broadening the in vivo usage capabilities of both materials [66,67]. However, the literature review indicates that researchers have primarily investigated simple, complex, and graded $CaPO_4$-based composites and hybrid formulations, as well as fibrous, laminar, and particulate ones (refer to Section 2 for the classification types of composites). $CaPO_4$-containing composites and hybrid formulations have already been developed in various forms, including scaf-

folds [1291], coatings [1292,1293], injectable [567,904], self-hardening formulations [478], and concretes [517,518]. However, in the future, further attention should be given to elaborating and developing both hierarchical and hybrid biocomposites. In addition, the research will continue to prioritize shape memory biocomposites [389–391], further developments of functionally graded composites [1294], biocomposites with novel properties, such as piezoelectric ones [1295], and biocomposites with therapeutic properties for bone tissue engineering applications. These innovative formulations offer multiple benefits, including reduced incision length, mimicking of bone porosity, controlled and increased strength, and potential antibacterial and anti-inflammatory effects. Furthermore, in accordance with current trends in tissue engineering, next-generation $CaPO_4$-based composites and hybrid formulations should incorporate various biological components, such as hormones, bioactive factors, drugs, and living cells [1269,1296,1297]. These components could augment the biomaterials' osteoconductivity, osteointegration potential, and biocompatibility, thus making them suitable for biomedical applications.

Funding: This research received no external funding.

Conflicts of Interest: The authors declare no conflict of interest.

Abbreviations

A-W	apatite-wollastonite
BMP	bone morphogenetic protein
BSA	bovine serum albumin
CMC	carboxymethylcellulose
DNA	desoxynucleic acid
EVOHa	copolymer of ethylene and vinyl alcohol
IBS	injectable bone substitute
HDPE	high-density polyethylene
HPMC	hydroxypropylmethylcellulose
PA	polyamide
PAA	polyacrylic acid
PBT	polybutyleneterephthalate
PCL	poly(ε-caprolactone)
PDLA	poly(D-lactic acid)
PDLLA	poly(D,L-lactic acid)
PE	polyethylene
PEEK	polyetheretherketone
PEG	polyethylene glycol
PGA	polyglycolic acid
PHB	polyhydroxybutyrate
PHBHV	poly(hydroxybutyrate-*co*-hydroxyvalerate)
PHEMA	polyhydroxyethyl methacrylate
PLA	polylactic acid
PLGA	poly(lactic-*co*-glycolic) acid
PLGC	*co*-polyester lactide-*co*-glycolide-*co*-ε-caprolactone
PLLA	poly(L-lactic acid)
PMMA	polymethylmethacrylate
PP	polypropylene
PPF	poly(propylene-*co*-fumarate)
PSZ	partially stabilized zirconia
PTMC	poly(trimethylene carbonate)
PU	polyurethane
PVA	polyvinyl alcohol
PVAP	polyvinyl alcohol phosphate

References

1. Kaveh, K.; Ibrahim, R.; Bakar, M.Z.A.; Ibrahim, T.A. Bone grafting and bone graft substitutes. *J. Anim. Vet. Adv.* **2010**, *9*, 1055–1067. [CrossRef]
2. Shibuya, N.; Jupiter, D.C. Bone graft substitute: Allograft and xenograft. *Clin. Podiatr. Med. Surg.* **2015**, *32*, 21–34. [CrossRef]
3. Georgeanu, V.A.; Gingu, O.; Antoniac, I.V.; Manolea, H.O. Current options and future perspectives on bone graft and biomaterials substitutes for bone repair, from clinical needs to advanced biomaterials research. *Appl. Sci.* **2023**, *13*, 8471. [CrossRef]
4. Li, S.; Chen, Y.; Lin, Z.; Cui, W.; Zhao, J.; Su, W. A systematic review of randomized controlled clinical trials comparing hamstring autografts versus bone-patellar tendon-bone autografts for the reconstruction of the anterior cruciate ligament. *Arch. Orthop. Trauma Surg.* **2012**, *132*, 1287–1297. [CrossRef]
5. Gillman, C.E.; Jayasuriya, A.C. FDA-approved bone grafts and bone graft substitute devices in bone regeneration. *Mater. Sci. Eng. C* **2021**, *130*, 112466. [CrossRef]
6. Keller, E.E.; Triplett, W.W. Iliac crest bone grafting: Review of 160 consecutive cases. *J. Oral Maxillofac. Surg.* **1987**, *45*, 11–14. [CrossRef]
7. Giladi, A.M.; Rinkinen, J.R.; Higgins, J.P.; Iorio, M.L. Donor-site morbidity of vascularized bone flaps from the distal femur: A systematic review. *Plast. Reconstr. Surg.* **2018**, *142*, 363E–372E. [CrossRef]
8. Boehm, K.S.; Al-Taha, M.; Morzycki, A.; Samargandi, O.A.; Al-Youha, S.; Leblanc, M.R. Donor site morbidities of iliac crest bone graft in craniofacial surgery: A systematic review. *Ann. Plas. Surg.* **2019**, *83*, 352–358. [CrossRef]
9. Attia, A.K.; Mahmoud, K.; ElSweify, K.; Bariteau, J.; Labib, S.A. Donor site morbidity of calcaneal, distal tibial and proximal tibial cancellous bone autografts in foot and ankle surgery. A systematic review and meta-analysis of 2296 bone grafts. *Foot Ankle Surg.* **2022**, *28*, 680–690. [CrossRef]
10. Li, Z.; Kawashita, M. Current progress in inorganic artificial biomaterials. *J. Artif. Organ.* **2011**, *14*, 163–170. [CrossRef]
11. Bojar, W.; Kucharska, M.; Ciach, T.; Koperski, Ł.; Jastrzębski, Z.; Szałwiński, M. Bone regeneration potential of the new chitosan-based alloplastic biomaterial. *J. Biomater. Appl.* **2014**, *28*, 1060–1068. [CrossRef]
12. Wickramasinghe, M.L.; Dias, G.J.; Premadasa, K.M.G.P. A novel classification of bone graft materials. *J. Biomed. Mater. Res. B Appl. Biomater.* **2022**, *110*, 1724–1749. [CrossRef]
13. Panchbhavi, V.K. Synthetic bone grafting in foot and ankle surgery. *Foot Ankle Clin.* **2010**, *15*, 559–576. [CrossRef]
14. Weiner, S.; Wagner, H.D. The material bone: Structure-mechanical function relations. *Ann. Rev. Mater. Sci.* **1998**, *28*, 271–298. [CrossRef]
15. Rey, C.; Combes, C.; Drouet, C.; Glimcher, M.J. Bone mineral: Update on chemical composition and structure. *Osteoporos. Int.* **2009**, *20*, 1013–1021. [CrossRef]
16. Dorozhkin, S.V. *Calcium Orthophosphates: Applications in Nature, Biology and Medicine*; Pan Stanford: Singapore, 2012; p. 854.
17. Dorozhkin, S.V. *Calcium Orthophosphate-Based Bioceramics and Biocomposites*; Wiley-VCH: Weinheim, Germany, 2016; p. 405.
18. Burr, D.B. The contribution of the organic matrix to bone's material properties. *Bone* **2002**, *31*, 8–11. [CrossRef]
19. Fratzl, P.; Gupta, H.S.; Paschalis, E.P.; Roschger, P. Structure and mechanical quality of the collagen-mineral nano-composite in bone. *J. Mater. Chem.* **2004**, *14*, 2115–2123. [CrossRef]
20. Olszta, M.J.; Cheng, X.G.; Jee, S.S.; Kumar, B.R.; Kim, Y.Y.; Kaufman, M.J.; Douglas, E.P.; Gower, L.B. Bone structure and formation: A new perspective. *Mater. Sci. Eng. R* **2007**, *58*, 77–116. [CrossRef]
21. Fonseca, H.; Moreira-Gonçalves, D.; Coriolano, H.J.A.; Duarte, J.A. Bone quality: The determinants of bone strength and fragility. *Sports Med.* **2014**, *44*, 37–53. [CrossRef]
22. Murugan, R.; Ramakrishna, S. Development of nanocomposites for bone grafting. *Compos. Sci. Technol.* **2005**, *65*, 2385–2406. [CrossRef]
23. Suchanek, W.; Yoshimura, M. Processing and properties of hydroxyapatite-based biomaterials for use as hard tissue replacement implants. *J. Mater. Res.* **1998**, *13*, 94–117. [CrossRef]
24. Vallet-Regi, M.; Arcos, D. Nanostructured hybrid materials for bone tissue regeneration. *Curr. Nanosci.* **2006**, *2*, 179–189. [CrossRef]
25. Doblaré, M.; Garcia, J.M.; Gómez, M.J. Modelling bone tissue fracture and healing: A review. *Eng. Fract. Mech.* **2004**, *71*, 1809–1840. [CrossRef]
26. Vallet-Regi, M. Revisiting ceramics for medical applications. *Dalton Trans.* **2006**, *44*, 5211–5220. [CrossRef]
27. Pioletti, D.P. Biomechanics in bone tissue engineering. *Comput. Methods Biomech. Biomed. Eng.* **2010**, *13*, 837–846. [CrossRef]
28. Huiskes, R.; Ruimerman, R.; van Lenthe, H.G.; Janssen, J.D. Effects of mechanical forces on maintenance and adaptation of form in trabecular bone. *Nature* **2000**, *405*, 704–706. [CrossRef]
29. Boccaccini, A.R.; Blaker, J.J. Bioactive composite materials for tissue engineering scaffolds. *Expert Rev. Med. Dev.* **2005**, *2*, 303–317. [CrossRef]
30. Hutmacher, D.W.; Schantz, J.T.; Lam, C.X.F.; Tan, K.C.; Lim, T.C. State of the art and future directions of scaffold-based bone engineering from a biomaterials perspective. *J. Tissue Eng. Regen. Med.* **2007**, *1*, 245–260. [CrossRef]
31. Guarino, V.; Causa, F.; Ambrosio, L. Bioactive scaffolds for bone and ligament tissue. *Expert Rev. Med. Dev.* **2007**, *4*, 405–418. [CrossRef]
32. Yunos, D.M.; Bretcanu, O.; Boccaccini, A.R. Polymer-bioceramic composites for tissue engineering scaffolds. *J. Mater. Sci.* **2008**, *43*, 4433–4442. [CrossRef]

33. Zhao, H.X. Progress of study on drug-loaded chitosan/hydroxyapatite composite in bone tissue engineering. *J. Funct. Mater.* **2014**, *45*, 13006–13012+13020.
34. Hench, L.L.; Polak, J.M. Third-generation biomedical materials. *Science* **2002**, *295*, 1014–1017. [CrossRef]
35. Mathijsen, A. *Nieuwe Wijze van Aanwending van het Gips-Verband bij Beenbreuken*; J.B. van Loghem: Haarlem, The Netherlands, 1852; p. 21.
36. Dreesman, H. Über Knochenplombierung. *Beitr. Klin. Chir.* **1892**, *9*, 804–810.
37. Wang, M. Developing bioactive composite materials for tissue replacement. *Biomaterials* **2003**, *24*, 2133–2151. [CrossRef]
38. Available online: https://en.wikipedia.org/wiki/Composite_material (accessed on 10 May 2024).
39. Gibson, R.F. A review of recent research on mechanics of multifunctional composite materials and structures. *Compos. Struct.* **2010**, *92*, 2793–2810. [CrossRef]
40. Evans, S.L.; Gregson, P.J. Composite technology in load-bearing orthopaedic implants. *Biomaterials* **1998**, *19*, 1329–1342. [CrossRef]
41. Wan, Y.Z.; Hong, L.; Jia, S.R.; Huang, Y.; Zhu, Y.; Wang, Y.L.; Jiang, H.J. Synthesis and characterization of hydroxyapatite-bacterial cellulose nanocomposites. *Compos. Sci. Technol.* **2006**, *66*, 1825–1832. [CrossRef]
42. Oyane, A. Development of apatite-based composites by a biomimetic process for biomedical applications. *J. Ceram. Soc. Jpn.* **2010**, *118*, 77–81. [CrossRef]
43. Dorozhkin, S.V. Calcium orthophosphate coatings on magnesium and its biodegradable alloys. *Acta Biomater.* **2014**, *10*, 2919–2934. [CrossRef]
44. Varadavenkatesan, T.; Vinayagam, R.; Pai, S.; Kathirvel, B.; Pugazhendhi, A.; Selvaraj, R. Synthesis, biological and environmental applications of hydroxyapatite and its composites with organic and inorganic coatings. *Prog. Org. Coat.* **2021**, *151*, 106056. [CrossRef]
45. Wysokowski, M.; Machałowski, T.; Idaszek, J.; Chlanda, A.; Jaroszewicz, J.; Heljak, M.; Niemczak, M.; Piasecki, A.; Gajewska, M.; Ehrlich, H.; et al. Deep eutectic solvent-assisted fabrication of bioinspired 3D carbon–calcium phosphate scaffolds for bone tissue engineering. *RSC Adv.* **2023**, *13*, 21971–21981. [CrossRef]
46. Dorozhkin, S.V. There are over 60 ways to produce biocompatible calcium orthophosphate ($CaPO_4$) deposits on various substrates. *J. Compos. Sci.* **2023**, *7*, 273. [CrossRef]
47. Zhao, J.; Guo, L.Y.; Yang, X.B.; Weng, J. Preparation of bioactive porous HA/PCL composite scaffolds. *Appl. Surf. Sci.* **2008**, *255*, 2942–2946. [CrossRef]
48. Dorozhkin, S.; Ajaal, T. Strengthening of dense bioceramic samples using bioresorbable polymers—A statistical approach. *J. Biomim. Biomater. Tiss. Eng.* **2009**, *4*, 27–39. [CrossRef]
49. Woo, A.S.; Jang, J.L.; Liberman, R.F.; Weinzweig, J. Creation of a vascularized composite graft with acellular dermal matrix and hydroxyapatite. *Plast. Reconstr. Surg.* **2010**, *125*, 1661–1669. [CrossRef]
50. Vila, M.; Sánchez-Salcedo, S.; Cicuéndez, M.; Izquierdo-Barba, I.; Vallet-Regí, M. Novel biopolymer-coated hydroxyapatite foams for removing heavy-metals from polluted water. *J. Hazard. Mater.* **2011**, *192*, 71–77. [CrossRef]
51. Furko, M.; Detsch, R.; Tolnai, I.; Tolnai, I.; Balázsi, K.; Boccaccini, A.R.; Balázsi, C. Biomimetic mineralized amorphous carbonated calcium phosphate-polycaprolactone bioadhesive composites as potential coatings on implant materials. *Ceram. Int.* **2023**, *49 Pt B*, 18565–18576. [CrossRef]
52. Dong, J.; Uemura, T.; Kojima, H.; Kikuchi, M.; Tanaka, J.; Tateishi, T. Application of low-pressure system to sustain in vivo bone formation in osteoblast/porous hydroxyapatite composite. *Mater. Sci. Eng. C* **2001**, *17*, 37–43. [CrossRef]
53. Mikán, J.; Villamil, M.; Montes, T.; Carretero, C.; Bernal, C.; Torres, M.L.; Zakaria, F.A. Porcine model for hybrid material of carbonated apatite and osteoprogenitor cells. *Mater. Res. Innov.* **2009**, *13*, 323–326. [CrossRef]
54. Oe, K.; Miwa, M.; Nagamune, K.; Sakai, Y.; Lee, S.Y.; Niikura, T.; Iwakura, T.; Hasegawa, T.; Shibanuma, N.; Hata, Y.; et al. Nondestructive evaluation of cell numbers in bone marrow stromal cell/β-tricalcium phosphate composites using ultrasound. *Tissue Eng. C* **2010**, *16*, 347–353. [CrossRef]
55. Kundu, B.; Soundrapandian, C.; Nandi, S.K.; Mukherjee, P.; Dandapat, N.; Roy, S.; Datta, B.K.; Mandal, T.K.; Basu, D.; Bhattacharya, R.N. Development of new localized drug delivery system based on ceftriaxone-sulbactam composite drug impregnated porous hydroxyapatite: A systematic approach for in vitro and in vivo animal trial. *Pharm. Res.* **2010**, *27*, 1659–1676. [CrossRef]
56. Skrinda-Melne, M.; Locs, J.; Grava, A.; Dubnika, A. Calcium phosphates enhanced with liposomes—The future of bone regeneration and drug delivery. *J. Liposome Res.* **2024**. *early view*. [CrossRef]
57. Holzmeister, I.; Schamel, M.; Groll, J.; Gbureck, U.; Vorndran, E. Artificial inorganic biohybrids: The functional combination of microorganisms and cells with inorganic materials. *Acta Biomater.* **2018**, *74*, 17–35. [CrossRef]
58. Kickelbick, G. (Ed.) *Hybrid Materials. Synthesis, Characterization and Applications*; Wiley-VCH Verlag: Weinheim, Germany, 2007; p. 498.
59. Matthews, F.L.; Rawlings, R.D. *Composite Materials: Engineering and Science*; CRC Press: Boca Raton, FL, USA, 2000; p. 480.
60. Xia, Z.; Riester, L.; Curtin, W.A.; Li, H.; Sheldon, B.W.; Liang, J.; Chang, B.; Xu, J.M. Direct observation of toughening mechanisms in carbon nanotube ceramic matrix composites. *Acta Mater.* **2004**, *52*, 931–944. [CrossRef]
61. Tavares, M.I.B.; Ferreira, O.; Preto, M.; Miguez, E.; Soares, I.L.; da Silva, E.P. Evaluation of composites miscibility by low field NMR. *Int. J. Polym. Mater.* **2007**, *56*, 1113–1118. [CrossRef]

62. Kiran, E. Polymer miscibility, phase separation, morphological modifications and polymorphic transformations in dense fluids. *J. Supercrit. Fluids* **2009**, *47*, 466–483. [CrossRef]
63. Šupová, M. Problem of hydroxyapatite dispersion in polymer matrices: A review. *J. Mater. Sci. Mater. Med.* **2009**, *20*, 1201–1213. [CrossRef]
64. Böstman, O.; Pihlajamäki, H. Clinical biocompatibility of biodegradable orthopaedic implants for internal fixation: A review. *Biomaterials* **2000**, *21*, 2615–2621. [CrossRef]
65. Zhang, X.D.; Williams, D.F. (Eds.) Definitions of biomaterials for the twenty-first century. In Proceedings of the Consensus Conference, Chengdu, China, 11–12 June 2018; Materials Today. Elsevier: Amsterdam, The Netherlands, 2019; p. 290.
66. John, M.J.; Thomas, S. Biofibres and biocomposites. *Carbohydr. Polym.* **2008**, *71*, 343–364. [CrossRef]
67. Tanner, K.E. Bioactive ceramic-reinforced composites for bone augmentation. *J. R. Soc. Interface* **2010**, *7*, S541–S557. [CrossRef]
68. Gravitis, Y.A.; Tééyaér, R.E.; Kallavus, U.L.; Andersons, B.A.; Ozol'-Kalnin, V.G.; Kokorevich, A.G.; Érin'sh, P.P.; Veveris, G.P. Biocomposite structure of wood cell membranes and their destruction by explosive autohydrolysis. *Mech. Compos. Mater.* **1987**, *22*, 721–725. [CrossRef]
69. Bernard, S.L.; Picha, G.J. The use of coralline hydroxyapatite in a 'biocomposite' free flap. *Plast. Reconstr. Surg.* **1991**, *87*, 96–107. [CrossRef]
70. Rao, H.; Thompson, W.A.; Katz, J.L.; Harper, R.A. Elastic constants of the composite system hydroxyapatite-dicalcium phosphate dihydrate. *J. Dent. Res.* **1976**, *55*, 708. [CrossRef]
71. Dorozhkin, S.V. Calcium orthophosphates and human beings. A historical perspective from the 1770s until 1940. *Biomatter* **2012**, *2*, 53–70. [CrossRef]
72. Dorozhkin, S.V. A detailed history of calcium orthophosphates from 1770s till 1950. *Mater. Sci. Eng. C* **2013**, *33*, 3085–3110. [CrossRef]
73. Hing, K.A. Bioceramic bone graft substitutes: Influence of porosity and chemistry. *Int. J. Appl. Ceram. Technol.* **2005**, *2*, 184–199. [CrossRef]
74. Naqshbandi, A.R.; Sopyan, I. Development of porous calcium phosphate bioceramics for bone implant applications: A review. *Rec. Pat. Mater. Sci.* **2013**, *6*, 238–252.
75. LeGeros, R.Z. Calcium Phosphates in Oral Biology and Medicine. In *Monographs in Oral Science*; Myers, H.M., Ed.; Karger: Basel, Switzerland, 1991; Volume 15, p. 201.
76. Elliott, J.C. *Structure and Chemistry of the Apatites and Other Calcium Orthophosphates, Studies in Inorganic Chemistry*; Elsevier: Amsterdam, The Netherlands, 1994; Volume 18, p. 389.
77. Heimann, R.B. (Ed.) *Calcium Phosphate: Structure, Synthesis, Properties and Applications*; Nova Science: New York, NY, USA, 2012; p. 498.
78. Gshalaev, V.S.; Demirchan, A.C. (Eds.) *Hydroxyapatite: Synthesis, Properties and Applications*; Nova Science: New York, NY, USA, 2012; p. 477.
79. Carraher, C.E., Jr. *Introduction to Polymer Chemistry*, 2nd ed.; CRC Press: Boca Raton, FL, USA, 2010; p. 534.
80. Young, R.J.; Lovell, P.A. *Introduction to Polymers*, 3rd ed.; CRC Press: Boca Raton, FL, USA, 2011; p. 688.
81. Thomson, R.C.; Ak, S.; Yaszemski, M.J.; Mikos, A.G. Polymer scaffold processing. In *Principles of Tissue Engineering*; Academic Press: New York, NY, USA, 2000; pp. 251–262.
82. Khan, M.U.A.; Aslam, M.A.; Abdullah, M.F.B.; Hasan, A.; Shah, S.A.; Stojanović, G.M. Recent perspective of polymeric biomaterial in tissue engineering—A review. *Mater. Today Chem.* **2023**, *34*, 101818. [CrossRef]
83. Shastri, V.P. Non-degradable biocompatible polymers in medicine: Past, present and future. *Curr. Pharm. Biotechnol.* **2003**, *4*, 331–337. [CrossRef]
84. Chen, H.; Yuan, L.; Song, W.; Wu, Z.; Li, D. Biocompatible polymer materials: Role of protein-surface interactions. *Prog. Polym. Sci.* **2008**, *33*, 1059–1087. [CrossRef]
85. Tanaka, M.; Sato, K.; Kitakami, E.; Kobayashi, S.; Hoshiba, T.; Fukushima, K. Design of biocompatible and biodegradable polymers based on intermediate water concept. *Polym. J.* **2015**, *47*, 114–121. [CrossRef]
86. Lanza, R.P.; Hayes, J.L.; Chick, W.L. Encapsulated cell technology. *Nat. Biotechnol.* **1996**, *14*, 1107–1111. [CrossRef]
87. Shukla, S.C.; Singh, A.; Pandey, A.K.; Mishra, A. Review on production and medical applications of ε-polylysine. *Biochem. Eng. J.* **2012**, *65*, 70–81. [CrossRef]
88. Agrawal, C.M.; Ray, R.B. Biodegradable polymeric scaffolds for musculoskeletal tissue engineering. *J. Biomed. Mater. Res.* **2001**, *55*, 141–150. [CrossRef]
89. Kweon, H.; Yoo, M.; Park, I.; Kim, T.; Lee, H.; Lee, S.; Oh, J.; Akaike, T.; Cho, C. A novel degradable polycaprolactone network for tissue engineering. *Biomaterials* **2003**, *24*, 801–808. [CrossRef]
90. Wang, Y.C.; Zhang, P.H. Electrospun absorbable polycaprolactone (PCL) scaffolds for medical applications. *Adv. Mater. Res.* **2014**, *906*, 221–225. [CrossRef]
91. Sartori, S.; Chiono, V.; Tonda-Turo, C.; Mattu, C.; Gianluca, C. Biomimetic polyurethanes in nano and regenerative medicine. *J. Mater. Chem. B* **2014**, *2*, 5128–5144. [CrossRef]
92. Temenoff, J.S.; Mikos, A.G. Injectable biodegradable materials for orthopedic tissue engineering. *Biomaterials* **2000**, *21*, 2405–2412. [CrossRef]

93. Behravesh, E.; Yasko, A.W.; Engel, P.S.; Mikos, A.G. Synthetic biodegradable polymers for orthopaedic applications. *Clin. Orthop. Rel. Res.* **1999**, *367S*, S118–S125. [CrossRef]
94. Lewandrowski, K.U.; Gresser, J.D.; Wise, D.L.; White, R.L.; Trantolo, D.J. Osteoconductivity of an injectable and bioresorbable poly(propyleneglycol-co-fumaric acid) bone cement. *Biomaterials* **2000**, *21*, 293–298. [CrossRef]
95. Lee, K.W.; Wang, S.; Fox, B.C.; Ritman, E.L.; Yaszemski, M.J.; Lu, L. Poly(propylene fumarate) bone tissue engineering scaffold fabrication using stereolithography: Effects of resin formulations and laser parameters. *Biomacromolecules* **2007**, *8*, 1077–1084. [CrossRef]
96. Xu, J.; Feng, E.; Song, J. Renaissance of aliphatic polycarbonates: New techniques and biomedical applications. *J. Appl. Polym. Sci.* **2014**, *131*, 39822. [CrossRef]
97. Boland, E.D.; Coleman, B.D.; Barnes, C.P.; Simpson, D.G.; Wnek, G.E.; Bowlin, G.L. Electrospinning polydioxanone for biomedical applications. *Acta Biomater.* **2005**, *1*, 115–123. [CrossRef]
98. Swain, S.K.; Prusty, K. Biomedical applications of acrylic-based nanohydrogels. *J. Mater. Sci.* **2018**, *53*, 2303–2325. [CrossRef]
99. Frazer, R.Q.; Byron, R.T.; Osborne, P.B.; West, K.P. PMMA: An essential material in medicine and dentistry. *J. Long-Term Eff. Med. Implants* **2005**, *15*, 629–639. [CrossRef]
100. Li, Y.W.; Leong, J.C.Y.; Lu, W.W.; Luk, K.D.K.; Cheung, K.M.C.; Chiu, K.Y.; Chow, S.P. A novel injectable bioactive bone cement for spinal surgery: A developmental and preclinical study. *J. Biomed. Mater. Res.* **2000**, *52*, 164–170. [CrossRef]
101. Mckellop, H.; Shen, F.; Lu, B.; Campbell, P.; Salovey, R. Development of an extremely wear resistant UHMW polyethylene for total hip replacements. *J. Orthop. Res.* **1999**, *17*, 157–167. [CrossRef]
102. Kurtz, S.M.; Muratoglu, O.K.; Evans, M.; Edidin, A.A. Advances in the processing, sterilization and crosslinking of ultra-high molecular weight polyethylene for total joint arthroplasty. *Biomaterials* **1999**, *20*, 1659–1688. [CrossRef]
103. Laurencin, C.T.; Ambrosio, M.A.; Borden, M.D.; Cooper, J.A., Jr. Tissue engineering: Orthopedic applications. *Ann. Rev. Biomed. Eng.* **1999**, *1*, 19–46. [CrossRef]
104. Meijer, G.J.; Cune, M.S.; van Dooren, M.; de Putter, C.; van Blitterswijk, C.A. A comparative study of flexible (Polyactive™) versus rigid (hydroxylapatite) permucosal dental implants. I. Clinical aspects. *J. Oral Rehabil.* **1997**, *24*, 85–92. [CrossRef]
105. Meijer, G.J.; Dalmeijer, R.A.; de Putter, C.; van Blitterswijk, C.A. A comparative study of flexible (Polyactive™) versus rigid (hydroxylapatite) permucosal dental implants. II. Histological aspects. *J. Oral Rehabil.* **1997**, *24*, 93–101. [CrossRef]
106. Waris, E.; Ashammakhi, N.; Lehtimäki, M.; Tulamo, R.M.; Törmälä, P.; Kellomäki, M.; Konttinen, Y.T. Long-term bone tissue reaction to polyethylene oxide/polybutylene terephthalate copolymer (Polyactive®) in metacarpophalangeal joint reconstruction. *Biomaterials* **2008**, *29*, 2509–2515. [CrossRef]
107. Svensson, A.; Nicklasson, E.; Harrah, T.; Panilaitis, B.; Kaplan, D.L.; Brittberg, M.; Gatenholm, P. Bacterial cellulose as a potential scaffold for tissue engineering of cartilage. *Biomaterials* **2005**, *26*, 419–431. [CrossRef]
108. Rampinelli, G.; di Landro, L.; Fujii, T. Characterization of biomaterials based on microfibrillated cellulose with different modifications. *J. Reinf. Plast. Compos.* **2010**, *29*, 1793–1803. [CrossRef]
109. Granja, P.L.; Barbosa, M.A.; Pouysége, L.; de Jéso, B.; Rouais, F.; Baquuey, C. Cellulose phosphates as biomaterials. Mineralization of chemically modified regenerated cellulose hydrogels. *J. Mater. Sci.* **2001**, *36*, 2163–2172. [CrossRef]
110. Granja, P.L.; Jéso, B.D.; Bareille, R.; Rouais, F.; Baquey, C.; Barbosa, M.A. Cellulose phosphates as biomaterials. In vitro biocompatibility studies. *React. Funct. Polym.* **2006**, *66*, 728–739. [CrossRef]
111. De Stefano, V.; Khan, S.; Tabada, A. Applications of PLA in modern medicine. *Eng. Regen.* **2020**, *1*, 76–87.
112. Budak, K.; Sogut, O.; Sezer, U.A. A review on synthesis and biomedical applications of polyglycolic acid. *J. Polym. Res.* **2020**, *27*, 208. [CrossRef]
113. Ashammakhi, N.; Rokkanen, P. Absorbable polyglycolide devices in trauma and bone surgery. *Biomaterials* **1997**, *18*, 3–9. [CrossRef]
114. Boyan, B.; Lohmann, C.; Somers, A.; Neiderauer, G.; Wozney, J.; Dean, D.; Carnes, D.; Schwartz, Z. Potential of porous poly-D,L-lactide-co-glycolide particles as a carrier for recombinant human bone morphogenetic protein-2 during osteoinduction in vivo. *J. Biomed. Mater. Res.* **1999**, *46*, 51–59. [CrossRef]
115. Gentile, P.; Chiono, V.; Carmagnola, I.; Hatton, P.V. An overview of poly(lactic-co-glycolic) acid (PLGA)-based biomaterials for bone tissue engineering. *Int. J. Mol. Sci.* **2014**, *15*, 3640–3659. [CrossRef]
116. Kalirajan, C.; Dukle, A.; Nathanael, A.J.; Oh, T.H.; Manivasagam, G. A critical review on polymeric biomaterials for biomedical applications. *Polymers* **2021**, *13*, 3015. [CrossRef]
117. Lacambra-Andreu, X.; Maazouz, A.; Lamnawar, K.; Chenal, J.M. A review on manufacturing processes of biocomposites based on poly(α-esters) and bioactive glass fillers for bone regeneration. *Biomimetics* **2023**, *8*, 81. [CrossRef]
118. Ishuang, S.L.; Payne, R.G.; Yaszemski, M.J.; Aufdemorte, T.B.; Bizios, R.; Mikos, A.G. Osteoblast migration on poly(α-hydroxy esters). *Biotechnol. Bioeng.* **1996**, *50*, 443–451.
119. Shikinami, Y.; Okuno, M. Bioresorbable devices made of forged composites of hydroxyapatite (HA) particles and poly-L-lactide (PLLA): Part I. Basic characteristics. *Biomaterials* **1999**, *20*, 859–877. [CrossRef]
120. Khor, E.; Lim, L.Y. Implantable applications of chitin and chitosan. *Biomaterials* **2003**, *24*, 2339–2349. [CrossRef]
121. Ali, A.; Ahmed, S. A review on chitosan and its nanocomposites in drug delivery. *Int. J. Biol. Macromol.* **2018**, *109*, 273–286. [CrossRef]

122. Piskin, E.; Bölgen, N.; Egri, S.; Isoglu, I.A. Electrospun matrices made of poly(α-hydroxy acids) for medical use. *Nanomedicine* **2007**, *2*, 441–457. [CrossRef]
123. Rezwana, K.; Chena, Q.Z.; Blakera, J.J.; Boccaccini, A.R. Biodegradable and bioactive porous polymer/inorganic composite scaffolds for bone tissue engineering. *Biomaterials* **2006**, *27*, 3413–3431. [CrossRef]
124. Seal, B.L.; Otero, T.C.; Panitch, A. Polymeric biomaterials for tissue and organ regeneration. *Mater. Sci. Eng. R* **2001**, *34*, 147–230. [CrossRef]
125. Mano, J.F.; Sousa, R.A.; Boesel, L.F.; Neves, N.M.; Reis, R.L. Bioinert, biodegradable and injectable polymeric matrix composites for hard tissue replacement: State of the art and recent developments. *Compos. Sci. Technol.* **2004**, *64*, 789–817. [CrossRef]
126. de las Heras Alarcón, C.; Pennadam, S.; Alexander, C. Stimuli responsive polymers for biomedical applications. *Chem. Soc. Rev.* **2005**, *34*, 276–285. [CrossRef]
127. Kohane, D.S.; Langer, R. Polymeric biomaterials in tissue engineering. *Pediatr. Res.* **2008**, *63*, 487–491. [CrossRef]
128. Arzhakova, O.V.; Arzhakov, M.S.; Badamshina, E.R.; Bryuzgina, E.B.; Bryuzgin, E.V.; Bystrova, A.V.; Vaganov, G.V.; Vasilevskaya, V.V.; Vdovichenko, A.Y.; Gallyamov, M.O.; et al. Polymers for the future. *Rus. Chem. Rev.* **2022**, *91*, RCR5062. [CrossRef]
129. Benalaya, I.; Alves, G.; Lopes, J.; Silva, L.R. A review of natural polysaccharides: Sources, characteristics, properties, food, and pharmaceutical applications. *Int. J. Mol. Sci.* **2024**, *25*, 1322. [CrossRef]
130. Okada, M. Chemical syntheses of biodegradable polymers. *Prog. Polym. Sci.* **2002**, *27*, 87–133. [CrossRef]
131. Jordan, J.; Jacob, K.I.; Tannenbaum, R.; Sharaf, M.A.; Jasiuk, I. Experimental trends in polymer nanocomposites—A review. *Mater. Sci. Eng. A* **2005**, *393*, 1–11. [CrossRef]
132. Liu, X.; Chu, P.K.; Ding, C. Surface modification of titanium, titanium alloys and related materials for biomedical applications. *Mater. Sci. Eng. R* **2004**, *47*, 49–121. [CrossRef]
133. Hanawa, T. Biofunctionalization of titanium for dental implant. *Jpn. Dent. Sci. Rev.* **2010**, *46*, 93–101. [CrossRef]
134. Nasab, M.B.; Hassan, M.R.; Sahari, B.B. Metallic biomaterials of knee and hip—A review. *Trends Biomater. Artif. Organ.* **2010**, *24*, 69–82.
135. Cheng, J.; Liu, B.; Wu, Y.H.; Zheng, Y.F. Comparative in vitro study on pure metals (Fe, Mn, Mg, Zn and W) as biodegradable metals. *J. Mater. Sci. Technol.* **2013**, *29*, 619–627. [CrossRef]
136. Chen, Q.; Thouas, G.A. Metallic implant biomaterials. *Mater. Sci. Eng. R* **2015**, *87*, 1–57. [CrossRef]
137. Ryan, G.; Pandit, A.; Apatsidis, D.P. Fabrication methods of porous metals for use in orthopaedic applications. *Biomaterials* **2006**, *27*, 2651–2670. [CrossRef]
138. Levine, B. A new era in porous metals: Applications in orthopaedics. *Adv. Eng. Mater.* **2008**, *10*, 788–792. [CrossRef]
139. Chen, C.; Zhang, M. Fabrication methods of porous tantalum metal implants for use as biomaterials. *Adv. Mater. Res.* **2012**, *476–478*, 2063–2066. [CrossRef]
140. Ma, P.X. Biomimetic materials for tissue engineering. *Adv. Drug Deliv. Rev.* **2008**, *60*, 184–198. [CrossRef]
141. Kathuria, Y.P. The potential of biocompatible metallic stents and preventing restenosis. *Mater. Sci. Eng. A* **2006**, *417*, 40–48. [CrossRef]
142. Purnama, A.; Hermawan, H.; Couet, J.; Mantovani, D. Assessing the biocompatibility of degradable metallic materials: State-of-the-art and focus on the potential of genetic regulation. *Acta Biomater.* **2010**, *6*, 1800–1807. [CrossRef]
143. Li, G.; Yang, H.; Zheng, Y.; Chen, X.H.; Yang, J.A.; Zhu, D.; Ruan, L.; Takashima, K. Challenges in the use of zinc and its alloys as biodegradable metals: Perspective from biomechanical compatibility. *Acta Biomater.* **2019**, *97*, 23–45. [CrossRef]
144. Knowles, J.C. Phosphate based glasses for biomedical applications. *J. Mater. Chem.* **2003**, *13*, 2395–2401. [CrossRef]
145. Tilocca, A. Current challenges in atomistic simulations of glasses for biomedical applications. *Phys. Chem. Chem. Phys.* **2014**, *16*, 3874–3880. [CrossRef]
146. Kasuga, T. Development of phosphate glass-ceramics for biomedical applications. *J. Ceram. Soc. Jpn.* **2007**, *115*, 455–459. [CrossRef]
147. Abdelghany, A.M.; El Batal, F.H.; El Batal, H.A. Zinc containing borate glasses and glass-ceramics: Search for biomedical applications. *Process. Appl. Ceram.* **2014**, *8*, 185–193. [CrossRef]
148. Shearer, A.; Montazerian, M.; Mauro, J.C. Modern definition of bioactive glasses and glass-ceramics. *J. Non-Cryst. Solids* **2023**, *608*, 122228. [CrossRef]
149. Hench, L.L. The story of Bioglass®. *J. Mater. Sci. Mater. Med.* **2006**, *17*, 967–978. [CrossRef]
150. Jones, J.R. Review of bioactive glass: From Hench to hybrids. *Acta Biomater.* **2013**, *9*, 4457–4486. [CrossRef]
151. Weizhong, Y.; Dali, Z.; Guangfu, Y. Research and development of A-W bioactive glass ceramic. *J. Biomed. Eng.* **2003**, *20*, 541–545.
152. Li, G.; Zhou, D.; Xue, M.; Yang, W.; Long, Q.; Cao, B.; Feng, D. Study on the surface bioactivity of novel magnetic A-W glass ceramic in vitro. *Appl. Surf. Sci.* **2008**, *255*, 559–561. [CrossRef]
153. Höland, W.; Schweiger, M.; Watzke, R.; Peschke, A.; Kappert, H. Ceramics as biomaterials for dental restoration. *Expert Rev. Med. Dev.* **2008**, *5*, 729–745. [CrossRef]
154. Li, R.W.K.; Chow, T.W.; Matinlinna, J.P. Ceramic dental biomaterials and CAD/CAM technology: State of the art. *J. Prosthodont. Res.* **2014**, *58*, 208–216. [CrossRef]
155. Ramesh, T.R.; Gangaiah, M.; Harish, P.V.; Krishnakumar, U.; Nandakishore, B. Zirconia ceramics as a dental biomaterial—An over view. *Trends Biomater. Artif. Organs* **2012**, *26*, 154–160.
156. Wang, C.H.; Wang, M.C.; Du, J.K.; Sie, Y.Y.; Hsi, C.S.; Lee, H.E. Phase transformation and nanocrystallite growth behavior of 2 mol% yttria-partially stabilized zirconia (2Y-PSZ) powders. *Ceram. Int.* **2013**, *39*, 5165–5174. [CrossRef]

157. Garvie, R.C. A personal history of the development of transformation toughened PSZ ceramics. *J. Aust. Ceram. Soc.* **2014**, *50*, 15–22.
158. Benson, J. Elemental carbon as a biomaterial. *J. Biomed. Mater. Res.* **1972**, *5*, 41–47. [CrossRef]
159. Olborska, A.; Swider, M.; Wolowiec, R.; Niedzielski, P.; Rylski, A.; Mitura, S. Amorphous carbon–biomaterial for implant coatings. *Diam. Relat. Mater.* **1994**, *3*, 899–901. [CrossRef]
160. Saito, N.; Usui, Y.; Aoki, K.; Narita, N.; Shimizu, M.; Hara, K.; Ogiwara, N.; Nakamura, K.; Ishigaki, N.; Kato, H.; et al. Carbon nanotubes: Biomaterial applications. *Chem. Soc. Rev.* **2009**, *38*, 1897–1903. [CrossRef]
161. Saito, N.; Haniu, H.; Usui, Y.; Aoki, K.; Hara, K.; Takanashi, S.; Shimizu, M.; Narita, N.; Okamoto, M.; Kobayashi, S.; et al. Safe clinical use of carbon nanotubes as innovative biomaterials. *Chem. Rev.* **2014**, *114*, 6040–6079. [CrossRef]
162. Harrison, B.S.; Atala, A. Carbon nanotube applications for tissue engineering. *Biomaterials* **2007**, *28*, 344–353. [CrossRef]
163. Saito, N.; Usui, Y.; Aoki, K.; Narita, N.; Shimizu, M.; Ogiwara, N.; Nakamura, K.; Ishigaki, N.; Kato, H.; Taruta, S. Carbon nanotubes for biomaterials in contact with bone. *Curr. Med. Chem.* **2008**, *15*, 523–527. [CrossRef]
164. Ma, P.C.; Siddiqui, N.A.; Marom, G.; Kim, J.K. Dispersion and functionalization of carbon nanotubes for polymer-based nanocomposites: A review. *Compos. Part A Appl. Sci. Manuf.* **2010**, *41*, 1345–1367. [CrossRef]
165. Kharissova, O.V.; González, C.M.O.; Kharisov, B.I. Solubilization and dispersion of carbon allotropes in water and non-aqueous solvents. *Ind. Eng. Chem. Res.* **2018**, *57*, 12624–12645. [CrossRef]
166. Beuvelot, J.; Bergeret, C.; Mallet, R.; Fernandez, V.; Cousseau, J.; Baslé, M.F.; Chappard, D. In vitro calcification of chemically functionalized carbon nanotubes. *Acta Biomater.* **2010**, *6*, 4110–4117. [CrossRef]
167. Vardharajula, S.; Ali, S.Z.; Tiwari, P.M.; Eroğlu, E.; Vig, K.; Dennis, V.A.; Singh, S.R. Functionalized carbon nanotubes: Biomedical applications. *Int. J. Nanomed.* **2012**, *7*, 5361–5374.
168. Partha, R.; Conyers, J.L. Biomedical applications of functionalized fullerene-based nanomaterials. *Int. J. Nanomed.* **2009**, *4*, 261–275.
169. Xiao, Y.; Pang, Y.X.; Yan, Y.; Qian, P.; Zhao, H.; Manickam, S.; Wu, T.; Pang, C.H. Synthesis and functionalization of graphene materials for biomedical applications: Recent advances, challenges and perspectives. *Adv. Sci.* **2023**, *10*, 2205292. [CrossRef]
170. Mathieu, L.M.; Bourban, P.E.; Manson, J.A.E. Processing of homogeneous ceramic/polymer blends for bioresorbable composites. *Compos. Sci. Technol.* **2006**, *66*, 1606–1614. [CrossRef]
171. Nair, M.; Nancy, D.; Krishnan, A.G.; Anjusree, G.S.; Vadukumpully, S.; Nair, S.V. Graphene oxide nanoflakes incorporated gelatin-hydroxyapatite scaffolds enhance osteogenic differentiation of human mesenchymal stem cells. *Nanotechnology* **2015**, *26*, 161001. [CrossRef]
172. Schappo, H.; Giry, K.; Salmoria, G.; Damia, C.; Hotza, D. Polymer/calcium phosphate biocomposites manufactured by selective laser sintering: An overview. *Prog. Addit. Manuf.* **2023**, *8*, 285–301. [CrossRef]
173. Gao, X.; Wang, H.; Luan, S.; Zhou, G. Biofabrication of poly(aryletherketone)-hydroxyapatite composite scaffolds via low-temperature printing. *Adv. Mater. Technol.* **2023**, *8*, 2201676. [CrossRef]
174. Soleymani, S.; Naghib, S.M. 3D and 4D printing hydroxyapatite-based scaffolds for bone tissue engineering and regeneration. *Heliyon* **2023**, *9*, e19363. [CrossRef]
175. Pezzotti, G.; Asmus, S.M.F. Fracture behavior of hydroxyapatite/polymer interpenetrating network composites prepared by in situ polymerization process. *Mater. Sci. Eng. A* **2001**, *316*, 231–237. [CrossRef]
176. Weickmann, H.; Gurr, M.; Meincke, O.; Thomann, R.; Mülhaupt, R. A versatile solvent-free "one-pot" route to polymer nanocomposites and the in situ formation of calcium phosphate/layered silicate hybrid nanoparticles. *Adv. Funct. Mater.* **2010**, *20*, 1778–1786. [CrossRef]
177. Wei, G.; Gong, C.; Hu, K.; Wang, Y.; Zhang, Y. Biomimetic hydroxyapatite on graphene supports for biomedical applications: A review. *Nanomaterials* **2019**, *9*, 1435. [CrossRef]
178. Boyapati, P.C.S.; Srinivas, K.; Akhil, S.; Bollikolla, H.B.; Chandu, B. A comprehensive review on novel graphene-hydroxyapatite nanocomposites for potential bioimplant applications. *ChemistrySelect* **2023**, *8*, e202204585. [CrossRef]
179. Aryal, S.; Bhattarai, S.R.; Bahadur, K.C.R.; Khil, M.S.; Lee, D.R.; Kim, H.Y. Carbon nanotubes assisted biomimetic synthesis of hydroxyapatite from simulated body fluid. *Mater. Sci. Eng. A* **2006**, *426*, 202–207. [CrossRef]
180. Kealley, C.; Ben-Nissan, B.; van Riessen, A.; Elcombe, M. Development of carbon nanotube reinforced hydroxyapatite bioceramics. *Key Eng. Mater.* **2006**, *309–311*, 597–602. [CrossRef]
181. Kealley, C.; Elcombe, M.; van Riessen, A.; Ben-Nissan, B. Development of carbon nanotube reinforced hydroxyapatite bioceramics. *Phys. B* **2006**, *385–386*, 496–498. [CrossRef]
182. Aryal, S.; Bahadur, K.C.R.; Dharmaraj, N.; Kim, K.W.; Kim, H.Y. Synthesis and characterization of hydroxyapatite using carbon nanotubes as a nano-matrix. *Scr. Mater.* **2006**, *54*, 131–135. [CrossRef]
183. Kim, H.; Mondal, S.; Jang, B.; Manivasagan, P.; Moorthy, M.S.; Oh, J. Biomimetic synthesis of metal–hydroxyapatite (Au-HAp, Ag-HAp, Au-Ag-HAp): Structural analysis, spectroscopic characterization and biomedical application. *Ceram. Int.* **2018**, *44*, 20490–20500. [CrossRef]
184. Rabadjieva, D.; Gergulova, R.; Ruseva, K.; Bonchev, A.; Shestakova, P.; Simeonov, M.; Vasileva, R.; Tatchev, D.; Titorenkova, R.; Vassileva, E. Polycarboxy/sulfo betaine–calcium phosphate hybrid materials with a remineralization potential. *Materials* **2023**, *16*, 6640. [CrossRef]

185. Rautaray, D.; Mandal, S.; Sastry, M. Synthesis of hydroxyapatite crystals using amino acid-capped gold nanoparticles as a scaffold. *Langmuir* **2005**, *21*, 5185–5191. [CrossRef]
186. Wang, X.J.; Li, Y.; Wei, J.; de Groot, K. Development of biomimetic nano-hydroxyapatite/poly(hexamethylene adipamide) composites. *Biomaterials* **2002**, *23*, 4787–4791. [CrossRef]
187. Wei, J.; Li, Y. Tissue engineering scaffold material of nano-apatite crystals and polyamide composite. *Eur. Polym. J.* **2004**, *40*, 509–515.
188. Memoto, R.; Nakamura, S.; Isobe, T.; Senna, M. Direct synthesis of hydroxyapatite-silk fibroin nano-composite sol via a mechano-chemical route. *J. Sol Gel Sci. Technol.* **2001**, *21*, 7–12.
189. Yoshida, A.; Miyazaki, T.; Ashizuka, M.; Ishida, E. Bioactivity and mechanical properties of cellulose/carbonate hydroxyapatite composites prepared in situ through mechanochemical reaction. *J. Biomater. Appl.* **2006**, *21*, 179–194. [CrossRef]
190. Fujiwara, M.; Shiokawa, K.; Morigaki, K.; Tatsu, Y.; Nakahara, Y. Calcium phosphate composite materials including inorganic powders, BSA or duplex DNA prepared by W/O/W interfacial reaction method. *Mater. Sci. Eng. C* **2008**, *28*, 280–288. [CrossRef]
191. Nagata, F.; Miyajima, T.; Yokogawa, Y. A method to fabricate hydroxyapatite/poly(lactic acid) microspheres intended for biomedical application. *J. Eur. Ceram. Soc.* **2006**, *26*, 533–535. [CrossRef]
192. Russias, J.; Saiz, E.; Nalla, R.K.; Tomsia, A.P. Microspheres as building blocks for hydroxyapatite/polylactide biodegradable composites. *J. Mater. Sci.* **2006**, *41*, 5127–5133. [CrossRef]
193. Khan, Y.M.; Cushnie, E.K.; Kelleher, J.K.; Laurencin, C.T. In situ synthesized ceramic-polymer composites for bone tissue engineering: Bioactivity and degradation studies. *J. Mater. Sci.* **2007**, *42*, 4183–4190. [CrossRef]
194. Liu, X.; Okada, M.; Maeda, H.; Fujii, S.; Furuzono, T. Hydroxyapatite/biodegradable poly(L-lactide-co-ε-caprolactone) composite microparticles as injectable scaffolds by a Pickering emulsion route. *Acta Biomater.* **2011**, *7*, 821–828. [CrossRef]
195. Hu, Y.; Zou, S.; Chen, W.; Tong, Z.; Wang, C. Mineralization and drug release of hydroxyapatite/poly(L-lactic acid) nanocomposite scaffolds prepared by Pickering emulsion templating. *Colloid Surface B* **2014**, *122*, 559–565. [CrossRef]
196. Kim, H.W.; Knowles, J.C.; Kim, H.E. Hydroxyapatite and gelatin composite foams processed via novel freeze-drying and crosslinking for use as temporary hard tissue scaffolds. *J. Biomed. Mater. Res. A* **2005**, *72A*, 136–145. [CrossRef]
197. Mohandes, F.; Salavati-Niasari, M. Freeze-drying synthesis, characterization and in vitro bioactivity of chitosan/graphene oxide/hydroxyapatite nanocomposite. *RSC Adv.* **2014**, *4*, 25993–26001. [CrossRef]
198. Sinha, A.; Das, G.; Sharma, B.K.; Roy, R.P.; Pramanick, A.K.; Nayar, S. Poly(vinyl alcohol)-hydroxyapatite biomimetic scaffold for tissue regeneration. *Mater. Sci. Eng. C* **2007**, *27*, 70–74. [CrossRef]
199. Sugawara, A.; Yamane, S.; Akiyoshi, K. Nanogel-templated mineralization: Polymer-calcium phosphate hybrid nanomaterials. *Macromol. Rapid Commun.* **2006**, *27*, 441–446. [CrossRef]
200. Liu, M.; Wang, Y.; Liu, X.; Wei, Q.; Bao, C.; Zhang, K. Comprehensive review on fabricating bioactive ceramic bone scaffold using vat photopolymerization. *ACS Biomater. Sci. Eng.* **2023**, *9*, 3032–3057. [CrossRef]
201. Chu, C.; Zhu, J.; Yin, Z.; Wang, S. Hydroxyapatite-Ti functionally graded biomaterial fabricated by powder metallurgy. *Mater. Sci. Eng. A* **1999**, *271*, 95–100.
202. Ul Haq, E.; Ahmed, F.; Rehman, F.U.; Channa, I.A.; Makhdoom, M.A.; Shahzad, J.; Shafiq, T.; Zain-ul-Abdein, M.; Shar, M.A.; Alhazaa, A. Synthesis and characterization of a titanium-based functionally graded material-structured biocomposite using powder metallurgy. *ACS Omega* **2023**, *8*, 28976–28983. [CrossRef]
203. Escalera, C.H.; Figueroa, I.A.; Casas-Luna, M.; Rodríguez-Gómez, F.J.; Piña-Barba, C.; Montufar, E.B.; Čelko, L. Magnesium strengthening in 3D printed TCP scaffold composites. *J. Compos. Sci.* **2023**, *7*, 467. [CrossRef]
204. Avila, J.D.; Stenberg, K.; Bose, S.; Bandyopadhyay, A. Hydroxyapatite reinforced Ti6Al4V composites for load-bearing implants. *Acta Biomater.* **2021**, *123*, 379–392. [CrossRef]
205. Afrouzian, A.; Bandyopadhyay, A. 3D printed silicon nitride, alumina and hydroxyapatite ceramic reinforced Ti6Al4V composites–tailored microstructures to enhance bio-tribo-corrosion and antibacterial properties. *J. Mech. Behav. Biomed. Mater.* **2023**, *144*, 105973. [CrossRef]
206. Juhasz, J.A.; Best, S.M. Bioactive ceramics: Processing, structures and properties. *J. Mater. Sci.* **2012**, *47*, 610–624. [CrossRef]
207. Wang, S.F.; Zhang, J.; Luo, D.W.; Gu, F.; Tang, D.Y.; Dong, Z.L.; Tan, G.E.B.; Que, W.X.; Zhang, T.S.; Li, S.; et al. Transparent ceramics: Processing, materials and applications. *Prog. Solid State Chem.* **2013**, *41*, 20–54. [CrossRef]
208. Mortensen, A.; Suresh, S. Functionally graded metals and metal-ceramic composites: Part 1 processing. *Int. Mater. Rev.* **1995**, *40*, 239–265. [CrossRef]
209. Suresh, S.; Mortensen, A. Functionally graded metals and metal-ceramic composites: Part 2 thermomechanical behaviour. *Int. Mater. Rev.* **1997**, *42*, 85–116. [CrossRef]
210. Travitzky, N. Processing of ceramic-metal composites. *Adv. Appl. Ceram.* **2012**, *111*, 286–300. [CrossRef]
211. Dhandayuthapani, B.; Yoshida, Y.; Maekawa, T.; Kumar, D.S. Polymeric scaffolds in tissue engineering application: A review. *Int. J. Polym. Sci.* **2011**, *2011*, 290602. [CrossRef]
212. Wang, W.; Zhang, B.; Li, M.; Li, J.; Zhang, C.; Han, Y.; Wang, L.; Wang, K.; Zhou, C.; Liu, L.; et al. 3D printing of PLA/n-HA composite scaffolds with customized mechanical properties and biological functions for bone tissue engineering. *Compos. Part B Eng.* **2021**, *224*, 109192. [CrossRef]
213. Han, Y.; Wei, Q.; Chang, P.; Hu, K.; Okoro, O.V.; Shavandi, A.; Nie, L. Three-dimensional printing of hydroxyapatite composites for biomedical application. *Crystals* **2021**, *11*, 353. [CrossRef]

214. Ojo, S.A.; Abere, D.V.; Adejo, H.O.; Robert, R.A.; Oluwasegun, K.M. Additive manufacturing of hydroxyapatite-based composites for bioengineering applications. *Bioprinting* **2023**, *32*, e00278. [CrossRef]
215. Fuchs, A.; Bartolf-Kopp, M.; Böhm, H.; Straub, A.; Kübler, A.C.; Linz, C.; Gbureck, U. Composite grafts made of polycaprolactone fiber mats and oil-based calcium phosphate cement pastes for the reconstruction of cranial and maxillofacial defects. *Clin. Oral Investig.* **2023**, *27*, 3199–3209. [CrossRef]
216. Baji, A.; Wong, S.C.; Srivatsan, T.S.; Njus, G.O.; Mathur, G. Processing methodologies for polycaprolactone-hydroxyapatite composites: A review. *Mater. Manuf. Process.* **2006**, *21*, 211–218. [CrossRef]
217. Guan, L.; Davies, J.E. Preparation and characterization of a highly macroporous biodegradable composite tissue engineering scaffold. *J. Biomed. Mater. Res. A* **2004**, *71A*, 480–487. [CrossRef]
218. Sun, F.; Zhou, H.; Lee, J. Various preparation methods of highly porous hydroxyapatite/polymer nanoscale biocomposites for bone regeneration. *Acta Biomater.* **2011**, *7*, 3813–3828. [CrossRef]
219. Kumar, A.; Negi, Y.S.; Choudhary, V.; Bhardwaj, N.K. Microstructural and mechanical properties of porous biocomposite scaffolds based on polyvinyl alcohol, nano-hydroxyapatite and cellulose nanocrystals. *Cellulose* **2015**, *21*, 3409–3426. [CrossRef]
220. Teng, X.R.; Ren, J.; Gu, S.Y. Preparation and characterization of porous PDLLA/HA composite foams by supercritical carbon dioxide technology. *J. Biomed. Mater. Res. B Appl. Biomater.* **2007**, *81B*, 185–193. [CrossRef]
221. Ren, J.; Zhao, P.; Ren, T.; Gu, S.; Pan, K. Poly (D,L-lactide)/nano-hydroxyapatite composite scaffolds for bone tissue engineering and biocompatibility evaluation. *J. Mater. Sci. Mater. Med.* **2008**, *19*, 1075–1082. [CrossRef]
222. Yang, X.; Qi, D.; Xu, K.; Alimu, A.; Cao, L. Bio-compatible n-HAPs/polymer monolithic composites templated from CO_2-in-water high internal phase emulsions. *React. Funct. Polym.* **2022**, *181*, 105417. [CrossRef]
223. Ohji, T.; Fukushima, M. Macro-porous ceramics: Processing and properties. *Int. Mater. Rev.* **2012**, *57*, 115–131. [CrossRef]
224. Dorozhkin, S.V. Calcium orthophosphate ($CaPO_4$)-based bioceramics: Preparation, properties and applications. *Coatings* **2022**, *12*, 1380. [CrossRef]
225. Babilotte, J.; Guduric, V.; le Nihouannen, D.; Naveau, A.; Fricain, J.C.; Catros, S. 3D printed polymer-mineral composite biomaterials for bone tissue engineering: Fabrication and characterization. *J. Biomed. Mater. Res. B Appl. Biomater.* **2019**, *107B*, 2579–2595. [CrossRef]
226. Converse, G.L.; Yue, W.; Roeder, R.K. Processing and tensile properties of hydroxyapatite-whisker-reinforced polyetheretherketone. *Biomaterials* **2007**, *28*, 927–935. [CrossRef]
227. Converse, G.L.; Roeder, R.K. Tensile properties of hydroxyapatite whisker reinforced polyetheretherketone. *Mater. Res. Soc. Symp. Proc.* **2005**, *898*, 44–49. [CrossRef]
228. Zhang, H.; Darvell, B.W. Failure and behavior in water of hydroxyapatite whisker-reinforced bis-GMA-based resin composites. *J. Mech. Behav. Biomed. Mater.* **2012**, *10*, 39–47. [CrossRef]
229. Liu, F.W.; Bao, S.; Jin, Y.; Jiang, X.Z.; Zhu, M.F. Novel bionic dental resin composite reinforced by hydroxyapatite whisker. *Mater. Res. Innov.* **2014**, *18*, S4854–S4858. [CrossRef]
230. Nouri-Felekori, M.; Mesgar, A.S.M.; Mohammadi, Z. Development of composite scaffolds in the system of gelatin–calcium phosphate whiskers/fibrous spherulites for bone tissue engineering. *Ceram. Int.* **2015**, *41*, 6013–6019. [CrossRef]
231. Watanabe, T.; Ban, S.; Ito, T.; Tsuruta, S.; Kawai, T.; Nakamura, H. Biocompatibility of composite membrane consisting of oriented needle-like apatite and biodegradable copolymer with soft and hard tissues in rats. *Dental Mater. J.* **2004**, *23*, 609–612. [CrossRef]
232. Li, H.; Chen, Y.; Xie, Y. Photo-crosslinking polymerization to prepare polyanhydride/needle-like hydroxyapatite biodegradable nanocomposite for orthopedic application. *Mater. Lett.* **2003**, *57*, 2848–2854. [CrossRef]
233. Nejati, E.; Firouzdor, V.; Eslaminejad, M.B.; Bagheri, F. Needle-like nano hydroxyapatite/poly(L-lactide acid) composite scaffold for bone tissue engineering application. *Mater. Sci. Eng. C* **2009**, *29*, 942–949. [CrossRef]
234. Sun, S.P.; Wei, M.; Olson, J.R.; Shaw, M.T. A modified pultrusion process for preparing composites reinforced with continuous fibers and aligned hydroxyapatite nano needles. *Polym. Compos.* **2015**, *36*, 931–938. [CrossRef]
235. Kasuga, T.; Ota, Y.; Nogami, M.; Abe, Y. Preparation and mechanical properties of polylactic acid composites containing hydroxyapatite fibers. *Biomaterials* **2000**, *22*, 19–23. [CrossRef]
236. Smith, L. Ceramic-plastic material as a bone substitute. *Arch. Surg.* **1963**, *87*, 653–661. [CrossRef]
237. Bonfield, W.; Grynpas, M.D.; Tully, A.E.; Bowman, J.; Abram, J. Hydroxyapatite reinforced polyethylene—A mechanically compatible implant material for bone replacement. *Biomaterials* **1981**, *2*, 185–189. [CrossRef]
238. Bonfield, W.; Bowman, J.; Grynpas, M.D. Composite Material for Use in Orthopaedics. UK Patent 8032647, 9 October 1981.
239. Bonfield, W. Composites for bone replacement. *J. Biomed. Eng.* **1988**, *10*, 522–526. [CrossRef]
240. Guild, F.J.; Bonfield, W. Predictive character of hydroxyapatite-polyethelene HAPEX^{TM} composite. *Biomaterials* **1993**, *14*, 985–993. [CrossRef]
241. Wang, M.; Joseph, R.; Bonfield, W. Hydroxyapatite-polyethylene composites for bone substitution: Effect of ceramic particle size and morphology. *Biomaterials* **1998**, *19*, 2357–2366. [CrossRef]
242. Nazhat, S.N.; Joseph, R.; Wang, M.; Smith, R.; Tanner, K.E.; Bonfield, W. Dynamic mechanical characterisation of hydroxyapatite reinforced polyethylene: Effect of particle size. *J. Mater. Sci. Mater. Med.* **2000**, *11*, 621–628. [CrossRef]
243. Guild, F.J.; Bonfield, W. Predictive modelling of the mechanical properties and failure processes of hydroxyapatite-polyethylene (HAPEX^{TM}) composite. *J. Mater. Sci. Mater. Med.* **1998**, *9*, 497–502. [CrossRef]

244. Wang, M.; Ladizesky, N.H.; Tanner, K.E.; Ward, I.M.; Bonfield, W. Hydrostatically extruded HAPEX^{TM}. *J. Mater. Sci.* **2000**, *35*, 1023–1030. [CrossRef]
245. Bonner, M.; Saunders, L.S.; Ward, I.M.; Davies, G.W.; Wang, M.; Tanner, K.E.; Bonfield, W. Anisotropic mechanical properties of oriented HAPEX^{TM}. *J. Mater. Sci.* **2002**, *37*, 325–334. [CrossRef]
246. di Silvio, L.; Dalby, M.J.; Bonfield, W. Osteoblast behaviour on HA/PE composite surfaces with different HA volumes. *Biomaterials* **2002**, *23*, 101–107. [CrossRef]
247. Dalby, M.J.; Kayser, M.V.; Bonfield, W.; di Silvio, L. Initial attachment of osteoblasts to an optimised HAPEX^{TM} topography. *Biomaterials* **2002**, *23*, 681–690. [CrossRef]
248. Zhang, Y.; Tanner, K.E.; Gurav, N.; di Silvio, L. In vitro osteoblastic response to 30 vol% hydroxyapatite-polyethylene composite. *J. Biomed. Mater. Res. A* **2007**, *81A*, 409–417. [CrossRef]
249. Rea, S.M.; Brooks, R.A.; Schneider, A.; Best, S.M.; Bonfield, W. Osteoblast-like cell response to bioactive composites-surface-topography and composition effects. *J. Biomed. Mater. Res. B Appl. Biomater.* **2004**, *70B*, 250–261. [CrossRef]
250. Hench, L.L.; Wilson, J. Surface-active biomaterials. *Science* **1984**, *226*, 630–636. [CrossRef]
251. Salernitano, E.; Migliaresi, C. Composite materials for biomedical applications: A review. *J. Appl. Biomater. Biomech.* **2003**, *1*, 3–18.
252. Pandey, A.; Jan, E.; Aswath, P.B. Physical and mechanical behavior of hot rolled HDPE/HA composites. *J. Mater. Sci.* **2006**, *41*, 3369–3376. [CrossRef]
253. Bonner, M.; Ward, I.M.; McGregor, W.; Tanner, K.E.; Bonfield, W. Hydroxyapatite/polypropylene composite: A novel bone substitute material. *J. Mater. Sci. Lett.* **2001**, *20*, 2049–2052. [CrossRef]
254. Suppakarn, N.; Sanmaung, S.; Ruksakulpiwa, Y.; Sutapun, W. Effect of surface modification on properties of natural hydroxyapatite/polypropylene composites. *Key Eng. Mater.* **2008**, *361–363*, 511–514.
255. Younesi, M.; Bahrololoom, M.E. Formulating the effects of applied temperature and pressure of hot pressing process on the mechanical properties of polypropylene-hydroxyapatite bio-composites by response surface methodology. *Mater. Des.* **2010**, *31*, 4621–4630. [CrossRef]
256. Younesi, M.; Bahrololoom, M.E. Effect of polypropylene molecular weight, hydroxyapatite particle size and Ringer's solution on creep and impact behavior of polypropylene-surface treated hydroxyapatite biocomposites. *J. Compos. Mater.* **2011**, *45*, 513–523. [CrossRef]
257. Sousa, R.A.; Reis, R.L.; Cunha, A.M.; Bevis, M.J. Processing and properties of bone-analogue biodegradable and bioinert polymeric composites. *Compos. Sci. Technol.* **2003**, *63*, 389–402. [CrossRef]
258. Wang, M.; Deb, S.; Bonfield, W. Chemically coupled hydroxyapatite-polyethylene composites: Processing and characterisation. *Mater. Lett.* **2000**, *44*, 119–124. [CrossRef]
259. Wang, M.; Bonfield, W. Chemically coupled hydroxyapatite-polyethylene composites: Structure and properties. *Biomaterials* **2001**, *22*, 1311–1320. [CrossRef]
260. Homaeigohar, S.S.; Shokrgozar, M.A.; Khavandi, A.; Sadi, A.Y. In vitro biological evaluation of β-TCP/HDPE—A novel orthopedic composite: A survey using human osteoblast and fibroblast bone cells. *J. Biomed. Mater. Res. A* **2008**, *84A*, 491–499. [CrossRef]
261. Sadi, A.Y.; Homaeigohar, S.S.; Khavandi, A.R.; Javadpour, J. The effect of partially stabilized zirconia on the mechanical properties of the hydroxyapatite-polyethylene composites. *J. Mater. Sci. Mater. Med.* **2004**, *15*, 853–858. [CrossRef]
262. Nath, S.; Bodhak, S.; Basu, B. HDPE-Al_2O_3-HAp composites for biomedical applications: Processing and characterizations. *J. Biomed. Mater. Res. B Appl. Biomater.* **2009**, *88B*, 1–11. [CrossRef]
263. Downes, R.N.; Vardy, S.; Tanner, K.E.; Bonfield, W. Hydroxyapatite-polyethylene composite in orbital surgery. Bioceramics 4. In Proceedings of the 4th International Symposium on Ceramics in Medicine, London, UK, 11–13 September 1991; pp. 239–246.
264. Bonfield, W.; Tanner, E. Hydroxyapatite composite biomaterials–evolution and applications. *Mater. World* **1997**, *5*, 18–20.
265. Dornhoffer, H.L. Hearing results with the dornhoffer ossicular replacement prostheses. *Laryngoscope* **1998**, *108*, 531–536. [CrossRef]
266. Swain, R.E.; Wang, M.; Beale, B.; Bonfield, W. HAPEX^{TM} for otologic applications. *Biomed. Eng. Appl. Basis Commun.* **1999**, *11*, 315–320.
267. Reis, R.L.; Cunha, A.M.; Oliveira, M.J.; Campos, A.R.; Bevis, M.J. Relationship between processing and mechanical properties of injection molded high molecular mass polyethylene + hydroxyapatite composites. *Mater. Res. Inn.* **2001**, *4*, 263–272. [CrossRef]
268. Sousa, R.A.; Reis, R.L.; Cunha, A.M.; Bevis, M.J. Structure development and interfacial interactions in high-density polyethylene/hydroxyapatite (HDPE/HA) composites molded with preferred orientation. *J. Appl. Polym. Sci.* **2002**, *86*, 2873–2886. [CrossRef]
269. Yi, Z.; Li, Y.; Jidong, L.; Xiang, Z.; Hongbing, L.; Yuanyuan, W.; Weihu, Y. Novel bio-composite of hydroxyapatite reinforced polyamide and polyethylene: Composition and properties. *Mater. Sci. Eng. A* **2007**, *452–453*, 512–517.
270. Unwin, A.P.; Ward, I.M.; Ukleja, P.; Weng, J. The role of pressure annealing in improving the stiffness of polyethylene/hydroxyapatite composites. *J. Mater. Sci.* **2001**, *36*, 3165–3177. [CrossRef]
271. Fang, L.M.; Leng, Y.; Gao, P. Processing and mechanical properties of HA/UHMWPE nanocomposites. *Biomaterials* **2006**, *27*, 3701–3707. [CrossRef]
272. Fang, L.M.; Gao, P.; Leng, Y. High strength and bioactive hydroxyapatite nano-particles reinforced ultrahigh molecular weight polyethylene. *Compos. B* **2007**, *38*, 345–351. [CrossRef]

273. Mirsalehi, S.A.; Khavandi, A.; Mirdamadi, S.; Naimi-Jamal, M.R.; Kalantari, S.M. Nanomechanical and tribological behavior of hydroxyapatite reinforced ultrahigh molecular weight polyethylene nanocomposites for biomedical applications. *J. Appl. Polym. Sci.* **2015**, *132*, 42052. [CrossRef]
274. Ramakrishna, S.; Mayer, J.; Wintermantel, E.; Leong, K.W. Biomedical applications of polymer-composite materials: A review. *Compos. Sci. Technol.* **2001**, *61*, 1189–1224. [CrossRef]
275. Donners, J.J.J.M.; Nolte, R.J.M.; Sommerdijk, N.A.J.M. Dendrimer-based hydroxyapatite composites with remarkable materials properties. *Adv. Mater.* **2003**, *15*, 313–316. [CrossRef]
276. Schneider, O.D.; Stepuk, A.; Mohn, D.; Luechinger, N.A.; Feldman, K.; Stark, W.J. Light-curable polymer/calcium phosphate nanocomposite glue for bone defect treatment. *Acta Biomater.* **2010**, *6*, 2704–2710. [CrossRef]
277. Ignjatovic, N.L.; Plavsic, M.; Miljkovic, M.S.; Zivkovic, L.M.; Uskokovic, D.P. Microstructural characteristics of calcium hydroxyapatite/poly-L-lactide based composites. *J. Microsc.* **1999**, *196*, 243–248. [CrossRef]
278. Skrtic, D.; Antonucci, J.M.; Eanes, E.D. Amorphous calcium phosphate-based bioactive polymeric composites for mineralized tissue regeneration. *J. Res. Natl. Inst. Stand. Technol.* **2003**, *108*, 167–182. [CrossRef]
279. Rizzi, S.C.; Heath, D.J.; Coombes, A.G.A.; Bock, N.; Textor, M.; Downes, S. Biodegradable polymer/hydroxyapatite composites: Surface analysis and initial attachment of human osteoblasts. *J. Biomed. Mater. Res.* **2001**, *55*, 475–486. [CrossRef]
280. Navarro, M.; Planell, J.A. Bioactive composites based on calcium phosphates for bone regeneration. *Key Eng. Mater.* **2010**, *441*, 203–233. [CrossRef]
281. Zhang, R.Y.; Ma, P.X. Porous poly(L-lactic acid)/apatite composites created by biomimetic process. *J. Biomed. Mater. Res.* **1999**, *45*, 285–293. [CrossRef]
282. Liu, Q.; de Wijn, J.R.; van Blitterswijk, C.A. Composite biomaterials with chemical bonding between hydroxyapatite filler particles and PEG/PBT copolymer matrix. *J. Biomed. Mater. Res.* **1998**, *40*, 490–497. [CrossRef]
283. Cerrai, P.; Guerra, G.D.; Tricoli, M.; Krajewski, A.; Ravaglioli, A.; Martinetti, R.; Dolcini, L.; Fini, M.; Scarano, A.; Piattelli, A. Periodontal membranes from composites of hydroxyapatite and bioresorbable block copolymers. *J. Mater. Sci. Mater. Med.* **1999**, *10*, 677–682. [CrossRef]
284. Roeder, R.K.; Sproul, M.M.; Turner, C.H. Hydroxyapatite whiskers provide improved mechanical properties in reinforced polymer composites. *J. Biomed. Mater. Res. A* **2003**, *67A*, 801–812. [CrossRef]
285. Wagoner Johnson, A.J.; Herschler, B.A. A review of the mechanical behavior of CaP and CaP/polymer composites for applications in bone replacement and repair. *Acta Biomater.* **2011**, *7*, 16–30. [CrossRef]
286. Hutmacher, D.W. Scaffolds in tissue engineering bone and cartilage. *Biomaterials* **2000**, *21*, 2529–2543. [CrossRef]
287. Owji, N.; Mandakhbayar, N.; Cha, J.R.; Padalhin, A.R.; Erdogan, Z.K.; Aldaadaa, A.; Shakouri, T.; Sawadkar, P.; Frost, O.; Kim, H.W.; et al. Inclusion of calcium phosphate does not further improve in vitro and in vivo osteogenesis in a novel, highly biocompatible, mechanically stable and 3D printable polymer. *Sci. Rep.* **2022**, *12*, 16977. [CrossRef]
288. Wang, M.; Yue, C.Y.; Chua, B. Production and evaluation of hydroxyapatite reinforced polysulfone for tissue replacement. *J. Mater. Sci. Mater. Med.* **2001**, *12*, 821–826. [CrossRef]
289. Chlopek, J.; Rosol, P.; Morawska-Chochol, A. Durability of polymer-ceramics composite implants determined in creep tests. *Compos. Sci. Technol.* **2006**, *66*, 1615–1622. [CrossRef]
290. Robinson, P.; Wilson, C.; Mecholsky, J. Processing and mechanical properties of hydroxyapatite-polysulfone laminated composites. *J. Eur. Ceram. Soc.* **2014**, *34*, 1387–1396. [CrossRef]
291. Xu, F.; Li, Y.; Yao, X.; Liao, H.; Zhang, L. Preparation and in vivo investigation of artificial cornea made of nano-hydroxyapatite/poly(vinyl alcohol) hydrogel composite. *J. Mater. Sci. Mater. Med.* **2007**, *18*, 635–640.
292. Xu, F.; Li, Y.; Deng, Y.; Xiong, G. Porous nano-hydroxyapatite/poly(vinyl alcohol) composite hydrogel as artificial cornea fringe: Characterization and evaluation in vitro. *J. Biomater. Sci. Polym. Edn.* **2008**, *19*, 431–439. [CrossRef]
293. Poursamar, S.A.; Orang, F.; Bonakdar, S.; Savar, M.K. Preparation and characterisation of poly vinyl alcohol/hydroxyapatite nanocomposite via in situ synthesis: A potential material as bone tissue engineering scaffolds. *Int. J. Nanomanuf.* **2010**, *5*, 330–334. [CrossRef]
294. Timofejeva, A.; Loca, D. Hydroxyapatite/polyvinyl alcohol composite hydrogels for bone and cartilage tissue engineering. *Key Eng. Mater.* **2018**, *762*, 54–58. [CrossRef]
295. Pramanik, N.; Biswas, S.K.; Pramanik, P. Synthesis and characterization of hydroxyapatite/poly(vinyl alcohol phosphate) nanocomposite biomaterials. *Int. J. Appl. Ceram. Technol.* **2008**, *5*, 20–28. [CrossRef]
296. Bigi, A.; Boanini, E.; Gazzano, M.; Rubini, K. Structural and morphological modifications of hydroxyapatite-polyaspartate composite crystals induced by heat treatment. *Cryst. Res. Technol.* **2005**, *40*, 1094–1098. [CrossRef]
297. Bertoni, E.; Bigi, A.; Falini, G.; Panzavolta, S.; Roveri, N. Hydroxyapatite polyacrylic acid nanocrystals. *J. Mater. Chem.* **1999**, *9*, 779–782. [CrossRef]
298. Qiu, H.J.; Yang, J.; Kodali, P.; Koh, J.; Ameer, G.A. A citric acid-based hydroxyapatite composite for orthopedic implants. *Biomaterials* **2006**, *27*, 5845–5854. [CrossRef]
299. Greish, Y.E.; Brown, P.W. Chemically formed HAp-Ca poly(vinyl phosphonate) composites. *Biomaterials* **2001**, *22*, 807–816. [CrossRef]
300. Greish, Y.E.; Brown, P.W. Formation and properties of hydroxyapatite-calcium poly(vinyl phosphonate) composites. *J. Am. Ceram. Soc.* **2002**, *85*, 1738–1744. [CrossRef]

301. Sailaja, G.S.; Velayudhan, S.; Sunny, M.C.; Sreenivasan, K.; Varma, H.K.; Ramesh, P. Hydroxyapatite filled chitosan-polyacrylic acid polyelectrolyte complexes. *J. Mater. Sci.* **2003**, *38*, 3653–3662. [CrossRef]
302. Piticescu, R.M.; Chitanu, G.C.; Albulescu, M.; Giurginca, M.; Popescu, M.L.; Łojkowski, W. Hybrid HAp-maleic anhydride copolymer nanocomposites obtained by in-situ functionalisation. *Solid State Phenom.* **2005**, *106*, 47–56. [CrossRef]
303. Song, J.; Saiz, E.; Bertozzi, C.R. A new approach to mineralization of biocompatible hydrogel scaffolds: An efficient process toward 3-dimensional bonelike composites. *J. Am. Chem. Soc.* **2003**, *125*, 1236–1243. [CrossRef]
304. Kutikov, A.B.; Song, J. An amphiphilic degradable polymer/hydroxyapatite composite with enhanced handling characteristics promotes osteogenic gene expression in bone marrow stromal cells. *Acta Biomater.* **2013**, *9*, 8354–8364. [CrossRef]
305. Wu, S.; Wang, J.; Zou, L.; Jin, L.; Wang, Z.; Li, Y. A three-dimensional hydroxyapatite/polyacrylonitrile composite scaffold designed for bone tissue engineering. *RSC Adv.* **2018**, *8*, 1730–1736. [CrossRef]
306. Borkowski, L.; Lübek, T.; Jojczuk, M.; Nogalski, A.; Belcarz, A.; Hajnos, M.; Ginalska, G. Behavior of new hydroxyapatite/glucan composite in human serum. *J. Biomed. Mater. Res. B Appl. Biomater.* **2018**, *106B*, 2653–2664. [CrossRef]
307. Abu Bakar, M.S.; Cheng, M.H.W.; Tang, S.M.; Yu, S.C.; Liao, K.; Tan, C.T.; Khor, K.A.; Cheang, P. Tensile properties, tension-tension fatigue and biological response of polyetheretherketone-hydroxyapatite composites for load-bearing orthopedic implants. *Biomaterials* **2003**, *24*, 2245–2250. [CrossRef]
308. Abu Bakar, M.S.; Cheang, P.; Khor, K.A. Mechanical properties of injection molded hydroxyapatite-polyetheretherketone biocomposites. *Compos. Sci. Technol.* **2003**, *63*, 421–425. [CrossRef]
309. Fan, J.P.; Tsui, C.P.; Tang, C.Y. Modeling of the mechanical behavior of HA/PEEK biocomposite under quasi-static tensile load. *Mater. Sci. Eng. A* **2004**, *382*, 341–350. [CrossRef]
310. Chan, K.W.; Liao, C.Z.; Wong, H.M.; Yeung, K.W.K.; Tjong, S.C. Preparation of polyetheretherketone composites with nanohydroxyapatite rods and carbon nanofibers having high strength, good biocompatibility and excellent thermal stability. *RSC Adv.* **2016**, *6*, 19417–19429. [CrossRef]
311. Qi, D.; Wang, N.; Wang, S.; Liu, L.; Zhu, S.; She, P.; Yue, X. High-strength porous polyetheretherketone/hydroxyapatite composite for the treatment of bone defect. *Compos. Comm.* **2023**, *38*, 101473. [CrossRef]
312. Li, S.; Li, G.; Lian, X.; Hu, J.; Li, M.; Wang, B.; Zou, Y.; Zhou, Z. Integrated porous polyetheretherketone/hydroxyapatite scaffolds: Design, manufacturing and performance evaluation. *Compos. Part A—Appl. Sci.* **2023**, *173*, 107656. [CrossRef]
313. Gong, X.H.; Tang, C.Y.; Hu, H.C.; Zhou, X.P. Improved mechanical properties of HIPS/hydroxyapatite composites by surface modification of hydroxyapatite via in situ polymerization of styrene. *J. Mater. Sci. Mater. Med.* **2004**, *15*, 1141–1146. [CrossRef]
314. Fu, G.; Xia, Z.; Jiang, J.; Jing, B.; Zhang, X. Fabrication and characterization of nanocomposites with high-impact polystyrene and hydroxyapatite with well-defined polystyrene via ATRP. *J. Reinf. Plast. Comp.* **2011**, *30*, 1445–1453. [CrossRef]
315. Petricca, S.E.; Marra, K.G.; Kumta, P.N. Chemical synthesis of poly(lactic-co-glycolic acid)/hydroxyapatite composites for orthopaedic applications. *Acta Biomater.* **2006**, *2*, 277–286. [CrossRef]
316. Zhou, H.; Lawrence, J.G.; Bhaduri, S.B. Fabrication aspects of PLA-CaP/PLGA-CaP composites for orthopedic applications: A review. *Acta Biomater.* **2012**, *8*, 1999–2016. [CrossRef]
317. Hoekstra, J.W.M.; Ma, J.; Plachokova, A.S.; Bronkhorst, E.M.; Bohner, M.; Pan, J.; Meijer, G.J.; Jansen, J.A.; van den Beucken, J.J.J.P. The in vivo performance of CaP/PLGA composites with varied PLGA microsphere sizes and inorganic compositions. *Acta Biomater.* **2013**, *9*, 7518–7526. [CrossRef]
318. Leung, L.H.; Naguib, H.E. Characterizing the viscoelastic behaviour of poly(lactide-co-glycolide acid)–hydroxyapatite foams. *J. Cell. Plast.* **2013**, *49*, 497–505. [CrossRef]
319. Fisher, P.D.; Venugopal, G.; Milbrandt, T.A.; Hilt, J.Z.; Puleo, D.A. Hydroxyapatite-reinforced in situ forming PLGA systems for intraosseous injection. *J. Biomed. Mater. Res. A* **2015**, *103A*, 2365–2373. [CrossRef]
320. Athanasiou, K.A.; Schmitz, J.P.; Agrawal, C.M. The effects of porosity on in vitro degradation of polylactic acid–polyglycolic acid implants used in repair of articular cartilage. *Tissue Eng.* **1998**, *4*, 53–63. [CrossRef]
321. Verheyen, C.C.P.M.; Klein, C.P.A.T.; de Blieck-Hogervorst, J.M.A.; Wolke, J.G.C.; de Wijin, J.R.; van Blitterswijk, C.A.; de Groot, K. Evaluation of hydroxylapatite poly(L-lactide) composites: Physico-chemical properties. *J. Mater. Sci. Mater. Med.* **1993**, *4*, 58–65. [CrossRef]
322. Agrawal, C.M.; Athanasiou, K.A. Technique to control pH in vicinity of biodegrading PLA-PGA implants. *J. Biomed. Mater. Res. Appl. Biomater.* **1997**, *38*, 105–114. [CrossRef]
323. Li, H.; Chang, J. pH-compensation effect of bioactive inorganic fillers on the degradation of PLGA. *Compos. Sci. Technol.* **2005**, *65*, 2226–2232. [CrossRef]
324. Peter, S.J.; Miller, S.T.; Zhu, G.; Yasko, A.W.; Mikos, A.G. In vivo degradation of a poly(propylene fumarate)/β-tricalcium phosphate injectable composite scaffold. *J. Biomed. Mater. Res.* **1998**, *41*, 1–7. [CrossRef]
325. Ara, M.; Watanabe, M.; Imai, Y. Effect of blending calcium compounds on hydrolitic degradation of poly(D,L-lactic acid-co-glycolic acid). *Biomaterials* **2002**, *23*, 2479–2483. [CrossRef]
326. Schiller, C.; Epple, M. Carbonated apatites can be used as pH-stabilizing filler for biodegradable polyesters. *Biomaterials* **2003**, *24*, 2037–2043. [CrossRef]
327. Schiller, C.; Rasche, C.; Wehmöller, M.; Beckmann, F.; Eufinger, H.; Epple, M.; Weihe, S. Geometrically structured implants for cranial reconstruction made of biodegradable polyesters and calcium phosphate/calcium carbonate. *Biomaterials* **2004**, *25*, 1239–1247. [CrossRef]

328. Shikinami, Y.; Okuno, M. Bioresorbable devices made of forged composites of hydroxyapatite (HA) particles and poly L-lactide (PLLA). Part II: Practical properties of miniscrews and miniplates. *Biomaterials* **2001**, *22*, 3197–3211. [CrossRef]
329. Russias, J.; Saiz, E.; Nalla, R.K.; Gryn, K.; Ritchie, R.O.; Tomsia, A.P. Fabrication and mechanical properties of PLA/HA composites: A study of in vitro degradation. *Mater. Sci. Eng. C* **2006**, *26*, 1289–1295. [CrossRef]
330. Akagi, H.; Iwata, M.; Ichinohe, T.; Amimoto, H.; Hayashi, Y.; Kannno, N.; Ochi, H.; Fujita, Y.; Harada, Y.; Tagawa, M.; et al. Hydroxyapatite/poly-L-lactide acid screws have better biocompatibility and femoral burr hole closure than does poly-L-lactide acid alone. *J. Biomater. Appl.* **2014**, *28*, 954–962. [CrossRef]
331. Pérez-Davila, S.; Garrido-Gulías, N.; González-Rodríguez, L.; López-Álvarez, M.; Serra, J.; López-Periago, J.E.; González, P. Physicochemical properties of 3D-printed polylactic acid/hydroxyapatite scaffolds. *Polymers* **2023**, *15*, 2849. [CrossRef]
332. Kim, H.W.; Lee, H.H.; Knowles, J.C. Electrospinning biomedical nanocomposite fibers of hydroxyapaite/poly(lactic acid) for bone regeneration. *J. Biomed. Mater. Res. A* **2006**, *79A*, 643–649. [CrossRef]
333. Gross, K.A.; Rodríguez-Lorenzo, L.M. Biodegradable composite scaffolds with an interconnected spherical network for bone tissue engineering. *Biomaterials* **2004**, *25*, 4955–4962. [CrossRef]
334. Zhang, H.; Chen, Z. Fabrication and characterization of electrospun PLGA/MWNTs/hydroxyapatite biocomposite scaffolds for bone tissue engineering. *J. Bioact. Compat. Polym.* **2010**, *25*, 241–259. [CrossRef]
335. Durucan, C.; Brown, P.W. Low temperature formation of calcium-deficient hydroxyapatite-PLA/PLGA composites. *J. Biomed. Mater. Res.* **2000**, *51*, 717–725. [CrossRef]
336. Durucan, C.; Brown, P.W. Calcium-deficient hydroxyapatite-PLGA composites: Mechanical and microstructural investigation. *J. Biomed. Mater. Res.* **2000**, *51*, 726–734. [CrossRef]
337. Durucan, C.; Brown, P.W. Biodegradable hydroxyapatite-polymer composites. *Adv. Eng. Mater.* **2001**, *3*, 227–231. [CrossRef]
338. Nazhat, S.N.; Kellomäki, M.; Törmälä, P.; Tanner, K.E.; Bonfield, W. Dynamic mechanical characterization of biodegradable composites of hydroxyapatite and polylactides. *J. Biomed. Mater. Res.* **2001**, *58*, 335–343. [CrossRef]
339. Ignjatovic, N.; Suljovrujic, E.; Biudinski-Simendic, J.; Krakovsky, I.; Uskokovic, D. Evaluation of hot-presses hydroxyapatite/poly-L-lactide composite biomaterial characteristics. *J. Biomed. Mater. Res. B Appl. Biomater.* **2004**, *71B*, 284–294. [CrossRef]
340. Wang, X.; Lou, T.; Yang, J.; Yang, Z.; He, K. Preparation of PLLA/HAP/β-TCP composite scaffold for bone tissue engineering. *Appl. Mech. Mater.* **2014**, *513–517*, 143–146. [CrossRef]
341. Hasegawa, S.; Tamura, J.; Neo, M.; Goto, K.; Shikinami, Y.; Saito, M.; Kita, M.; Nakamura, T. In vivo evaluation of a porous hydroxyapatite/poly-D,L-lactide composite for use as a bone substitute. *J. Biomed. Mater. Res. A* **2005**, *75A*, 567–579. [CrossRef]
342. Hasegawa, S.; Neo, M.; Tamura, J.; Fujibayashi, S.; Takemoto, M.; Shikinami, Y.; Okazaki, K.; Nakamura, T. In vivo evaluation of a porous hydroxyapatite/poly-D,L-lactide composite for bone tissue engineering. *J. Biomed. Mater. Res. A* **2007**, *81A*, 930–938. [CrossRef]
343. Kim, S.S.; Park, M.S.; Jeon, Q.; Choi, C.Y.; Kim, B.S. Poly(lactide-co-glycolide)/hydroxyapatite composite scaffolds for bone tissue engineering. *Biomaterials* **2006**, *27*, 1399–1409. [CrossRef]
344. Mao, D.; Li, Q.; Bai, N.; Dong, H.; Li, D. Porous stable poly(lactic acid)/ethyl cellulose/hydroxyapatite composite scaffolds prepared by a combined method for bone regeneration. *Carbohyd. Polym.* **2018**, *180*, 104–111. [CrossRef]
345. Carvalho, T.S.S.; Ribeiro, N.; Torres, P.M.C.; Almeida, J.C.; Belo, J.H.; Araújo, J.P.; Ramos, A.; Oliveira, M.; Olhero, S.M. Magnetic polylactic acid-calcium phosphate-based biocomposite as a potential biomaterial for tissue engineering applications. *Mater. Chem. Phys.* **2023**, *296*, 127175. [CrossRef]
346. Alonso-Fernández, I.; Haugen, H.J.; López-Peña, M.; González-Cantalapiedra, A.; Muñoz, F. Use of 3D-printed polylactic acid/bioceramic composite scaffolds for bone tissue engineering in preclinical in vivo studies: A systematic review. *Acta Biomater.* **2023**, *168*, 1–21. [CrossRef]
347. Reis, R.L.; Cunha, A.M. New degradable load-bearing biomaterials composed of reinforced starch based blends. *J. Appl. Med. Polym.* **2000**, *4*, 1–5.
348. Sousa, R.A.; Mano, J.F.; Reis, R.L.; Cunha, A.M.; Bevis, M.J. Mechanical performance of starch based bioactive composites moulded with preferred orientation for potential medical applications. *Polym. Eng. Sci.* **2002**, *42*, 1032–1045. [CrossRef]
349. Marques, A.P.; Reis, R.L. Hydroxyapatite reinforcement of different starch-based polymers affects osteoblast-like cells adhesion/spreading and proliferation. *Mater. Sci. Eng. C* **2005**, *25*, 215–229. [CrossRef]
350. Reis, R.L.; Cunha, A.M.; Allan, P.S.; Bevis, M.J. Structure development and control of injection-molded hydroxylapatite-reinforced starch/EVOH composites. *Adv. Polym. Technol.* **1997**, *16*, 263–277. [CrossRef]
351. Vaz, C.M.; Reis, R.L.; Cunha, A.M. Use of coupling agents to enhance the interfacial interactions in starch-EVOH/hydroxylapatite composites. *Biomaterials* **2002**, *23*, 629–635. [CrossRef]
352. Leonor, I.B.; Ito, A.; Onuma, K.; Kanzaki, N.; Reis, R.L. In vitro bioactivity of starch thermoplastic/hydroxyapatite composite biomaterials: An in situ study using atomic force microscopy. *Biomaterials* **2003**, *24*, 579–585. [CrossRef]
353. Vaz, C.M.; Reis, R.L.; Cunha, A.M. Degradation model of starch-EVOH+HA composites. *Mater. Res. Innov.* **2001**, *4*, 375–380. [CrossRef]
354. Chen, L.J.; Wang, M. Production and evaluation of biodegradable composites based on PHB-PHV copolymer. *Biomaterials* **2002**, *23*, 2631–2639. [CrossRef]
355. Ni, J.; Wang, M. In vitro evaluation of hydroxyapatite reinforced polyhydroxybutyrate composite. *Mater. Sci. Eng. C* **2002**, *20*, 101–109. [CrossRef]

356. Carlo, E.C.; Borges, A.P.B.; Del Carlo, R.J.; Martinez, M.M.M.; Oliveira, P.M.; Morato, G.O.; Eleotério, R.B.; Reis, M.S. Comparison of in vivo properties of hydroxyapatite-polyhydroxybutyrate composites assessed for bone substitution. *J. Craniofac. Surg.* **2009**, *20*, 853–859. [CrossRef]
357. Sadat-Shojai, M.; Khorasani, M.T.; Jamshidi, A.; Irani, S. Nano-hydroxyapatite reinforced polyhydroxybutyrate composites: A comprehensive study on the structural and in vitro biological properties. *Mater. Sci. Eng. C* **2013**, *33*, 2776–2787. [CrossRef]
358. Tyubaeva, P.M.; Gasparyan, K.G.; Fedotov, A.Y.; Lobzhanidze, P.V.; Baranov, O.V.; Egorov, A.A.; Sirotinkin, V.P.; Komlev, V.S.; Olkhov, A.A. Development of nonwoven fibrous materials based on poly-3-hydroxybutyrate with a high content of α-tricalcium phosphate. *Polymers* **2023**, *15*, 3167. [CrossRef]
359. Chen, D.Z.; Tang, C.Y.; Chan, K.C.; Tsui, C.P.; Yu, P.H.F.; Leung, M.C.P.; Uskokovic, P.S. Dynamic mechanical properties and in vitro bioactivity of PHBHV/HA nanocomposite. *Compos. Sci. Technol.* **2007**, *67*, 1617–1626. [CrossRef]
360. Rai, B.; Noohom, W.; Kithva, P.H.; Grøndahl, L.; Trau, M. Bionanohydroxyapatite/poly(3-hydroxybutyrate-co-3-hydroxyvalerate) composites with improved particle dispersion and superior mechanical properties. *Chem. Mater.* **2008**, *20*, 2802–2808. [CrossRef]
361. Wang, Y.W.; Wu, Q.; Chen, J.; Chen, G.Q. Evaluation of three-dimensional scaffolds made of blends of hydroxyapatite and poly(3-hydroxybutyrate-co-3-hydroxyhexanoate) for bone reconstruction. *Biomaterials* **2005**, *26*, 899–904. [CrossRef]
362. Linhart, W.; Lehmann, W.; Siedler, M.; Peters, F.; Schilling, A.F.; Schwarz, K.; Amling, M.; Rueger, J.M.; Epple, M. Composites of amorphous calcium phosphate and poly(hydroxybutyrate) and poly(hydroxybutyrate-co-hydroxyvalerate) for bone substitution: Assessment of the biocompatibility. *J. Mater. Sci.* **2006**, *41*, 4806–4813. [CrossRef]
363. Azevedo, M.; Reis, R.L.; Claase, M.; Grijpma, D.; Feijen, J. Development and properties of polycaprolactone/hydroxyapatite composite biomaterials. *J. Mater. Sci. Mater. Med.* **2003**, *14*, 103–107. [CrossRef]
364. Walsh, D.; Furuzono, T.; Tanaka, J. Preparation of porous composite implant materials by in situ polymerization of porous apatite containing ε-caprolactone or methyl methacrylate. *Biomaterials* **2001**, *22*, 1205–1212. [CrossRef]
365. Kim, H.W. Biomedical nanocomposites of hydroxyapatite/polycaprolactone obtained by surfactant mediation. *J. Biomed. Mater. Res. A* **2007**, *83A*, 169–177. [CrossRef]
366. Chuenjitkuntaworn, B.; Inrung, W.; Damrongsri, D.; Mekaapiruk, K.; Supaphol, P.; Pavasant, P. Polycaprolactone/hydroxyapatite composite scaffolds: Preparation, characterization and in vitro and in vivo biological responses of human primary bone cells. *J. Biomed. Mater. Res. A* **2010**, *94A*, 241–251. [CrossRef]
367. Kim, B.S.; Yang, S.S.; Lee, J. A polycaprolactone/cuttlefish bone-derived hydroxyapatite composite porous scaffold for bone tissue engineering. *J. Biomed. Mater. Res. B Appl. Biomater.* **2014**, *102B*, 943–951. [CrossRef]
368. Hajiali, F.; Tajbakhsh, S.; Shojaei, A. Fabrication and properties of polycaprolactone composites containing calcium phosphate-based ceramics and bioactive glasses in bone tissue engineering: A review. *Polym. Rev.* **2017**, *58*, 164–207. [CrossRef]
369. Huang, B.; Caetano, G.; Vyas, C.; Blaker, J.J.; Diver, C.; Bártolo, P. Polymer-ceramic composite scaffolds: The effect of hydroxyapatite and β-tri-calcium phosphate. *Materials* **2018**, *11*, 129. [CrossRef]
370. Causa, F.; Netti, P.A.; Ambrosio, L.; Ciapetti, G.; Baldini, N.; Pagani, S.; Martini, D.; Giunti, A. Poly-ε-caprolactone/hydroxyapatite composites for bone regeneration: In vitro characterization and human osteoblast response. *J. Biomed. Mater. Res. A* **2006**, *76A*, 151–162. [CrossRef]
371. Thomas, V.; Jagani, S.; Johnson, K.; Jose, M.V.; Dean, D.R.; Vohra, Y.K.; Nyairo, E. Electrospun bioactive nanocomposite scaffolds of polycaprolactone and nanohydroxyapatite for bone tissue engineering. *J. Nanosci. Nanotechol.* **2006**, *6*, 487–493. [CrossRef]
372. Marra, K.G.; Szem, J.W.; Kumta, P.N.; DiMilla, P.A.; Weiss, L.E. In vitro analysis of biodegradable polymer blend/hydroxyapatite composites for bone tissue engineering. *J. Biomed. Mater. Res.* **1999**, *47*, 324–335. [CrossRef]
373. Dunn, A.; Campbell, P.; Marra, K.G. The influence of polymer blend composition on the degradation of polymer/hydroxyapatite biomaterials. *J. Mater. Sci. Mater. Med.* **2001**, *12*, 673–677. [CrossRef]
374. Calandrelli, L.; Immirzi, B.; Malinconico, M.; Volpe, M.; Oliva, A.; Ragione, F. Preparation and characterization of composites based on biodegradable polymers for in vivo application. *Polymer* **2000**, *41*, 8027–8033. [CrossRef]
375. Chen, B.; Sun, K. Poly(ε-caprolactone)/hydroxyapatite composites: Effects of particle size, molecular weight distribution and irradiation on interfacial interaction and properties. *Polym. Test.* **2005**, *24*, 64–70. [CrossRef]
376. Kim, H.W.; Knowles, J.C.; Kim, H.E. Hydroxyapatite/poly(ε-caprolactone) composite coatings on hydroxyapatite porous bone scaffold for drug delivery. *Biomaterials* **2004**, *25*, 1279–1287. [CrossRef]
377. Ural, E.; Kesenci, K.; Fambri, L.; Migliaresi, C.; Piskin, E. Poly(D,L-lactide/ε-caprolactone)/hydroxyapatite composites. *Biomaterials* **2000**, *21*, 2147–2154. [CrossRef]
378. Rodenas-Rochina, J.; Vidaurre, A.; Cortázar, I.C.; Lebourg, M. Effects of hydroxyapatite filler on long-term hydrolytic degradation of PLLA/PCL porous scaffolds. *Polym. Degrad. Stabil.* **2015**, *119*, 121–131. [CrossRef]
379. Kim, H.W.; Lee, E.J.; Kim, H.E.; Salih, V.; Knowles, J.C. Effect of fluoridation of hydroxyapatite in hydroxyapatite/polycaprolactone composites on osteoblast activity. *Biomaterials* **2005**, *26*, 4395–4404. [CrossRef]
380. Reyna-Urrutia, V.A.; Estevez, M.; González-González, A.M.; Rosales-Ibáñez, R. 3D scaffolds of caprolactone/chitosan/polyvinyl alcohol/hydroxyapatite stabilized by physical bonds seeded with swine dental pulp stem cell for bone tissue engineering. *J. Mater. Sci. Mater. Med.* **2022**, *33*, 81. [CrossRef]
381. Gloria, A.; Russo, T.; D'Amora, U.; Zeppetelli, S.; D'Alessandro, T.; Sandri, M.; Bañobre-López, M.; Piñeiro-Redondo, Y.; Uhlarz, M.; Tampieri, A.; et al. Magnetic poly(ε-caprolactone)/iron-doped hydroxyapatite nanocomposite substrates for advanced bone tissue engineering. *J. R. Soc. Interface* **2013**, *10*, 20120833. [CrossRef]

382. Shokrollahi, P.; Mirzadeh, H.; Scherman, O.A.; Huck, W.T.S. Biological and mechanical properties of novel composites based on supramolecular polycaprolactone and functionalized hydroxyapatite. *J. Biomed. Mater. Res. A* **2010**, *95A*, 209–221. [CrossRef]
383. Mehmanchi, M.; Shokrollahi, P.; Atai, M.; Omidian, H.; Bagheri, R. Supramolecular polycaprolactone nanocomposite based on functionalized hydroxyapatite. *J. Bioact. Compat. Polym.* **2012**, *27*, 467–480. [CrossRef]
384. Bose, S.; Razack, S.A.; Arthanari, S.; Kim, Y.; Lee, H.; Kang, H.W. Near-infrared light-responsive Cu_2O@$CuFeS_2$-hydroxyapatite-chitosan based antibacterial coating on titanium bioimplant. *Prog. Org. Coat.* **2023**, *183*, 107714. [CrossRef]
385. Popkov, A.; Tverdokhlebov, S.; Muradisinov, S.; Popkov, D. First clinical case of Ilizarov femur lengthening over a bioactive and degradable intramedullary implant. *Case Rep. Orthop.* **2023**, *2023*, 7547590. [CrossRef]
386. Cojocaru, F.D.; Gardikiotis, I.; Dodi, G.; Rotaru, A.; Balan, V.; Rezus, E.; Verestiuc, L. Polysaccharides-calcium phosphates composite beads as bone substitutes for fractures repair and regeneration. *Polymers* **2023**, *15*, 1509. [CrossRef]
387. Klimek, L.; Kopacz, K.; Smielak, B.; Kula, Z. An evaluation of the mechanical properties of a hybrid composite containing hydroxyapatite. *Materials* **2023**, *16*, 4548. [CrossRef]
388. Forysenkova, A.A.; Fadeeva, I.V.; Deyneko, D.V.; Gosteva, A.N.; Mamin, G.V.; Shurtakova, D.V.; Davydova, G.A.; Yankova, V.G.; Antoniac, I.V.; Rau, J.V. Polyvinylpyrrolidone–alginate–carbonate hydroxyapatite porous composites for dental applications. *Materials* **2023**, *16*, 4478. [CrossRef]
389. Deng, C.; Wang, B.; Dongqin, X.; Zhou, S.; Duan, K.; Weng, J. Preparation and shape memory property of hydroxyapatite/poly (vinyl alcohol) composite. *Polym.—Plast. Technol. Eng.* **2012**, *51*, 1315–1318. [CrossRef]
390. Kutikov, A.B.; Reyer, K.A.; Song, J. Shape-memory performance of thermoplastic amphiphilic triblock copolymer poly(D,L-lactic acid-co-ethylene glycol-co-D,L-lactic acid) (PELA)/hydroxyapatite composites. *Macromol. Chem. Phys.* **2014**, *215*, 2482–2490. [CrossRef]
391. Bao, M.; Wang, X.; Yuan, H.; Lou, X.; Zhao, Q.; Zhang, Y. HAp incorporated ultrafine polymeric fibers with shape memory effect for potential use in bone screw hole healing. *J. Mater. Chem. B* **2016**, *4*, 5308–5320. [CrossRef]
392. Esposti, M.D.; Chiellini, F.; Bondioli, F.; Morselli, D.; Fabbri, P. Highly porous PHB-based bioactive scaffolds for bone tissue engineering by in situ synthesis of hydroxyapatite. *Mater. Sci. Eng. C* **2019**, *100*, 286–296. [CrossRef]
393. Guillaume, O.; Geven, M.A.; Varjas, V.; Gehweiler, D.; Stadelmann, V.A.; Smidt, T.; Zeiter, S.; Sprecher, C.; Bos, R.R.M.; Grijpma, D.W.; et al. Orbital floor repair using patient specific osteoinductive implant made by stereolithography. *Biomaterials* **2020**, *233*, 119721. [CrossRef]
394. Sikkema, R.; Keohan, B.; Zhitomirsky, I. Alginic acid polymer-hydroxyapatite composites for bone tissue engineering. *Polymers* **2021**, *13*, 3070. [CrossRef]
395. Novesar, J.; Dinda, A.; Rahmayeni; Upita, S.; Vivi, S. The effect of temperature on the synthesis and characterization of hydroxyapatite-polyethylene glycol composites by in-situ process. *Hybrid Adv.* **2023**, *2*, 100031.
396. Ghasroldasht, M.M.; Mastrogiacomo, M.; Akbarian, F.; Rezaeian, A. Polyurethane and polyurethane/hydroxyapatite scaffold in a three-dimensional culture system. *Cell Biol. Int.* **2022**, *46*, 2041–2049. [CrossRef]
397. Behl, M.; Razzaq, M.Y.; Lendlein, A. Multifunctional shape-memory polymers. *Adv. Mater.* **2010**, *22*, 3388–3410. [CrossRef]
398. Cojocaru, F.D.; Balan, V.; Popa, M.I.; Lobiuc, A.; Antoniac, A.; Antoniac, I.V.; Verestiuc, L. Biopolymers–calcium phosphates composites with inclusions of magnetic nanoparticles for bone tissue engineering. *Int. J. Biol. Macromol.* **2019**, *125*, 612–620. [CrossRef]
399. Carvalho, T.S.S.; Torres, P.M.C.; Belo, J.H.; Mano, J.; Olhero, S.M. Bioactive magnetic materials in bone tissue engineering: A review of recent findings in CaP-based particles and 3D-printed scaffolds. *Adv. NanoBiomed. Res.* **2023**, *3*, 2300035. [CrossRef]
400. Ramesh, N.; Moratti, S.C.; Dias, G.J. Hydroxyapatite-polymer biocomposites for bone regeneration: A review of current trends. *J. Biomed. Mater. Res. B Appl. Biomater.* **2018**, *106B*, 2046–2057. [CrossRef]
401. Ielo, I.; Calabrese, G.; de Luca, G.; Conoci, S. Recent advances in hydroxyapatite-based biocomposites for bone tissue regeneration in orthopedics. *Int. J. Mol. Sci.* **2022**, *23*, 9721. [CrossRef]
402. Furko, M.; Balázsi, K.; Balázsi, C. Calcium phosphate loaded biopolymer composites—A comprehensive review on the most recent progress and promising trends. *Coatings* **2023**, *13*, 360. [CrossRef]
403. Aoki, K.; Ideta, H.; Komatsu, Y.; Tanaka, A.; Kito, M.; Okamoto, M.; Takahashi, J.; Suzuki, S.; Saito, N. Bone-regeneration therapy using biodegradable scaffolds: Calcium phosphate bioceramics and biodegradable polymers. *Bioengineering* **2024**, *11*, 180. [CrossRef]
404. Handschel, J.; Wiesmann, H.P.; Stratmann, U.; Kleinheinz, J.; Meyer, U.; Joos, U. TCP is hardly resorbed and not osteoconductive in a non-loading calvarial model. *Biomaterials* **2002**, *23*, 1689–1695. [CrossRef]
405. Kikuchi, M.; Tanaka, J. Chemical interaction in β-tricalcium phosphate/copolymerized poly-L-lactide composites. *J. Ceram. Soc. Jpn.* **2000**, *108*, 642–645. [CrossRef]
406. Haaparanta, A.M.; Haimi, S.; Ellä, V.; Hopper, N.; Miettinen, S.; Suuronen, R.; Kellomäki, M. Porous polylactide/β-tricalcium phosphate composite scaffolds for tissue engineering applications. *J. Tissue Eng. Regen. Med.* **2010**, *4*, 366–373. [CrossRef]
407. Shin, D.Y.; Kang, M.H.; Kang, I.G.; Kim, H.E.; Jeong, S.H. In vitro and in vivo evaluation of polylactic acid-based composite with tricalcium phosphate microsphere for enhanced biodegradability and osseointegration. *J. Biomater. Appl.* **2018**, *32*, 1360–1370. [CrossRef]

408. Kikuchi, M.; Koyama, Y.; Yamada, T.; Imamura, Y.; Okada, T.; Shirahama, N.; Akita, K.; Takakuda, K.; Tanaka, J. Development of guided bone regeneration membrane composed of β-tricalcium phosphate and poly(L-lactide-co-glycolide-co-ε-caprolactone) composites. *Biomaterials* **2004**, *25*, 5979–5986. [CrossRef]
409. Chen, T.M.; Yao, C.H.; Wang, H.J.; Chou, G.H.; Lee, T.W.; Lin, F.H. Evaluation of a novel malleable, biodegradable osteoconductive composite in a rabbit cranial defect model. *Mater. Chem. Phys.* **1998**, *55*, 44–50. [CrossRef]
410. Dong, G.C.; Chen, H.M.; Yao, C.H. A novel bone substitute composite composed of tricalcium phosphate, gelatin and drynaria fortunei herbal extract. *J. Biomed. Mater. Res. A* **2008**, *84A*, 167–177. [CrossRef]
411. Ji, J.; Yuan, X.; Xia, Z.; Liu, P.; Chen, J. Porous β-tricalcium phosphate composite scaffold reinforced by K_2HPO_4 and gelatin. *Key Eng. Mater.* **2010**, *434–435*, 620–623. [CrossRef]
412. Yao, C.H.; Liu, B.S.; Hsu, S.H.; Chen, Y.S.; Tsai, C.C. Biocompatibility and biodegradation of a bone composite containing tricalcium phosphate and genipin crosslinked gelatin. *J. Biomed. Mater. Res. A* **2004**, *69A*, 709–717. [CrossRef]
413. Eslaminejad, M.B.; Mirzadeh, H.; Mohamadi, Y.; Nickmahzar, A. Bone differentiation of marrow-derived mesenchymal stem cells using β-tricalcium phosphate-alginate-gelatin hybrid scaffolds. *J. Tissue Eng. Regen. Med.* **2007**, *1*, 417–424. [CrossRef]
414. Bigi, A.; Cantelli, I.; Panzavolta, S.; Rubini, K. α-tricalcium phosphate-gelatin composite cements. *J. Appl. Biomater. Biomech.* **2004**, *2*, 81–87.
415. Yang, S.H.; Hsu, C.K.; Wang, K.C.; Hou, S.M.; Lin, F.H. Tricalcium phosphate and glutaraldehyde crosslinked gelatin incorporating bone morphogenetic protein—A viable scaffold for bone tissue engineering. *J. Biomed. Mater. Res. B Appl. Biomater.* **2005**, *74B*, 468–475. [CrossRef]
416. Muramatsu, K.; Oba, K.; Mukai, D.; Hasegawa, K.; Masuda, S.; Yoshihara, Y. Subacute systemic toxicity assessment of β-tricalcium phosphate/carboxymethyl-chitin composite implanted in rat femur. *J. Mater. Sci. Mater. Med.* **2007**, *18*, 513–522. [CrossRef]
417. Panzavolta, S.; Fini, M.; Nicoletti, A.; Bracci, B.; Rubini, K.; Giardino, R.; Bigi, A. Porous composite scaffolds based on gelatin and partially hydrolyzed α-tricalcium phosphate. *Acta Biomater.* **2009**, *5*, 636–643. [CrossRef]
418. Uchino, T.; Kamitakahara, M.; Otsuka, M.; Ohtsuki, C. Hydroxyapatite-forming capability and mechanical properties of organic-inorganic hybrids and α-tricalcium phosphate porous bodies. *J. Ceram. Soc. Jpn.* **2010**, *118*, 57–61. [CrossRef]
419. Flauder, S.; Sajzew, R.; Müller, F.A. Mechanical properties of porous β-tricalcium phosphate composites prepared by ice-templating and poly(σ-caprolactone) impregnation. *ACS Appl. Mater. Interfaces* **2015**, *7*, 845–851. [CrossRef]
420. Ramanathan, M.; Shijirbold, A.; Okui, T.; Tatsumi, H.; Kotani, T.; Shimamura, Y.; Morioka, R.; Ayasaka, K.; Kanno, T. In vivo evaluation of bone regenerative capacity of the novel nanobiomaterial: β-tricalcium phosphate polylactic acid-co-glycolide (β-TCP/PLLA/PGA) for use in maxillofacial bone defects. *Nanomaterials* **2024**, *14*, 91. [CrossRef]
421. Liao, L.; Zhu, W.; Tao, C.; Li, D.; Mao, M. *Cissus quadrangularis* L. extract-loaded tricalcium phosphate reinforced natural polymer composite for guided bone regeneration. *J. Mater. Sci. Mater. Med.* **2023**, *34*, 33. [CrossRef]
422. Ritschl, L.; Schilling, P.; Wittmer, A.; Bohner, M.; Bernstein, A.; Schmal, H.; Seidenstuecker, M. Composite material consisting of microporous beta-TCP ceramic and alginate-dialdehyde-gelatin for controlled dual release of clindamycin and bone morphogenetic protein 2. *J. Mater. Sci. Mater. Med.* **2023**, *34*, 39. [CrossRef]
423. Cohen, B.; Panker, M.; Zuckerman, E.; Foox, M.; Zilberman, M. Effect of calcium phosphate-based fillers on the structure and bonding strength of novel gelatin-alginate bioadhesives. *J. Biomater. Appl.* **2014**, *28*, 1366–1375. [CrossRef]
424. Bleach, N.C.; Tanner, K.E.; Kellomäki, M.; Törmälä, P. Effect of filler type on the mechanical properties of self-reinforced polylactide-calcium phosphate composites. *J. Mater. Sci. Mater. Med.* **2001**, *12*, 911–915. [CrossRef]
425. Liu, L.; Xiong, Z.; Yan, Y.N.; Hu, Y.Y.; Zhang, R.J.; Wang, S.G. Porous morphology, porosity, mechanical properties of poly(α-hydroxy acid)-tricalcium phosphate composite scaffolds fabricated by low-temperature deposition. *J. Biomed. Mater. Res. A* **2007**, *82A*, 618–629. [CrossRef]
426. Zhang, Y.; Zhang, M.Q. Synthesis and characterization of macroporous chitosan/calcium phosphate composite scaffolds for tissue engineering. *J. Biomed. Mater. Res.* **2001**, *55*, 304–312. [CrossRef]
427. Rai, B.; Teoh, S.H.; Hutmacher, D.W.; Cao, T.; Ho, K.H. Novel PCL-based honeycomb scaffolds as drug delivery systems for rhBMP-2. *Biomaterials* **2005**, *26*, 3739–3748. [CrossRef]
428. Rai, B.; Teoh, S.H.; Ho, K.H.; Hutmacher, D.W.; Cao, T.; Chen, F.; Yacob, K. The effect of rhBMP-2 on canine osteoblasts seeded onto 3D bioactive polycaprolactone scaffolds. *Biomaterials* **2004**, *25*, 5499–5506. [CrossRef]
429. Lei, Y.; Rai, B.; Ho, K.H.; Teoh, S.H. In vitro degradation of novel bioactive polycaprolactone—20% tricalcium phosphate composite scaffolds for bone engineering. *Mater. Sci. Eng. C* **2007**, *27*, 293–298. [CrossRef]
430. Miyai, T.; Ito, A.; Tamazawa, G.; Matsuno, T.; Sogo, Y.; Nakamura, C.; Yamazaki, A.; Satoh, T. Antibiotic-loaded poly-ε-caprolactone and porous β-tricalcium phosphate composite for treating osteomyelitis. *Biomaterials* **2008**, *29*, 350–358. [CrossRef]
431. Li, Y.; Wu, Z.G.; Li, X.K.; Guo, Z.; Wu, S.H.; Zhang, Y.Q.; Shi, L.; Teoh, S.H.; Liu, Y.C.; Zhang, Z.Y. A polycaprolactone-tricalcium phosphate composite scaffold as an autograft-free spinal fusion cage in a sheep model. *Biomaterials* **2014**, *35*, 5647–5659. [CrossRef]
432. Takahashi, Y.; Yamamoto, M.; Tabata, Y. Enhanced osteoinduction by controlled release of bone morphogenetic protein-2 from biodegradable sponge composed of gelatin and β-tricalcium phosphate. *Biomaterials* **2005**, *26*, 4856–4865. [CrossRef]
433. Ignatius, A.A.; Betz, O.; Augat, P.; Claes, L.E. In vivo investigations on composites made of resorbable ceramics and poly(lactide) used as bone graft substitutes. *J. Biomed. Mater. Res. Appl. Biomater.* **2001**, *58*, 701–709. [CrossRef]
434. Miao, X.; Lim, W.K.; Huang, X.; Chen, Y. Preparation and characterization of interpenetrating phased TCP/HA/PLGA composites. *Mater. Lett.* **2005**, *59*, 4000–4005. [CrossRef]

435. Ozbek, B.; Erdogan, B.; Ekren, N.; Oktar, F.N.; Akyol, S.; Ben-Nissan, B.; Sasmazel, H.T.; Kalkandelen, C.; Mergen, A.; Kuruca, S.E.; et al. Production of the novel fibrous structure of poly(ε-caprolactone)/tri-calcium phosphate/hexagonal boron nitride composites for bone tissue engineering. *J. Austral. Ceram. Soc.* **2018**, *54*, 251–260. [CrossRef]
436. Dorozhkin, S.V. Multiphasic calcium orthophosphate ($CaPO_4$) bioceramics and their biomedical applications. *Ceram. Int.* **2016**, *42*, 6529–6554. [CrossRef]
437. Zhang, L.F.; Sun, R.; Xu, L.; Du, J.; Xiong, Z.C.; Chen, H.C.; Xiong, C.D. Hydrophilic poly (ethylene glycol) coating on PDLLA/BCP bone scaffold for drug delivery and cell culture. *Mater. Sci. Eng. C* **2008**, *28*, 141–149. [CrossRef]
438. Ignjatovic, N.; Ninkov, P.; Ajdukovic, Z.; Konstantinovic, V.; Uskokovic, D. Biphasic calcium phosphate/poly-(D,L-lactide-co-glycolide) biocomposite as filler and blocks for reparation of bone tissue. *Mater. Sci. Forum* **2005**, *494*, 519–524. [CrossRef]
439. Ignjatovic, N.; Ninkov, P.; Ajdukovic, Z.; Vasiljevic-Radovic, D.; Uskokovic, D. Biphasic calcium phosphate coated with poly-D,L-lactide-co-glycolide biomaterial as a bone substitute. *J. Eur. Ceram. Soc.* **2007**, *27*, 1589–1594. [CrossRef]
440. Yang, W.; Yin, G.; Zhou, D.; Gu, J.; Li, Y. In vitro characteristics of surface-modified biphasic calcium phosphate/poly(L-Lactide) biocomposite. *Adv. Eng. Mater.* **2010**, *12*, B128–B132. [CrossRef]
441. Ignjatovic, N.; Ninkov, P.; Kojic, V.; Bokurov, M.; Srdic, V.; Krnojelac, D.; Selakovic, S.; Uskokovic, D. Cytotoxicity and fibroblast properties during in vitro test of biphasic calcium phosphate/poly-D,L-lactide-co-glycolide biocomposites and different phosphate materials. *Microsc. Res. Techniq.* **2006**, *69*, 976–982. [CrossRef]
442. Ajdukovic, Z.; Ignjatovic, N.; Petrovic, D.; Uskokovic, D. Substitution of osteoporotic alveolar bone by biphasic calcium phosphate/poly-D,L-lactide-co-glycolide biomaterials. *J. Biomater. Appl.* **2007**, *21*, 317–328. [CrossRef]
443. Kim, H.W.; Knowles, J.C.; Kim, H.E. Effect of biphasic calcium phosphates on drug release and biological and mechanical properties of poly(ε-caprolactone) composite membranes. *J. Biomed. Mater. Res. A* **2004**, *70A*, 467–479. [CrossRef]
444. Kwak, K.A.; Jyoti, M.A.; Song, H.Y. In vitro and in vivo studies of three dimensional porous composites of biphasic calcium phosphate/poly ε-caprolactone: Effect of bio-functionalization for bone tissue engineering. *Appl. Surf. Sci.* **2014**, *301*, 307–314. [CrossRef]
445. van Leeuwen, A.C.; Yuan, H.; Passanisi, G.; van der Meer, J.W.; de Bruijn, J.D.; van Kooten, T.G.; Grijpma, D.W.; Bos, R.R. Poly(trimethylene carbonate) and biphasic calcium phosphate composites for orbital floor reconstruction: A feasibility study in sheep. *Eur. Cell. Mater.* **2014**, *27*, 81–96; discussion 96–97. [CrossRef]
446. Hossain, M.; Jeong, J.H.; Sultana, T.; Kim, J.H.; Moon, J.E.; Im, S. A composite of polymethylmethacrylate, hydroxyapatite and β-tricalcium phosphate for bone regeneration in an osteoporotic rat model. *J. Biomed. Mater. Res. B Appl. Biomater.* **2023**, *111*, 1813–1823. [CrossRef]
447. Bakhtiari, L.; Rezai, H.R.; Hosseinalipour, S.M.; Shokrgozar, M.A. Investigation of biphasic calcium phosphate/gelatin nanocomposite scaffolds as a bone tissue engineering. *Ceram. Int.* **2010**, *36*, 2421–2426. [CrossRef]
448. Bakhtiari, L.; Rezai, H.R.; Hosseinalipour, S.M.; Shokrgozar, M.A. Preparation of porous Biphasic calcium phosphate-gelatin nanocomposite for bone tissue engineering. *J. Nano Res.* **2010**, *11*, 67–72. [CrossRef]
449. Hassouna, A.; Elgharbawy, H.; Morsy, R. Development of porous scaffolds based on the in situ synthesis of biphasic calcium phosphate in a gelatin-polyvinyl alcohol matrix for bone tissue engineering. *J. Mol. Struct.* **2023**, *1279*, 134951. [CrossRef]
450. Matsuda, A.; Ikoma, T.; Kobayashi, H.; Tanaka, J. Preparation and mechanical property of core-shell type chitosan/calcium phosphate composite fiber. *Mater. Sci. Eng. C* **2004**, *24*, 723–728. [CrossRef]
451. Rattanachan, S.; Lorprayoon, C.; Boonphayak, P. Synthesis of chitosan/brushite powders for bone cement composites. *J. Ceram. Soc. Jpn.* **2008**, *116*, 36–41. [CrossRef]
452. Ohsawa, H.; Ito, A.; Sogo, Y.; Yamazaki, A.; Ohno, T. Synthesis of albumin/DCP nano-composite particles. *Key Eng. Mater.* **2007**, *330–332*, 239–242. [CrossRef]
453. Mohammad, F.; Arfin, T.; Al-Lohedan, H.A. Synthesis, characterization and applications of ethyl cellulose-based polymeric calcium (II) hydrogen phosphate composite. *J. Electron. Mater.* **2018**, *47*, 2954–2963. [CrossRef]
454. Li, X.; Noshadi, B.; Motamedi, K.; Movahed, E.; Behfarnia, P.; Semiroumi, D.T. Bioceramic calcium phosphate-polymer scaffolds: A promising strategy for osteochondral repair and regenerative medicine. *Mater. Chem. Phys.* **2023**, *304*, 127855. [CrossRef]
455. Xu, H.H.K.; Sun, L.; Weir, M.D.; Antonucci, J.M.; Takagi, S.; Chow, L.C.; Peltz, M. Nano DCPA-whisker composites with high strength and Ca and PO_4 release. *J. Dent. Res.* **2006**, *85*, 722–727. [CrossRef]
456. Xu, H.H.K.; Weir, M.D.; Sun, L.; Takagi, S.; Chow, L.C. Effects of calcium phosphate nanoparticles on Ca-PO_4 composite. *J. Dent. Res.* **2007**, *86*, 378–383. [CrossRef]
457. Xu, H.H.K.; Weir, M.D.; Sun, L. Nanocomposites with Ca and PO_4 release: Effects of reinforcement, dicalcium phosphate particle size and silanization. *Dent. Mater.* **2007**, *23*, 1482–1491. [CrossRef]
458. Chen, W.C.; Chang, K.C.; Wu, H.Y.; Ko, C.L.; Huang, C.L. Thermal cycling effect of dicalcium phosphate-reinforced composites on auto-mineralized dental resin. *Mater. Sci. Eng. C* **2014**, *45*, 359–368. [CrossRef]
459. El-Meliegy, E.; Mabrouk, M.; Kamal, G.M.; Awad, S.M.; El-Tohamy, A.M.; El Gohary, M.I. Anticancer drug carriers using dicalcium phosphate/dextran/CMCnanocomposite scaffolds. *J. Drug Deliv. Sci. Technol.* **2018**, *45*, 315–322. [CrossRef]
460. Tortet, L.; Gavarri, J.R.; Nihoul, G.; Dianoux, A.J. Proton mobilities in brushite and brushite/polymer composites. *Solid State Ion.* **1997**, *97*, 253–256. [CrossRef]
461. Tortet, L.; Gavarri, J.R.; Musso, J.; Nihoul, G.; Sarychev, A.K. Percolation and modeling of proton conduction in polymer/brushite composites. *J. Solid State Chem.* **1998**, *141*, 392–403. [CrossRef]

462. Dorozhkin, S.V. Synthetic amorphous calcium phosphates (ACPs): Preparation, structure, properties and biomedical applications. *Biomater. Sci.* **2021**, *9*, 7748–7798. [CrossRef]
463. Dorozhkin, S.V. Dental applications of calcium orthophosphates ($CaPO_4$). *J. Dent. Res.* **2019**, *1*, 24–54.
464. Zhang, L.; Weir, M.D.; Chow, L.C.; Antonucci, J.M.; Chen, J.; Xu, H.H.K. Novel rechargeable calcium phosphate dental nanocomposite. *Dent. Mater.* **2016**, *32*, 285–293. [CrossRef]
465. Zhang, L.; Weir, M.D.; Chow, L.C.; Reynolds, M.A.; Xu, H.H.K. Rechargeable calcium phosphate orthodontic cement with sustained ion release and re-release. *Sci. Rep.* **2016**, *6*, 36476. [CrossRef]
466. Xie, X.J.; Xing, D.; Wang, L.; Zhou, H.; Weir, M.D.; Bai, Y.X.; Xu, H.H.K. Novel rechargeable calcium phosphate nanoparticle-containing orthodontic cement. *Int. J. Oral Sci.* **2018**, *9*, 24–32. [CrossRef]
467. Liang, K.; Xiao, S.; Wu, J.; Li, J.; Weir, M.D.; Cheng, L.; Reynolds, M.A.; Zhou, X.; Xu, H.H.K. Long-term dentin remineralization by poly(amido amine) and rechargeable calcium phosphate nanocomposite after fluid challenges. *Dent. Mater.* **2018**, *34*, 607–618. [CrossRef]
468. Gutierrez, M.C.; Jobbágy, M.; Ferrer, M.L.; del Monte, F. Enzymatic synthesis of amorphous calcium phosphate-chitosan nanocomposites and their processing into hierarchical structures. *Chem. Mater.* **2008**, *20*, 11–13. [CrossRef]
469. Hakimimehr, D.; Liu, D.M.; Troczynski, T. In-situ preparation of poly(propylene fumarate)–hydroxyapatite composite. *Biomaterials* **2005**, *26*, 7297–7303. [CrossRef]
470. Antonucci, J.M.; Regnault, W.F.; Skrtic, D. Polymerization shrinkage and stress development in amorphous calcium phosphate/urethane dimethacrylate polymeric composites. *J. Compos. Mater.* **2010**, *44*, 355–367. [CrossRef]
471. Wang, K.W.; Zhu, Y.J.; Chen, F.; Cao, S.W. Calcium phosphate/block copolymer hybrid porous nanospheres: Preparation and application in drug delivery. *Mater. Lett.* **2010**, *64*, 2299–2301. [CrossRef]
472. Cao, S.W.; Zhu, Y.J.; Wu, J.; Wang, K.W.; Tang, Q.L. Preparation and sustained-release property of triblock copolymer/calcium phosphate nanocomposite as nanocarrier for hydrophobic drug. *Nanoscale Res. Lett.* **2010**, *5*, 781–785. [CrossRef]
473. Iwama, R.; Anada, T.; Shiwaku, Y.; Tsuchiya, K.; Takahashi, T.; Suzuki, O. Osteogenic cellular activity around onlaid octacalcium phosphate-gelatin composite onto rat calvaria. *J. Biomed. Mater. Res. A* **2018**, *106A*, 1322–1333. [CrossRef]
474. Yokoi, T. The development of novel calcium phosphate-polymer composite biomaterials with macro- to nano-level controlled hierarchical structures. *J. Ceram. Soc. Jpn.* **2019**, *127*, 715–721. [CrossRef]
475. Suzuki, O. Octacalcium phosphate (OCP)-based bone substitute materials. *Jpn. Dent. Sci. Rev.* **2013**, *49*, 58–71. [CrossRef]
476. Derakhshani, A.; Hesaraki, S.; Nezafati, N.; Azami, M. Wound closure, angiogenesis and antibacterial behaviors of tetracalcium phosphate/hydroxyethyl cellulose/hyaluronic acid/gelatin composite dermal scaffolds. *J. Biomat. Sci. Polym. Ed.* **2022**, *33*, 605–626. [CrossRef]
477. Li, D.; Guo, X.; Du, H.; Ding, W.; Li, M.; Xu, Y. Tetracalcium phosphate/polycaprolactone composite scaffold: Mechanical reinforcement, biodegradability regulation and bioactivity induction. *J. Mech. Behav. Biomed. Mater.* **2023**, *147*, 106144. [CrossRef]
478. Dorozhkin, S.V. Self-setting calcium orthophosphate ($CaPO_4$) formulations and their biomedical applications. *Adv. Nano-Bio. Mater. Dev.* **2019**, *3*, 321–421.
479. Brückner, T.; Schamel, M.; Kübler, A.C.; Groll, J.; Gbureck, U. Novel bone wax based on poly(ethylene glycol)–calcium phosphate cement mixtures. *Acta Biomater.* **2016**, *33*, 252–263. [CrossRef]
480. Rödel, M.; Teßmar, J.; Groll, J.; Gbureck, U. Tough and elastic α-tricalcium phosphate cement composites with degradable PEG-based cross-linker. *Materials* **2019**, *12*, 53. [CrossRef]
481. Lou, C.W.; Huang, C.C.; Chen, W.C.; Hu, J.J.; Lu, C.T.; Lin, J.H. Preliminary studies in composite scaffolds of calcium phosphate bone cement with polylactide. *Appl. Mech. Mater.* **2012**, *184–185*, 1098–1101. [CrossRef]
482. Zhong, M.L.; Chen, X.Q.; Fan, H.S.; Zhang, X.D. Incorporation of salmon calcitonin-loaded poly(lactide-co-glycolide) (PLGA) microspheres into calcium phosphate bone cement and the biocompatibility evaluation in vitro. *J. Bioact. Compat. Polym.* **2012**, *27*, 133–147. [CrossRef]
483. Bigi, A.; Bracci, B.; Panzavolta, S. Effect of added gelatin on the properties of calcium phosphate cement. *Biomaterials* **2004**, *25*, 2893–2899. [CrossRef]
484. Bigi, A.; Panzavolta, S.; Sturba, L.; Torricelli, P.; Fini, M.; Giardino, R. Normal and osteopenic bone-derived osteoblast response to a biomimetic gelatin-calcium phosphate bone cement. *J. Biomed. Mater. Res. A* **2006**, *78A*, 739–745. [CrossRef]
485. Panzavolta, S.; Torricelli, P.; Sturba, L.; Bracci, B.; Giardino, R.; Bigi, A. Setting properties and in vitro bioactivity of strontium-enriched gelatin-calcium phosphate bone cements. *J. Biomed. Mater. Res. A* **2008**, *84A*, 965–972. [CrossRef]
486. Maazouz, Y.; Montufar, E.B.; Guillem-Marti, J.; Fleps, I.; Öhman, C.; Persson, C.; Ginebra, M.P. Robocasting of biomimetic hydroxyapatite scaffolds using self-setting inks. *J. Mater. Chem. B* **2014**, *2*, 5378–5386. [CrossRef]
487. Rammelt, S.; Neumann, M.; Hanisch, U.; Reinstorf, A.; Pompe, W.; Zwipp, H.; Biewener, A. Osteocalcin enhances bone remodeling around hydroxyapatite/collagen composites. *J. Biomed. Mater. Res. A* **2005**, *73A*, 284–294. [CrossRef]
488. Park, J.H.; Lee, E.J.; Knowles, J.C.; Kim, H.W. Preparation of in situ hardening composite microcarriers: Calcium phosphate cement combined with alginate for bone regeneration. *J. Biomater. Appl.* **2014**, *28*, 1079–1084. [CrossRef]
489. Wang, X.; Ma, J.; Feng, Q.; Cui, F.Z. Skeletal repair in rabbits with calcium phosphate cements incorporated phosphorylated chitin. *Biomaterials* **2002**, *23*, 4591–4600. [CrossRef]

490. Xue, B.; Zhang, C.; Wang, Y.; Wang, J.; Zhang, J.; Lu, M.; Li, G.; Cao, Z.; Huang, Q. A novel controlled-release system for antibacterial enzyme lysostaphin delivery using hydroxyapatite/chitosan composite bone cement. *PLoS ONE* **2014**, *9*, e113797. [CrossRef]
491. Cui, G.; Li, J.; Lei, W.; Bi, L.; Tang, P.; Liang, Y.; Tao, S.; Wang, Y. The mechanical and biological properties of an injectable calcium phosphate cement-fibrin glue composite for bone regeneration. *J. Biomed. Mater. Res. B Appl. Biomater.* **2010**, *92B*, 377–385. [CrossRef]
492. Han, F.; Shi, C.; Yang, H.; Li, B. Calcium phosphate-silk fibroin composites: Bone cement and beyond. In *Developments and Applications of Calcium Phosphate Bone Cements*; Liu, C., He, H., Eds.; Springer Series in Biomaterials Science and Engineering; Springer: Singapore, 2018; Volume 9, pp. 449–472.
493. Cassel, J.B.; Tronco, M.C.; de Melo, B.A.; Oliveira, F.D.S.D.; dos Santos, L.A.L. α-Tricalcium phosphate cement reinforced with silk fibroin: A high strength biomimetic bone cement with chloride-substituted hydroxyapatite. *J. Mech. Behav. Biomed. Mater.* **2023**, *143*, 105936. [CrossRef]
494. Liu, W.; Zhang, J.; Rethore, G.; Khairoun, K.; Pilet, P.; Tancret, F.; Bouler, J.M.; Weiss, P. A novel injectable, cohesive and toughened Si-HPMC (silanized-hydroxypropyl methylcellulose) composite calcium phosphate cement for bone substitution. *Acta Biomater.* **2014**, *10*, 3335–3345. [CrossRef]
495. Mirkiani, S.; Mesgar, A.S.; Mohammadi, Z.; Matinfar, M. Synergetic reinforcement of brushite cements by monetite/apatite whisker-like fibers and carboxymethylcellulose. *Materialia* **2022**, *21*, 101329. [CrossRef]
496. de Lacerda Schickert, S.; Pinto, J.C.; Jansen, J.; Leeuwenburgh, S.C.G.; van den Beucken, J.J.J.P. Tough and injectable fiber reinforced calcium phosphate cement as an alternative to polymethylmethacrylate cement for vertebral augmentation: A biomechanical study. *Biomater. Sci.* **2020**, *8*, 4239. [CrossRef]
497. Luo, J.; Faivre, J.; Engqvist, H.; Persson, C. The addition of poly(vinyl alcohol) fibers to apatitic calcium phosphate cement can improve its toughness. *Materials* **2019**, *12*, 1531. [CrossRef]
498. Duru, İ.; Büyük, N.İ.; Köse, G.T.; Marques, D.W.; Bruce, K.A.; Martin, J.R.; Ege, D. Incorporating the antioxidant fullerenol into calcium phosphate bone cements increases cellular osteogenesis without compromising physical cement characteristics. *Adv. Eng. Mater.* **2023**, *25*, 2300301. [CrossRef]
499. Sadiasa, A.; Sarkar, S.K.; Franco, R.A.; Min, Y.K.; Lee, B.T. Bioactive glass incorporation in calcium phosphate cement-based injectable bone substitute for improved in vitro biocompatibility and in vivo bone regeneration. *J. Biomater. Appl.* **2014**, *28*, 739–756. [CrossRef]
500. El-Fiqi, A.; Kim, J.H.; Kim, H.W. Highly bioactive bone cement microspheres based on α-tricalcium phosphate microparticles/mesoporous bioactive glass nanoparticles: Formulation, physico-chemical characterization and in vivo bone regeneration. *Colloids Surface B* **2022**, *217*, 112650. [CrossRef]
501. Demir-Oğuz, Ö.; Boccaccini, A.R.; Loca, D. Injectable bone cements: What benefits the combination of calcium phosphates and bioactive glasses could bring? *Bioact. Mater.* **2023**, *19*, 217–236. [CrossRef]
502. Richter, R.F.; Ahlfeld, T.; Gelinsky, M.; Lode, A. Composites consisting of calcium phosphate cements and mesoporous bioactive glasses as a 3D plottable drug delivery system. *Acta Biomater.* **2023**, *156*, 146–157. [CrossRef]
503. Richter, R.F.; Vater, C.; Korn, M.; Ahlfeld, T.; Rauner, M.; Pradel, W.; Stadlinger, B.; Gelinsky, M.; Lode, A.; Korn, P. Treatment of critical bone defects using calcium phosphate cement and mesoporous bioactive glass providing spatiotemporal drug delivery. *Bioact. Mater.* **2023**, *28*, 402–419. [CrossRef]
504. Zhou, S.; Ma, J.; Shen, Y.; Haapasalo, M.; Ruse, N.D.; Yang, Q.; Troczynski, T. In vitro studies of calcium phosphate silicate bone cements. *J. Mater. Sci. Mater. Med.* **2013**, *24*, 355–364. [CrossRef]
505. Motisuke, M.; Santos, V.R.; Bazanini, N.C.; Bertran, C.A. Apatite bone cement reinforced with calcium silicate fibers. *J. Mater. Sci. Mater. Med.* **2014**, *25*, 2357–2363. [CrossRef]
506. Correa, D.; Almirall, A.; Carrodeguas, R.G.; dos Santos, L.A.; de Aza, A.H.; Parra, J.; Morejon, L.; Delgado, J.A. α-Tricalcium phosphate cements modified with β-dicalcium silicate and tricalcium aluminate: Physicochemical characterization, in vitro bioactivity and cytotoxicity. *J. Biomed. Mater. Res. B Appl. Biomater.* **2015**, *103B*, 72–83. [CrossRef]
507. Cho, E.; Kim, J.E.; Lee, J.; Park, S.; Lee, S.; Chung, J.H.; Kim, J.; Seonwoo, H. Development of 3D printable calcium phosphate cement scaffolds with cockle shell powders. *Materials* **2023**, *16*, 6154. [CrossRef]
508. Wan, Y.; Ma, H.; Ma, Z.; Tan, L.; Miao, L. Enhanced degradability of the apatite-based calcium phosphate cement incorporated with amorphous MgZnCa alloy. *ACS Biomater. Sci. Eng.* **2023**, *9*, 6084–6093. [CrossRef]
509. Perez, R.A.; Patel, K.D.; Kim, H.W. Novel magnetic nanocomposite injectables: Calcium phosphate cements impregnated with ultrafine magnetic nanoparticles for bone regeneration. *RSC Adv.* **2015**, *5*, 13411–13419. [CrossRef]
510. Elahpour, N.; Rabiee, S.M.; Ebrahimzadeh, M.H.; Moradi, A. In-vitro formation and growth kinetics of apatite on a new light-cured composite calcium phosphate cement. *Ceram. Int.* **2018**, *44*, 15317–15322. [CrossRef]
511. Wang, Y.; Peng, Z.; Zhang, D.; Song, D. Tough, injectable calcium phosphate cement based composite hydrogels to promote osteogenesis. *Gels* **2023**, *9*, 302. [CrossRef]
512. Canal, C.; Ginebra, M.P. Fibre-reinforced calcium phosphate cements: A review. *J. Mech. Behav. Biomed. Mater.* **2011**, *4*, 1658–1671. [CrossRef]
513. Hasan, M.S.; Carpenter, N.; Wei, T.L.; McNally, D.; Ahmed, I.; Boszczyk, B.M. Effects of adding resorbable phosphate glass fibres and PLA to calcium phosphate bone cements. *J. Appl. Biomater. Funct. Mater.* **2014**, *12*, 203–209. [CrossRef]

514. Low, K.L.; Tan, S.H.; Zein, S.H.S.; McPhail, D.S.; Boccaccini, A.R. Optimization of the mechanical properties of calcium phosphate/multi-walled carbon nanotubes/bovine serum albumin composites using response surface methodology. *Mater. Des.* **2011**, *32*, 3312–3319. [CrossRef]
515. Chew, K.K.; Low, K.L.; Zein, S.H.S.; McPhail, D.S.; Gerhardt, L.C.; Roether, J.A.; Boccaccini, A.R. Reinforcement of calcium phosphate cement with multiwalled carbon nanotubes and bovine serum albumin for injectable bone substitute applications. *J. Mech. Behav. Biomed. Mater.* **2011**, *4*, 331–339. [CrossRef]
516. Ruiz, J.; Moreno, D.; Copete, H.; Vargas, F.; López, M.E. Calcium phosphate cements improved by addition of carbonated hydroxyapatite type B. *Bol. Soc. Esp. Ceram. V* **2023**, *62*, 315–328. [CrossRef]
517. Zima, A.; Czechowska, J.; Szponder, T.; Ślósarczyk, A. In vivo behavior of biomicroconcretes based on α-tricalcium phosphate and hybrid hydroxyapatite/chitosan granules and sodium alginate. *J. Biomed. Mater. Res. A* **2020**, *108A*, 1243–1255. [CrossRef]
518. Czechowska, J.; Cichoń, E.; Belcarz, A.; Ślósarczyk, A.; Zima, A. Effect of gold nanoparticles and silicon on the bioactivity and antibacterial properties of hydroxyapatite/chitosan/tricalcium phosphate-based biomicroconcretes. *Materials* **2021**, *14*, 3854. [CrossRef]
519. Kim, S.B.; Kim, Y.J.; Yoon, T.L.; Park, S.A.; Cho, I.H.; Kim, E.J.; Kim, I.A.; Shin, J.W. The characteristics of a hydroxyapatite-chitosan-PMMA bone cement. *Biomaterials* **2004**, *25*, 5715–5723. [CrossRef]
520. Vallo, C.I.; Montemartini, P.E.; Fanovich, M.A.; Lópes, J.M.P.; Cuadrado, T.R. Polymethylmethacrylate-based bone cement modified with hydroxyapatite. *J. Biomed. Mater. Res. B Appl. Biomater.* **1999**, *48*, 150–158. [CrossRef]
521. Moursi, A.M.; Winnard, A.V.; Winnard, P.L.; Lannutti, J.J.; Seghi, R.R. Enhanced osteoblast response to a PMMA–HA composite. *Biomaterials* **2002**, *23*, 133–144. [CrossRef]
522. Dalby, M.J.; di Silvio, L.; Harper, E.J.; Bonfield, W. Increasing hydroxyapatite incorporation into poly(methylmethacrylate) cement increases osteoblast adhesion and response. *Biomaterials* **2002**, *23*, 569–576. [CrossRef]
523. Itokawa, H.; Hiraide, T.; Moriya, M.; Fujimoto, M.; Nagashima, G.; Suzuki, R.; Fujimoto, T. A 12 month in vivo study on the response of bone to a hydroxyapatite-polymethylmethacrylate cranioplasty composite. *Biomaterials* **2007**, *28*, 4922–4927. [CrossRef]
524. Tham, W.L.; Chow, W.S.; Ishak, Z.A.M. Flexural and morphological properties of poly(methyl methacrylate)/hydroxyapatite composites: Effects of planetary ball mill grinding time. *J. Reinf. Plastics Compos.* **2010**, *29*, 2065–2075. [CrossRef]
525. Bai, H.; Walsh, F.; Gludovatz, B.; Delattre, B.; Huang, C.; Chen, Y.; Tomsia, A.P.; Ritchie, R.O. Bioinspired hydroxyapatite/poly(methyl methacrylate) composite with a nacre-mimetic architecture by a bidirectional freezing method. *Adv. Mater.* **2016**, *28*, 50–56. [CrossRef]
526. Harper, E.J.; Behiri, J.C.; Bonfield, W. Flexural and fatigue properties of a bone cement based upon polyethylmethacrylate and hydroxyapatite. *J. Mater. Sci. Mater. Med.* **1995**, *6*, 799–803. [CrossRef]
527. Arnold, J.C.; Venditti, N.P. Prediction of the long-term creep behaviour of hydroxyapatite-filled polyethylmethacrylate bone cements. *J. Mater. Sci. Mater. Med.* **2007**, *18*, 1849–1858. [CrossRef]
528. Ohgaki, M.; Yamashita, K. Preparation of polymethylmethacrylate-reinforced functionally graded hydroxyapatite composites. *J. Am. Ceram. Soc.* **2003**, *86*, 1440–1442. [CrossRef]
529. Del Real, R.P.; Padilla, S.; Vallet-Regi, M. Gentamicin release from hydroxyapatite/poly(ethyl methacrylate)/poly(methyl methacrylate)composites. *J. Biomed. Mater. Res.* **2000**, *52*, 1–7. [CrossRef]
530. Bakina, O.; Svarovskaya, N.; Ivanova, L.; Glazkova, E.; Rodkevich, N.; Evstigneev, V.; Evstigneev, M.; Mosunov, A.; Lerner, M. New PMMA-based hydroxyapatite/$ZnFe_2O_4$/ZnO composite with antibacterial performance and low toxicity. *Biomimetics* **2023**, *8*, 488. [CrossRef]
531. Saito, M.; Maruoka, A.; Mori, T.; Sugano, N.; Hino, K. Experimental studies on a new bioactive bone cement: Hydroxyapatite composite resin. *Biomaterials* **1994**, *15*, 156–160. [CrossRef]
532. Kawagoe, K.; Saito, M.; Shibuya, T.; Nakashima, T.; Hino, K.; Yoshikawa, H. Augmentation of cancellous screw fixation with hydroxyapatite composite resin (CAP) in vivo. *J. Biomed. Mater. Res.* **2000**, *53*, 678–684. [CrossRef]
533. Turner, A.W.L.; Gillies, R.M.; Svehla, M.J.; Saito, M.; Walsh, W.R. Hydroxyapatite composite resin cement augmentation of pedicle screw fixation. *Clin. Orthop. Rel. Res.* **2003**, *406*, 253–261. [CrossRef]
534. Watson, K.E.; Ten Huisen, K.S.; Brown, P.W. The formation of hydroxyapatite–calcium polyacrylate composites. *J. Mater. Sci. Mater. Med.* **1999**, *10*, 205–213. [CrossRef]
535. Reed, C.S.; Ten Huisen, K.S.; Brown, P.W.; Allcock, H.R. Thermal stability and compressive strength of calcium-deficient hydroxyapatite–poly[bis(carboxylatophenoxy)phosphazene] composites. *Chem. Mater.* **1996**, *8*, 440–447. [CrossRef]
536. Peter, S.J.; Kim, P.; Yasko, A.W.; Yaszemski, M.J.; Mikos, A.G. Crosslinking characteristics of an injectable poly(propylene fumarate)/β-tricalcium phosphate paste and mechanical properties of the crosslinked composite for use as a biodegradable bone cement. *J. Biomed. Mater. Res.* **1999**, *44*, 314–321. [CrossRef]
537. He, S.; Yaszemski, M.J.; Yasko, A.W.; Engel, P.S.; Mikos, A.G. Injectable biodegradable polymer composites based on poly (propylene fumarate) crosslinked with poly(ethylene glycol)-dimethacrylate. *Biomaterials* **2000**, *21*, 2389–2394. [CrossRef]
538. Ignjatovic, N.; Jovanovic, J.; Suljovrujic, E.; Uskokovic, D. Injectable polydimethylsiloxane/hydroxyapatite composite cement. *Biomed. Mater. Eng.* **2003**, *13*, 401–410.
539. Fei, Z.; Hu, Y.; Wu, D.; Wu, H.; Lu, R.; Bai, J.; Song, H. Preparation and property of a novel bone graft composite consisting of rhBMP-2 loaded PLGA microspheres and calcium phosphate cement. *J. Mater. Sci. Mater. Med.* **2008**, *19*, 1109–1116. [CrossRef]

540. Link, D.P.; van den Dolder, J.; van den Beucken, J.J.J.P.; Cuijpers, V.M.; Wolke, J.G.C.; Mikos, A.G.; Jansen, J.A. Evaluation of the biocompatibility of calcium phosphate cement/PLGA microparticle composites. *J. Biomed. Mater. Res. A* **2008**, *87A*, 760–769. [CrossRef]
541. Chiang, T.Y.; Ho, C.C.; Chen, D.C.H.; Lai, M.H.; Ding, S.J. Physicochemical properties and biocompatibility of chitosan oligosaccharide/gelatin/calcium phosphate hybrid cements. *Mater. Chem. Phys.* **2010**, *120*, 282–288. [CrossRef]
542. Fujishiro, Y.; Takahashi, K.; Sato, T. Preparation and compressive strength of α-tricalcium phosphate/gelatin gel composite cement. *J. Biomed. Mater. Res.* **2001**, *54*, 525–530. [CrossRef]
543. Miyazaki, K.; Horibe, T.; Antonucci, J.M.; Takagi, S.; Chow, L.C. Polymeric calcium phosphate cements: Analysis of reaction products and properties. *Dental Mater.* **1993**, *9*, 41–45. [CrossRef]
544. Miyazaki, K.; Horibe, T.; Antonucci, J.M.; Takagi, S.; Chow, L.C. Polymeric calcium phosphate cements: Setting reaction modifiers. *Dental Mater.* **1993**, *9*, 46–50. [CrossRef]
545. Dos Santos, L.A.; de Oliveira, L.C.; Rigo, E.C.S.; Carrodeguas, R.G.; Boschi, A.O.; de Arruda, A.C.F. Influence of polymeric additives on the mechanical properties of α-tricalcium phosphate cement. *Bone* **1999**, *25*, 99S–102S. [CrossRef]
546. Greish, Y.E.; Brown, P.W.; Bender, J.D.; Allcockm, H.R.; Lakshmim, S.; Laurencin, C.T. Hydroxyapatite-polyphosphazane composites prepared at low temperatures. *J. Am. Ceram. Soc.* **2007**, *90*, 2728–2734. [CrossRef]
547. Greish, Y.E.; Bender, J.D.; Lakshmi, S.; Brown, P.W.; Allcock, H.R.; Laurencin, C.T. Formation of hydroxyapatite-polyphosphazene polymer composites at physiologic temperature. *J. Biomed. Mater. Res. A* **2006**, *77A*, 416–425. [CrossRef]
548. Greish, Y.E.; Bender, J.D.; Lakshmi, S.; Brown, P.W.; Allcock, H.R.; Laurencin, C.T. Low temperature formation of hydroxyapatite-poly(alkyl oxybenzoate) phosphazene composites for biomedical applications. *Biomaterials* **2005**, *26*, 1–9. [CrossRef]
549. Mickiewicz, R.A.; Mayes, A.M.; Knaack, D. Polymer–calcium phosphate cement composites for bone substitutes. *J. Biomed. Mater. Res.* **2002**, *61*, 581–592. [CrossRef]
550. Carey, L.E.; Xu, H.H.K.; Simon, C.G.; Takagi, S.; Chow, L.C. Premixed rapid-setting calcium phosphate composites for bone repair. *Biomaterials* **2005**, *26*, 5002–5014. [CrossRef]
551. Krüger, R.; Seitz, J.M.; Ewald, A.; Bach, F.W.; Groll, J. Strong and tough magnesium wire reinforced phosphate cement composites for load-bearing bone replacement. *J. Mech. Behav. Biomed. Mater.* **2013**, *20*, 36–44. [CrossRef]
552. Miao, X.; Tan, L.P.; Tan, L.S.; Huang, X. Porous calcium phosphate ceramics modified with PLGA–bioactive glass. *Mater. Sci. Eng. C* **2007**, *27*, 274–279. [CrossRef]
553. Lickorish, D.; Guan, L.; Davies, J.E. A three-phase, fully resorbable, polyester/calcium phosphate scaffold for bone tissue engineering: Evolution of scaffold design. *Biomaterials* **2007**, *28*, 1495–1502. [CrossRef]
554. Qian, G.; Fan, P.; He, F.; Ye, J. Novel strategy to accelerate bone regeneration of calcium phosphate cement by incorporating 3D plotted poly(lactic-co-glycolic acid) network and bioactive wollastonite. *Adv. Healthc. Mater.* **2019**, *8*, 1801325. [CrossRef]
555. Iwasakia, Y.; Takahataa, Y.; Fujii, S. Self-setting particle-stabilized emulsion for hard-tissue engineering. *Colloid Surface B* **2015**, *126*, 394–400. [CrossRef]
556. Xu, H.H.K.; Simon, C.G. Fast setting calcium phosphate-chitosan scaffold: Mechanical properties and biocompatibility. *Biomaterials* **2005**, *26*, 1337–1348. [CrossRef]
557. Zhang, L.; Li, Y.; Zhou, G.; Lu, G.Y.; Zuo, Y. Setting mechanism of nano-hydroxyapatite/chitosan bone cement. *J. Inorg. Mater.* **2006**, *21*, 1197–1202.
558. Ruhe, P.Q.; Hedberg, E.L.; Padron, N.T.; Spauwen, P.H.M.; Jansen, J.A.; Mikos, A.G. Biocompatibility and degradation of poly(D,L-lactic-co-glycolic acid)/calcium phosphate cement composites. *J. Biomed. Mater. Res. A* **2005**, *74A*, 533–544. [CrossRef]
559. Guo, D.G.; Sun, H.L.; Xu, K.W.; Han, Y. Long-term variations in mechanical properties and in vivo degradability of CPC/PLGA composite. *J. Biomed. Mater. Res. B Appl. Biomater.* **2007**, *82B*, 533–544.
560. Habraken, W.J.E.M.; Wolke, J.G.C.; Mikos, A.G.; Jansen, J.A. Injectable PLGA microsphere/calcium phosphate cements: Physical properties and degradation characteristics. *J. Biomater. Sci. Polym. Edn.* **2006**, *17*, 1057–1074. [CrossRef]
561. Ruhe, P.Q.; Hedberg-Dirk, E.L.; Padron, N.T.; Spauwen, P.H.M.; Jansen, J.A.; Mikos, A.G. Porous poly (D,L-lactic-co-glycolic acid)/calcium phosphate cement composite for reconstruction of bone defects. *Tissue Eng.* **2006**, *12*, 789–800. [CrossRef]
562. Ruhe, P.Q.; Hedberg, E.L.; Padron, N.T.; Spauwen, P.H.M.; Jansen, J.A.; Mikos, A.G. rhBMP-2 release from injectable poly (D,L-lactic-co-glycolic acid)/calcium phosphate composites. *J. Bone Joint Surg.* **2003**, *85A* (Suppl. S3), 75–81. [CrossRef]
563. Plachokova, A.; Link, D.; van den Dolder, J.; van den Beucken, J.; Jansen, J.A. Bone regenerative properties of injectable PGLA–CaP composite with TGF-β1 in a rat augmentation model. *J. Tissue Eng. Regen. Med.* **2007**, *1*, 457–464. [CrossRef]
564. Roy, A.; Jhunjhunwala, S.; Bayer, E.; Fedorchak, M.; Little, S.R.; Kumta, P.N. Porous calcium phosphate–poly (lactic-co-glycolic) acid composite bone cement: A viable tunable drug delivery system. *Mater. Sci. Eng. C* **2016**, *59*, 92–101. [CrossRef]
565. Bian, T.; Zhao, K.; Meng, Q.; Jiao, H.; Tang, Y.; Luo, J. Fabrication and performance of calcium phosphate cement/small intestinal submucosa composite bionic bone scaffolds with different microstructures. *Ceram. Int.* **2018**, *44*, 9181–9187. [CrossRef]
566. Moussi, H.; Weiss, P.; le Bideau, J.; Gautier, H.; Charbonnier, B. Injectable macromolecule-based calcium phosphate bone substitutes. *Mater. Adv.* **2022**, *3*, 6125–6141. [CrossRef]
567. Liu, S.; Hu, Y.; Zhang, J.; Bao, S.; Xian, L.; Dong, X.; Zheng, W.; Li, Y.; Gao, H.; Zhou, W. Bioactive and biocompatible macroporous scaffolds with tunable performances prepared based on 3D printing of the pre-crosslinked sodium alginate/hydroxyapatite hydrogel ink. *Macromol. Mater. Eng.* **2019**, *304*, 1800698. [CrossRef]

568. Zhou, Z.X.; Buchanan, F.; Mitchell, C.; Dunne, N. Printability of calcium phosphate: Calcium sulfate powders for the application of tissue engineered bone scaffolds using the 3D printing technique. *Mater. Sci. Eng. C* **2014**, *38*, 1–10. [CrossRef]
569. Torrejon-Moya, A.; Apalimova, A.; González-Navarro, B.; Zaera-Le Gal, R.; Marí-Roig, A.; López-López, J. Calcium sulfate in implantology (biphasic calcium sulfate/hydroxyapatite, BCS/HA, Bond Apatite®): Review of the literature and case reports. *Coatings* **2022**, *12*, 1350. [CrossRef]
570. Zhang, Y.; Xie, L.; Jiao, X.; Yue, X.; Xu, Y.; Wang, C.; Li, Y.; Yang, X.; Yang, G.; Xu, S.; et al. Preferentially biodegradable gypsum fibers endowing invisible microporous structures and enhancing osteogenic capability of calcium phosphate cements. *ACS Biomater. Sci. Eng.* **2024**, *10*, 1077–1089. [CrossRef]
571. Liu, J.; Qiu, F.; Zou, Y.; Zhang, Z.; Wang, A.; Zhang, Y. Physicochemical and biological properties of composite bone cement based on octacalcium phosphate and tricalcium silicate. *Ceram. Int.* **2023**, *49*, 20315–20325. [CrossRef]
572. Stepanova, K.; Lytkina, D.; Sadykov, R.; Shalygina, K.; Khojazoda, T.; Mahmadbegov, R.; Kurzina, I. Composite cement materials based on β-tricalcium phosphate, calcium sulfate and a mixture of polyvinyl alcohol and polyvinylpyrrolidone intended for osteanagenesis. *Polymers* **2023**, *15*, 210. [CrossRef]
573. Gao, H.; Ji, B.; Jager, I.L.; Arzt, E.; Fratzl, P. Materials become insensitive to flaws at nanoscale: Lessons from nature. *Proc. Nat. Acad. Sci. USA* **2003**, *100*, 5597–5600. [CrossRef]
574. Webster, T.J. Nanophase ceramics: The future orthopedic and dental implant material. *Adv. Chem. Eng.* **2001**, *27*, 125–166.
575. Webster, T.J.; Ergun, C.; Doremus, R.H.; Siegel, R.W.; Bizios, R. Enhanced functions of osteoblasts on nanophase ceramics. *Biomaterials* **2000**, *21*, 1803–1810. [CrossRef]
576. Zakaria, S.M.; Zein, S.H.S.; Othman, M.R.; Yang, F.; Jansen, J.A. Nanophase hydroxyapatite as a biomaterial in advanced hard tissue engineering: A review. *Tissue Eng. B* **2013**, *19*, 431–441. [CrossRef]
577. Dorozhkin, S.V. Nanometric calcium orthophosphates ($CaPO_4$): Preparation, properties and biomedical applications. *Adv. Nano-Bio. Mater. Dev.* **2019**, *3*, 422–513.
578. Li, G.; Huang, J.; Li, Y.; Zhang, R.; Deng, B.; Zhang, J.; Aoki, H. In vitro study on influence of a discrete nano-hydroxyapatite on leukemia P388 cell behavior. *Biomed. Mater. Eng.* **2007**, *17*, 321–327.
579. Mizutani, T.; Okuda, N. Bioinspired mechanical materials–development of high-toughness ceramics through complexation of calcium phosphate and organic polymers. *Ceramics* **2023**, *6*, 2117–2133. [CrossRef]
580. Xu, H.H.K.; Sun, L.; Weir, M.D.; Takagi, S.; Chow, L.C.; Hockey, B. Effects of incorporating nanosized calcium phosphate particles on properties of whisker-reinforced dental composites. *J. Biomed. Mater. Res. B Appl. Biomater.* **2007**, *81B*, 116–125. [CrossRef]
581. Shu, X.; Shi, Q.; Feng, J.; Xie, X.; Chen, Y. Design and in vitro evaluation of novel γ-PGA/hydroxyapatite nanocomposites for bone tissue engineering. *J. Mater. Sci.* **2014**, *49*, 7742–7749. [CrossRef]
582. Hong, Z.K.; Zhang, P.B.; He, C.L.; Qiu, X.Y.; Liu, A.X.; Chen, L.; Chen, X.; Jing, X. Nanocomposite of poly(L-lactide) and surface grafted hydroxyapatite: Mechanical properties and biocompatibility. *Biomaterials* **2005**, *26*, 6296–6304. [CrossRef]
583. Kothapalli, C.R.; Shaw, M.T.; Wei, M. Biodegradable HA-PLA 3-D porous scaffolds: Effect of nano-sized filler content on scaffold properties. *Acta Biomater.* **2005**, *1*, 653–662. [CrossRef]
584. Aydin, E.; Planell, J.A.; Hasirci, V. Hydroxyapatite nanorod-reinforced biodegradable poly(L-lactic acid) composites for bone plate applications. *J. Mater. Sci. Mater. Med.* **2011**, *22*, 2413–2427. [CrossRef]
585. Chae, T.; Yang, H.; Ko, F.; Troczynski, T. Bio-inspired dicalcium phosphate anhydrate/poly(lactic acid) nanocomposite fibrous scaffolds for hard tissue regeneration: In situ synthesis and electrospinning. *J. Biomed. Mater. Res. A* **2014**, *102A*, 514–522. [CrossRef]
586. Liu, Z.; Chen, Y.; Ding, W.; Zhang, C. Filling behavior, morphology evolution and crystallization behavior of microinjection molded poly(lactic acid)/hydroxyapatite nanocomposites. *Compos. A* **2015**, *72*, 85–95. [CrossRef]
587. Nguyen, N.M.; Kakarla, A.B.; Nukala, S.G.; Kong, C.; Baji, A.; Kong, I. Evaluation of physicochemical properties of a hydroxyapatite polymer nanocomposite for use in fused filament fabrication. *Polymers* **2023**, *15*, 3980. [CrossRef]
588. Hong, Z.; Zhang, P.; Liu, A.; Chen, L.; Chen, X.; Jing, X. Composites of poly(lactide-co-glycolide) and the surface modified carbonated hydroxyapatite nanoparticles. *J. Biomed. Mater. Res. A* **2007**, *81A*, 515–522. [CrossRef]
589. Huang, Y.X.; Ren, J.; Chen, C.; Ren, T.B.; Zhou, X.Y. Preparation and properties of poly(lactide-co-glycolide) (PLGA)/nano-hydroxyapatite (NHA) scaffolds by thermally induced phase separation and rabbit MSCs culture on scaffolds. *J. Biomater. Appl.* **2008**, *22*, 409–432. [CrossRef]
590. Xue, D.; Zheng, Q.; Zong, C.; Li, Q.; Li, H.; Qian, S.; Zhang, B.; Yu, L.; Pan, Z. Osteochondral repair using porous poly(lactide-co-glycolide)/nano-hydroxyapatite hybrid scaffolds with undifferentiated mesenchymal stem cells in a rat model. *J. Biomed. Mater. Res. A* **2010**, *94A*, 259–270. [CrossRef]
591. Torabinejad, B.; Mohammadi-Rovshandeh, J.; Davachi, S.M.; Zamanian, A. Synthesis and characterization of nanocomposite scaffolds based on triblock copolymer of L-lactide, ε-caprolactone and nano-hydroxyapatite for bone tissue engineering. *Mater. Sci. Eng. C* **2014**, *42*, 199–210. [CrossRef]
592. Solechan, S.; Suprihanto, A.; Widyanto, S.A.; Triyono, J.; Fitriyana, D.F.; Siregar, J.P.; Cionita, T. Characterization of PLA/PCL/nano-hydroxyapatite (nHA) biocomposites prepared via cold isostatic pressing. *Polymers* **2023**, *15*, 559. [CrossRef]
593. Yazdanpanah, Z.; Sharma, N.K.; Raquin, A.; Cooper, D.M.L.; Chen, X.; Johnston, J.D. Printing tissue-engineered scaffolds made of polycaprolactone and nano-hydroxyapatite with mechanical properties appropriate for trabecular bone substitutes. *BioMed. Eng. OnLine* **2023**, *22*, 73. [CrossRef]

594. Kikuchi, M.; Itoh, S.; Ichinose, S.; Shinomiya, K.; Tanaka, J. Self-organization mechanism in a bone-like hydroxyapatite/collagen nanocomposite synthesized in vitro and its biological reaction in vivo. *Biomaterials* **2001**, *22*, 1705–1711. [CrossRef]
595. Kikuchi, M.; Matsumoto, H.N.; Yamada, T.; Koyama, Y.; Takakuda, K.; Tanaka, J. Glutaraldehyde cross-linked hydroxyapatite/collagen self-organized nanocomposites. *Biomaterials* **2004**, *25*, 63–69. [CrossRef]
596. Lynn, A.K.; Nakamura, T.; Patel, N.; Porter, A.E.; Renouf, A.C.; Laity, P.R.; Best, S.M.; Cameron, R.E.; Shimizu, Y.; Bonfield, W. Composition-controlled nanocomposites of apatite and collagen incorporating silicon as osseopromotive agent. *J. Biomed. Mater. Res. A* **2005**, *74A*, 447–453. [CrossRef]
597. Chang, M.C.; Tanaka, J. FTIR study for hydroxyapatite/collagen nanocomposite cross-linked by glutaraldehyde. *Biomaterials* **2002**, *23*, 4811–4818. [CrossRef]
598. Chang, M.C.; Tanaka, J. XPS study for the microstructure development of hydroxyapatite-collagen nanocomposites cross-linked using glutaraldehyde. *Biomaterials* **2002**, *23*, 3879–3885. [CrossRef]
599. Fukui, N.; Sato, T.; Kuboki, Y.; Aoki, H. Bone tissue reaction of nano-hydroxyapatite/collagen composite at the early stage of implantation. *Biomed. Mater. Eng.* **2008**, *18*, 25–33.
600. Kim, T.G.; Park, S.H.; Chung, H.J.; Yang, D.Y.; Park, T.G. Microstructured scaffold coated with hydroxyapatite/collagen nanocomposite multilayer for enhanced osteogenic induction of human mesenchymal stem cells. *J. Mater. Chem.* **2010**, *20*, 8927–8933. [CrossRef]
601. Chen, L.; Hu, J.; Ran, J.; Shen, X.; Tong, H. Synthesis and cytocompatibility of collagen/hydroxyapatite nanocomposite scaffold for bone tissue engineering. *Polym. Compos.* **2016**, *37*, 81–90. [CrossRef]
602. Sri, A.K.; Arthi, C.; Neya, N.R.; Hikku, G.S. Nano-hydroxyapatite/collagen composite as scaffold material for bone regeneration. *Biomed. Mater.* **2023**, *18*, 032002.
603. Liao, S.S.; Cui, F.Z.; Zhu, Y. Osteoblasts adherence and migration through three-dimensional porous mineralized collagen based composite: nHAC/PLA. *J. Bioact. Compat. Polym.* **2004**, *19*, 117–130. [CrossRef]
604. Liao, S.S.; Cui, F.Z.; Zhang, W.; Feng, Q.L. Hierarchically biomimetic bone scaffold materials: Nano-HA/collagen/PLA composite. *J. Biomed. Mater. Res. B Appl. Biomater.* **2004**, *69B*, 158–165. [CrossRef]
605. Liao, S.S.; Cui, F.Z. In vitro and in vivo degradation of the mineralized collagen based composite scaffold: Nanohydroxyapatite/collagen/poly(L-lactide). *Tissue Eng.* **2004**, *10*, 73–80. [CrossRef]
606. Liao, S.S.; Wang, W.; Uo, M.; Ohkawa, S.; Akasaka, T.; Tamura, K.; Cui, F.Z.; Watari, F. A three-layered nano-carbonated hydroxyapatite/collagen/PLGA composite membrane for guided tissue regeneration. *Biomaterials* **2005**, *26*, 7564–7571. [CrossRef]
607. Liao, S.; Watari, F.; Zhu, Y.; Uo, M.; Akasaka, T.; Wang, W.; Xu, G.; Cui, F.Z. The degradation of the three layered nano-carbonated hydroxyapatite/collagen/PLGA composite membrane in vitro. *Dent. Mater.* **2007**, *23*, 1120–1128. [CrossRef]
608. Degirmenbasi, N.; Kalyon, D.M.; Birinci, E. Biocomposites of nanohydroxyapatite with collagen and poly(vinyl alcohol). *Colloids Surf. B* **2006**, *48*, 42–49. [CrossRef]
609. Zhang, S.M.; Cui, F.Z.; Liao, S.S.; Zhu, Y.; Han, L. Synthesis and biocompatibility of porous nanohydroxyapatite/collagen/alginate composite. *J. Mater. Sci. Mater. Med.* **2003**, *14*, 641–645. [CrossRef]
610. Sotome, S.; Uemura, T.; Kikuchi, M.; Chen, J.; Itoh, S.; Tanaka, J.; Tateishi, T.; Shinomiya, K. Synthesis and in vivo evaluation of a novel hydroxyapatite/collagen-alginate as a bone filler and a drug delivery carrier of bone morphogenetic protein. *Mater. Sci. Eng. C* **2004**, *24*, 341–347. [CrossRef]
611. Chang, M.C.; Ikoma, T.; Tanaka, J. Cross-linkage of hydroxyapatite/gelatin nanocomposite using EGDE. *J. Mater. Sci.* **2004**, *39*, 5547–5550. [CrossRef]
612. Teng, S.; Shi, J.; Peng, B.; Chen, L. The effect of alginate addition on the structure and morphology of hydroxyapatite/gelatin nanocomposites. *Compos. Sci. Technol.* **2006**, *66*, 1532–1538. [CrossRef]
613. Mobini, S.; Javadpour, J.; Hosseinalipour, M.; Ghazi-Khansari, M.; Khavandi, A.; Rezaie, H.R. Synthesis and characterisation of gelatin-nano hydroxyapatite composite scaffolds for bone tissue engineering. *Adv. Appl. Ceram.* **2008**, *107*, 4–8. [CrossRef]
614. Wang, H.; Bongio, M.; Farbod, K.; Nijhuis, A.W.; van den Beucken, J.; Boerman, O.C.; van Hest, J.C.; Li, Y.; Jansen, J.A.; Leeuwenburgh, S.C.G. Development of injectable organic/inorganic colloidal composite gels made of self-assembling gelatin nanospheres and calcium phosphate nanocrystals. *Acta Biomater.* **2014**, *10*, 508–519. [CrossRef]
615. Maulida, H.N.; Hikmawati, D.; Budiatin, A.S. Injectable bone substitute paste based on hydroxyapatite, gelatin and streptomycin for spinal tuberculosis. *J. Spine* **2015**, *4*, 1000266. [CrossRef]
616. Hachinohe, Y.; Taira, M.; Hoshi, M.; Yoshida, D.; Hatakeyama, W.; Sawada, T.; Kondo, H. Self-prepared hyaluronic acid/alkaline gelatin composite with nano-hydroxyapatite and bone morphogenetic protein for cranial bone formation. *Int. J. Mol. Sci.* **2023**, *24*, 1104. [CrossRef]
617. Lewandrowski, K.U.; Bondre, S.P.; Wise, D.L.; Trantolo, D.J. Enhanced bioactivity of a poly(propylene fumarate) bone graft substitute by augmentation with nano-hydroxyapatite. *Biomed. Mater. Eng.* **2003**, *13*, 115–124.
618. Klein, T.R.; Kirillova, A.; Galla, K.; Becker, M.L. Influence of post-processing on the properties of 3D-printed poly(propylene fumarate) star polymer hydroxyapatite nanocomposites. *RSC Appl. Polym.* **2023**, *1*, 73–81. [CrossRef]
619. Wei, J.; Li, Y.; Chen, W.; Zuo, Y. A study on nano-composite of hydroxyapatite and polyamide. *J. Mater. Sci.* **2003**, *38*, 3303–3306. [CrossRef]
620. Wang, H.; Li, Y.; Zuo, Y.; Li, J.; Ma, S.; Cheng, L. Biocompatibility and osteogenesis of biomimetic nano-hydroxyapatite/polyamide composite scaffolds for bone tissue engineering. *Biomaterials* **2007**, *28*, 3338–3348. [CrossRef]

621. Zhang, X.; Li, Y.; Zuo, Y.; Lv, G.Y.; Mu, Y.H.; Li, H. Morphology, hydrogen-bonding and crystallinity of nano-hydroxyapatite/polyamide 66 biocomposites. *Compos. A* **2007**, *38*, 843–848. [CrossRef]
622. Zhang, X.; Li, Y.; Lv, G.Y.; Zuo, Y.; Mu, Y.H.; Lan, W. The study on interaction mechanism between n-HA and PA66 in n-HA/PA66 biocomposites. *Funct. Mater.* **2005**, *36*, 896–899.
623. Menon, D.; Anand, K.A.; Anitha, V.C.; Nair, S. Hydroxyapatite-reinforced polyamide 6,6 nanocomposites through melt compounding. *Int. J. Polym. Mater.* **2010**, *59*, 498–509. [CrossRef]
624. Hu, G.; Wang, H.; Yao, X.; Bi, D.; Zhu, G.; Tang, S.; Wei, J.; Yang, L.; Tong, P.; Xiao, L. Development of nanofluorapatite polymer-based composite for bioactive orthopedic implants and prostheses. *Int. J. Nanomed.* **2014**, *9*, 3875–3884. [CrossRef]
625. Yusong, P.; Dangsheng, X.; Xiaolin, C. Mechanical properties of nanohydroxyapatite reinforced poly(vinyl alcohol) gel composites as biomaterial. *J. Mater. Sci.* **2007**, *42*, 5129–5134. [CrossRef]
626. Xu, F.; Li, Y.; Wang, X.; Wei, J.; Yang, A. Preparation and characterization of nano-hydroxyapatite/poly(vinyl alcohol) hydrogel biocomposite. *J. Mater. Sci.* **2004**, *39*, 5669–5672.
627. Wang, H.S.; Wang, G.X.; Pan, Q.X. Electrochemical study of the interactions of DNA with redox-active molecules based on the immobilization of dsDNA on the sol-gel derived nano porous hydroxyapatite-polyvinyl alcohol hybrid material coating. *Electroanalysis* **2005**, *17*, 1854–1860. [CrossRef]
628. Bobrowska, K.; Sadowska, K.; Golec, P.; Bilewicz, R.; Stolarczyk, K.; Przesniak-Welenc, M. Bovine serum albumin–hydroxyapatite nanoflowers as potential local drug delivery system of ciprofloxacin. *Int. J. Nanomed.* **2023**, *18*, 6449–6467. [CrossRef]
629. Pramanik, N.; Mohapatra, S.; Pramanik, P.; Bhargava, P. Processing and properties of nano-hydroxyapatite (n-HAp)/poly(ethylene-co-acrylic acid) (EAA) composite using a phosphonic acid coupling agent for orthopedic applications. *J. Am. Ceram. Soc.* **2007**, *90*, 369–375. [CrossRef]
630. Pramanik, N.; Bhargava, P.; Alam, S.; Pramanik, P. Processing and properties of nano- and macro-hydroxyapatite/poly(ethylene-co-acrylic acid) composites. *Polym. Compos.* **2006**, *27*, 633–641. [CrossRef]
631. Zhang, Y.F.; Cheng, X.R.; Chen, Y.; Shi, B.; Chen, X.H.; Xu, D.X.; Ke, J. Three-dimensional nanohydroxyapatite/chitosan scaffolds as potential tissue engineered periodontal tissue. *J. Biomater. Appl.* **2007**, *21*, 333–349. [CrossRef]
632. Thein-Han, W.W.; Misra, R.D.K. Biomimetic chitosan-nanohydroxyapatite composite scaffolds for bone tissue engineering. *Acta Biomater.* **2009**, *5*, 1182–1197. [CrossRef]
633. Ma, X.; Wang, Y.; Guo, H.; Wang, J. Nano-hydroxyapatite/chitosan sponge-like biocomposite for repairing of rat calvarial critical-sized bone defect. *J. Bioact. Compat. Polym.* **2011**, *26*, 335–346.
634. Reves, B.T.; Jennings, J.A.; Bumgardner, J.D.; Haggard, W.O. Preparation and functional assessment of composite chitosan-nano-hydroxyapatite scaffolds for bone regeneration. *J. Funct. Biomater.* **2012**, *3*, 114–130. [CrossRef]
635. Roy, P.; Sailaja, R.R.N. Chitosan-nanohydroxyapatite composites: Mechanical, thermal and bio-compatibility studies. *Int. J. Biol. Macromol.* **2015**, *73*, 170–181. [CrossRef]
636. Thomas, S.P.; Alghamdi, M.N. Chitosan composites with nanohydroxyapatite prepared by wet chemical reaction along with microwave irradiation: Permeability and swelling aspects. *Polym. Compos.* **2018**, *39*, 718–729. [CrossRef]
637. Chakraborty, H.; Bhowmik, N. Structure and stability analysis of biocompatible hydroxyapatite reinforced chitosan nanocomposite. *Polym. Compos.* **2018**, *39*, E573–E583. [CrossRef]
638. le Grill, S.; Coppel, S.Y.; Soulie, J.; Bertrand, G.; Rey, C.; Brouille, F. Towards chitosan-amorphous calcium phosphate nanocomposite: Co-precipitation induced by spray drying. *Next Mater.* **2024**, *4*, 100095. [CrossRef]
639. Lu, Y.; Zhu, A.; Wang, W.; Shi, H. New bioactive hybrid material of nano-hydroxyapatite based on N-carboxyethylchitosan for bone tissue engineering. *Appl. Surf. Sci.* **2010**, *256*, 7228–7233. [CrossRef]
640. Zhou, G.; Li, Y.; Zhang, L.; Li, H.; Wang, M.; Cheng, L.; Wang, Y.; Wang, H.; Shi, P. The study of tri-phasic interactions in nano-hydroxyapatite/konjac glucomannan/chitosan composite. *J. Mater. Sci.* **2007**, *42*, 2591–2597.
641. Zhou, G.; Li, Y.; Zhang, L.; Zuo, Y.; Jansen, J.A. Preparation and characterization of nano-hydroxyapatite/chitosan/konjac glucomannan composite. *J. Biomed. Mater. Res. A* **2007**, *83A*, 931–939. [CrossRef]
642. Mohamed, K.R.; El-Rashidy, Z.M.; Salama, A.A. Preparation and characterization of nano hydroxyapatite/polymeric composites materials. Part I. *Mater. Chem. Phys.* **2011**, *130*, 561–568. [CrossRef]
643. Singh, Y.P.; Dasgupta, S.; Bhaskar, R. Preparation, characterization and bioactivities of nano anhydrous calcium phosphate added gelatin–chitosan scaffolds for bone tissue engineering. *J. Biomat. Sci. Polym. Ed.* **2019**, *30*, 1756–1778. [CrossRef]
644. Wu, M.Y.; Kao, I.F.; Fu, C.Y.; Yen, S.K. Effects of adding chitosan on drug entrapment efficiency and release duration for paclitaxel-loaded hydroxyapatite–gelatin composite microspheres. *Pharmaceutics* **2023**, *15*, 2025. [CrossRef]
645. Bueno, V.B.; Bentini, R.; Catalani, L.H.; Barbosa, L.R.S.; Petri, D.F.S. Synthesis and characterization of xanthan-hydroxyapatite nanocomposites for cellular uptake. *Mater. Sci. Eng. C* **2014**, *37*, 195–230. [CrossRef]
646. Huang, J.; Lin, Y.W.; Fu, X.W.; Best, S.M.; Brooks, R.A.; Rushton, N.; Bonfield, W. Development of nano-sized hydroxyapatite reinforced composites for tissue engineering scaffolds. *J. Mater. Sci. Mater. Med.* **2007**, *18*, 2151–2157. [CrossRef]
647. Lee, H.J.; Choi, H.W.; Kim, K.J.; Lee, S.C. Modification of hydroxyapatite nanosurfaces for enhanced colloidal stability and improved interfacial adhesion in nanocomposites. *Chem. Mater.* **2006**, *18*, 5111–5118. [CrossRef]
648. Lee, H.J.; Kim, S.E.; Choi, H.W.; Kim, C.W.; Kim, K.J.; Lee, S.C. The effect of surface-modified nano-hydroxyapatite on biocompatibility of poly(ε-caprolactone) / hydroxyapatite nanocomposites. *Eur. Polym. J.* **2007**, *43*, 1602–1608. [CrossRef]

649. Hao, J.Y.; Liu, Y.; Zhou, S.; Li, Z.; Deng, X. Investigation of nanocomposites based on semi-interpenetrating network of [L-poly (ε-caprolactone)]/[net-poly (ε-caprolactone)] and hydroxyapatite nanocrystals. *Biomaterials* **2003**, *24*, 1531–1539. [CrossRef]
650. Meskinfam, M.; Bertoldi, S.; Albanese, N.; Cerri, A.; Tanzi, M.C.; Imani, R.; Baheiraei, N.; Farokhi, M.; Farè, S. Polyurethane foam/nano hydroxyapatite composite as a suitable scaffold for bone tissue regeneration. *Mater. Sci. Eng. C* **2018**, *82*, 130–140. [CrossRef]
651. Sultan, M. Hydroxyapatite/polyurethane composites as promising biomaterials. *Chem. Pap.* **2018**, *72*, 2375–2395. [CrossRef]
652. Zhang, T.; Li, J.; Wang, Y.; Han, W.; Wei, Y.; Hu, Y.; Liang, Z.; Lian, X.; Huang, D. Hydroxyapatite/polyurethane scaffolds for bone tissue engineering. *Tissue Eng. Part B-Rev.* **2024**, *30*, 60–73. [CrossRef]
653. Ghassemi, B.; Estaji, S.; Mousavi, S.R.; Nemati, M.S.; Shojaei, S.; Mostafaiyan, M.; Arjmand, M.; Khonakdar, H.A. In-depth study of mechanical properties of poly(lactic acid)/thermoplastic polyurethane/hydroxyapatite blend nanocomposites. *J. Mater. Sci.* **2022**, *57*, 7250–7264. [CrossRef]
654. Revilla-López, G.; Casanovas, J.; Bertran, O.; Turon, P.; Puiggalí, J.; Alemán, C. Modeling biominerals formed by apatites and DNA. *Biointerphases* **2013**, *8*, 10. [CrossRef]
655. Bertran, O.; del Valle, L.J.; Revilla-López, G.; Chaves, G.; Cardús, L.; Casas, M.T.; Casanovas, J.; Turon, P.; Puiggalí, J.; Alemán, C. Mineralization of DNA into nanoparticles of hydroxyapatite. *Dalton Trans.* **2014**, *43*, 317–327. [CrossRef]
656. Grande, C.J.; Torres, F.G.; Gomez, C.M.; Bañó, M.C. Nanocomposites of bacterial cellulose/hydroxyapatite for biomedical applications. *Acta Biomater.* **2009**, *5*, 1605–1615. [CrossRef]
657. Zadegan, S.; Hossainalipour, M.; Ghassai, H.; Rezaie, H.R.; Naimi-Jamal, M.R. Synthesis of cellulose-nanohydroxyapatite composite in 1-n-butyl-3-methylimidazolium chloride. *Ceram. Int.* **2010**, *36*, 2375–2381. [CrossRef]
658. Fu, L.H.; Qi, C.; Liu, Y.J.; Cao, W.T.; Ma, M.G. Sonochemical synthesis of cellulose/hydroxyapatite nanocomposites and their application in protein adsorption. *Sci. Rep.* **2018**, *8*, 8292. [CrossRef]
659. Salama, A. Cellulose/calcium phosphate hybrids: New materials for biomedical and environmental applications. *Int. J. Biol. Macromol.* **2019**, *127*, 606–617. [CrossRef]
660. Pang, P.; Li, W.; Liu, Y. Effect of ball milling process on the microstructure of titanium-nanohydroxyapatite composite powder. *Rare Metals* **2007**, *26*, 118–123. [CrossRef]
661. Li, W.; Pang, P.; Liu, Y. Microstructure and phase composition of Ti-based biocomposites with different contents of nano-hydroxyapatite. *Trans. Nonferrous Met. Soc. China* **2007**, *17*, S1148–S1151.
662. Niespodziana, K.; Jurczyk, K.; Jakubowicz, J.; Jurczyk, M. Fabrication and properties of titanium-hydroxyapatite nanocomposites. *Mater. Chem. Phys.* **2010**, *123*, 160–165. [CrossRef]
663. Hesaraki, S.; Ebadzadeh, T.; Ahmadzadeh-Asl, S. Nanosilicon carbide/hydroxyapatite nanocomposites: Structural, mechanical and in vitro cellular properties. *J. Mater. Sci. Mater. Med.* **2010**, *21*, 2141–2149. [CrossRef]
664. Zhao, X.; Yang, J.; Xin, H.; Wang, X.; Zhang, L.; He, F.; Liu, Q.; Zhang, W. Improved dispersion of SiC whisker in nano hydroxyapatite and effect of atmospheres on sintering of the SiC whisker reinforced nano hydroxyapatite composites. *Mater. Sci. Eng. C* **2018**, *91*, 135–145. [CrossRef]
665. Brook, I.; Freeman, C.; Grubb, S.; Cummins, N.; Curran, D.; Reidy, C.; Hampshire, S.; Towler, M. Biological evaluation of nano-hydroxyapatite-zirconia (HA-ZrO_2) composites and strontium-hydroxyapatite (Sr-HA) for load-bearing applications. *J. Biomater. Appl.* **2012**, *27*, 291–298. [CrossRef]
666. Chaudhry, A.A.; Yan, H.; Viola, G.; Reece, M.J.; Knowles, J.C.; Gong, K.; Rehman, I.; Darr, J.A. Phase stability and rapid consolidation of hydroxyapatite-zirconia nano-coprecipitates made using continuous hydrothermal flow synthesis. *J. Biomater. Appl.* **2012**, *27*, 79–90. [CrossRef]
667. Gain, A.K.; Zhang, L.; Liu, W. Microstructure and material properties of porous hydroxyapatite-zirconia nanocomposites using polymethyl methacrylate powders. *Mater. Des.* **2015**, *67*, 136–144. [CrossRef]
668. Cicuéndez, M.; Portolés, M.T.; Izquierdo-Barba, I.; Vallet-Regí, M. New nanocomposite system with nanocrystalline apatite embedded into mesoporous bioactive glass. *Chem. Mater.* **2012**, *24*, 1100–1106. [CrossRef]
669. Govindan, R.; Girija, E.K. Drug loaded phosphate glass/hydroxyapatite nanocomposite for orthopedic applications. *J. Mater. Chem. B* **2014**, *2*, 5468–5477. [CrossRef]
670. Akhavan, A.; Sheikh, N.; Khoylou, F.; Naimian, F.; Ataeivarjovi, E. Synthesis of antimicrobial silver/hydroxyapatite nanocomposite by gamma irradiation. *Radiat. Phys. Chem.* **2014**, *98*, 46–50. [CrossRef]
671. Bahrami, M.; Fathi, M.H.; Ahmadian, M. The effect of nanobioceramic reinforcement on mechanical and biological properties of Co-base alloy/hydroxyapatite nanocomposite. *Mater. Sci. Eng. C* **2015**, *48*, 572–578. [CrossRef]
672. Chung, H.K.; Wongso, V.; Sambudi, N.S.; Isnaeni. Biowaste-derived carbon dots/hydroxyapatite nanocomposite as drug delivery vehicle for acetaminophen. *J. Sol-Gel Sci. Technol.* **2020**, *93*, 214–223. [CrossRef]
673. Irfan, A.; Jeshurun, A.; Baraneedharan, P.; Reddy, B.M. A photoluminescence study of nitrogen-doped carbon quantum dots/hydroxyapatite (NCQDs/HAp) nanocomposites. *Mater. Technol.* **2022**, *37*, 768–779. [CrossRef]
674. Ofudje, E.A.; Akande, J.A.; Sodiya, E.F.; Ajayi, G.O.; Ademoyegun, A.J.; Al-Sehemi, A.G.; Kavil, Y.N.; Bakheet, A.M. Bioactivity properties of hydroxyapatite/clay nanocomposites. *Sci. Rep.* **2023**, *13*, 19896. [CrossRef]
675. Šupová, M. Calcium orthophosphate-clay composites—Preparation, characterisation, and applications: A review. *Minerals* **2024**, *14*, 169. [CrossRef]

676. Yan, Y.; Li, Y.; Zheng, Y.; Yi, Z.; Wei, J.; Xia, C.; Chen, Y. Synthesis and properties of a copolymer of poly(1,4-phenylene sulfide)-poly(2,4-phenylene sulfide acid) and its nano-apatite reinforced composite. *Eur. Polym. J.* **2003**, *39*, 411–416.
677. Yang, K.; Wang, C.; Wei, J. A study on biocomposite of nano apatite/poly (1,4-phenylene-sulfide)-poly (2,4-phenylene sulfide acid). *Compos. B* **2007**, *38*, 306–310. [CrossRef]
678. Jiang, L.; Li, Y.; Zhang, L.; Liao, J. Preparation and properties of a novel bone repair composite: Nano-hydroxyapatite/chitosan/carboxymethyl cellulose. *J. Mater. Sci. Mater. Med.* **2008**, *19*, 981–987.
679. Liu, L.; Liu, J.; Wang, M.; Min, S.; Cai, Y.; Zhu, L.; Yao, J. Preparation and characterization of nano-hydroxyapatite/silk fibroin porous scaffolds. *J. Biomater. Sci. Polym. Edn.* **2008**, *19*, 325–338. [CrossRef]
680. Ren, Y.J.; Sun, X.D.; Cui, F.Z.; Wei, Y.T.; Cheng, Z.J.; Kong, X.D. Preparation and characterization of antheraea pernyi silk fibroin based nanohydroxyapatite composites. *J. Bioact. Compat. Polym.* **2007**, *22*, 465–474. [CrossRef]
681. Sundaraseelan, J.; Sastry, T.P. Fabrication of a biomimetic compound containing nano hydroxyapatite–demineralised bone matrix. *J. Biomed. Nanotechnol.* **2007**, *3*, 401–405. [CrossRef]
682. Niu, Y.; Cao, L.; Wei, J.; Ma, Y.; Song, S.; Weng, W.; Li, H.; Liu, C.; Su, J. Development of a bioactive composite of nano fluorapatite and poly(butylene succinate) for bone tissue regeneration. *J. Mater. Chem. B* **2014**, *2*, 1174–1181. [CrossRef]
683. Li, H.; Yang, L.; Dong, X.; Gu, Y.; Lv, G.; Yan, Y. Composite scaffolds of nano calcium deficient hydroxyapatite/multi-(amino acid) copolymer for bone tissue regeneration. *J. Mater. Sci. Mater. Med.* **2014**, *25*, 1257–1265. [CrossRef]
684. Pourdanesh, F.; Jebali, A.; Hekmatimoghaddam, S.; Allaveisie, A. In vitro and in vivo evaluation of a new nanocomposite, containing high density polyethylene, tricalcium phosphate, hydroxyapatite and magnesium oxide nanoparticles. *Mater. Sci. Eng. C* **2014**, *40*, 382–388. [CrossRef]
685. Li, Z.; Mi, W.; Wang, H.; Su, Y.; He, C. Nano-hydroxyapatite/polyacrylamide composite hydrogels with high mechanical strengths and cell adhesion properties. *Colloid Surface B* **2014**, *123*, 959–964. [CrossRef]
686. Gheisari, H.; Karamian, E.; Abdellahi, M. A novel hydroxyapatite–hardystonite nanocomposite ceramic. *Ceram. Int.* **2015**, *41*, 5967–5975. [CrossRef]
687. Tempesti, P.; Nicotera, G.S.; Bonini, M.; Fratini, E.; Baglioni, P. Poly(N-isopropylacrylamide)-hydroxyapatite nanocomposites as thermoresponsive filling materials on dentinal surface and tubules. *J. Colloid Interf. Sci.* **2018**, *509*, 123–131. [CrossRef]
688. Demétrio, K.B.; Cioato, M.J.G.; Moreschi, A.; Oliveira, G.A.; Lorenzi, W.B.; de Oliveira, F.H.; Neto, A.V.M.; Sanches, P.R.S.; Xavier, R.G.; dos Santos, L.A.L. Polydimethylsiloxane/nano calcium phosphate composite tracheal stents: Mechanical and physiological properties. *J. Biomed. Mater. Res. B Appl. Biomater.* **2019**, *107B*, 545–553. [CrossRef]
689. Afifi, M.; El-Naggar, M.E.; Muhammad, S.; Alghamdi, N.A.; Wageh, S.; Salem, S.R.; Alhashmialameer, D. Nanocomposites based on hydroxyapatite/lithium oxide and graphene oxide nanosheets for medical applications. *J. Mater. Sci.* **2022**, *57*, 11300–11316. [CrossRef]
690. Zandi, M.; Mirzadeh, H.; Mayer, C.; Urch, H.; Eslaminejad, M.B.; Bagheri, F.; Mivehchi, H. Biocompatibility evaluation of nano-rod hydroxyapatite/gelatin coated with nano-HAp as a novel scaffold using mesenchymal stem cells. *J. Biomed. Mater. Res. A* **2010**, *92A*, 1244–1255. [CrossRef]
691. Sun, T.S.; Guan, K.; Shi, S.S.; Zhu, B.; Zheng, Y.J.; Cui, F.Z.; Zhang, W.; Liao, S.S. Effect of nano-hydroxyapatite/collagen composite and bone morphogenetic protein-2 on lumbar intertransverse fusion in rabbits. *Chin. J. Traumatol.* **2004**, *7*, 18–24.
692. Itoh, S.; Kikuehi, M.; Koyama, Y.; Takakuda, K.; Shinomiya, K.; Tanaka, J. Development of a hydroxyapatite/collagen nanocomposite as a medical device. *Cell Transp.* **2004**, *13*, 451–461. [CrossRef]
693. Kester, M.; Heakal, Y.; Fox, T.; Sharma, A.; Robertson, G.P.; Morgan, T.T.; Altinoğlu, E.I.; Tabaković, A.; Parette, M.R.; Rouse, S.M.; et al. Calcium phosphate nanocomposite particles for in vitro imaging and encapsulated chemotherapeutic drug delivery to cancer cells. *Nano Lett.* **2008**, *8*, 4116–4121. [CrossRef]
694. Wang, K.W.; Zhou, L.Z.; Sun, Y.; Wu, G.J.; Gu, H.C.; Duan, Y.R.; Chen, F.; Zhu, Y.J. Calcium phosphate/PLGA-mPEG hybrid porous nanospheres: A promising vector with ultrahigh gene loading and transfection efficiency. *J. Mater. Chem.* **2010**, *20*, 1161–1166. [CrossRef]
695. Gelinsky, M.; Welzel, P.B.; Simon, P.; Bernhardt, A.; König, U. Porous three-dimensional scaffolds made of mineralized collagen: Preparation and properties of a biomimetic nanocomposite material for tissue engineering of bone. *Chem. Eng. J.* **2008**, *137*, 84–96. [CrossRef]
696. Hu, Q.; Li, B.Q.; Wang, M.; Shen, J.C. Preparation and characterization of biodegradable chitosan/hydroxyapatite nanocomposite rods via in situ hybridization: A potential material as internal fixation of bone fracture. *Biomaterials* **2004**, *25*, 779–785. [CrossRef]
697. Wei, G.; Ma, P.X. Structure and properties of nano-hydroxyapatite/polymer composite scaffolds for bone tissue engineering. *Biomaterials* **2004**, *25*, 4749–4757. [CrossRef]
698. Liou, S.C.; Chen, S.Y.; Liu, D.M. Synthesis and characterization of needlelike apatitic nanocomposite with controlled aspect ratios. *Biomaterials* **2003**, *24*, 3981–3988. [CrossRef]
699. Liou, S.C.; Chen, S.Y.; Liu, D.M. Manipulation of nanoneedle and nanosphere apatite/poly(acrylic acid) nanocomposites. *J. Biomed. Mater. Res. B Appl. Biomater.* **2005**, *73B*, 117–122. [CrossRef]
700. Nakayama, M.; Lim, W.Q.; Kajiyama, S.; Kumamoto, A.; Ikuhara, Y.; Kato, T.; Zhao, Y. Liquid-crystalline hydroxyapatite/polymer nanorod hybrids: Potential bioplatform for photodynamic therapy and cellular scaffolds. *ACS Appl. Mater. Interfaces* **2019**, *11*, 17759–17765. [CrossRef]

701. Huang, J.; Best, S.M.; Bonfield, W.; Brooks, R.A.; Rushton, N.; Jayasinghe, S.N.; Edirisinghe, M.J. In vitro assessment of the biological response to nano-size hydroxyapatite. *J. Mater. Sci. Mater. Med.* **2004**, *15*, 441–445. [CrossRef]
702. Kong, L.; Gao, Y.; Cao, W.; Gong, Y.; Zhao, N.; Zhang, X. Preparation and characterization of nano-hydroxyapatite/chitosan composite scaffolds. *J. Biomed. Mater. Res. A* **2005**, *75A*, 275–282. [CrossRef]
703. Venkatesan, J.; Kim, S.K. Nano-hydroxyapatite composite biomaterials for bone tissue engineering—A review. *J. Biomed. Nanotechnol.* **2014**, *10*, 3124–3140. [CrossRef]
704. Christenson, E.M.; Anseth, K.S.; van den Beucken, J.J.J.P.; Chan, C.K.; Ercan, B.; Jansen, J.A.; Laurencin, C.T.; Li, W.J.; Murugan, R.; Nair, L.S.; et al. Nanobiomaterial applications in orthopedics. *J. Orthop. Res.* **2007**, *25*, 11–22. [CrossRef]
705. Ridi, F.; Meazzini, I.; Castroflorio, B.; Bonini, M.; Berti, D.; Baglioni, P. Functional calcium phosphate composites in nanomedicine. *Adv. Colloid Interface Sci.* **2017**, *244*, 281–295. [CrossRef]
706. Pielichowska, K.; Blazewicz, S. Bioactive polymer/hydroxyapatite (nano)composites for bone tissue regeneration. *Adv. Polym. Sci.* **2010**, *232*, 97–207.
707. Liao, J.; Li, Y.; Duan, X.; Zhu, L. Nano-hydroxyapatite/polymer composite as bone repair materials. *Prog. Chem.* **2015**, *27*, 220–228.
708. Du, M.; Chen, J.; Liu, K.; Xing, H.; Song, C. Recent advances in biomedical engineering of nano-hydroxyapatite including dentistry, cancer treatment and bone repair. *Compos. B* **2021**, *215*, 108790. [CrossRef]
709. Radha, G.; Manjubaashini, N.; Balakumar, S. Nano-hydroxyapatite/natural polymer composite scaffolds for bone tissue engineering: A brief review of recent trend. *Vitr. Models* **2023**, *2*, 125–151. [CrossRef]
710. Liu, C. Collagen–hydroxyapatite composite scaffolds for tissue engineering. In *Hydroxyapatite (HAp) for Biomedical Applications*; Mucalo, M.R., Ed.; Woodhead Publishing Series in Biomaterials: Number 95; Elsevier: Cambridge, UK, 2015; pp. 211–234.
711. Bedell, M.L.; Navara, A.M.; Du, Y.; Zhang, S.; Mikos, A.G. Polymeric Systems for Bioprinting. *Chem. Rev.* **2020**, *120*, 10744–10792. [CrossRef]
712. Hellmich, C.; Ulm, F.J. Are mineralized tissues open crystal foams reinforced by crosslinked collagen?—Some energy arguments. *J. Biomech.* **2002**, *35*, 1199–1212. [CrossRef]
713. Veiga, A.; Castro, F.; Rocha, F.; Oliveira, A.L. An update on hydroxyapatite/collagen composites: What is there left to say about these bioinspired materials? *J. Biomed. Mater. Res. B Appl. Biomater.* **2022**, *110B*, 1192–1205. [CrossRef]
714. Roveri, N.; Falini, G.; Sidoti, M.C.; Tampieri, A.; Landi, E.; Sandri, M.; Parma, B. Biologically inspired growth of hydroxyapatite nanocrystals inside self-assembled collagen fibers. *Mater. Sci. Eng. C* **2003**, *23*, 441–446. [CrossRef]
715. Tampieri, A.; Celotti, G.; Landi, E. From biomimetic apatites to biologically inspired composites. *Anal. Bioanal. Chem.* **2005**, *381*, 568–576. [CrossRef]
716. Tampieri, A.; Celotti, G.; Landi, E.; Sandri, M.; Roveri, N.; Falini, G. Biologically inspired synthesis of bone-like composite: Self-assembled collagen fibers/hydroxyapatite nanocrystals. *J. Biomed. Mater. Res. A* **2003**, *67A*, 618–625. [CrossRef]
717. Clarke, K.I.; Graves, S.E.; Wong, A.T.C.; Triffit, J.T.; Francis, M.J.O.; Czernuszka, J.T. Investigation into the formation and mechanical properties of a bioactive material based on collagen and calcium phosphate. *J. Mater. Sci. Mater. Med.* **1993**, *4*, 107–110. [CrossRef]
718. Ten Huisen, K.S.; Martin, R.I.; Klimkiewicz, M.; Brown, P.W. Formation and properties of a synthetic bone composite: Hydroxyapatite-collagen. *J. Biomed. Mater. Res.* **1995**, *29*, 803–810. [CrossRef]
719. Ishikawa, H.; Koshino, T.; Takeuchi, R.; Saito, T. Effects of collagen gel mixed with hydroxyapatite power on interface between newly formed bone and grafted Achilles tendon in rabbit femoral bone tunnel. *Biomaterials* **2001**, *22*, 1689–1694. [CrossRef]
720. ltoh, S.; Kikuchi, M.; Takakuda, K.; Koyama, Y.; Matsumoto, H.N.; Ichinose, S.; Tanaka, J.; Kawauchi, T.; Shinomiya, K. The biocompatibility and osteoconductive activity of a novel hydroxyapatite/collagen composite biomaterial and its function as a carrier of rhBMP-2. *J. Biomed. Mater. Res.* **2001**, *54*, 445–453.
721. Uskokovic, V.; Ignjatovic, N.; Petranovic, N. Synthesis and characterization of hydroxyapatite-collagen biocomposite materials. *Mater. Sci. Forum* **2002**, *413*, 269–274. [CrossRef]
722. Yoon, B.H.; Kim, H.W.; Lee, S.H.; Bae, C.J.; Koh, Y.H.; Kong, Y.M.; Kim, H.E. Stability and cellular responses to fluorapatite-collagen composites. *Biomaterials* **2005**, *26*, 2957–2963. [CrossRef]
723. Wahl, D.A.; Czernuszka, J.T. Collagen-hydroxyapatite composites for hard tissue repair. *Eur. Cell Mater.* **2006**, *11*, 43–56. [CrossRef]
724. Teng, S.H.; Lee, E.J.; Park, C.S.; Choi, W.Y.; Shin, D.S.; Kim, H.E. Bioactive nanocomposite coatings of collagen/hydroxyapatite on titanium substrates. *J. Mater. Sci. Mater. Med.* **2008**, *19*, 2453–2461. [CrossRef]
725. Song, J.H.; Kim, H.E.; Kim, H.W. Collagen-apatite nanocomposite membranes for guided bone regeneration. *J. Biomed. Mater. Res. B Appl. Biomater.* **2007**, *83B*, 248–257. [CrossRef]
726. Pek, Y.S.; Gao, S.; Arshad, M.S.M.; Leck, K.J.; Ying, J.Y. Porous collagen-apatite nanocomposite foams as bone regeneration scaffolds. *Biomaterials* **2008**, *29*, 4300–4305. [CrossRef]
727. Zhao, H.; Huang, C.; Jin, H.; Cai, J. A novel route for collagen/hydroxyapatite preparation by enzymatic decomposition of urea. *J. Compos. Mater.* **2010**, *44*, 2127–2133. [CrossRef]
728. Kozłowska, J.; Sionkowska, A. Effects of different crosslinking methods on the properties of collagen-calcium phosphate composite materials. *Int. J. Biol. Macromol.* **2015**, *74*, 397–403. [CrossRef]
729. Banglmaier, R.F.; Sander, E.A.; VandeVord, P.J. Induction and quantification of collagen fiber alignment in a three-dimensional hydroxyapatite–collagen composite scaffold. *Acta Biomater.* **2015**, *17*, 26–35. [CrossRef]

730. Banks, E.; Nakajima, S.; Shapiro, L.C.; Tilevitz, O.; Alonzo, J.R.; Chianelli, R.R. Fibrous apatite grown on modified collagen. *Science* **1977**, *198*, 1164–1166. [CrossRef]
731. Hayashi, K.; Yabuki, T.; Tabuchi, K.; Fujii, T. Repair of experimental bone defect with a collagen block containing synthesized apatite. *Arch. Orthop. Traum. Surg.* **1982**, *99*, 265–269. [CrossRef]
732. Mittelmeier, H.; Nizzard, M. Knochenregeneration mit industriell gefertigtem Collagen Apatit Implantat ("Collapat"). In *Osteogenese und Knochenwachstum*; Hackenbroch, M.H., Refior, H.J., Jäger, M.G., Eds.; Thieme: Stuttgart, Germany, 1982; pp. 194–197.
733. Serre, C.M.; Papillard, M.; Chavassieux, P.; Boivin, G. In vitro induction of a calcifying matrix by biomaterials constituted of collagen and/or hydroxyapatite: An ultrastructural comparison of three types of biomaterials. *Biomaterials* **1993**, *14*, 97–106. [CrossRef]
734. Scabbia, A.; Trombelli, L. A comparative study on the use of a HA/collagen/chondroitin sulphate biomaterial (Biostite®) and a bovine-derived HA xenograft (Bio-Oss®) in the treatment of deep intraosseous defects. *J. Clin. Periodontol.* **2004**, *31*, 348–355. [CrossRef]
735. Yamasaki, Y.; Yoshida, Y.; Okazaki, M.; Shimazu, A.; Kubo, T.; Akagawa, Y.; Uchida, T. Action of FGMgCO$_3$Ap-collagen composite in promoting bone formation. *Biomaterials* **2003**, *24*, 4913–4920. [CrossRef]
736. Wang, X.; Grogan, S.P.; Rieser, F.; Winkelmann, V.; Maquet, V.; Berge, M.L.; Mainil-Varlet, P. Tissue engineering of biphasic cartilage constructs using various biodegradable scaffolds: An in vitro study. *Biomaterials* **2004**, *25*, 3681–3688. [CrossRef]
737. Zahn, D. Multi-scale simulations of apatite–collagen composites: From molecules to materials. *Front. Mater. Sci.* **2017**, *11*, 1–12. [CrossRef]
738. Chang, M.C.; Ikoma, T.; Kikuchi, M.; Tanaka, J. The cross-linkage effect of hydroxyapatite/collagen nanocomposites on a self-organization phenomenon. *J. Mater. Sci. Mater. Med.* **2002**, *13*, 993–997. [CrossRef]
739. Iijima, M.; Moriwaki, Y.; Kuboki, Y. Oriented growth of octacalcium phosphate on and inside the collagenous matrix in vitro. *Connect. Tissue Res.* **1996**, *32*, 519–524.
740. Ortiz, F.; Díaz-Barrios, A.; Lopez-Cabaña, Z.E.; González, G. Effect of the electric field on the biomineralization of collagen. *Polymers* **2023**, *15*, 3121. [CrossRef]
741. Miyamoto, Y.; Ishikawa, K.; Takechi, M.; Toh, T.; Yuasa, T.; Nagayama, M.; Suzuki, K. Basic properties of calcium phosphate cement containing atelocollagen in its liquid or powder phases. *Biomaterials* **1998**, *19*, 707–715. [CrossRef]
742. Iijima, M.; Moriwaki, Y.; Kuboki, Y. In vitro crystal growth of octacalcium phosphate on type I collagen fiber. *J. Cryst. Growth* **1994**, *137*, 553–560. [CrossRef]
743. Iijima, M.; Iijima, K.; Moriwaki, Y.; Kuboki, Y. Oriented growth of octacalcium phosphate crystals on type I collagen fibrils under physiological conditions. *J. Cryst. Growth* **1994**, *140*, 91–99. [CrossRef]
744. Lawson, A.C.; Czernuszka, J.T. Collagen–calcium phosphate composites. *Proc. Inst. Mech. Eng. H* **1998**, *212*, 413–425. [CrossRef]
745. Kamakura, S.; Sasaki, K.; Honda, Y.; Anada, T.; Suzuki, O. Octacalcium phosphate combined with collagen orthotopically enhances bone regeneration. *J. Biomed. Mater. Res. B Appl. Biomater.* **2006**, *79B*, 210–217. [CrossRef]
746. Kawai, T.; Anada, T.; Honda, Y.; Kamakura, S.; Matsui, K.; Matsui, A.; Sasaki, K.; Morimoto, S.; Echigo, S.; Suzuki, O. Synthetic octacalcium phosphate augments bone regeneration correlated with its content in collagen scaffold. *Tissue Eng. A* **2009**, *15*, 23–32. [CrossRef]
747. Masuda, T.; Kawai, T.; Anada, T.; Kamakura, S.; Suzuki, O. Quality of regenerated bone enhanced by implantation of octacalcium phosphate-collagen composite. *Tissue Eng. C* **2010**, *16*, 471–478. [CrossRef]
748. Kikuchi, M.; Ikoma, T.; Itoh, S.; Matsumoto, H.N.; Koyama, Y.; Takakuda, K.; Shinomiya, K.; Tanaka, J. Biomimetic synthesis of bone-like nanocomposites using the self-organization mechanism of hydroxyapatite and collagen. *Compos. Sci. Technol.* **2004**, *64*, 819–825. [CrossRef]
749. Li, X.; Chang, J. Preparation of bone-like apatite-collagen nanocomposites by a biomimetic process with phosphorylated collagen. *J. Biomed. Mater. Res. A* **2008**, *85A*, 293–300. [CrossRef]
750. Jee, S.S.; Thula, T.T.; Gower, L.B. Development of bone-like composites via the polymer-induced liquid-precursor (PILP) process. Part 1: Influence of polymer molecular weight. *Acta Biomater.* **2010**, *6*, 3676–3686. [CrossRef]
751. Aaddouz, M.; Azzaoui, K.; Sabbahi, R.; Youssoufi, M.H.; Yahyaoui, M.I.; Asehraou, A.; El Miz, M.; Hammouti, B.; Shityakov, S.; Siaj, M.; et al. Cheminformatics-based design and synthesis of hydroxyapatite/collagen nanocomposites for biomedical applications. *Polymers* **2024**, *16*, 85. [CrossRef]
752. Bu, H.; Li, G. Comparative investigation of hydroxyapatite/collagen composites prepared by $CaCl_2$ addition at different time points in collagen self-assembly process. *J. Mater. Sci.* **2018**, *53*, 6313–6324. [CrossRef]
753. Bian, T.; Zhao, K.; Meng, Q.; Tang, Y.; Jiao, H.; Luo, J. The construction and performance of multi-level hierarchical hydroxyapatite (HA)/collagen composite implant based on biomimetic bone Haversian motif. *Mater. Des.* **2019**, *162*, 60–69. [CrossRef]
754. Manjushree, M.B.; Archana, R.; Deepak, P.; Nibedita, L. Fabrication and characterization of ceramic-polymer composite 3D scaffolds and demonstration of osteoinductive propensity with gingival mesenchymal stem cells. *RSC Adv.* **2023**, *13*, 26967–26982.
755. Andronescu, E.; Ficai, M.; Voicu, G.; Ficai, D.; Maganu, M.; Ficai, A. Synthesis and characterization of collagen/hydroxyapatite: Magnetite composite material for bone cancer treatment. *J. Mater. Sci. Mater. Med.* **2010**, *21*, 2237–2242. [CrossRef]
756. Ficai, M.; Andronescu, E.; Ficai, D.; Voicu, G.; Ficai, A. Synthesis and characterization of COLL-PVA/HA hybrid materials with stratified morphology. *Colloid Surface B* **2010**, *81*, 614–619. [CrossRef]

757. Chacon, E.L.; Bertolo, M.R.V.; de Guzzi Plepis, A.M.; da Conceição Amaro Martins, V.; dos Santos, G.R.; Pinto, C.A.L.; Pelegrine, A.A.; Teixeira, M.L.; Buchaim, D.V.; Nazari, F.M.; et al. Collagen-chitosan-hydroxyapatite composite scaffolds for bone repair in ovariectomized rats. *Sci. Rep.* **2023**, *13*, 28. [CrossRef]
758. Hoshi, M.; Taira, M.; Sawada, T.; Hachinohe, Y.; Hatakeyama, W.; Takafuji, K.; Tekemoto, S.; Kondo, H. Preparation of collagen/hydroxyapatite composites using the alternate immersion method and evaluation of the cranial bone-forming capability of composites complexed with acidic gelatin and b-FGF. *Materials* **2022**, *15*, 8802. [CrossRef]
759. Animut, T.Y.; Ningsih, H.S.; Shih, H.H.; Wu, M.H.; Shih, S.J. Effect of calcium silicate and β-tricalcium phosphate reinforcement on the mechanical–biological properties of freeze-dried collagen composite scaffolds for bone tissue engineering applications. *Ceramics* **2023**, *6*, 548–560. [CrossRef]
760. Inzana, J.A.; Olvera, D.; Fuller, S.M.; Kelly, J.P.; Graeve, O.A.; Schwarz, E.M.; Kates, S.L.; Awad, H.A. 3D printing of composite calcium phosphate and collagen scaffolds for bone regeneration. *Biomaterials* **2014**, *35*, 4026–4034. [CrossRef]
761. Tamimi, F.; Kumarasami, B.; Doillon, C.; Gbureck, U.; Nihouannen, D.L.; Cabarcos, E.L.; Barralet, J.E. Brushite-collagen composites for bone regeneration. *Acta Biomater.* **2008**, *4*, 1315–1321. [CrossRef]
762. Mai, R.; Reinstorf, A.; Pilling, E.; Hlawitschka, M.; Jung, R.; Gelinsky, M.; Schneider, M.; Loukota, R.; Pompe, W.; Eckelt, U.; et al. Histologic study of incorporation and resorption of a bone cement-collagen composite: An in vivo study in the minipig. *Oral Surg. Oral Med. Oral Pathol. Oral Radiol. Endod.* **2008**, *105*, e9–e14. [CrossRef]
763. Moreau, J.L.; Weir, M.D.; Xu, H.H.K. Self-setting collagen-calcium phosphate bone cement: Mechanical and cellular properties. *J. Biomed. Mater. Res. A* **2009**, *91A*, 605–613. [CrossRef]
764. Liu, X.; Wang, X.M.; Chen, Z.; Cui, F.Z.; Liu, H.Y.; Mao, K.; Wang, Y. Injectable bone cement based on mineralized collagen. *J. Biomed. Mater. Res. B Appl. Biomater.* **2010**, *94B*, 72–79. [CrossRef]
765. Otsuka, M.; Nakagawa, H.; Ito, A.; Higuchi, W.I. Effect of geometrical structure on drug release rate of a three-dimensionally perforated porous apatite/collagen composite cement. *J. Pharm. Sci.* **2010**, *99*, 286–292. [CrossRef]
766. Cui, F.Z.; Li, Y.; Ge, J. Self-assembly of mineralized collagen composites. *Mater. Sci. Eng. R* **2007**, *57*, 1–27. [CrossRef]
767. Hirota, K.; Nishihara, K.; Tanaka, H. Pressure sintering of apatite-collagen composite. *Biomed. Mater. Eng.* **1993**, *3*, 147–151. [CrossRef]
768. Zahn, D.; Hochrein, O.; Kawska, A.; Brickmann, J.; Kniep, R. Towards an atomistic understanding of apatite-collagen biomaterials: Linking molecular simulation studies of complex-, crystal- and composite-formation to experimental findings. *J. Mater. Sci.* **2007**, *42*, 8966–8973. [CrossRef]
769. Silva, C.C.; Pinheiro, A.G.; Figueiro, S.D.; Goes, J.C.; Sasaki, J.M.; Miranda, M.A.R.; Sombra, A.S.B. Piezoelectric properties of collagen-nanocrystalline hydroxyapatite composites. *J. Mater. Sci.* **2002**, *37*, 2061–2070. [CrossRef]
770. Yunoki, S.; Ikoma, T.; Tsuchiya, A.; Monkawa, A.; Ohta, K.; Sotome, S.; Shinomiya, K.; Tanaka, J. Fabrication and mechanical and tissue ingrowth properties of unidirectionally porous hydroxyapatite/collagen composite. *J. Biomed. Mater. Res. B Appl. Biomater.* **2007**, *80B*, 166–173. [CrossRef]
771. Keeney, M.; Collin, E.; Pandit, A. Multi-channelled collagen-calcium phosphate scaffolds: Their physical properties and human cell response. *Tissue Eng. C* **2009**, *15*, 265–273. [CrossRef]
772. Chapman, M.W.; Bucholz, R.; Cornell, C. Treatment of acute fractures with a collagen-calcium phosphate graft material: A randomized clinical trial. *J. Bone Joint Surg.* **1997**, *79A*, 495–502. [CrossRef]
773. Rodrigues, C.V.M.; Serricella, P.; Linhares, A.B.R.; Guerdes, R.M.; Borojevic, R.; Rossi, M.A.; Duarte, M.E.L.; Farina, M. Characterization of a bovine collagen-hydroxyapatite composite scaffold for bone tissue engineering. *Biomaterials* **2003**, *24*, 4987–4997. [CrossRef]
774. Miura, K.I.; Anada, T.; Honda, Y.; Shiwaku, Y.; Kawai, T.; Echigo, S.; Takahashi, T.; Suzuki, O. Characterization and bioactivity of nano-submicro octacalcium phosphate/gelatin composite. *Appl. Surf. Sci.* **2013**, *282*, 138–145. [CrossRef]
775. Kawai, T.; Echigo, S.; Matsui, K.; Tanuma, Y.; Takahashi, T.; Suzuki, O.; Kamakura, S. First clinical application of octacalcium phosphate collagen composite in human bone defect. *Tissue Eng. A* **2014**, *20*, 1336–1341. [CrossRef]
776. Lickorish, D.; Ramshaw, J.A.M.; Werkmeister, J.A.; Glattauer, V.; Howlett, C.R. Development of a collagen-hydroxyapatite composite biomaterial via biomimetic process. *J. Biomed. Mater. Res. A* **2004**, *68A*, 19–27. [CrossRef]
777. Sionkowska, A.; Kozłowska, J. Characterization of collagen/hydroxyapatite composite sponges as a potential bone substitute. *Int. J. Biol. Macromol.* **2010**, *47*, 483–487. [CrossRef]
778. Hsu, F.Y.; Chueh, S.C.; Wang, J.Y. Microspheres of hydroxyapatite/reconstituted collagen as supports for osteoblast cell growth. *Biomaterials* **1999**, *20*, 1931–1936. [CrossRef]
779. Wu, T.J.; Huang, H.H.; Lan, C.W.; Lin, C.H.; Hsu, F.Y.; Wang, Y.J. Studies on the microspheres comprised of reconstituted collagen and hydroxyapatite. *Biomaterials* **2004**, *25*, 651–658. [CrossRef]
780. Wei, Q.; Lu, J.; Wang, Q.; Fan, H.; Zhang, X. Novel synthesis strategy for composite hydrogel of collagen/hydroxyapatite-microsphere originating from conversion of $CaCO_3$ templates. *Nanotechnology* **2015**, *26*, 115605. [CrossRef]
781. Liao, S.S.; Watari, F.; Uo, M.; Ohkawa, S.; Tamura, K.; Wang, W.; Cui, F.Z. The preparation and characteristics of a carbonated hydroxyapatite/collagen composite at room temperature. *J. Biomed. Mater. Res. B Appl. Biomater.* **2005**, *74B*, 817–821. [CrossRef]
782. Yokoyama, A.; Gelinsky, M.; Kawasaki, T.; Kohgo, T.; König, U.; Pompe, W.; Watari, F. Biomimetic porous scaffolds with high elasticity made from mineralized collagen—An animal study. *J. Biomed. Mater. Res. B Appl. Biomater.* **2005**, *75B*, 464–472. [CrossRef]

783. Zou, C.; Weng, W.; Deng, X.J.; Cheng, K.; Liu, X.; Du, P.; Shen, G.; Han, G. Preparation and characterization of porous β-tricalcium phosphate/collagen composites with an integrated structure. *Biomaterials* **2005**, *26*, 5276–5284. [CrossRef]
784. Available online: https://en.wikipedia.org/wiki/Bioconjugation (accessed on 1 May 2024).
785. Gotterbarm, T.; Richter, W.; Jung, M.; Berardi-Vilei, S.; Mainil-Varlet, P.; Yamashita, T.; Breusch, S.J. An in vivo study of a growth-factor enhanced, cell free, two-layered collagen-tricalcium phosphate in deep osteochondral defects. *Biomaterials* **2006**, *27*, 3387–3395. [CrossRef]
786. Sobczak-Kupiec, A.; Drabczyk, A.; Florkiewicz, W.; Głąb, M.; Kudłacik-Kramarczyk, S.; Słota, D.; Tomala, A.; Tyliszczak, B. Review of the applications of biomedical compositions containing hydroxyapatite and collagen modified by bioactive components. *Materials* **2021**, *14*, 2096. [CrossRef]
787. Xie, H.; Ruan, S.; Zhao, M.; Long, J.; Ma, X.; Guo, J.; Lin, X. Preparation and characterization of 3D hydroxyapatite/collagen scaffolds and its application in bone regeneration with bone morphogenetic protein-2. *RSC Adv.* **2023**, *13*, 23010–23020. [CrossRef]
788. Jayaraman, M.; Subramanian, M.V. Preparation and characterization of two new composites: Collagen-brushite and collagen-octacalcium phosphate. *Med. Sci. Monitor* **2002**, *8*, BR481–BR487.
789. Matsui, K.; Matsui, A.; Handa, T.; Kawai, T.; Suzuki, O.; Kamakura, S.; Echigo, S. Bone regeneration by octacalcium phosphate collagen composites in a dog alveolar cleft model. *Int. J. Oral Maxillofac. Surg.* **2010**, *39*, 1218–1225. [CrossRef]
790. Iibuchi, S.; Matsui, K.; Kawai, T.; Sasaki, K.; Suzuki, O.; Kamakura, S.; Echigo, S. Octacalcium phosphate (OCP) collagen composites enhance bone healing in a dog tooth extraction socket model. *Int. J. Oral Maxillofac. Surg.* **2010**, *39*, 161–168. [CrossRef]
791. Kawai, T.; Matsui, K.; Ezoe, Y.; Kajii, F.; Suzuki, O.; Takahashi, T.; Kamakura, S. Efficacy of octacalcium phosphate collagen composite for titanium dental implants in dogs. *Materials* **2018**, *11*, 229. [CrossRef]
792. Ni, T.; Zhu, Y.; Hao, L.; Chen, Y.; Cheng, T. Preparation of photothermal-sensitive PDGF@ZIF-8-PDA@COL/PLGA-TCP composite scaffolds for bone defect repair. *Mater. Des.* **2022**, *217*, 110643. [CrossRef]
793. Kołodziejska, B.; Kaflak, A.; Kolmas, J. Biologically inspired collagen/apatite composite biomaterials for potential use in bone tissue regeneration—A review. *Materials* **2020**, *13*, 1748. [CrossRef]
794. Ikeda, H.; Yamaza, T.; Yoshinari, M.; Ohsaki, Y.; Ayukawa, Y.; Kido, M.A.; Inoue, T.; Shimono, M.; Koyano, K.; Tanaka, T. Ultrastructural and immunoelectron microscopic studies of the peri-implant epithelium-implant (Ti-6Al-4V) interface of rat maxilla. *J. Periodontol.* **2000**, *71*, 961–973. [CrossRef]
795. Uchida, M.; Oyane, A.; Kim, H.M.; Kokubo, T.; Ito, A. Biomimetic coating of laminin-apatite composite on titanium metal and its excellent cell-adhesive properties. *Adv. Mater.* **2004**, *16*, 1071–1074. [CrossRef]
796. Oyane, A.; Uchida, M.; Ito, A. Laminin-apatite composite coating to enhance cell adhesion to ethylene-vinyl alcohol copolymer. *J. Biomed. Mater. Res. A* **2005**, *72A*, 168–174. [CrossRef]
797. Oyane, A.; Uchida, M.; Onuma, K.; Ito, A. Spontaneous growth of a laminin-apatite nano-composite in a metastable calcium phosphate solution. *Biomaterials* **2006**, *27*, 167–175. [CrossRef]
798. Oyane, A.; Tsurushima, H.; Ito, A. Highly efficient gene transfer system using a laminin-DNA-apatite composite layer. *J. Gene Med.* **2010**, *12*, 194–206. [CrossRef]
799. Oyane, A.; Wang, X.; Sogo, Y.; Ito, A.; Tsurushima, H. Calcium phosphate composite layers for surface-mediated gene transfer. *Acta Biomater.* **2012**, *8*, 2034–2046. [CrossRef]
800. Yaylaoglu, M.B.; Korkusuz, P.; Ors, U.; Korkusuz, F.; Hasirci, V. Development of a calcium phosphate-gelatin composite as a bone substitute and its use in drug release. *Biomaterials* **1999**, *20*, 711–719. [CrossRef]
801. Kim, H.W.; Knowles, J.C.; Kim, H.E. Porous scaffolds of gelatin-hydroxyapatite nanocomposites obtained by biomimetic approach: Characterization and antibiotic drug release. *J. Biomed. Mater. Res. B Appl. Biomater.* **2005**, *74B*, 686–698. [CrossRef]
802. Chang, M.C.; Douglas, W.H.; Tanaka, J. Organic-inorganic interaction and the growth mechanism of hydroxyapatite crystals in gelatin matrices between 37 and 80 °C. *J. Mater. Sci. Mater. Med.* **2006**, *17*, 387–396. [CrossRef]
803. Chang, M.C.; Douglas, W.H. Cross-linkage of hydroxyapatite/gelatin nanocomposite using imide-based zero-length cross-linker. *J. Mater. Sci. Mater. Med.* **2007**, *18*, 2045–2051. [CrossRef]
804. Han, Y.; Dal-Fabbro, R.; Mahmoud, A.H.; Rahimnejad, M.; Xu, J.; Castilho, M.; Dissanayaka, W.L.; Bottino, M.C. GelMA/TCP nanocomposite scaffold for vital pulp therapy. *Acta Biomater.* **2024**, *173*, 495–508. [CrossRef]
805. Wise, E.R.; Maltsev, S.; Davies, M.E.; Duer, M.J.; Jaeger, C.; Loveridge, N.; Murray, R.C.; Reid, D.G. The organic-mineral interface in bone is predominantly polysaccharide. *Chem. Mater.* **2007**, *19*, 5055–5057. [CrossRef]
806. Lin, H.R.; Yeh, Y.J. Porous alginate/hydroxyapatite composite scaffolds for bone tissue engineering: Preparation, characterization and in vitro studies. *J. Biomed. Mater. Res. B Appl. Biomater.* **2004**, *71B*, 52–65. [CrossRef]
807. Chae, T.; Yang, H.; Leung, V.; Ko, F.; Troczynski, T. Novel biomimetic hydroxyapatite/alginate nanocomposite fibrous scaffolds for bone tissue regeneration. *J. Mater. Sci. Mater. Med.* **2013**, *24*, 1885–1894. [CrossRef]
808. Li, S.; Kan, B.; Zhao, K.; Ren, T.; Lin, B.; Wei, J.; Chen, T. Preparation of tricalcium phosphate-calcium alginate composite flat sheet membranes and their application for protein release. *Polym. Compos.* **2015**, *36*, 1899–1906. [CrossRef]
809. Wulandari, W.; Islami, D.M.; Wellia, D.V.; Emriadi, E.; Sisca, V.; Jamarun, N. The effect of alginate concentration on crystallinity, morphology and thermal stability properties of hydroxyapatite/alginate composite. *Polymers* **2023**, *15*, 614. [CrossRef]
810. Yamaguchi, I.; Tokuchi, K.; Fukuzaki, H.; Koyama, Y.; Takakuda, K.; Monma, H.; Tanaka, J. Preparation and microstructure analysis of chitosan/hydroxyapatite nanocomposites. *J. Biomed. Mater. Res.* **2001**, *55*, 20–27. [CrossRef]

811. Tang, X.J.; Gui, L.; Lü, X.Y. Hard tissue compatibility of natural hydroxyapatite/chitosan composite. *Biomed. Mater.* **2008**, *3*, 044115. [CrossRef]
812. Ge, H.; Zhao, B.; Lai, Y.; Hu, X.; Zhang, D.; Hu, K. From crabshell to chitosan-hydroxyapatite composite material via a biomorphic mineralization synthesis method. *J. Mater. Sci. Mater. Med.* **2010**, *21*, 1781–1787. [CrossRef]
813. Onoki, T.; Nakahira, A.; Tago, T.; Hasegawa, Y.; Kuno, T. Novel low temperature processing techniques for apatite ceramics and chitosan polymer composite bulk materials and its mechanical properties. *Appl. Surf. Sci.* **2012**, *262*, 263–266. [CrossRef]
814. Fernández, T.; Olave, G.; Valencia, C.H.; Arce, S.; Quinn, J.M.W.; Thouas, G.A.; Chen, Q.Z. Effects of calcium phosphate/chitosan composite on bone healing in rats: Calcium phosphate induces osteon formation. *Tissue Eng. A* **2014**, *20*, 1948–1960. [CrossRef]
815. Boudemagh, D.; Venturini, P.; Fleutot, S.; Cleymand, F. Elaboration of hydroxyapatite nanoparticles and chitosan/hydroxyapatite composites: A present status. *Polym. Bull.* **2019**, *76*, 2621–2653. [CrossRef]
816. Galotta, A.; Demir, Ö.; Marsan, O.; Sglavo, V.M.; Loca, D.; Combes, C.; Locs, J. Apatite/chitosan composites formed by cold sintering for drug delivery and bone tissue engineering applications. *Nanomaterials* **2024**, *14*, 441. [CrossRef]
817. Zamora, I.; Morales, G.A.; Castro, J.I.; Rojas, L.M.R.; Valencia-Llano, C.H.; Hernandez, J.H.M.; Zapata, M.E.V.; Grande-Tovar, C.D. Chitosan (CS)/hydroxyapatite (HA)/tricalcium phosphate (β-TCP)-based composites as a potential material for pulp tissue regeneration. *Polymers* **2023**, *15*, 3213. [CrossRef]
818. Ait Said, H.; Noukrati, H.; Ben Youcef, H.; Mahdi, I.; Oudadesse, H.; Barroug, A. In situ precipitated hydroxyapatite-chitosan composite loaded with ciprofloxacin: Formulation, mechanical, in vitro antibiotic uptake, release and antibacterial properties. *Mater. Chem. Phys.* **2023**, *294*, 127008. [CrossRef]
819. Scalera, F.; Pereira, S.I.A.; Bucciarelli, A.; Tobaldi, D.M.; Quarta, A.; Gervaso, F.; Castro, P.M.L.; Polini, A.; Piccirillo, C. Chitosan-hydroxyapatite composites made from sustainable sources: A morphology and antibacterial study. *Mater. Today Sustain.* **2023**, *21*, 100334. [CrossRef]
820. Zhou, K.; Azaman, F.A.; Cao, Z.; Fournet, M.B.; Devine, D.M. Bone tissue engineering scaffold optimisation through modification of chitosan/ceramic composition. *Macromol* **2023**, *3*, 326–342. [CrossRef]
821. Predoi, D.; Iconaru, S.L.; Ciobanu, S.C.; Buton, N.; Predoi, M.V. Complex evaluation of nanocomposite-based hydroxyapatite for biomedical applications. *Biomimetics* **2023**, *8*, 528. [CrossRef]
822. Wan, A.C.A.; Khor, E.; Hastings, G.W. Preparation of a chitin-apatite composite by in situ precipitation onto porous chitin scaffolds. *J. Biomed. Mater. Res.* **1998**, *41*, 541–548. [CrossRef]
823. Wan, A.C.A.; Khor, E.; Hastings, G.W. Hydroxyapatite modified chitin as potential hard tissue substitute material. *J. Biomed. Mater. Res.* **1997**, *38*, 235–241. [CrossRef]
824. Geçer, A.; Yldz, N.; Erol, M.; Çalml, A. Synthesis of chitin calcium phosphate composite in different growth media. *Polym. Compos.* **2008**, *29*, 84–91. [CrossRef]
825. Silva, S.S.; Duarte, A.R.C.; Oliveira, J.M.; Mano, J.F.; Reis, R.L. Alternative methodology for chitin–hydroxyapatite composites using ionic liquids and supercritical fluid technology. *J. Bioact. Compat. Polym.* **2013**, *28*, 481–491. [CrossRef]
826. Machałowski, T.; Kozłowski, M.; Kołodziejczak-Radzimska, A.; Jakubowicz, J.; Jesionowski, T. Chitin nanofibres as reinforcement for hydroxyapatite-based composite preparation. *Prog. Chem. Appl. Chitin Its Deriv.* **2022**, *27*, 162–174. [CrossRef]
827. Wang, J.; Sun, Q.Z.; Gao, J.; Liu, D.M.; Meng, X.C.; Li, M.Q. Preparation and properties on silk fibers reinforced hydroxyapatite/chitosan composites. *Adv. Mater. Res.* **2010**, *105–106*, 557–560. [CrossRef]
828. Zhang, Y.; Reddy, V.J.; Wong, S.Y.; Li, X.; Su, B.; Ramakrishna, S.; Lim, C.T. Enhanced biomineralization in osteoblasts on a novel electrospun biocomposite nanofibrous substrate of hydroxyapatite/collagen/chitosan. *Tissue Eng. A* **2010**, *16*, 1949–1960. [CrossRef]
829. Dehghani, N.; Haghiralsadat, F.; Yazdian, F.; Sadeghian-Nodoushan, F.; Ghasemi, N.; Mazaheri, F.; Pourmadadi, M.; Naghib, S.M. Chitosan/silk fibroin/nitrogen-doped carbon quantum dot/α-tricalcium phosphate nanocomposite electrospinned as a scaffold for wound healing application: In vitro and in vivo studies. *Int. J. Biol. Macromol.* **2023**, *238*, 124078. [CrossRef]
830. Won, J.E.; El-Fiqi, A.; Jegal, S.H.; Han, C.M.; Lee, E.J.; Knowles, J.C.; Kim, H.W. Gelatin-apatite bone mimetic co-precipitates incorporated within biopolymer matrix to improve mechanical and biological properties useful for hard tissue repair. *J. Biomater. Appl.* **2014**, *28*, 1213–1225. [CrossRef]
831. Sarkar, C.; Kumari, P.; Anuvrat, K.; Sahu, S.K.; Chakraborty, J.; Garai, S. Synthesis and characterization of mechanically strong carboxymethyl cellulose–gelatin–hydroxyapatite nanocomposite for load-bearing orthopedic application. *J. Mater. Sci.* **2018**, *53*, 230–246. [CrossRef]
832. Xu, Z.; Li, K.; Zhou, K.; Li, S.; Chen, H.; Zeng, J.; Hu, R. 3D printing silk fibroin/hydroxyapatite/sodium alginate composite scaffolds for bone tissue engineering. *Fiber. Polym.* **2023**, *24*, 275–283. [CrossRef]
833. Sukhodub, L.; Fediv, V.; Kumeda, M.; Sukhodub, L.; Kulchynskyi, V.; Tkachuk, I.; Cherepanov, V.; Prylutskyy, Y. Electrical properties of biodegradable chitosan-calcium phosphate nerve conduits doped with inorganic nanoparticles. *Colloids Surf. A* **2023**, *678*, 132425. [CrossRef]
834. Kousalya, G.N.; Gandhi, R.M.; Sundaram, S.C.; Meenakshi, S. Synthesis of nano-hydroxyapatite chitin/chitosan hybrid biocomposites for the removal of Fe(III). *Carbohydr. Polym.* **2010**, *82*, 594–599. [CrossRef]
835. Sundaram, C.S.; Viswanathan, N.; Meenakshi, S. Uptake of fluoride by nano-hydroxyapatite/chitosan, a bioinorganic composite. *Bioresour. Technol.* **2008**, *99*, 8226–8230. [CrossRef]

836. Sundaram, C.S.; Viswanathan, N.; Meenakshi, S. Fluoride sorption by nano-hydroxyapatite/chitin composite. *J. Hazard. Mater.* **2009**, *172*, 147–151. [CrossRef]
837. Salama, A. Recent progress in preparation and applications of chitosan/calcium phosphate composite materials. *Int. J. Biol. Macromol.* **2021**, *178*, 240–252. [CrossRef]
838. Ait Said, H.; Mabroum, H.; Lahcini, M.; Oudadesse, H.; Barroug, A.; Ben Youcef, H.; Noukrati, H. Manufacturing methods, properties and potential applications in bone tissue regeneration of hydroxyapatite-chitosan biocomposites: A review. *Int. J. Biol. Macromol.* **2023**, *243*, 125150. [CrossRef]
839. Wen, H.B.; de Wijn, J.R.; van Blitterswijk, C.A.; de Groot, K. Incorporation of bovine serum albumin in calcium phosphate coating on titanium. *J. Biomed. Mater. Res.* **1999**, *46*, 245–252. [CrossRef]
840. Liu, T.Y.; Chen, S.Y.; Liu, D.M.; Liou, S.C. On the study of BSA-loaded calcium-deficient hydroxyapatite nano-carriers for controlled drug delivery. *J. Control. Release* **2005**, *107*, 112–121. [CrossRef]
841. Liu, Y.; Hunziker, E.; Randall, N.; de Groot, K.; Layrolle, P. Proteins incorporated into biomimetically prepared calcium phosphate coatings modulate their mechanical strength and dissolution rate. *Biomaterials* **2003**, *24*, 65–70. [CrossRef]
842. Dorozhkin, S.V.; Dorozhkina, E.I. The influence of bovine serum albumin on the crystallization of calcium phosphates from a revised simulated body fluid. *Colloid Surface A* **2003**, *215*, 191–199. [CrossRef]
843. Fu, H.H.; Hu, Y.H.; McNelis, T.; Hollinger, J.O. A calcium phosphate-based gene delivery system. *J. Biomed. Mater. Res. A* **2005**, *74A*, 40–48. [CrossRef]
844. Bisht, S.; Bhakta, G.; Mitra, S.; Maitra, A. pDNA loaded calcium phosphate nanoparticles: Highly efficient non-viral vector for gene delivery. *Int. J. Pharm.* **2005**, *288*, 157–168. [CrossRef]
845. Kakizawa, Y.; Miyata, K.; Furukawa, S.; Kataoka, K. Size-controlled formation of a calcium phosphate-based organic-inorganic hybrid vector for gene delivery using poly(ethylene glycol)-block-poly(aspartic acid). *Adv. Mater.* **2004**, *16*, 699–702. [CrossRef]
846. Singh, R.; Saxena, A.; Mozumdar, S. Calcium phosphate—DNA nanocomposites: Morphological studies and their bile duct infusion for liver-directed gene therapy. *Int. J. Appl. Ceram. Technol.* **2008**, *5*, 1–10. [CrossRef]
847. Oyane, A.; Araki, H.; Sogo, Y.; Ito, A.; Tsurushima, H. Coprecipitation of DNA and calcium phosphate using an infusion fluid mixture. *Key Eng. Mater.* **2013**, *529–530*, 465–470. [CrossRef]
848. Sporysh, I.; Shynkaruk, E.; Lysko, O.; Shynkaruk, A.; Dubok, V.; Buzaneva, E.; Ritter, U.; Scharff, P. Biomimetic hydroxyapatite nanocrystals in composites with C60 and Au-DNA nanoparticles: IR-spectral study. *Mater. Sci. Eng. B* **2010**, *169*, 128–133. [CrossRef]
849. Taguchi, T.; Kishida, A.; Akashi, M. Hydroxyapatite formation on/in poly(vinyl alcohol) hydrogel matrices using a novel alternate soaking process. *Chem. Lett.* **1998**, *8*, 711–712. [CrossRef]
850. Tachaboonyakiat, W.; Serizawa, T.; Akashi, M. Hydroxyapatite formation on/in biodegradable chitosan hydrogels by an alternate soaking process. *Polym. J.* **2001**, *33*, 177–181. [CrossRef]
851. Schnepp, Z.A.C.; Gonzalez-McQuire, R.; Mann, S. Hybrid biocomposites based on calcium phosphate mineralization of self-assembled supramolecular hydrogels. *Adv. Mater.* **2006**, *18*, 1869–1872. [CrossRef]
852. Patel, M.; Patel, K.J.; Caccamese, J.F.; Coletti, D.P.; Sauk, J.J.; Fisher, J.P. Characterization of cyclic acetal hydroxyapatite nanocomposites for craniofacial tissue engineering. *J. Biomed. Mater. Res. A* **2010**, *94A*, 408–418. [CrossRef]
853. Yu, H.; Song, J.; Zhang, X.; Jiang, K.; Fan, H.; Li, Y.; Zhao, Y.; Liu, S.; Hao, D.; Li, G. Hydroxyapatite-tethered peptide hydrogel promotes osteogenesis. *Gels* **2022**, *8*, 804. [CrossRef]
854. Bigi, A.; Boanini, E.; Gazzano, M.; Kojdecki, M.A.; Rubini, K. Microstructural investigation of hydroxyapatite-polyelectrolyte composites. *J. Mater. Chem.* **2004**, *14*, 274–279. [CrossRef]
855. Bigi, A.; Boanini, E.; Gazzano, M.; Rubini, K.; Torricelli, P. Nanocrystalline hydroxyapatite-polyaspartate composites. *Biomed. Mater. Eng.* **2004**, *14*, 573–579.
856. Boanini, E.; Fini, M.; Gazzano, M.; Bigi, A. Hydroxyapatite nanocrystals modified with acidic amino acids. *Eur. J. Inorg. Chem.* **2006**, 4821–4826. [CrossRef]
857. Boanini, E.; Torricelli, P.; Gazzano, M.; Giardino, R.; Bigi, A. Nanocomposites of hydroxyapatite with aspartic acid and glutamic acid and their interaction with osteoblast-like cells. *Biomaterials* **2006**, *27*, 4428–4433. [CrossRef]
858. Ikawa, N.; Kimura, T.; Oumi, Y.; Sano, T. Amino acid containing amorphous calcium phosphates and the rapid transformation into apatite. *J. Mater. Chem.* **2009**, *19*, 4906–4913. [CrossRef]
859. Sánchez-Salcedo, S.; Nieto, A.; Vallet-Regi, M. Hydroxyapatite/β-tricalcium phosphate/agarose macroporous scaffolds for bone tissue engineering. *Chem. Eng. J.* **2005**, *137*, 62–71. [CrossRef]
860. Román, J.; Cabañas, M.V.; Peña, J.; Doadrio, J.C.; Vallet-Regi, M. An optimized β-tricalcium phosphate and agarose scaffold fabrication technique. *J. Biomed. Mater. Res. A* **2008**, *84A*, 99–107. [CrossRef]
861. Alcaide, M.; Serrano, M.C.; Pagani, R.; Sánchez-Salcedo, S.; Nieto, A.; Vallet-Regí, M.; Portolés, M.T. L929 fibroblast and SAOS-2 osteoblast response to hydroxyapatite-βTCP/ agarose biomaterial. *J. Biomed. Mater. Res. A* **2009**, *89A*, 539–549. [CrossRef]
862. Abiraman, S.; Varma, H.; Umashankar, P.; John, A. Fibrin sealant as an osteoinductive protein in a mouse model. *Biomaterials* **2002**, *23*, 3023–3031. [CrossRef]
863. Wittkampf, A. Fibrin sealant as sealant for hydroxyapatite granules. *J. Craniomaxillofac. Surg.* **1989**, *17*, 179–181. [CrossRef]
864. Le Nihouannen, D.; Guehennec, L.L.; Rouillon, T.; Pilet, P.; Bilban, M.; Layrolle, P.; Daculsi, G. Micro-architecture of calcium phosphate granules and fibrin glue composites for bone tissue engineering. *Biomaterials* **2006**, *27*, 2716–2722. [CrossRef]

865. Le Nihouannen, D.; Goyenvalle, E.; Aguado, E.; Pilet, P.; Bilban, M.; Daculsi, G.; Layrolle, P. Hybrid composites of calcium phosphate granules, fibrin glue and bone marrow for skeletal repair. *J. Biomed. Mater. Res. A* **2007**, *81A*, 399–408. [CrossRef]
866. Boanini, E.; Torricelli, P.; Gazzano, M.; Giardino, R.; Bigi, A. Alendronate-hydroxyapatite nanocomposites and their interaction with osteoclasts and osteoblast-like cells. *Biomaterials* **2008**, *29*, 790–796. [CrossRef]
867. Wang, L.; Nemoto, R.; Senna, M. Microstructure and chemical states of hydroxyapatite/silk fibroin nanocomposites synthesized via a wet-mechanochemical route. *J. Nanopart. Res.* **2002**, *4*, 535–540. [CrossRef]
868. Wang, L.; Li, C.Z.; Senna, M. High-affinity integration of hydroxyapatite nanoparticles with chemically modified silk fibroin. *J. Nanopart. Res.* **2007**, *9*, 919–929. [CrossRef]
869. Fan, C.; Li, J.; Xu, G.; He, H.; Ye, X.; Chen, Y.; Sheng, X.; Fu, J.; He, D. Facile fabrication of nano-hydroxyapatite/silk fibroin composite via a simplified coprecipitation route. *J. Mater. Sci.* **2010**, *45*, 5814–5819. [CrossRef]
870. Liu, H.; Xu, G.W.; Wang, Y.F.; Zhao, H.S.; Xiong, S.; Wu, Y.; Heng, B.C.; An, C.R.; Zhu, G.H.; Xie, D.H. Composite scaffolds of nano-hydroxyapatite and silk fibroin enhance mesenchymal stem cell-based bone regeneration via the interleukin 1 alpha autocrine/paracrine signaling loop. *Biomaterials* **2015**, *49*, 103–112. [CrossRef]
871. Farokhi, M.; Mottaghitalab, F.; Samani, S.; Shokrgozar, M.A.; Kundu, S.C.; Reis, R.L.; Fatahi, Y.; Kaplan, D.L. Silk fibroin/hydroxyapatite composites for bone tissue engineering. *Biotechnol. Adv.* **2018**, *36*, 68–91. [CrossRef]
872. Milazzo, M.; Fitzpatrick, V.; Owens, C.E.; Carraretto, I.M.; McKinley, G.H.; Kaplan, D.L.; Buehler, M.J. 3D printability of silk/hydroxyapatite composites for microprosthetic applications. *ACS Biomater. Sci. Eng.* **2023**, *9*, 1285–1295.
873. Salama, A.; Neumann, M.; Günter, C.; Taubert, A. Ionic liquid-assisted formation of cellulose/calcium phosphate hybrid materials. *Beilstein J. Nanotechnol.* **2014**, *5*, 1553–1568. [CrossRef]
874. Okuda, K.; Kido, E.; Hirota, K.; Mizutani, T. Water-resistant tough composites of cellulose nanofibers and hydroxyapatite. *ACS Appl. Polym. Mater.* **2023**, *5*, 8082–8088. [CrossRef]
875. Wang, L.; Li, C.Z. Preparation and physicochemical properties of a novel hydroxyapatite/chitosan-silk fibroin composite. *Carbohydr. Polym.* **2007**, *68*, 740–745. [CrossRef]
876. Shahbazarab, Z.; Teimouri, A.; Chermahini, A.N.; Azadi, M. Fabrication and characterization of nanobiocomposite scaffold of zein/chitosan/nanohydroxyapatite prepared by freeze-drying method for bone tissue engineering. *Int. J. Biol. Macromol.* **2018**, *108*, 1017–1027. [CrossRef]
877. Oliveira, J.M.; Costa, S.A.; Leonor, I.B.; Malafaya, P.B.; Mano, J.F.; Reis, R.L. Novel hydroxyapatite/carboxymethylchitosan composite scaffolds prepared through an innovative "autocatalytic" electroless coprecipitation route. *J. Biomed. Mater. Res. A* **2009**, *88*, 470–480. [CrossRef]
878. Sogo, Y.; Ito, A.; Matsuno, T.; Oyane, A.; Tamazawa, G.; Satoh, T.; Yamazaki, A.; Uchimura, E.; Ohno, T. Fibronectin-calcium phosphate composite layer on hydroxyapatite to enhance adhesion, cell spread and osteogenic differentiation of human mesenchymal stem cells in vitro. *Biomed. Mater.* **2007**, *2*, 116–123. [CrossRef]
879. Lin, J.; Fan, Y.; Hutchinson, D.J.; Malkoch, M. Soft hydroxyapatite composites based on triazine-trione systems as potential biomedical engineering frameworks. *ACS Appl. Mater. Interfaces* **2023**, *15*, 7329–7339. [CrossRef]
880. Rhee, S.H.; Suetsugu, Y.; Tanaka, J. Biomimetic configurational arrays of hydroxyapatite nanocrystals on bio-organics. *Biomaterials* **2001**, *22*, 2843–2847. [CrossRef]
881. Cross, K.J.; Huq, N.L.; Palamara, J.E.; Perich, J.W.; Reynolds, E.C. Physicochemical characterization of casein phosphopeptide-amorphous calcium phosphate nanocomplexes. *J. Biol. Chem.* **2005**, *280*, 15362–15369. [CrossRef]
882. Dimopoulou, M.; Ritzoulis, C.; Papastergiadis, E.S.; Panayiotou, C. Composite materials based on okra hydrocolloids and hydroxyapatite. *Food Hydrocoll.* **2014**, *42*, 348–354. [CrossRef]
883. Nakata, R.; Tachibana, A.; Tanabe, T. Preparation of keratin hydrogel/hydroxyapatite composite and its evaluation as a controlled drug release carrier. *Mater. Sci. Eng. C* **2014**, *41*, 59–64. [CrossRef]
884. Manda, M.G.; da Silva, L.P.; Cerqueira, M.T.; Pereira, D.R.; Oliveira, M.B.; Mano, J.F.; Marques, A.P.; Oliveira, J.M.; Correlo, V.M.; Reis, R.L. Gellan gum-hydroxyapatite composite spongy-like hydrogels for bone tissue engineering. *J. Biomed. Mater. Res. A* **2018**, *106A*, 479–490. [CrossRef]
885. Yu, P.; Bao, R.Y.; Shi, X.J.; Yang, W.; Yang, M.B. Self-assembled high-strength hydroxyapatite/graphene oxide/chitosan composite hydrogel for bone tissue engineering. *Carbohyd. Polym.* **2017**, *155*, 507–515. [CrossRef]
886. Li, C.; Born, A.K.; Schweizer, T.; Zenobi-Wong, M.; Cerruti, M.; Mezzenga, R. Amyloid-hydroxyapatite bone biomimetic composites. *Adv. Mater.* **2014**, *26*, 3207–3212. [CrossRef]
887. Kolanthai, E.; Colon, V.S.D.; Sindu, P.A.; Chandra, V.S.; Karthikeyan, K.R.; Babu, M.S.; Sundaram, S.M.; Palanichamy, M.; Kalkura, S.N. Effect of solvent; enhancing the wettability and engineering the porous structure of a calcium phosphate/agarose composite for drug delivery. *RSC Adv.* **2015**, *5*, 18301–18311. [CrossRef]
888. Krukowski, S.; Lysenko, N.; Kolodziejski, W. Synthesis and characterization of nanocrystalline composites containing calcium hydroxyapatite and glycine. *J.Solid State Chem.* **2018**, *264*, 59–67. [CrossRef]
889. Jung, J.Y.; Hong, Y.J.; Choi, Y.S.; Jeong, S.; Lee, W.K. A new method for the preparation of bioactive calcium phosphate films hybridized with 1α,25-dihydroxyvitamin D3. *J. Mater. Sci. Mater. Med.* **2010**, *20*, 2441–2453. [CrossRef]
890. Vu, B.T.; Le, A.N.M.; Tang, T.N.; Dang, N.N.T.; Duong, T.T.; Hua, H.T.N.; Phan, T.B.; Ta, H.T.K.; Pham, V.H.; Tran, Q.N.; et al. Fabrication of novel bone substitute alginate—N,O-carboxymethyl chitosan—Aldehyde hyaluronic acid—Biphasic calcium phosphate for bone regeneration. *React. Funct. Polym.* **2023**, *191*, 105691. [CrossRef]

891. Killion, J.A.; Geever, L.M.; Devine, D.M.; Higginbotham, C.L. Fabrication and in vitro biological evaluation of photopolymerisable hydroxyapatite hydrogel composites for bone regeneration. *J. Biomater. Appl.* **2014**, *28*, 1274–1283. [CrossRef]
892. Pontons-Melo, J.C.; Balbinot, G.d.S.; Sauro, S.; Collares, F.M. Experimental composite resin with myristyltrimethylammonium bromide (MYTAB) and alpha-tricalcium phosphate (α-TCP): Antibacterial and remineralizing effect. *J. Funct. Biomater.* **2023**, *14*, 303. [CrossRef]
893. Shchukin, D.G.; Sukhorukov, G.B.; Möhwald, H. Biomimetic fabrication of nanoengineered hydroxyapatite/polyelectrolyte composite shell. *Chem. Mater.* **2003**, *15*, 3947–3950. [CrossRef]
894. Busch, S.; Dolhaine, H.; DuChesne, A.; Heinz, S.; Hochrein, O.; Laeri, F.; Podebrad, O.; Vietze, U.; Weiland, T.; Kniep, R. Biomimetic morphogenesis of fluorapatite-gelatin composites: Fractal growth, the question of intrinsic electric fields, core/shell assemblies, hollow spheres and reorganization of denatured collagen. *Eur. J. Inorg. Chem.* **1999**, *1999*, 1643–1653. [CrossRef]
895. Tlatlik, H.; Simon, P.; Kawska, A.; Zahn, D.; Kniep, R. Biomimetic fluorapatite-gelatin nanocomposites: Pre-structuring of gelatin matrices by ion impregnation and its effect on form development. *Angew. Chem. Int. Ed. Engl.* **2006**, *45*, 1905–1910. [CrossRef]
896. Kniep, R.; Simon, P. "Hidden" hierarchy of microfibrils within 3D-periodic fluorapatite-gelatin nanocomposites: Development of complexity and form in a biomimetic system. *Angew. Chem. Int. Ed. Engl.* **2008**, *47*, 1405–1409. [CrossRef]
897. Brickmann, J.; Paparcone, R.; Kokolakis, S.; Zahn, D.; Duchstein, P.; Carrillocabrera, W.; Simon, P.; Kniep, R. Fluorapatite-gelatine nanocomposite superstructures: New insights into a biomimetic system of high complexity. *ChemPhysChem* **2010**, *11*, 1851–1853. [CrossRef]
898. Vyalikh, A.; Simon, P.; Rosseeva, E.; Buder, J.; Kniep, R.; Scheler, U. Intergrowth and interfacial structure of biomimetic fluorapatite-gelatin nanocomposite: A solid-state NMR study. *J. Phys. Chem. B* **2014**, *118*, 724–730. [CrossRef]
899. Gashti, M.P.; Stir, M.; Hulliger, J. Synthesis of bone-like micro-porous calcium phosphate/iota-carrageenan composites by gel diffusion. *Colloid Surface B* **2013**, *110*, 426–433. [CrossRef]
900. Aguilera, S.B.; McCarthy, A.; Khalifian, S.; Lorenc, Z.P.; Goldie, K.; Chernoff, W.G. The role of calcium hydroxylapatite (Radiesse) as a regenerative aesthetic treatment: A narrative review. *Aesthet. Surg. J.* **2023**, *43*, 1063–1090. [CrossRef]
901. Galadari, H.; Guida, S. A systematic review of Radiesse® (calcium hydroxylapatite): Evidence and recommendations for the body. *Int. J. Dermatol.* **2024**, *63*, 150–160. [CrossRef]
902. Klesing, J.; Chernousova, S.; Kovtun, A.; Neumann, S.; Ruiz, L.; Gonzalez-Calbet, J.M.; Vallet-Regi, M.; Heumann, R.; Epple, M. An injectable paste of calcium phosphate nanorods, functionalized with nucleic acids, for cell transfection and gene silencing. *J. Mater. Chem.* **2010**, *20*, 6144–6148. [CrossRef]
903. Thai, V.V.; Lee, B.T. Fabrication of calcium phosphate-calcium sulfate injectable bone substitute using hydroxy-propyl-methyl-cellulose and citric acid. *J. Mater. Sci. Mater. Med.* **2010**, *21*, 1867–1874. [CrossRef]
904. Low, K.L.; Tan, S.H.; Zein, S.H.S.; Roether, J.A.; Mouriño, V.; Boccaccini, A.R. Calcium phosphate-based composites as injectable bone substitute materials. *J. Biomed. Mater. Res. B Appl. Biomater.* **2010**, *94B*, 273–286. [CrossRef]
905. D'Este, M.; Eglin, D. Hydrogels in calcium phosphate moldable and injectable bone substitutes: Sticky excipients or advanced 3-D carriers? *Acta Biomater.* **2013**, *9*, 5421–5430. [CrossRef]
906. Daculsi, G.; Weiss, P.; Bouler, J.M.; Gauthier, O.; Millot, F.; Aguado, E. Biphasic calcium phosphate/hydrosoluble polymer composites: A new concept for bone and dental substitution biomaterials. *Bone* **1999**, *25* (Suppl. S2), 59S–61S. [CrossRef]
907. Turczyn, R.; Weiss, P.; Lapkowski, M.; Daculsi, G. In situ self-hardening bioactive composite for bone and dental surgery. *J. Biomater. Sci. Polym. Edn.* **2000**, *11*, 217–223. [CrossRef]
908. Bennett, S.; Connolly, K.; Lee, D.R.; Jiang, Y.; Buck, D.; Hollinger, J.O.; Gruskin, E.A. Initial biocompatibility studies of a novel degradable polymeric bone substitute that hardens in situ. *Bone* **1996**, *19*, 101S–107S. [CrossRef]
909. Shalygina, K.; Lytkina, D.; Sadykov, R.; Kurzina, I. Composite cryogels based on hydroxyapatite and polyvinyl alcohol and the study of physicochemical and mechanical properties. *Materials* **2024**, *17*, 403. [CrossRef]
910. Bongio, M.; van den Beucken, J.J.J.P.; Nejadnik, M.R.; Birgani, Z.T.; Habibovic, P.; Kinard, L.A.; Kasper, F.K.; Mikos, A.G.; Leeuwenburgh, S.C.G.; Jansen, J.A. Subcutaneous tissue response and osteogenic performance of calcium phosphate nanoparticle-enriched hydrogels in the tibial medullary cavity of guinea pigs. *Acta Biomater.* **2013**, *9*, 5464–5474. [CrossRef]
911. Chernousova, S.; Klesing, J.; Soklakova, N.; Epple, M. A genetically active nano-calcium phosphate paste for bone substitution, encoding the formation of BMP-7 and VEGF-A. *RSC Adv.* **2013**, *3*, 11155–11161. [CrossRef]
912. Yu, B.; Zhang, Y.; Li, X.; Wang, Q.; Ouyang, Y.; Xia, Y.; Lin, B.; Li, S.; Fan, Y.; Chen, Y. The use of injectable chitosan/nanohydroxyapatite/collagen composites with bone marrow mesenchymal stem cells to promote ectopic bone formation in vivo. *J. Nanomater.* **2013**, *2013*, 506593. [CrossRef]
913. Phewchan, P.; Laoruengthana, A.; Tiyaboonchai, W. Calcium phosphate incorporated in silk fibroin/methylcellulose based injectable hydrogel: Preparation, characterization and in vitro biological evaluation for bone defect treatment. *J. Biomed. Mater. Res. B Appl. Biomater.* **2023**, *111*, 1640–1652. [CrossRef]
914. Bodakhe, S.; Verma, S.; Garkhal, K.; Samal, S.K.; Sharma, S.S.; Kumar, N. Injectable photocrosslinkable nanocomposite based on poly(glycerol sebacate) fumarate and hydroxyapatite: Development, biocompatibility and bone regeneration in a rat calvarial bone defect model. *Nanomedicine* **2013**, *8*, 1777–1795. [CrossRef]
915. Fricain, J.C.; Aid, R.; Lanouar, S.; Maurel, D.B.; le Nihouannen, D.; Delmond, S.; Letourneur, D.; Vilamitjana, J.A.; Catros, S. In-vitro and in-vivo design and validation of an injectable polysaccharide-hydroxyapatite composite material for sinus floor augmentation. *Dent. Mater.* **2018**, *34*, 1024–1035. [CrossRef]

916. Şahin, E. Enhanced injectability of aqueous β-tricalcium phosphate suspensions through PAA incorporation, gelling and preshearing. *J. Mech. Behav. Biomed. Mater.* **2023**, *145*, 106026. [CrossRef]
917. Lin, G.; Cosimbescu, L.; Karin, N.J.; Tarasevich, B.J. Injectable and thermosensitive PLGA-g-PEG hydrogels containing hydroxyapatite: Preparation, characterization and in vitro release behavior. *Biomed. Mater.* **2012**, *7*, 024107. [CrossRef]
918. Nejadnik, M.R.; Yang, X.; Bongio, M.; Alghamdi, H.S.; van den Beucken, J.J.J.P.; Huysmans, M.C.; Jansen, J.A.; Hilborn, J.; Ossipov, D.; Leeuwenburgh, S.C.G. Self-healing hybrid nanocomposites consisting of bisphosphonated hyaluronan and calcium phosphate nanoparticles. *Biomaterials* **2014**, *35*, 6918–6929. [CrossRef]
919. Munarin, F.; Petrini, P.; Gentilini, R.; Pillai, R.S.; Dirè, S.; Tanzi, M.C.; Sglavo, V.M. Micro- and nano-hydroxyapatite as active reinforcement for soft biocomposites. *Int. J. Biol. Macromol.* **2015**, *72*, 199–209. [CrossRef]
920. Douglas, T.E.L.; Schietse, J.; Zima, A.; Gorodzha, S.; Parakhonskiy, B.V.; Khalenkow, D.; Shkarin, R.; Ivanova, A.; Baumbach, T.; Weinhardt, V.; et al. Novel self-gelling injectable hydrogel/alpha-tricalcium phosphate composites for bone regeneration: Physiochemical and microcomputer tomographical characterization. *J. Biomed. Mater. Res. A* **2018**, *106A*, 822–828. [CrossRef]
921. Daculsi, G.; Rohanizadeh, R.; Weiss, P.; Bouler, J.M. Crystal polymer interaction with new injectable bone substitute: SEM and HrTEM study. *J. Biomed. Mater. Res.* **2000**, *50*, 1–7. [CrossRef]
922. Weiss, P.; Lapkowski, M.; LeGeros, R.Z.; Bouler, J.M.; Jean, A.; Daculsi, G. FTIR spectroscopic study of an organic/mineral composite for bone and dental substitute materials. *J. Mater. Sci. Mater. Med.* **1997**, *8*, 621–629. [CrossRef]
923. Weiss, P.; Bohic, S.; Lapkowski, M.; Daculsi, G. Application of FTIR microspectroscopy to the study of an injectable composite for bone and dental surgery. *J. Biomed. Mater. Res.* **1998**, *41*, 167–170. [CrossRef]
924. Weiss, P.; Layrolle, P.; Clergeau, L.P.; Enckel, B.; Pilet, P.; Amouriq, Y.; Daculsi, G.; Giumelli, B. The safety and efficacy of an injectable bone substitute in dental sockets demonstrated in a human clinical trial. *Biomaterials* **2007**, *28*, 3295–3305. [CrossRef]
925. Fatimi, A.; Tassin, J.F.; Axelos, M.A.V.; Weiss, P. The stability mechanisms of an injectable calcium phosphate ceramic suspension. *J. Mater. Sci. Mater. Med.* **2010**, *21*, 1799–1809. [CrossRef]
926. Trojani, C.; Boukhechba, F.; Scimeca, J.C.; Vandenbos, F.; Michiels, J.F.; Daculsi, G.; Boileau, P.; Weiss, P.; Carle, G.F.; Rochet, N. Ectopic bone formation using an injectable biphasic calcium phosphate/Si-HPMC hydrogel composite loaded with undifferentiated bone marrow stromal cells. *Biomaterials* **2006**, *27*, 3256–3264. [CrossRef]
927. Zhang, S.M.; Lü, G. Clinical application of compound injectable bone substitutes in bone injury repair. *J. Clin. Rehabil. Tissue Eng. Res.* **2009**, *13*, 10117–10120.
928. Daculsi, G.; Uzel, P.A.; Bourgeois, N.; le François, T.; Rouvillain, J.L.; Bourges, X.; Baroth, S. New injectable bone substitute using reversible thermosensitive hydrogel and BCP granules: In vivo rabbit experiments. *Key Eng. Mater.* **2009**, *396–398*, 457–460. [CrossRef]
929. Iooss, P.; le Ray, A.M.; Grimandi, G.; Daculsi, G.; Merle, C. A new injectable bone substitute combining poly(ε-caprolactone) microparticles with biphasic calcium phosphate granules. *Biomaterials* **2001**, *22*, 2785–2794. [CrossRef]
930. Bohner, M. Design of ceramic-based cements and putties for bone graft substitution. *Eur. Cell Mater.* **2010**, *20*, 1–12. [CrossRef]
931. Evis, Z.; Ergun, C.; Doremus, R.H. Hydroxylapatite-zirconia composites: Thermal stability of phases and sinterability as related to the CaO-ZrO_2 phase diagram. *J. Mater. Sci.* **2005**, *40*, 1127–1134. [CrossRef]
932. Rao, R.R.; Kannan, T.S. Synthesis and sintering of hydroxyapatite-zirconia composites. *Mater. Sci. Eng. C* **2002**, *20*, 187–193.
933. Mansur, C.; Pope, M.; Pascucci, M.R.; Shivkumar, S. Zirconia-calcium phosphate composites for bone replacement. *Ceram. Int.* **1998**, *24*, 77–79. [CrossRef]
934. Kim, H.W.; Kim, H.E.; Salih, V.; Knowles, J.C. Dissolution control and cellular responses of calcium phosphate coatings on zirconia porous scaffold. *J. Biomed. Mater. Res. A* **2004**, *68A*, 522–530. [CrossRef]
935. Milella, E.; Cosentino, F.; Licciulli, A.; Massaro, C. Preparation and characterisation of titania/hydroxyapatite composite coatings obtained by sol-gel process. *Biomaterials* **2001**, *22*, 1425–1431. [CrossRef]
936. Tancred, D.C.; Carr, A.J.; McCormack, B.A. The sintering and mechanical behaviour of hydroxyapatite with bioglass additions. *J. Mater. Sci. Mater. Med.* **2001**, *12*, 81–93. [CrossRef]
937. Goller, G.; Demirkiran, H.; Oktar, F.N.; Demirkesen, E. Processing and characterization of Bioglass reinforced hydroxyapatite composites. *Ceram. Int.* **2003**, *29*, 721–724. [CrossRef]
938. Lopes, M.A.; Silva, R.F.; Monteiro, F.J.; Santos, J.D. Microstructural dependence of Young's moduli of P_2O_5 glass reinforced hydroxyapatite for biomedical applications. *Biomaterials* **2000**, *21*, 749–754. [CrossRef]
939. Amaral, S.S.; de Sousa Lima, B.S.; Avelino, S.O.M.; Spirandeli, B.R.; Campos, T.M.B.; Thim, G.P.; de Sousa Trichês, E.; do Prado, R.F.; de Vasconcellos, L.M.R. β-TCP/S53P4 scaffolds obtained by gel casting: Synthesis, properties and biomedical applications. *Bioengineering* **2023**, *10*, 597. [CrossRef]
940. Ruiz-Aguilar, C. Porous phosphate-based bioactive glass/β-TCP scaffold for tooth remineralization. *PLoS ONE* **2023**, *18*, e0284885. [CrossRef]
941. Juang, H.Y.; Hon, M.H. Fabrication and mechanical properties of hydroxyapatite-alumina composites. *Mater. Sci. Eng. C* **1994**, *2*, 77–81. [CrossRef]
942. Li, J.; Forbreg, S.; Hermansson, L. Evaluation of the mechanical properties of hot isotatically pressed titania and titania-calcium phosphate composites. *Biomaterials* **1991**, *12*, 438–440. [CrossRef]
943. Noma, T.; Shoji, N.; Wada, S.; Suzuki, T. Preparation of spherical Al_2O_3 particle dispersed hydroxyapatite ceramics. *J. Ceram. Soc. Jpn.* **1993**, *101*, 923–927. [CrossRef]

944. Gautier, S.; Champion, E.; Bernache-Assollant, D. Toughening characterization in alumina platelet-hydroxyapatite matrix composites. *J. Mater. Sci. Mater. Med.* **1999**, *10*, 533–540. [CrossRef]
945. Fang, Y.; Roy, D.M.; Cheng, J.; Roy, R.; Agrawal, D.K. Microwave sintering of hydroxyapatite-based composites. *Ceram. Trans.* **1993**, *36*, 397–407.
946. Park, K.; Vasilosa, T. Microstructure and mechanical properties of silicon carbide whisker/calcium phosphate composites produced by hot pressing. *Mater. Lett.* **1997**, *32*, 229–233. [CrossRef]
947. Jin, H.B.; Oktar, F.N.; Dorozhkin, S.; Agathopoulos, S. Sintering behavior and properties of reinforced hydroxyapatite/TCP biphasic bioceramics with ZnO-whiskers. *J. Compos. Mater.* **2011**, *45*, 1435–1445. [CrossRef]
948. de With, G.; Corbijn, A.T. Metal fibre reinforced hydroxyapatite ceramics. *J. Mater. Sci.* **1989**, *24*, 3411–3415. [CrossRef]
949. Ruys, A.J.; Simpson, S.A.; Sorrell, C.C. Thixotropic casting of fibre-reinforced ceramic matrix composites. *J. Mater. Sci. Lett.* **1994**, *13*, 1323–1325. [CrossRef]
950. Miao, X.; Ruys, A.J.; Milthorpe, B.K. Hydroxyapatite-316L fibre composites prepared by vibration assisted slip casting. *J. Mater. Sci.* **2001**, *36*, 3323–3332. [CrossRef]
951. Kim, H.M.; Chae, W.P.; Chang, K.W.; Chun, S.; Kim, S.; Jeong, Y.; Kang, I.K. Composite nanofiber mats consisting of hydroxyapatite and titania for biomedical applications. *J. Biomed. Mater. Res. B Appl. Biomater.* **2010**, *94B*, 380–387. [CrossRef]
952. Hirakura, S.; Kobayashi, T.; Ono, S.; Oaki, Y.; Imai, H. Fibrous nanocrystals of hydroxyapatite loaded with TiO_2 nanoparticles for the capture and photocatalytic decomposition of specific proteins. *Colloid Surface B* **2010**, *79*, 131–135. [CrossRef]
953. Wu, J.M.; Yeh, T.S. Sintering of hydroxylapatite-zirconia composite materials. *J. Mater. Sci.* **1988**, *23*, 3771–3777. [CrossRef]
954. Li, J.; Liao, H.; Hermansson, L. Sintering of partially-stabilized zirconia and partially-stabilized zirconia-hydroxyapatite composites by hot isostatic pressing and pressureless sintering. *Biomaterials* **1996**, *17*, 1787–1790. [CrossRef]
955. Takagi, M.; Mochida, M.; Uchida, N.; Saito, K.; Uematsu, K. Filter cake forming and hot isostatic pressing for TZP-dispersed hydroxyapatite composite. *J. Mater. Sci. Mater. Med.* **1992**, *3*, 199–203. [CrossRef]
956. Shen, Z.; Adolfsson, E.; Nygren, M.; Gao, L.; Kawaoka, H.; Niihara, K. Dense hydroxyapatite-zirconia ceramic composites with high strength for biological applications. *Adv. Mater.* **2001**, *13*, 214–216. [CrossRef]
957. Nagarajan, V.S.; Rao, K.J. Structural, mechanical and biocompatibility studies of hydroxyapatite-derived composites toughened by zirconia addition. *J. Mater. Chem.* **1993**, *3*, 43–51. [CrossRef]
958. Quan, R.; Yang, D.; Wu, X.; Wang, H.; Miao, X.; Li, W. In vitro and in vivo biocompatibility of graded hydroxyapatite-zirconia composite bioceramic. *J. Mater. Sci. Mater. Med.* **2008**, *19*, 183–187. [CrossRef]
959. Wang, L.L.; Wang, X.F.; Jiang, H.T.; Yu, C.L. Preparation of porous hydroxyapatite-zirconia composite scaffolds by combination of gel-casting and polymer sponge methods. *Adv. Mater. Res.* **2010**, *105–106*, 616–619. [CrossRef]
960. Cao, Y.; Li, C.; Xia, Y.; Ren, K.; Zhu, S. Study on the fabrication and mechanical properties of HAp-3YSZ composites by flash sintering. *Ceram. Int.* **2022**, *48*, 16300–16305. [CrossRef]
961. Koushik, T.M.; Miller, C.M.; Antunes, E. Optimisation of two-step sintering parameters to produce bioactive and dense zirconia-hydroxyapatite composite ceramics. *J. Eur. Ceram. Soc.* **2023**, *43*, 2222–2233. [CrossRef]
962. Ge, M.; Xie, D.; Yang, Y.; Tian, Z. Sintering densification mechanism and mechanical properties of the 3D-printed high-melting-point-difference magnesium oxide/calcium phosphate composite bio-ceramic scaffold. *J. Mech. Behav. Biomed. Mater.* **2023**, *144*, 105978. [CrossRef]
963. Li, J.; Fartash, B.; Hermansson, L. Hydroxyapatite-alumina composites and bone-bonding. *Biomaterials* **1995**, *16*, 417–422. [CrossRef]
964. Jun, Y.K.; Kim, W.H.; Kweon, O.K.; Hong, S.H. The fabrication and biochemical evaluation of alumina reinforced calcium phosphate porous implants. *Biomaterials* **2003**, *24*, 3731–3739. [CrossRef]
965. Epure, L.M.; Dimitrievska, S.; Merhi, Y.; Yahia, L.H. The effect of varying Al_2O_3 percentage in hydroxyapatite/Al_2O_3 composite materials: Morphological, chemical and cytotoxic evaluation. *J. Biomed. Mater. Res. A* **2007**, *83A*, 1009–1023. [CrossRef]
966. Youness, R.A.; Saleh, H.A.; Taha, M.A. Microstructure and elastic properties of hydroxyapatite/alumina nanocomposites prepared by mechanical alloying technique for biomedical applications. *Biointerface Res. Appl. Chem.* **2023**, *13*, 395.
967. Shaly, A.A.; Priya, G.H.; Mahendiran, M.; Linet, J.M. A behavioural study of hydrothermally derived novel alumina/magnesia/hydroxyapatite (Al_2O_3/MgO/HA) bioceramic nanocomposite. *J. Mech. Behav. Biomed. Mater.* **2022**, *133*, 105313.
968. Lu, Y.P.; Li, M.S.; Li, S.T.; Wang, Z.G.; Zhu, R.F. Plasma-sprayed hydroxyapatite + titania composite bond coat for hydroxyapatite coating on titanium substrate. *Biomaterials* **2004**, *25*, 4393–4403. [CrossRef]
969. Pushpakanth, S.; Srinivasan, B.; Sreedhar, B.; Sastry, T.P. An in situ approach to prepare nanorods of titania-hydroxyapatite (TiO_2-HAp) nanocomposite by microwave hydrothermal technique. *Mater. Chem. Phys.* **2008**, *107*, 492–498. [CrossRef]
970. Nath, S.; Tripathi, R.; Basu, B. Understanding phase stability, microstructure development and biocompatibility in calcium phosphate-titania composites, synthesized from hydroxyapatite and titanium powder mix. *Mater. Sci. Eng. C* **2009**, *29*, 97–107. [CrossRef]
971. Swapna, Y.V.; Mathew, C.T.; Thomas, J.K. Resistive coupled microwave sintering of hydroxyapatite/titania nano-biocomposite and tailoring its mechanical properties. *J. Mech. Behav. Biomed. Mater.* **2023**, *141*, 105772. [CrossRef]
972. Sakka, S.; Bouaziz, J.; Ben Ayed, F. Sintering and mechanical properties of the alumina-tricalcium phosphate-titania composites. *Mater. Sci. Eng. C* **2014**, *40*, 92–101. [CrossRef]

973. Yang, Z.P.; Gong, X.Y.; Zhang, C.J. Recyclable Fe_3O_4/hydroxyapatite composite nanoparticles for photocatalytic applications. *Chem. Eng. J.* **2010**, *165*, 117–121. [CrossRef]
974. Liu, Y.; Zhong, H.; Li, L.; Zhang, C. Temperature dependence of magnetic property and photocatalytic activity of Fe_3O_4/hydroxyapatite nanoparticles. *Mater. Res. Bull.* **2010**, *45*, 2036–2039. [CrossRef]
975. Ignatovich, Z.; Novik, K.; Abakshonok, A.; Koroleva, E.; Beklemisheva, A.; Panina, L.; Kaniukov, E.; Anisovich, M.; Shumskaya, A. One-step synthesis of magnetic nanocomposite with embedded biologically active substance. *Molecules* **2021**, *26*, 937. [CrossRef]
976. Biedrzycka, A.; Skwarek, E.; Hanna, U.M. Hydroxyapatite with magnetic core: Synthesis methods, properties, adsorption and medical applications. *Adv. Colloid Interface Sci.* **2021**, *291*, 102401. [CrossRef]
977. Lee, B.T.; Lee, C.W.; Gain, A.K.; Song, H.Y. Microstructures and material properties of fibrous Ap/Al_2O_3-ZrO_2 composites fabricated by multi-pass extrusion process. *J. Eur. Ceram. Soc.* **2007**, *27*, 157–163. [CrossRef]
978. Oktar, F.N.; Agathopoulos, S.; Ozyegin, L.S.; Gunduz, O.; Demirkol, N.; Bozkurt, Y.; Salman, S. Mechanical properties of bovine hydroxyapatite (BHA) composites doped with SiO_2, MgO, Al_2O_3 and ZrO_2. *J. Mater. Sci. Mater. Med.* **2007**, *18*, 2137–2143. [CrossRef]
979. Gunduz, O.; Erkan, E.M.; Daglilar, S.; Salman, S.; Agathopoulos, S.; Oktar, F.N. Composites of bovine hydroxyapatite (BHA) and ZnO. *J. Mater. Sci.* **2008**, *43*, 2536–2540. [CrossRef]
980. Dong, L.; Zhu, Z.; Qiu, Y.; Zhao, J. Removal of lead from aqueous solution by hydroxyapatite/manganese dioxide composite. *Front. Environ. Sci. Eng.* **2016**, *10*, 28–36. [CrossRef]
981. Pandey, A.; Midha, S.; Sharma, R.K.; Maurya, R.; Nigam, V.K.; Ghosh, S.; Balani, K. Antioxidant and antibacterial hydroxyapatite-based biocomposite for orthopedic applications. *Mater. Sci. Eng. C* **2018**, *88*, 13–24. [CrossRef]
982. Mostafa, S.I.; Ismail, M.S.; Mohammed, H.A.; Osman, M.F.; Elwassefy, N.A. Magnetic hydroxyapatite bisphosphonate-based composites: A bone-targeting nanosystem. *Emergent Mater.* **2023**, *6*, 1273–1284. [CrossRef]
983. Lopes, M.A.; Monterio, F.J.; Santos, J.D. Glass-reinforced hydroxyapatite composites: Fracture toughness and hardness dependence on microstructural characteristics. *Biomaterials* **1999**, *20*, 2085–2090. [CrossRef]
984. Ragel, C.V.; Vallet-Regi, M.; Rodríguez-Lorenzo, L.M. Preparation and in vitro bioactivity of hydroxyapatite/sol-gel glass biphasic material. *Biomaterials* **2002**, *23*, 1865–1872. [CrossRef]
985. Li, X.W.; Yasuda, H.Y.; Umakoshi, Y. Bioactive ceramic composites sintered from hydroxyapatite and silica at 1200 °C: Preparation, microstructures and in vitro bone-like layer growth. *J. Mater. Sci. Mater. Med.* **2006**, *17*, 573–581. [CrossRef]
986. Padilla, S.; Sánchez-Salcedo, S.; Vallet-Regi, M. Bioactive and biocompatible pieces of HA/sol-gel glass mixtures obtained by the gel-casting method. *J. Biomed. Mater. Res. A* **2005**, *75A*, 63–72. [CrossRef]
987. Padilla, S.; Román, J.; Sánchez-Salcedo, S.; Vallet-Regi, M. Hydroxyapatite/SiO_2-CaO-P_2O_5 glass materials: In vitro bioactivity and biocompatibility. *Acta Biomater.* **2006**, *2*, 331–342. [CrossRef]
988. Sych, E.E.; Pinchuk, N.D.; Ivanchenko, L.A. Effect of sintering temperature on the properties of biogenic hydroxyapatite-glass composites. *Powder Metall. Metal Ceram.* **2010**, *49*, 153–158. [CrossRef]
989. Marovic, D.; Tarle, Z.; Hiller, K.A.; Müller, R.; Rosentritt, M.; Skrtic, D.; Schmalz, G. Reinforcement of experimental composite materials based on amorphous calcium phosphate with inert fillers. *Dent. Mater.* **2014**, *30*, 1052–1060. [CrossRef]
990. Bellucci, D.; Sola, A.; Lusvarghi, L.; Cannillo, V. Hydroxyapatite-tricalcium phosphate-bioactive glass ternary composites. *Ceram. Int.* **2014**, *40*, 3805–3808. [CrossRef]
991. Bellucci, D.; Sola, A.; Anesi, A.; Salvatori, R.; Chiarini, L.; Cannillo, V. Bioactive glass/hydroxyapatite composites: Mechanical properties and biological evaluation. *Mater. Sci. Eng. C* **2015**, *51*, 196–205. [CrossRef]
992. Yazdanpanah, Z.; Bahrololoom, M.E.; Hashemi, B. Evaluating morphology and mechanical properties of glass-reinforced natural hydroxyapatite composites. *J. Mech. Behav. Biomed. Mater.* **2015**, *41*, 36–42. [CrossRef]
993. Seyedmajidi, M.; Haghanifar, S.; Hajian-Tilaki, K.; Seyedmajidi, S. Histopathological, histomorphometrical and radiological evaluations of hydroxyapatite/bioactive glass and fluorapatite/bioactive glass nanocomposite foams as cell scaffolds in rat tibia: An in vivo study. *Biomed. Mater.* **2018**, *13*, 025015. [CrossRef]
994. Esposti, L.D.; Zheng, K.; Piancastelli, A.; Ionescu, A.C.; Adamiano, A.; Boccaccini, A.R.; Iafisco, M. Composite materials of amorphous calcium phosphate and bioactive glass nanoparticles for preventive dentistry. *Ceram. Int.* **2024**, *50*, 593–602. [CrossRef]
995. Makornpan, C.; Monmaturapoj, N.; Prahsarn, C.; Klinsukhon, W.; Chokevivat, W. Hydroxyapatite/titanium dioxide/bioactive glass composites with anti-microbial performance under multiple illumination conditions. *J. Mater. Sci.* **2023**, *58*, 17751–17764. [CrossRef]
996. Nishio, K.; Neo, M.; Akiyama, H.; Okada, Y.; Kokubo, T.; Nakamura, T. Effects of apatite and wollastonite containing glass-ceramic powder and two types of alumina powder in composites on osteoblastic differentiation of bone marrow cells. *J. Biomed. Mater. Res.* **2001**, *55*, 164–176. [CrossRef]
997. Encinas-Romero, M.A.; Aguayo-Salinas, S.; Valenzuela-García, J.L.; Payán, S.R.; Castillón-Barraza, F.F. Mechanical and bioactive behavior of hydroxyapatite-wollastonite sintered composites. *Int. J. Appl. Ceram. Technol.* **2010**, *7*, 164–177. [CrossRef]
998. Ha, N.R.; Yang, Z.X.; Hwang, K.H.; Kim, T.S.; Lee, J.K. Improvement of the stability of hydroxyapatite through glass ceramic reinforcement. *J. Nanosci. Nanotechnol.* **2010**, *10*, 3459–3462. [CrossRef]
999. Nath, S.; Biswas, K.; Wang, K.; Bordia, R.K.; Basu, B. Sintering, phase stability and properties of calcium phosphate-mullite composites. *J. Am. Ceram. Soc.* **2010**, *93*, 1639–1649. [CrossRef]

1000. Nath, S.; Ummethala, R.; Basu, B. Fretting wear behavior of calcium phosphate-mullite composites in dry and albumin-containing simulated body fluid conditions. *J. Mater. Sci. Mater. Med.* **2010**, *21*, 1151–1161. [CrossRef]
1001. Nath, S.; Dubey, A.K.; Basu, B. Mechanical properties of novel calcium phosphate-mullite biocomposites. *J. Biomater. Appl.* **2012**, *27*, 67–78. [CrossRef]
1002. Nath, S.; Kalmodia, S.; Basu, B. In vitro biocompatibility of novel biphasic calcium phosphate-mullite composites. *J. Biomater. Appl.* **2013**, *27*, 497–509. [CrossRef]
1003. Obada, D.O.; Osseni, S.A.; Sina, H.; Salami, K.A.; Oyedeji, A.N.; Dodoo-Arhin, D.; Bansod, N.D.; Csaki, S.; Atta, A.Y.; Fasanya, O.O.; et al. Fabrication of novel kaolin-reinforced hydroxyapatite scaffolds with robust compressive strengths for bone regeneration. *Appl. Clay Sci.* **2021**, *215*, 106298. [CrossRef]
1004. de Andrade, R.; Paim, T.C.; Bertaco, I.; Naasani, L.S.; Buchner, S.; Kovářík, T.; Hájek, J.; Wink, M.R. Hierarchically porous bioceramics based on geopolymer-hydroxyapatite composite as a novel biomaterial: Structure, mechanical properties and biocompatibility evaluation. *Appl. Mater. Today* **2023**, *33*, 101875. [CrossRef]
1005. Tseng, W.J.; Kao, W.H. Preparation of electrically conductive calcium phosphate composite foams by particle-stabilized emulsion route. *Ceramics* **2018**, *1*, 319–328. [CrossRef]
1006. Chaki, T.K.; Wang, P.E. Densification and strengthening of silver-reinforced hydroxyapatite-matrix composite prepared by sintering. *J. Mater. Sci. Mater. Med.* **1994**, *5*, 533–542. [CrossRef]
1007. Zhang, X.; Gubbels, G.H.M.; Terpstra, R.A.; Metselaar, R. Toughening of calcium hydroxyapatite with silver particles. *J. Mater. Sci.* **1997**, *32*, 235–243. [CrossRef]
1008. Chu, C.; Lin, P.; Dong, Y.; Xue, X.; Zhu, J.; Yin, Z. Fabrication and characterization of hydroxyapatite reinforced with 20 vol. % Ti particles for use as hard tissue replacement. *J. Mater. Sci. Mater. Med.* **2002**, *13*, 985–992. [CrossRef]
1009. Ning, C.Q.; Zhou, Y. In vitro bioactivity of a biocomposite fabricated from HA and Ti powders by powder metallurgy method. *Biomaterials* **2002**, *23*, 2909–2915. [CrossRef]
1010. Chu, C.; Xue, X.; Zhu, J.; Yin, Z. Mechanical and biological properties of hydroxyapatite reinforced with 40 vol. % titanium particles for use as hard tissue replacement. *J. Mater. Sci. Mater. Med.* **2004**, *15*, 665–670. [CrossRef]
1011. Karanjai, M.; Kumarb, M.B.V.; Sundaresan, R.; Basu, B.; Mohan, R.T.R.; Kashyap, B.P. Fretting wear study on Ti-Ca-P biocomposite in dry and simulated body fluid. *Mater. Sci. Eng. A* **2008**, *475*, 299–307. [CrossRef]
1012. Chu, C.; Xue, X.; Zhu, J.; Yin, Z. Fabrication and characterization of titanium-matrix composite with 20 vol. % hydroxyapatite for use as heavy load-bearing hard tissue replacement. *J. Mater. Sci. Mater. Med.* **2006**, *17*, 245–251. [CrossRef]
1013. Miranda, M.; Fernández, A.; Díaz, M.; Esteban-Tejeda, L.; López-Esteban, S.; Malpartida, F.; Torrecillas, R.; Moya, J.S. Silver-hydroxyapatite nanocomposites as bactericidal and fungicidal materials. *Int. J. Mater. Res.* **2010**, *101*, 122–127. [CrossRef]
1014. Khanra, A.K.; Jung, H.C.; Hong, K.S.; Shin, K.S. Comparative property study on extruded Mg–HAP and ZM61–HAP composites. *Mater. Sci. Eng. A* **2010**, *527*, 6283–6288. [CrossRef]
1015. Gu, X.N.; Wang, X.; Li, N.; Li, L.; Zheng, Y.F.; Miao, X. Microstructure and characteristics of the metal-ceramic composite (MgCa-HA/TCP) fabricated by liquid metal infiltration. *J. Biomed. Mater. Res. B Appl. Biomater.* **2011**, *99*, 127–134. [CrossRef]
1016. Liu, D.; Zuo, Y.; Meng, W.; Chen, M.; Fan, Z. Fabrication of biodegradable nano-sized β-TCP/Mg composite by a novel melt shearing technology. *Mater. Sci. Eng. C* **2012**, *32*, 1253–1258. [CrossRef]
1017. Kumar, A.; Biswas, K.; Basu, B. On the toughness enhancement in hydroxyapatite-based composites. *Acta Mater.* **2013**, *61*, 5198–5215. [CrossRef]
1018. Wang, X.; Dong, L.H.; Li, J.T.; Ma, X.L.; Zheng, Y.F. Microstructure, mechanical property and corrosion behavior of interpenetrating (HA+β-TCP)/MgCa composite fabricated by suction casting. *Mater. Sci. Eng. C* **2013**, *33*, 4266–4273. [CrossRef]
1019. Chang, Q.; Ru, H.Q.; Chen, D.L.; Zhang, C.P.; Yang, J.L.; Hu, S.L. Interfacial reactions in Ti–Fe particles reinforced hydroxyapatite matrix composites. *Mater. Lett.* **2014**, *128*, 245–247. [CrossRef]
1020. Sunil, B.R.; Kumar, T.S.S.; Chakkingal, U.; Nandakumar, V.; Doble, M. Friction stir processing of magnesium-nanohydroxyapatite composites with controlled in vitro degradation behavior. *Mater. Sci. Eng. C* **2014**, *39*, 315–324. [CrossRef]
1021. Buyong, S.A.; Jamaludin, S.B.; Malek, R.A. Effect of beta tricalcium phosphate (β-TCP) on properties of Mg-Zn composites. *Key Eng. Mater.* **2014**, *594–595*, 203–206. [CrossRef]
1022. Arifin, A.; Sulong, A.B.; Muhamad, N.; Syarif, J.; Ramli, M.I. Material processing of hydroxyapatite and titanium alloy (HA/Ti) composite as implant materials using powder metallurgy: A review. *Mater. Des.* **2014**, *55*, 165–175. [CrossRef]
1023. Ma, X.L.; Dong, L.H.; Wang, X. Microstructure, mechanical property and corrosion behavior of co-continuous β-TCP/MgCa composite manufactured by suction casting. *Mater. Des.* **2014**, *56*, 305–312. [CrossRef]
1024. Sunil, B.R.; Kumar, T.S.S.; Chakkingal, U.; Nandakumar, V.; Doble, M. Nano-hydroxyapatite reinforced AZ31 magnesium alloy by friction stir processing: A solid state processing for biodegradable metal matrix composites. *J. Mater. Sci. Mater. Med.* **2014**, *25*, 975–988. [CrossRef]
1025. Wakily, H.; Dabbagh, A.; Abdullah, H.; Abdul Halim, N.F.; Abu Kasim, N.H. Improved thermal and mechanical properties in hydroxyapatite–titanium composites by incorporating silica-coated titanium. *Mater. Lett.* **2015**, *143*, 322–325. [CrossRef]
1026. Kuśnierczyk, K.; Basista, M. Recent advances in research on magnesium alloys and magnesium-calcium phosphate composites as biodegradable implant materials. *J. Biomater. Appl.* **2017**, *31*, 878–900. [CrossRef]

1027. Montufar, E.B.; Casas-Luna, M.; Horynová, M.; Tkachenko, S.; Fohlerová, Z.; Diaz-de-la-Torre, S.; Dvořák, K.; Čelko, L.; Kaiser, J. High strength, biodegradable and cytocompatible alpha tricalcium phosphate-iron composites for temporal reduction of bone fractures. *Acta Biomater.* **2018**, *70*, 293–303. [CrossRef]
1028. Yang, H.; Qu, X.; Lin, W.; Wang, C.; Zhu, D.; Dai, K.; Zheng, Y. In vitro and in vivo studies on zinc-hydroxyapatite composites as novel biodegradable metal matrix composite for orthopedic applications. *Acta Biomater.* **2018**, *71*, 200–214. [CrossRef]
1029. Castañeda-Vía, J.; Landauro, C.V.; Quispe-Marcatoma, J.; Champi, A.; Montalvo, F.; Delgado, L.; Tay, L.Y.; Moya, M.J.; Guillén, R.; Rumiche, F.; et al. Improvement of mechanical properties of hydroxyapatite composites reinforced with *i*-$Al_{64}Cu_{23}Fe_{13}$ quasicrystal. *J. Compos. Mater.* **2020**, *55*, 1209. [CrossRef]
1030. Peng, Q.; Bin, X.; Xuxin, H.Y.; Wang, Y.H.; Peng, Z.W.; Tang, Z.G. Facile fabrication of boronized Ti6Al4V/HA composites for loadbearing applications. *J. Alloys Compd.* **2020**, *825*, 153102. [CrossRef]
1031. Verma, V.; Saha, J.; Gautam, A.; Pal, K. Investigation on microstructure, mechanical, biocorrosion and biocompatibility behavior of nano-sized TiO_2@Al_2O_3 reinforced Mg-HAp composites. *J. Alloys Compd.* **2022**, *910*, 164866. [CrossRef]
1032. Vidal, C.; Alves, P.; Alves, M.M.; Carmezim, M.J.; Fernandes, M.H.; Grenho, L.; Inácio, P.L.; Ferreira, F.B.; Santos, T.G.; Santos, C. Fabrication of a biodegradable and cytocompatible magnesium/nanohydroxyapatite/fluorapatite composite by upward friction stir processing for biomedical applications. *J. Mech. Behav. Biomed. Mater.* **2022**, *129*, 105137. [CrossRef]
1033. Venkatesh, V.S.S.; Kalapala, P.; Deoghare, A.B. Characterization of microwave sintered aluminium composite reinforced with hydroxyapatite extracted from Rihu fish scales. *Arch. Metall. Mater.* **2023**, *68*, 617–624. [CrossRef]
1034. Jayasathyakawin, S.; Ravichandran, M.; Ismail, S.O.; Srinivasan, D. Effects of hydroxyapatite addition on the microstructure and mechanical properties of sintered magnesium matrix composites. *Mater. Today Comm.* **2023**, *35*, 105582. [CrossRef]
1035. Chatterjee, T.; Maji, M.; Paul, S.; Ghosh, M.; Pradhan, S.K.; Meikap, A.K. Microstructural, electrical and mechanical characterizations of green-synthesized biocompatible calcium phosphate nanocomposites with morphological hierarchy. *Mater. Chem. Phys.* **2023**, *296*, 127245. [CrossRef]
1036. Aggarwal, D.; Kumar, V.; Sharma, S. Effect of rare earth oxide microparticles on mechanical, corrosion, antibacterial and hemolytic behavior of Mg-hydroxyapatite composite for orthopedic applications—A preliminary in-vitro study. *J. Biomed. Mater. Res. B Appl. Biomater.* **2023**, *111*, 1232–1246. [CrossRef]
1037. Chebodaeva, V.V.; Luginin, N.A.; Rezvanova, A.E.; Svarovskaya, N.V.; Suliz, K.V.; Ivanova, L.Y.; Khimich, M.A.; Toropkov, N.E.; Glukhov, I.A.; Miller, A.A.; et al. Formation of bioresorbable Fe-Cu-hydroxyapatite composite by 3D printing. *Coatings* **2023**, *13*, 803. [CrossRef]
1038. Yao, R.; Wang, H.; Shan, R.; Liu, L.; Zhao, Y.; Sun, Y.; Yao, X.; Huang, D.; Hang, R. Biodegradable porous Zn-1Mg-3βTCP scaffold for bone defect repair: In vitro and in vivo evaluation. *J. Mater. Sci. Technol.* **2023**, *162*, 189–202. [CrossRef]
1039. Papynov, E.K.; Shichalin, O.O.; Belov, A.A.; Buravlev, I.Y.; Mayorov, V.Y.; Fedorets, A.N.; Buravleva, A.A.; Lembikov, A.O.; Gritsuk, D.V.; Kapustina, O.V.; et al. $CaSiO_3$-HAp metal-reinforced biocomposite ceramics for bone tissue engineering. *J. Funct. Biomater.* **2023**, *14*, 259. [CrossRef]
1040. Yao, R.; Zhao, Y.; Han, S.; Shan, R.; Liu, L.; Sun, Y.; Yao, X.; Wang, X.; Hang, R. Microstructure, mechanical properties, in vitro degradation behavior and in vivo osteogenic activities of Zn-1Mg-β-TCP composites for bone defect repair. *Mater. Des.* **2023**, *225*, 111494. [CrossRef]
1041. Jia, Q.; Liang, S.; Wang, Q. Effect of HA content on microstructure and properties of Ti-27Nb-17Ta-8Zr/HA composite. *Materials* **2023**, *16*, 5095. [CrossRef]
1042. Damien, C.J.; Parsons, J.R.; Benedict, J.J.; Weisman, D.S. Investigation of a hydroxyapatite and calcium sulfate composite supplemented with an osteoinductive factor. *J. Biomed. Mater. Res.* **1990**, *24*, 639–654. [CrossRef]
1043. Rauschmann, M.A.; Wichelhaus, T.A.; Stirnal, V.; Dingeldein, E.; Zichner, L.; Schnettler, R.; Alt, V. Nanocrystalline hydroxyapatite and calcium sulphate as biodegradable composite carrier material for local delivery of antibiotics in bone infections. *Biomaterials* **2005**, *26*, 2677–2684. [CrossRef]
1044. Urban, R.M.; Turner, T.M.; Hall, D.J.; Inoue, N.; Gitelis, S. Increased bone formation using calcium sulfate-calcium phosphate composite graft. *Clin. Orthop. Relat. Res.* **2007**, *459*, 110–117. [CrossRef]
1045. Rauschmann, M.A.; Vogl, T.; Verheyden, A.; Pflugmacher, R.; Werba, T.; Schmidt, S.; Hierholzer, J. Bioceramic vertebral augmentation with a calcium sulphate/hydroxyapatite composite (Cerament^{TM} SpineSupport) in vertebral compression fractures due to osteoporosis. *Eur. Spine J.* **2010**, *19*, 887–892. [CrossRef]
1046. Nilsson, M.; Zheng, M.H.; Tägil, M. The composite of hydroxyapatite and calcium sulphate: A review of preclinical evaluation and clinical applications. *Expert Rev. Med. Dev.* **2013**, *10*, 675–684. [CrossRef]
1047. Du, M.K.; Kuang, Z.D.; Ji, H.R.; Mao, K.Y. Enhanced degradation and osteogenesis of β-tricalcium phosphate/calcium sulfate composite bioceramics: The effects of phase ratio. *J. Biomater. Tissue Eng.* **2014**, *4*, 389–398. [CrossRef]
1048. Kumar, G.S.; Girija, E.K.; Thamizhavel, A.; Yokogawa, Y.; Kalkura, S.N. Synthesis and characterization of bioactive hydroxyapatite-calcite nanocomposite for biomedical applications. *J. Colloid Interf. Sci.* **2010**, *349*, 56–62. [CrossRef]
1049. Smirnov, V.V.; Goldberg, M.A.; Shvorneva, L.I.; Fadeeva, I.V.; Shibaeva, T.V.; Barinov, S.M. Synthesis of composite biomaterials in the hydroxyapatite-calcite system. *Dokl. Chem.* **2010**, *432*, 151–154. [CrossRef]
1050. Polley, C.; Distler, T.; Detsch, R.; Lund, H.; Springer, A.; Boccaccini, A.R.; Seitz, H. 3D printing of piezoelectric barium titanate-hydroxyapatite scaffolds with interconnected porosity for bone tissue engineering. *Materials* **2020**, *13*, 1773. [CrossRef]

1051. Jiao, H.; Li, Z.; Zhou, X.; Zhao, K.; Tang, Y. Study on preparation and properties of tetragonal $BaTiO_3$/HA porous scaffolds. *Mater. Sci. Eng. B* **2023**, *296*, 116703. [CrossRef]
1052. Swain, S.; Bhaskar, R.; Narayanan, K.B.; Gupta, M.K.; Sharma, S.; Dasgupta, S.; Han, S.S.; Kumar, P. Physicochemical, mechanical, dielectric and biological properties of sintered hydroxyapatite/barium titanate nanocomposites for bone regeneration. *Biomed. Mater.* **2023**, *18*, 025016. [CrossRef]
1053. Watanabe, Y.; Ikoma, T.; Suetsugu, Y.; Yamada, H.; Tamura, K.; Komatsu, Y.; Tanaka, J.; Moriyoshi, Y. The densification of zeolite/apatite composites using a pulse electric current sintering method: A long-term assurance material for the disposal of radioactive waste. *J. Eur. Ceram. Soc.* **2006**, *26*, 481–486. [CrossRef]
1054. Lahiri, D.; Singh, V.; Benaduce, A.P.; Seal, S.; Kos, L.; Agarwal, A. Boron nitride nanotube reinforced hydroxyapatite composite: Mechanical and tribological performance and in-vitro biocompatibility to osteoblasts. *J. Mech. Behav. Biomed. Mater.* **2011**, *4*, 44–56. [CrossRef]
1055. Aguirre, T.G.; Cramer, C.L.; Torres, V.P.; Hammann, T.J.; Holland, T.B.; Ma, K. Effects of the addition of boron nitride nanoplate on the fracture toughness, flexural strength and Weibull distribution of hydroxyapatite composites prepared by spark plasma sintering. *J. Mech. Behav. Biomed. Mater.* **2019**, *93*, 105–117. [CrossRef]
1056. Nathanael, A.J.; Yuvakkumar, R.; Hong, S.I.; Oh, T.H. Novel zirconium nitride and hydroxyapatite nanocomposite coating: Detailed analysis and functional properties. *ACS Appl. Mater. Interfaces* **2014**, *6*, 9850–9857. [CrossRef]
1057. Liu, Y.; Huang, J.; Li, H. Synthesis of hydroxyapatite-reduced graphite oxide nanocomposites for biomedical applications: Oriented nucleation and epitaxial growth of hydroxyapatite. *J. Mater. Chem. B* **2013**, *1*, 1826–1834. [CrossRef]
1058. Zhao, X.; Chen, X.; Gui, Z.; Zheng, J.; Yang, P.; Liu, A.; Wei, S.; Yang, Z. Carbon fiber reinforced hydroxyapatite composites with excellent mechanical properties and biological activities prepared by spark plasma sintering. *Ceram. Int.* **2020**, *46*, 27446–27456. [CrossRef]
1059. Najafinezhad, A.; Abdellahi, M.; Saber-Samandari, S.; Ghayour, H.; Khandan, A. Hydroxyapatite-M-type strontium hexaferrite: A new composite for hyperthermia applications. *J. Alloys Compd.* **2018**, *734*, 290–300. [CrossRef]
1060. Agathopoulos, S.; Tulyaganov, D.U.; Marques, P.A.A.P.; Ferro, M.C.; Fernandes, M.H.V.; Correia, R.N. The fluorapatite-anorthite system in biomedicine. *Biomaterials* **2003**, *24*, 1317–1331. [CrossRef]
1061. Khor, K.A.; Gu, Y.W.; Pan, D.; Cheang, P. Microstructure and mechanical properties of plasma sprayed HA/YSZ/Ti-6Al-4V composite coatings. *Biomaterials* **2004**, *25*, 4009–4017. [CrossRef]
1062. Jodati, H.; Evis, Z.; Tezcaner, A.; Alshemary, A.Z.; Motameni, A. 3D porous bioceramic based boron-doped hydroxyapatite/baghdadite composite scaffolds for bone tissue engineering. *J. Mech. Behav. Biomed. Mater.* **2023**, *140*, 105722. [CrossRef]
1063. Mondal, S.; Manivasagan, P.; Bharathiraja, S.; Moorthy, M.S.; Kim, H.H.; Seo, H.; Lee, K.D.; Oh, J. Magnetic hydroxyapatite: A promising multifunctional platform for nanomedicine application. *Int. J. Nanomed.* **2017**, *12*, 8389–8410. [CrossRef]
1064. Mondal, S.; Manivasagan, P.; Bharathiraja, S.; Moorthy, M.S.; Nguyen, V.T.; Kim, H.H.; Nam, S.Y.; Lee, K.D.; Oh, J. Hydroxyapatite coated iron oxide nanoparticles: A promising nanomaterial for magnetic hyperthermia cancer treatment. *Nanomaterials* **2017**, *7*, 426. [CrossRef]
1065. Adamiano, A.; Wu, V.M.; Carella, F.; Lamura, G.; Canepa, F.; Tampieri, A.; Iafisco, M.; Uskoković, V. Magnetic calcium phosphates nanocomposites for the intracellular hyperthermia of cancers of bone and brain. *Nanomedicine* **2019**, *14*, 1267–1289. [CrossRef]
1066. Das, A.; Pamu, D. A comprehensive review on electrical properties of hydroxyapatite based ceramic composites. *Mater. Sci. Eng. C* **2019**, *101*, 539–563. [CrossRef]
1067. Kalmodia, S.; Goenka, S.; Laha, T.; Lahiri, D.; Basu, B.; Balani, K. Microstructure, mechanical properties and in vitro biocompatibility of spark plasma sintered hydroxyapatite-aluminum oxide-carbon nanotube composite. *Mater. Sci. Eng. C* **2010**, *30*, 1162–1169. [CrossRef]
1068. Al-Harbi, N.; Hussein, M.A.; Al-Hadeethi, Y.; Umar, A. Cellulose acetate-hydroxyapatite-bioglass-zirconia nanocomposite particles as potential biomaterial: Synthesis, characterization and biological properties for bone application. *Eng. Sci.* **2022**, *17*, 70–82. [CrossRef]
1069. El-Mehalawy, N.; Sayed, M.; El-Anwar, E.A.A.; Soliman, A.A.F.; Naga, S.M. Preparation and characterization of bioceramic composites based on anorthite and β-TCP from dolomitic phosphate and kaolin rocks. *Mater. Chem. Phys.* **2024**, *312*, 128625. [CrossRef]
1070. Best, S.M.; Porter, A.E.; Thian, E.S.; Huang, J. Bioceramics: Past, present and for the future. *J. Eur. Ceram. Soc.* **2008**, *28*, 1319–1327. [CrossRef]
1071. de Aza, P.N.; Guitián, F.; de Aza, S. Bioeutectic: A new ceramic material for human bone replacement. *Biomaterials* **1997**, *18*, 1285–1291. [CrossRef]
1072. Huang, X.; Jiang, D.; Tan, S. Apatite formation on the surface of wollastonite/tricalcium phosphate composite immersed in simulated body fluid. *J. Biomed. Mater. Res. B Appl. Biomater.* **2004**, *69B*, 70–72. [CrossRef]
1073. Zhang, F.; Chang, J.; Lin, K.; Lu, J. Preparation, mechanical properties and in vitro degradability of wollastonite/tricalcium phosphate macroporous scaffolds from nanocomposite powders. *J. Mater. Sci. Mater. Med.* **2008**, *19*, 167–173. [CrossRef]
1074. Baudín, C.; Pena, P. Review: Tailored microstructures in the system tricalcium phosphate-wollastonite-diopside for bone regeneration scaffolds. *Open Ceram.* **2023**, *16*, 100483. [CrossRef]

1075. Sugiura, Y.; Ono, F.; Nohara, M.; Takechi, A.; Kutara, K.; Kanda, T.; Saito, Y.; Yamada, E.; Oowada, K.; Endo, T.; et al. Inorganic silica hybrid octacalcium phosphate bone substitute: Harmonics to acceleration in biological metabolism and its curing process. *Materialia* **2023**, *28*, 101771. [CrossRef]
1076. Zhao, S.; Zhou, Z.; Wu, J.; Wang, S.; Guo, X.; Zhang, Q. Preparation and characterization of a novel hydroxyapatite-wollastonite/silk fibroin composite. *J. Compos. Mater.* **2012**, *46*, 1571–1581. [CrossRef]
1077. Greish, Y.E.; Brown, P.W. Characterization of wollastonite-reinforced HAp-Ca polycarboxylate composites. *J. Biomed. Mater. Res.* **2001**, *55*, 618–628, Erratum in *J. Biomed. Mater. Res.* **2001**, *56*, 459. [CrossRef]
1078. Greish, Y.E.; Brown, P.W. Characterization of bioactive glass-reinforced HAP-polymer composites. *J. Biomed. Mater. Res.* **2000**, *52*, 687–694. [CrossRef]
1079. Ren, Y.; Kong, W.; Liu, Y.; Yang, X.; Xu, X.; Qiang, L.; Mi, X.; Zhang, C.; Niu, H.; Wang, C.; et al. Photocurable 3D-printed PMBG/TCP scaffold coordinated with PTH (1-34) bidirectionally regulates bone homeostasis to accelerate bone regeneration. *Adv. Healthc. Mater.* **2023**, *12*, 2300292. [CrossRef]
1080. Radev, L.; Hristov, V.; Samuneva, B.; Ivanova, D. Organic/inorganic bioactive materials. Part II: In vitro bioactivity of collagen-calcium phosphate silicate/wollastonite hybrids. *Cent. Eur. J. Chem.* **2009**, *7*, 711–720. [CrossRef]
1081. Radev, L.; Hristov, V.; Fernandes, M.H.V.; Salvado, I.M.M. Organic/inorganic bioactive materials part IV: In vitro assessment of bioactivity of gelatin-calcium phosphate silicate/wollastonite hybrids. *Cent. Eur. J. Chem.* **2010**, *8*, 278–284. [CrossRef]
1082. Kangasniemi, I.; de Groot, K.; Wolke, J.; Andersson, O.; Luklinska, Z.; Becht, J.G.M.; Lakkisto, M.; Yli-Urpo, A. The stability of hydroxyapatite in an optimized bioactive glass matrix at sintering temperatures. *J. Mater. Sci. Mater. Med.* **1991**, *2*, 133–137. [CrossRef]
1083. Kangasniemi, I.M.O.; de Groot, K.; Becht, J.G.M.; Yli-Urpo, A. Preparation of dense hydroxylapatite or rhenanite containing bioactive glass composites. *J. Biomed. Mater. Res.* **1992**, *26*, 663–674. [CrossRef]
1084. Maruno, S.; Ban, S.; Wang, Y.F.; Iwata, H.; Itoh, H. Properties of functionally gradient composite consisting of hydroxyapatite containing glass coated titanium and characters for bioactive implant. *J. Ceram. Soc. Jpn.* **1992**, *100*, 362–367. [CrossRef]
1085. Bellucci, D.; Sola, A.; Cannillo, V. Hydroxyapatite and tricalcium phosphate composites with bioactive glass as second phase: State of the art and current applications. *J. Biomed. Mater. Res. A* **2016**, *104A*, 1030–1056. [CrossRef]
1086. Karadjian, M.; Essers, C.; Tsitlakidis, S.; Reible, B.; Moghaddam, A.; Boccaccini, A.R.; Westhauser, F. Biological properties of calcium phosphate bioactive glass composite bone substitutes: Current experimental evidence. *Int. J. Mol. Sci.* **2019**, *20*, 305. [CrossRef]
1087. Angioni, D.; Orrù, R.; Cao, G.; Garroni, S.; Bellucci, D.; Cannillo, V. Bioactivity enhancement by a ball milling treatment in novel bioactive glass-hydroxyapatite composites produced by spark plasma sintering. *J. Eur. Ceram. Soc.* **2023**, *43*, 1220–1229. [CrossRef]
1088. Angioni, D.; Orrù, R.; Cao, G.; Garroni, S.; Bellucci, D.; Cannillo, V. Recent advances on innovative bioactive glass-hydroxyapatite composites for bone tissue applications: Processing, mechanical properties and biological performance. *J. Eur. Ceram. Soc.* **2023**, *43*, 7688–7696. [CrossRef]
1089. Piccirillo, C.; Moreira, I.S.; Novais, R.M.; Fernandes, A.J.S.; Pullar, R.C.; Castro, P.M.L. Biphasic apatite-carbon materials derived from pyrolysed fish bones for effective adsorption of persistent pollutants and heavy metals. *J. Environ. Chem. Eng.* **2015**, *5*, 4884–4894. [CrossRef]
1090. Piccirillo, C. Preparation, characterisation and applications of bone char, a food waste-derived sustainable material: A review. *J. Environ. Manag.* **2023**, *339*, 117896. [CrossRef]
1091. White, A.A.; Best, S.M.; Kinloch, I.A. Hydroxyapatite-carbon nanotube composites for biomedical applications: A review. *Int. J. Appl. Ceram. Technol.* **2007**, *4*, 1–13. [CrossRef]
1092. Kharisov, B.I.; Kharissova, O.V.; González, L.T.; Méndez, Y.P.; Uflyand, I.E.; de la Fuente, I.G. Hydroxyapatite composites with carbon allotropes: Preparation, properties and applications. *Particuology* **2024**, *88*, 239–265. [CrossRef]
1093. Zhao, L.P.; Gao, L. Novel in situ synthesis of MWNT-hydroxyapatite composites. *Carbon* **2004**, *42*, 423–460. [CrossRef]
1094. Wei, Q.; Yang, X.P.; Chen, G.Q.; Tang, J.T.; Deng, X.L. The ultrasonic assisted synthesis of nano-hydroxyapatite and MWNT/hydroxyapatite composites. *New Carbon Mater.* **2005**, *20*, 164–170.
1095. Bai, Y.; Neupane, M.P.; Park, I.S.; Lee, M.H.; Bae, T.S.; Watari, F.; Uo, M. Electrophoretic deposition of carbon nanotubes-hydroxyapatite nanocomposites on titanium substrate. *Mater. Sci. Eng. C* **2010**, *30*, 1043–1049. [CrossRef]
1096. Shin, U.S.; Yoon, I.K.; Lee, G.S.; Jang, W.C.; Knowles, J.C.; Kim, H.W. Carbon nanotubes in nanocomposites and hybrids with hydroxyapatite for bone replacements. *J. Tissue Eng.* **2011**, *2011*, 674287. [CrossRef]
1097. Lahiri, D.; Ghosh, S.; Agarwal, A. Carbon nanotube reinforced hydroxyapatite composite for orthopedic application: A review. *Mater. Sci. Eng. C* **2012**, *32*, 1727–1758. [CrossRef]
1098. Kobayashi, S.; Kawai, W. Development of carbon nanofiber reinforced hydroxyapatite with enhanced mechanical properties. *Compos. A* **2007**, *38*, 114–123. [CrossRef]
1099. Gunawan, G.; Sopyan, I.; Nurfaezah, S.; 'Ammar, M. Development of triphasic calcium phosphate–carbon nanotubes (HA/TCP-CNT) composite: A preliminary study. *Key Eng. Mater.* **2013**, *531–532*, 258–261. [CrossRef]
1100. Balani, K.; Anderson, R.; Laha, T.; Andara, M.; Tercero, J.; Crumpler, E.; Agarwal, A. Plasma-sprayed carbon nanotube reinforced hydroxyapatite coatings and their interaction with human osteoblasts in vitro. *Biomaterials* **2007**, *28*, 618–624. [CrossRef]
1101. Chen, Y.; Gan, C.H.; Zhang, T.H.; Yu, G.; Bai, P.; Kaplan, A. Laser-surface-alloyed carbon nanotubes reinforced hydroxyapatite composite coatings. *Appl. Phys. Lett.* **2005**, *86*, 251905. [CrossRef]

1102. Chen, Y.; Zhang, T.H.; Gan, C.H.; Yu, G. Wear studies of hydroxyapatite composite coating reinforced by carbon nanotubes. *Carbon* **2007**, *45*, 998–1004. [CrossRef]
1103. Chen, Y.; Zhang, Y.Q.; Zhang, T.H.; Gan, C.H.; Zheng, C.Y.; Yu, G. Carbon nanotube reinforced hydroxyapatite composite coatings produced through laser surface alloying. *Carbon* **2006**, *44*, 37–45. [CrossRef]
1104. Xu, J.L.; Khor, K.A.; Sui, J.J.; Chen, W.N. Preparation and characterization of a novel hydroxyapatite/carbon nanotubes composite and its interaction with osteoblast-like cells. *Mater. Sci. Eng. C* **2009**, *29*, 44–49. [CrossRef]
1105. Mukherjee, S.; Kundu, B.; Sen, S.; Chanda, A. Improved properties of hydroxyapatite-carbon nanotube biocomposite: Mechanical, in vitro bioactivity and biological studies. *Ceram. Int.* **2014**, *40*, 5635–5643. [CrossRef]
1106. Hooshmand, T.; Abrishamchian, A.; Najafi, F.; Mohammadi, M.; Najafi, H.; Tahriri, M. Development of sol-gel-derived multi-wall carbon nanotube/hydroxyapatite nanocomposite powders for bone substitution. *J. Compos. Mater.* **2014**, *48*, 483–489. [CrossRef]
1107. Lee, H.H.; Shin, U.S.; Won, J.E.; Kim, H.W. Preparation of hydroxyapatite-carbon nanotube composite nanopowders. *Mater. Lett.* **2010**, *65*, 208–211. [CrossRef]
1108. White, A.A.; Kinloch, I.A.; Windle, A.H.; Best, S.M. Optimization of the sintering atmosphere for high-density hydroxyapatite-carbon nanotube composites. *J. R. Soc. Interface* **2010**, *7* (Suppl. S5), S529–S539. [CrossRef]
1109. Siqueira, I.A.W.B.; Oliveira, C.A.G.S.; Zanin, H.; Grinet, M.A.V.M.; Granato, A.E.C.; Porcionatto, M.A.; Marciano, F.R.; Lobo, A.O. Bioactivity behaviour of nano-hydroxyapatite/freestanding aligned carbon nanotube oxide composite. *J. Mater. Sci. Mater. Med.* **2015**, *26*, 1–10. [CrossRef]
1110. Figueroa-Rosales, E.X.; Martínez-Juárez, J.; García-Díaz, E.; Hernández-Cruz, D.; Sabinas-Hernández, S.A.; Robles-Águila, M.J. Photoluminescent properties of hydroxyapatite and hydroxyapatite/multi-walled carbon nanotube composites. *Crystals* **2021**, *11*, 832. [CrossRef]
1111. Ding, Y.; Liu, J.; Jin, X.; Lu, H.; Shen, G.; Yu, R. Poly-L-lysine/hydroxyapatite/carbon nanotube hybrid nanocomposite applied for piezoelectric immunoassay of carbohydrate antigen 19-9. *Analyst* **2008**, *133*, 184–190. [CrossRef]
1112. Liu, L.; Zhang, Y.; Ma, S.; Zhu, S.; Wu, S.; Wei, B.; Yang, G. Preparation and characterization of high-strength and high-modulus multi-walled carbon nanotube/hydroxyapatite/carbon fiber/polyetheretherketone composites. *Appl. Sci.* **2024**, *14*, 1723. [CrossRef]
1113. Slosarcyk, A.; Klisch, M.; Blazewicz, M.; Piekarczyk, J.; Stobierski, L.; Rapacz-Kmita, A. Hot pressed hydroxyapatite-carbon fibre composites. *J. Eur. Ceram. Soc.* **2000**, *20*, 1397–1402. [CrossRef]
1114. Dorner-Reisel, A.; Berroth, K.; Neubauer, R.; Nestler, K.; Marx, G.; Scislo, M.; Müller, E.; Slosarcyk, A. Unreinforced and carbon fibre reinforced hydroxyapatite: Resistance against microabrasion. *J. Eur. Ceram. Soc.* **2004**, *24*, 2131–2139. [CrossRef]
1115. Fu, T.; Zhao, J.L.; Wei, J.H.; Han, Y.; Xu, K.W. Preparation of carbon fiber fabric reinforced hydroxyapatite/epoxy composite by RTM processing. *J. Mater. Sci.* **2004**, *39*, 1411–1413. [CrossRef]
1116. Pecheva, E.; Pramatarova, L.; Hikov, T.; Fingarova, D.; Tanaka, Y.; Sakamoto, H.; Doi, H.; Tsutsumi, Y.; Hanawa, T. Apatite-nanodiamond composite as a functional coating of stainless steel. *Surf. Interf. Anal.* **2010**, *42*, 475–480. [CrossRef]
1117. Chen, X.; Zhang, B.; Gong, Y.; Zhou, P.; Li, H. Mechanical properties of nanodiamond-reinforced hydroxyapatite composite coatings deposited by suspension plasma spraying. *Appl. Surf. Sci.* **2018**, *439*, 60–65. [CrossRef]
1118. Azhari, A.; Toyserkani, E.; Villain, C. Additive manufacturing of graphene-hydroxyapatite nanocomposite structures. *Int. J. Appl. Ceram. Technol.* **2015**, *12*, 8–17. [CrossRef]
1119. Basirun, W.J.; Nasiri-Tabrizi, B.; Baradaran, S. Overview of hydroxyapatite–graphene nanoplatelets composite as bone graft substitute: Mechanical behavior and in-vitro biofunctionality. *Crit. Rev. Solid State Mater. Sci.* **2018**, *43*, 177–212. [CrossRef]
1120. Djordjevic, A.; Ignjatovic, N.; Seke, M.; Jovic, D.; Uskokovic, D.; Rakocevic, Z. Synthesis and characterization of hydroxyapatite/fullerenol nanocomposites. *J. Nanosci. Nanotechnol.* **2015**, *15*, 1538–1542. [CrossRef]
1121. Gao, Q.; Zhang, L.; Chen, Y.; Nie, H.; Zhang, B.; Li, H. Interfacial design and construction of carbon fiber composites by strongly bound hydroxyapatite nanobelt-carbon nanotubes for biological applications. *ACS Appl. Bio Mater.* **2023**, *6*, 874–882. [CrossRef]
1122. Egorov, A.; Smirnov, V.; Shvorneva, L.; Kutsev, S.; Barinov, S. High-temperature hydroxyapatite-titanium interaction. *Inorg. Mater.* **2010**, *46*, 168–171. [CrossRef]
1123. You, C.; Bi, Y.; Chen, M.F.; Sun, Y.; Liu, D.B. Effect of the addition of nano-β-TCP on the microstructure of Mg-Zn-Zr alloy. *Adv. Mater. Res.* **2012**, *535–537*, 259–263. [CrossRef]
1124. Monma, H. Tricalcium phosphate ceramics complexed with hydroxyapatite. *J. Ceram. Soc. Jpn.* **1987**, *96*, 60–64. [CrossRef]
1125. Farzadi, A.; Solati-Hashjin, M.; Bakhshi, F.; Aminian, A. Synthesis and characterization of hydroxyapatite/β-tricalcium phosphate nanocomposites using microwave irradiation. *Ceram. Int.* **2011**, *37*, 65–71. [CrossRef]
1126. Angioni, D.; Orrù, R.; Cao, G.; Garroni, S.; Ricci, P.C.; Manukyan, K.V. Combustion synthesis and spark plasma sintering of apatite-tricalcium phosphate nanocomposites. *Ceram. Int.* **2023**, *49*, 26825–26833. [CrossRef]
1127. Zerankeshi, M.M.; Mofakhami, S.; Salahinejad, E. 3D porous HA/TCP composite scaffolds for bone tissue engineering. *Ceram. Int.* **2022**, *48*, 22647–22663. [CrossRef]
1128. Wu, C.C.; Huang, S.T.; Tseng, T.W.; Rao, Q.L.; Lin, H.C. FT-IR and XRD investigations on sintered fluoridated hydroxyapatite composites. *J. Mol. Struct.* **2010**, *979*, 72–76. [CrossRef]
1129. Suchanek, W.; Yashima, M.; Kakihana, M.; Yoshimura, M. Processing and mechanical properties of hydroxyapatite reinforced with hydroxyapatite whiskers. *Biomaterials* **1996**, *17*, 1715–1723. [CrossRef]

1130. Suchanek, W.; Yashima, M.; Kakihana, M.; Yoshimura, M. Hydroxyapatite/hydroxyapatite-whisker composites without sintering additives: Mechanical properties and microstructural evolution. *J. Am. Ceram. Soc.* **1997**, *80*, 2805–2813. [CrossRef]
1131. Kaito, T.; Mukai, Y.; Nishikawa, M.; Ando, W.; Yoshikawa, H.; Myoui, A. Dual hydroxyapatite composite with porous and solid parts: Experimental study using canine lumbar interbody fusion model. *J. Biomed. Mater. Res. B Appl. Biomater.* **2006**, *78B*, 378–384. [CrossRef]
1132. Farrokhi-Rad, M. Electrophoretic deposition of hydroxyapatite fiber reinforced hydroxyapatite matrix nanocomposite coatings. *Surf. Coat. Technol.* **2017**, *329*, 155–162. [CrossRef]
1133. Ma, C.; Zeng, Q.; Yu, L.; Yu, S.; Song, J.; Ma, Y.; Dong, X. Preparation and characterization of 3D printed hydroxyapatite-whisker-strengthened hydroxyapatite scaffold coated with biphasic calcium phosphate. *Chin. J. Mech. Eng. Addit. Manuf. Front.* **2023**, *2*, 100097. [CrossRef]
1134. Ramay, H.R.; Zhang, M. Biphasic calcium phosphate nanocomposite porous scaffolds for load-bearing bone tissue engineering. *Biomaterials* **2004**, *21*, 5171–5180. [CrossRef]
1135. Kobayashi, S.; Murakoshi, T. Characterization of mechanical properties and bioactivity of hydroxyapatite/β-tricalcium phosphate composites. *Adv. Compos. Mater.* **2014**, *23*, 163–177. [CrossRef]
1136. Sasaki, K.; Ninomiya, Y.; Takechi, M.; Tsuru, K.; Ishikawa, K.; Shigeishi, H.; Ohta, K.; Aikawa, T. Physical properties and antimicrobial release ability of gentamicin-loaded apatite cement/α-TCP composites: An in vitro study. *Materials* **2023**, *16*, 995. [CrossRef]
1137. Wang, Z.; Li, Q.; Ren, S.; Zhang, H.; Chen, J.; Li, A.; Chen, Y. Composite monetite/amorphous calcium phosphate bone cement promotes bone regeneration. *Ceram. Int.* **2023**, *49*, 7888–7904. [CrossRef]
1138. Matsumoto, K.; Tsuru, K.; Kawachi, G.; Maruta, M.; Matsuya, S.; Takahashi, I.; Ishikawa, K. Reinforcement of carbonate apatite bone substitutes with carbonate apatite by Ca salt introduction. *J. Ceram. Soc. Jpn.* **2010**, *118*, 521–524. [CrossRef]
1139. Available online: https://en.wikipedia.org/wiki/3D_printing (accessed on 1 May 2024).
1140. Yan, M.; Awad, H.A. Optimizing rheological properties for printability: Low-temperature extrusion 3D printing of hydroxyapatite-polycaprolactone mixture inks for bone tissue engineering. *Front. Mater.* **2023**, *10*, 1239692. [CrossRef]
1141. Zhang, B.; Nguyen, A.K.; Narayan, R.J.; Huang, J. Direct ink writing of vancomycin-loaded polycaprolactone/polyethylene oxide/ hydroxyapatite 3D scaffolds. *J. Am. Ceram. Soc.* **2022**, *105*, 1821–1840. [CrossRef]
1142. Jahangir, S.; Vecstaudza, J.; Augurio, A.; Canciani, E.; Stipniece, L.; Locs, J.; Alini, M.; Serra, T. Cell-laden 3D printed GelMA/HAp and THA hydrogel bioinks: Development of osteochondral tissue-like bioinks. *Materials* **2023**, *16*, 7214. [CrossRef]
1143. Wu, X.; Chen, K.; Zhang, D.; Xu, L.; Yang, X. Study on the technology and properties of 3D bioprinting SF/GT/n-HA composite scaffolds. *Mater. Lett.* **2019**, *238*, 89–92. [CrossRef]
1144. Adhikari, J.; Perwez, M.S.; Das, A.; Saha, P. Development of hydroxyapatite reinforced alginate–chitosan based printable biomaterial-ink. *Nano-Struct. Nano-Objects* **2021**, *25*, 100630. [CrossRef]
1145. Rajabi, M.; Cabral, J.D.; Saunderson, S.; Gould, M.; Ali, M.A. Development and optimisation of hydroxyapatite-polyethylene glycol diacrylate hydrogel inks for 3D printing of bone tissue engineered scaffolds. *Biomed. Mater.* **2023**, *18*, 065009. [CrossRef]
1146. Tajvar, S.; Hadjizadeh, A.; Samandar, S.S. Development of bioinspired biphasic calcium phosphate inks for manufacturing bone scaffolds by robocasting. *3D Print. Addit. Manuf.* **2024**. *early view*. [CrossRef]
1147. Tolmacheva, N.; Bhattacharyya, A.; Noh, I. Calcium phosphate biomaterials for 3D bioprinting in bone tissue engineering. *Biomimetics* **2024**, *9*, 95. [CrossRef]
1148. Werner, J.; Linner-Krcmar, B.; Friess, W.; Greil, P. Mechanical properties and in vitro cell compatibility of hydroxyapatite ceramics with graded pore structure. *Biomaterials* **2002**, *23*, 4285–4294. [CrossRef]
1149. Hsu, Y.H.; Turner, I.G.; Miles, A.W. Fabrication of porous bioceramics with porosity gradients similar to the bimodal structure of cortical and cancellous bone. *J. Mater. Sci. Mater. Med.* **2007**, *18*, 2251–2256. [CrossRef]
1150. Macchetta, A.; Turner, I.G.; Bowen, C.R. Fabrication of HA/TCP scaffolds with a graded and porous structure using a camphene-based freeze-casting method. *Acta Biomater.* **2009**, *5*, 1319–1327. [CrossRef]
1151. Watari, F.; Yokoyama, A.; Saso, F.; Uo, M.; Kawasaki, T. Fabrication and properties of functionally graded dental implant. *Compos. B* **1997**, *28B*, 5–11. [CrossRef]
1152. Watari, F.; Yokoyama, A.; Omori, M.; Hirai, T.; Kondo, H.; Uo, M.; Kawasaki, T. Biocompatibility of materials and development to functionally graded implant for bio-medical application. *Compos. Sci. Technol.* **2004**, *64*, 893–908. [CrossRef]
1153. Chu, C.; Zhu, J.; Yin, Z.; Lin, P. Structure optimization and properties of hydroxyapatite-Ti symmetrical functionally graded biomaterial. *Mater. Sci. Eng. A* **2001**, *316*, 205–210. [CrossRef]
1154. Chu, C.; Zhu, J.; Yin, Z.; Lin, P. Optimal design and fabrication of hydroxyapatite-Ti asymmetrical functionally graded biomaterial. *Mater. Sci. Eng. A* **2003**, *348*, 244–250. [CrossRef]
1155. Bai, X.; More, K.; Rouleau, C.M.; Rabiei, A. Functionally graded hydroxyapatite coatings doped with antibacterial components. *Acta Biomater.* **2010**, *6*, 2264–2273. [CrossRef]
1156. Inagaki, M.; Yokogawa, Y.; Kameyama, T. Effects of plasma gas composition on bond strength of hydroxyapatite/titanium composite coatings prepared by rf-plasma spraying. *J. Eur. Ceram. Soc.* **2006**, *26*, 495–499. [CrossRef]
1157. Pei, X.; Wang, J.; Wan, Q.; Kang, L.; Xiao, M.; Bao, H. Functionally graded carbon nanotubes/hydroxyapatite composite coating by laser cladding. *Surf. Coat. Technol.* **2011**, *205*, 4380–4387. [CrossRef]

1158. Boanini, E.; Torricelli, P.; Sima, F.; Axente, E.; Fini, M.; Mihailescu, I.N.; Bigi, A. Strontium and zoledronate hydroxyapatites graded composite coatings for bone prostheses. *J. Colloid Interf. Sci.* **2015**, *448*, 1–7. [CrossRef]
1159. Liu, C.; Han, Z.; Czernuszka, J.T. Gradient collagen/nanohydroxyapatite composite scaffold: Development and characterization. *Acta Biomater.* **2009**, *5*, 661–669. [CrossRef]
1160. Jamuna-Thevi, K.; Saarani, N.N.; Kadir, M.R.A.; Hermawan, H. Triple-layered PLGA/nanoapatite/lauric acid graded composite membrane for periodontal guided bone regeneration. *Mater. Sci. Eng. C* **2014**, *43*, 253–263. [CrossRef]
1161. Erisken, C.; Kalyon, D.M.; Wang, H. Functionally graded electrospun polycaprolactone and β-tricalcium phosphate nanocomposites for tissue engineering applications. *Biomaterials* **2008**, *29*, 4065–4073. [CrossRef]
1162. Nindhia, T.G.T.; Koyoshi, Y.; Kaneko, A.; Sawada, H.; Ohta, M.; Hirai, S.; Uo, M. Hydroxyapatite-silk functionally graded material by pulse electric current sintering. *Trends Biomater. Artif. Organs* **2008**, *22*, 25–29.
1163. Ban, S.; Hasegawa, J.; Maruno, S. Fabrication and properties of functionally gradient bioactive composites comprising hydroxyapatite containing glass coated titanium. *Mater. Sci. Forum* **1999**, *308–311*, 350–355. [CrossRef]
1164. Stojanovic, D.; Jokic, B.; Veljovic, D.; Petrovic, R.; Uskokovic, P.S.; Janackovic, D. Bioactive glass-apatite composite coating for titanium implant synthesized by electrophoretic deposition. *J. Eur. Ceram. Soc.* **2007**, *27*, 1595–1599. [CrossRef]
1165. Wong, L.H.; Tio, B.; Miao, X. Functionally graded tricalcium phosphate/fluoroapatite composites. *Mater. Sci. Eng. C* **2002**, *20*, 111–115. [CrossRef]
1166. Afzal, M.A.F.; Kesarwani, P.; Reddy, K.M.; Kalmodia, S.; Basu, B.; Balani, K. Functionally graded hydroxyapatite-alumina-zirconia biocomposite: Synergy of toughness and biocompatibility Mater. *Sci. Eng. C* **2012**, *32*, 1164–1173. [CrossRef]
1167. Kuffner, B.H.B.; Capellato, P.; Ribeiro, L.M.S.; Sachs, D.; Silva, G. Production and characterization of a 316L stainless steel/β-TCP biocomposite using the functionally graded materials (FGMs) technique for dental and orthopedic applications. *Metals* **2021**, *11*, 1923. [CrossRef]
1168. Okazaki, M.; Miake, Y.; Tohda, H.; Yanagisawa, T.; Matsumoto, T.; Takahashi, J. Functionally graded fluoridated apatites. *Biomaterials* **1999**, *20*, 1421–1426. [CrossRef]
1169. Okazaki, M.; Takahashi, J. Synthesis of functionally graded CO_3 apatite as surface biodegradable crystals. *Biomaterials* **1999**, *20*, 1073–1078. [CrossRef]
1170. Peltola, T.; Patsi, M.; Rahiala, H.; Kangasniemi, I.; Yli-Urpo, A. Calcium phosphate induction by sol-gel-derived titania coatings on titanium substrates in vitro. *J. Biomed. Mater. Res.* **1998**, *41*, 504–510. [CrossRef]
1171. Heilmann, F.; Standard, O.C.; Müller, F.A.; Hoffman, M. Development of graded hydroxyapatite/$CaCO_3$ composite structures for bone ingrowth. *J. Mater. Sci. Mater. Med.* **2007**, *18*, 1817–1824. [CrossRef]
1172. Katti, K.S. Biomaterials in total joint replacement. *Colloid Surface B* **2004**, *39*, 133–142. [CrossRef]
1173. Cavalcanti, A.; Shirinzadeh, B.; Zhang, M.; Kretly, L.C. Nanorobot hardware architecture for medical defense. *Sensors* **2008**, *8*, 2932–2958. [CrossRef]
1174. Zhang, H.; Xu, J.J.; Chen, H.Y. Electrochemically deposited 2D nanowalls of calcium phosphate-PDDA on a glassy carbon electrode and their applications in biosensing. *J. Phys. Chem. C* **2007**, *111*, 16564–16570. [CrossRef]
1175. Ding, Y.; Liu, J.; Wang, H.; Shen, G.; Yu, R. A piezoelectric immunosensor for the detection of α-fetoprotein using an interface of gold/hydroxyapatite hybrid nanomaterial. *Biomaterials* **2007**, *28*, 2147–2154. [CrossRef]
1176. López, M.S.P.; Tamimi, F.; López-Cabarcos, E.; López-Ruiz, B. Highly sensitive amperometric biosensor based on a biocompatible calcium phosphate cement. *Biosens. Bioelectron.* **2009**, *24*, 2574–2579. [CrossRef]
1177. Wang, B.; Zhang, J.J.; Pan, Z.Y.; Tao, X.Q.; Wang, H.S. A novel hydrogen peroxide sensor based on the direct electron transfer of horseradish peroxidase immobilized on silica-hydroxyapatite hybrid film. *Biosens. Bioelectron.* **2009**, *24*, 1141–1145. [CrossRef]
1178. Lu, L.; Zhang, L.; Zhang, X.; Huan, S.; Shen, G.; Yu, R. A novel tyrosinase biosensor based on hydroxyapatite-chitosan nanocomposite for the detection of phenolic compounds. *Anal. Chim. Acta* **2010**, *665*, 146–151. [CrossRef]
1179. Huixia, L.; Yong, L.; Lanlan, L.; Yanni, T.; Qing, Z.; Kun, L. Development of ammonia sensors by using conductive polymer/hydroxyapatite composite materials. *Mater. Sci. Eng. C* **2016**, *59*, 438–444. [CrossRef]
1180. Ajab, H.; Dennis, J.O.; Abdullah, M.A. Synthesis and characterization of cellulose and hydroxyapatite-carbon electrode composite for trace plumbum ions detection and its validation in blood serum. *Int. J. Biol. Macromol.* **2018**, *113*, 376–385. [CrossRef]
1181. Mirzajani, R.; Karimi, S. Preparation of γ-Fe_2O_3/hydroxyapatite/Cu (II) magnetic nanocomposite and its application for electrochemical detection of metformin in urine and pharmaceutical samples. *Sens. Actuat. B-Chem.* **2018**, *270*, 405–416. [CrossRef]
1182. Anitta, S.; Sekar, C. HAP-TiO_2 nanocomposites based electrochemical sensor for selective and simultaneous detection of para-aminohippuric acid and uric acid. *Microchem. J.* **2022**, *181*, 107704. [CrossRef]
1183. Pompapathi, K.; Anantharaju, K.S.; Surendra, B.S.; Meena, S.; Uma, B.; Chowdhury, A.P.; Murthy, H.C.A. Synergistic effect of a $Bi_2Zr_2O_7$ and hydroxyapatite composite: Organic pollutant remediation, antibacterial and electrochemical sensing applications. *RSC Adv.* **2023**, *13*, 28198–28210. [CrossRef]
1184. Hartati, Y.W.; Devi, M.J.; Irkham, N.; Zulqaidah, S.; Noviyanti, A.R.; Rochani, S.; Topkaya, S.N.; Einaga, Y. Electrochemical investigation of hydroxyapatite–lanthanum strontium cobalt ferrite composites (HA–LSCF) for SARS-CoV-2 aptasensors. *RSC Adv.* **2023**, *13*, 20209–20216.
1185. Wypych, G. *Handbook of Fillers*, 3rd ed.; ChemTec Publishing: New York, NY, USA, 2009; p. 800.
1186. Almora-Barrios, N.; de Leeuw, N.H. A density functional theory study of the interaction of collagen peptides with hydroxyapatite surfaces. *Langmuir* **2010**, *26*, 14535–14542. [CrossRef]

1187. Zhang, H.P.; Lu, X.; Leng, Y.; Fang, L.; Qu, S.; Feng, B.; Weng, J.; Wang, J. Molecular dynamics simulations on the interaction between polymers and hydroxyapatite with and without coupling agents. *Acta Biomater.* **2009**, *5*, 1169–1181. [CrossRef]
1188. Wei, Q.; Wang, Y.; Chai, W.; Zhang, Y.; Chen, X. Molecular dynamics simulation and experimental study of the bonding properties of polymer binders in 3D powder printed hydroxyapatite bioceramic bone scaffolds. *Ceram. Int.* **2017**, *43*, 13702–13709. [CrossRef]
1189. Rhee, S.H.; Lee, J.D.; Tanaka, J. Nucleation of hydroxyapatite crystal through chemical interaction with collagen. *J. Am. Ceram. Soc.* **2000**, *83*, 2890–2892. [CrossRef]
1190. Lin, X.; Li, X.; Fan, H.; Wen, X.; Lu, J.; Zhang, X. In situ synthesis of bone-like apatite/collagen nano-composite at low temperature. *Mater. Lett.* **2004**, *58*, 3569–3572. [CrossRef]
1191. Zhang, W.; Liao, S.S.; Cui, F.Z. Hierarchical self-assembly of nanofibrils in mineralized collagen. *Chem. Mater.* **2003**, *15*, 3221–3226. [CrossRef]
1192. Liu, Q.; de Wijn, J.R.; van Blitterswijk, C.A. Covalent bonding of PMMA, PBMA and poly(HEMA) to hydroxyapatite particles. *J. Biomed. Mater. Res.* **1998**, *40*, 257–263. [CrossRef]
1193. Li, J.; Chen, Y.P.; Yin, Y.; Yao, F.; Yao, K. Modulation of nano-hydroxyapatite size via formation on chitosan-gelatin network film in situ. *Biomaterials* **2007**, *28*, 781–790. [CrossRef]
1194. Zhou, S.; Zheng, X.; Yu, X.; Wang, J.; Weng, J.; Li, X.; Feng, B.; Yin, M. Hydrogen bonding interaction of poly(D,L-lactide)/hydroxyapatite nanocomposites. *Chem. Mater.* **2007**, *19*, 247–253. [CrossRef]
1195. Ficai, A.; Andronescu, E.; Ghitulica, C.; Voicu, G.; Trandafir, V.; Manzu, D.; Ficai, M.; Pall, S. Collagen/hydroxyapatite interactions in composite biomaterials. *Mater. Plast.* **2009**, *46*, 11–15.
1196. Li, J.; Dou, Y.; Yang, J.; Yin, Y.; Zhang, H.; Yao, F.; Wang, H.; Yao, K. Surface characterization and biocompatibility of micro- and nano-hydroxyapatite/chitosan-gelatin network films. *Mater. Sci. Eng. C* **2009**, *29*, 1207–1215. [CrossRef]
1197. Danilchenko, S.N.; Kalinkevich, O.V.; Kuznetsov, V.N.; Kalinkevich, A.N.; Kalinichenko, T.G.; Poddubny, I.N.; Starikov, V.V.; Sklyar, A.M.; Sukhodub, L.F. Thermal transformations of the mineral component of composite biomaterials based on chitosan and apatite. *Cryst. Res. Technol.* **2010**, *45*, 685–691. [CrossRef]
1198. Popescu, L.M.; Rusti, C.F.; Piticescu, R.M.; Buruiana, T.; Valero, T.; Kintzios, S. Synthesis and characterization of acid polyurethane–hydroxyapatite composites for biomedical applications. *J. Compos. Mater.* **2013**, *47*, 603–612. [CrossRef]
1199. Ryabenkova, Y.; Jadav, N.; Conte, M.; Hippler, M.F.; Reeves-McLaren, N.; Coates, P.D.; Twigg, P.; Paradkar, A. Mechanism of hydrogen-bonded complex formation between ibuprofen and nanocrystalline hydroxyapatite. *Langmuir* **2017**, *33*, 2965–2976. [CrossRef]
1200. Sanchez, A.G.; Prokhorov, E.; Luna-Barcenas, G.; Mora-García, A.G.; Kovalenko, Y.; Rivera-Muñoz, E.M.; Raucci, M.G.; Buonocore, G. Chitosan-hydroxyapatite nanocomposites: Effect of interfacial layer on mechanical and dielectric properties. *Mater. Chem. Phys.* **2018**, *217*, 151–159. [CrossRef]
1201. Zarif, M.E.; Bita, B.; Yehia-Alexe, S.A.; Negut, I.; Groza, A. Spectral analysis of strontium-doped calcium phosphate/chitosan composite films. *Polymers* **2023**, *15*, 4245. [CrossRef]
1202. Boanini, E.; Gazzano, M.; Rubini, K.; Bigi, A. Composite nanocrystals provide new insight on alendronate interaction with hydroxyapatite structure. *Adv. Mater.* **2007**, *19*, 2499–2502. [CrossRef]
1203. Nastasović, A.B.; Ignjatović, N.L.; Uskoković, D.P.; Marković, D.D.; Ekmeščić, B.M.; Maksin, D.D.; Onjia, A.E. Determination of thermodynamic interactions of poly(L-lactide) and biphasic calcium phosphate/poly(L-lactide) composite by inverse gas chromatography at infinite dilution. *J. Mater. Sci.* **2014**, *49*, 5076–5086. [CrossRef]
1204. Tsuchiya, K.; Yoshioka, T.; Ikoma, T.; Tanaka, J. Chemical interaction between hydroxyapatite and organic molecules in biomaterials. *Ceram. Trans.* **2010**, *210*, 531–535.
1205. Dorozhkin, S.V. Is there a chemical interaction between calcium phosphates and hydroxypropylmethylcellulose (HPMC) in organic/inorganic composites? *J. Biomed. Mater. Res.* **2001**, *54*, 247–255. [CrossRef]
1206. Aminzare, M.; Eskandari, A.; Baroonian, M.H.; Berenov, A.; Hesabi, Z.R.; Taheri, M.; Sadrnezhaad, S.K. Hydroxyapatite nanocomposites: Synthesis, sintering and mechanical properties. *Ceram. Int.* **2013**, *39*, 2197–2206. [CrossRef]
1207. Shuai, C.; Yu, L.; Feng, P.; Gao, C.; Peng, S. Interfacial reinforcement in bioceramic/biopolymer composite bone scaffold: The role of coupling agent. *Colloid Surface B* **2020**, *193*, 111083. [CrossRef]
1208. Kickelbick, G. Concepts for the incorporation of inorganic building blocks into organic polymers on a nanoscale. *Prog. Polym. Sci.* **2003**, *28*, 83–114. [CrossRef]
1209. Uskokovic, P.S.; Tang, C.Y.; Tsui, C.P.; Ignjatovic, N.; Uskokovic, D.P. Micromechanical properties of a hydroxyapatite/poly-L-lactide biocomposite using nanoindentation and modulus mapping. *J. Eur. Ceram. Soc.* **2007**, *27*, 1559–1564. [CrossRef]
1210. Todo, M.; Kagawa, T. Improvement of fracture energy of HA/PLLA biocomposite material due to press processing. *J. Mater. Sci.* **2008**, *43*, 799–801. [CrossRef]
1211. Shuai, C.; Yu, L.; Feng, P.; Peng, S.; Pan, H.; Bai, X. Construction of a stereocomplex between poly(D-lactide) grafted hydroxyapatite and poly(L-lactide): Toward a bioactive composite scaffold with enhanced interfacial bonding. *J. Mater. Chem. B* **2022**, *10*, 214–223. [CrossRef]
1212. Grossman, R.F. Coupling agents. In *Polymer Modifiers and Additives*; Lutz, J.T., Jr., Grossman, R.F., Eds.; CRC Press: Boca Raton, FL, USA, 2000; pp. 95–106.
1213. Liu, Q.; de Wijn, J.R.; van Blitterswijk, C.A. Nanoapatite/polymer composites: Mechanical and physicochemical characteristics. *Biomaterials* **1997**, *18*, 1263–1270. [CrossRef]

1214. Yang, W.F.; Long, L.; Wang, R.; Chen, D.; Duan, S.; Xu, F.J. Surface-modified hydroxyapatite nanoparticle-reinforced polylactides for three-dimensional printed bone tissue engineering scaffolds. *J. Biomed. Nanotechnol.* **2018**, *14*, 294–303. [CrossRef]
1215. Pramanik, N.; Mohapatra, S.; Bhargava, P.; Pramanik, P. Chemical synthesis and characterization of hydroxyapatite (HAp)–poly(ethylene co vinyl alcohol) (EVA) nanocomposite using a phosphonic acid coupling agent for orthopedic applications. *Mater. Sci. Eng. C* **2009**, *29*, 228–236. [CrossRef]
1216. Cui, Y.; Liu, Y.; Cui, Y.; Jing, X.; Zhang, P.; Chen, X. The nanocomposite scaffold of poly(lactide-co-glycolide) and hydroxyapatite surface-grafted with L-lactic acid oligomer for bone repair. *Acta Biomater.* **2009**, *5*, 2680–2692. [CrossRef]
1217. Zhang, P.; Hong, Z.; Yu, T.; Chen, X.; Jing, X. In vivo mineralization and osteogenesis of nanocomposite scaffold of poly(lactide-co-glycolide) and hydroxyapatite surface-grafted with poly(L-lactide). *Biomaterials* **2009**, *30*, 58–70. [CrossRef]
1218. Chang, M.C.; Ikoma, T.; Kikuchi, M.; Tanaka, J. Preparation of a porous hydroxyapatite/collagen nanocomposite using glutataldehyde as a crosslinkage agent. *J. Mater. Sci. Lett.* **2001**, *20*, 1199–1201. [CrossRef]
1219. Sousa, R.A.; Reis, R.L.; Cunha, A.M.; Bevis, M.J. Coupling of HDPE/hydroxyapatite composites by silane-based methodologies. *J. Mater. Sci. Mater. Med.* **2003**, *14*, 475–487. [CrossRef]
1220. Dupraz, A.M.P.; de Wijn, J.R.; van der Meer, S.A.T.; Goedemoed, J.H. Biocompatibility screening of silane-treated hydroxyapatite powders for use as filler in resorbable composites. *J. Mater. Sci. Mater. Med.* **1996**, *7*, 731–738. [CrossRef]
1221. Dupraz, A.M.P.; de Wijn, J.R.; van der Meer, S.A.T.; de Groot, K. Characterization of silane-treated hydroxyapatite powders reinforced for use as filler in biodegradable composites. *J. Biomed. Mater. Res.* **1996**, *30*, 231–238. [CrossRef]
1222. Liao, J.G.; Wang, X.J.; Zuo, Y.; Zhang, L.; Wen, J.Q.; Li, Y. Surface modification of nano-hydroxyapatite with silane agent. *J. Inorg. Mater.* **2008**, *23*, 145–149. [CrossRef]
1223. Rakmae, S.; Ruksakulpiwat, Y.; Sutapun, W.; Suppakarn, N. Effect of silane coupling agent treated bovine bone based carbonated hydroxyapatite on in vitro degradation behavior and bioactivity of PLA composites. *Mater. Sci. Eng. C* **2012**, *32*, 1428–1436. [CrossRef]
1224. Marcomini, A.L.; Rego, B.T.; Bretas, R.E.S. Improvement of the short- and long-term mechanical properties of injection-molded poly(etheretherketone) and hydroxyapatite nanocomposites. *J. Appl. Polym. Sci.* **2017**, *134*, 44476. [CrossRef]
1225. Misra, D.N. Adsorption of zirconyl salts and their acids on hydroxyapatite: Use of salts as coupling agents to dental polymer composites. *J. Dent. Res.* **1985**, *12*, 1405–1408. [CrossRef]
1226. Carmen, A.; Rosestela, P.; Arquimedes, K.; Gema, G.; Nohemy, D.; Yanixia, S.; Luís, B.J. Characterization of HDPE/HA composites treated with titanate and zirconate coupling agents. *Macromol. Symp.* **2007**, *247*, 190–198. [CrossRef]
1227. Chow, W.S.; Tham, W.L.; Ishak, Z.A.M. Improvement of microstructure and properties of poly(methyl methacrylate)/hydroxyapatite composites treated with zirconate coupling agent. *J. Thermoplast. Compos. Mater.* **2012**, *25*, 165–180. [CrossRef]
1228. Tham, W.L.; Chow, W.S.; Ishak, Z.A.M. Effects of titanate coupling agent on the mechanical, thermal and morphological properties of poly(methyl methacrylate)/hydroxyapatite denture base composites. *J. Compos. Mater.* **2011**, *45*, 2335–2345. [CrossRef]
1229. Shen, D.; Fang, L.; Chen, X.; Tang, Y. Structure and properties of polyacrylic acid modified hydroxyapatite/liquid crystal polymer composite. *J. Reinfor. Plast. Comp.* **2011**, *30*, 1155–1163. [CrossRef]
1230. Qu, R.; Song, X.; Wang, Y.; Zhao, Y.; Fu, X. Hydroxyapatite cross-linked in situ polyvinyl alcohol hydrogel for bionic calcified cartilage layer. *Colloid Surface B* **2023**, *230*, 113510. [CrossRef]
1231. Liu, Q.; de Wijn, J.R.; van Blitterswijk, C.A. A study on the grafting reaction of isocyanates with hydroxyapatite particles. *J. Biomed. Mater. Res.* **1998**, *40*, 358–364. [CrossRef]
1232. Tanaka, H.; Yasukawa, A.; Kandori, K.; Ishikawa, T. Surface modification of calcium hydroxyapatite with hexyl and decyl phosphates. *Colloid Surface A* **1997**, *125*, 53–62. [CrossRef]
1233. Borum-Nicholas, L.; Wilson, O.C., Jr. Surface modification of hydroxyapatite. Part I. Dodecyl alcohol. *Biomaterials* **2003**, *24*, 3671–3679. [CrossRef]
1234. Borum, L.; Wilson, O.C., Jr. Surface modification of hydroxyapatite. Part II. Silica. *Biomaterials* **2003**, *24*, 3681–3688. [CrossRef]
1235. Li, Y.; Weng, W. Surface modification of hydroxyapatite by stearic acid: Characterization and in vitro behaviors. *J. Mater. Sci. Mater. Med.* **2008**, *19*, 19–25. [CrossRef]
1236. Lee, S.C.; Choi, H.W.; Lee, H.J.; Kim, K.J.; Chang, J.H.; Kim, S.Y.; Choi, J.; Oh, K.S.; Jeong, Y.K. In-situ synthesis of reactive hydroxyapatite nano-crystals for a novel approach of surface grafting polymerization. *J. Mater. Chem.* **2007**, *17*, 174–180. [CrossRef]
1237. Sánchez-Salcedo, S.; Colilla, M.; Izquierdo-Barba, I.; Vallet-Regi, M. Design and preparation of biocompatible zwitterionic hydroxyapatite. *J. Mater. Chem. B* **2013**, *1*, 1595–1606. [CrossRef]
1238. Dorozhkin, S.V. Functionalized calcium orthophosphates ($CaPO_4$) and their biomedical applications. *J. Mater. Chem. B* **2019**, *7*, 7471–7489. [CrossRef]
1239. Kennedy, B.M.; de Barra, E.; Hampshire, S.; Kelleher, M.C. Investigation of oleic acid as a dispersant for hydroxyapatite powders for use in ceramic filled photo-curable resins for stereolithography. *J. Eur. Ceram. Soc.* **2023**, *43*, 7146–7166. [CrossRef]
1240. Heidari, B.S.; Lopez, E.M.; Chen, P.; Ruan, R.; Vahabli, E.; Davachi, S.M.; Granero-Moltó, F.; De-Juan-Pardo, E.M.; Zheng, M.; Doyle, B. Silane-modified hydroxyapatite nanoparticles incorporated into polydioxanone/poly(lactide-co-caprolactone) creates a novel toughened nanocomposite with improved material properties and in vivo inflammatory responses. *Mater. Today Bio* **2023**, *22*, 100778.

1241. Morita, S.; Furuya, K.; Ishihara, K.; Nakabayashi, N. Performance of adhesive bone cement containing hydroxyapatite particles. *Biomaterials* **1998**, *19*, 1601–1606. [CrossRef]
1242. Shinzato, S.; Nakamura, T.; Tamura, J.; Kokubo, T.; Kitamura, Y. Bioactive bone cement: Effects of phosphoric ester monomer on mechanical properties and osteoconductivity. *J. Biomed. Mater. Res.* **2001**, *56*, 571–577. [CrossRef]
1243. Omori, M.; Okubo, A.; Otsubo, M.; Hashida, T.; Tohji, K. Consolidation of multi-walled carbon nanotube and hydroxyapatite coating by the spark plasma system (SPS). *Key Eng. Mater.* **2004**, *254–256*, 395–398. [CrossRef]
1244. Zhao, B.; Hu, H.; Mandal, S.K.; Haddon, R.C. A bone mimic based on the self-assembly of hydroxyapatite on chemically functionalized single-walled carbon nanotubes. *Chem. Mater.* **2005**, *17*, 3235–3241. [CrossRef]
1245. Zhang, H.; Zhou, L.; Zhang, W. Control of scaffold degradation in tissue engineering: A review. *Tissue Eng. B Rev.* **2014**, *20*, 492–502. [CrossRef]
1246. Wu, H.; Wei, X.; Liu, Y.; Dong, H.; Tang, Z.; Wang, N.; Bao, S.; Wu, Z.; Shi, L.; Zheng, X.; et al. Dynamic degradation patterns of porous polycaprolactone/β-tricalcium phosphate composites orchestrate macrophage responses and immunoregulatory bone regeneration. *Bioact. Mater.* **2023**, *21*, 595–611. [CrossRef]
1247. Ehrenfried, L.M.; Patel, M.H.; Cameron, R.E. The effect of tri-calcium phosphate (TCP) addition on the degradation of polylactide-co-glycolide (PLGA). *J. Mater. Sci. Mater. Med.* **2008**, *19*, 459–466. [CrossRef]
1248. Ehrenfried, L.M.; Farrar, D.; Cameron, R.E. Degradation properties of co-continuous calcium-phosphate-polyester composites. *Biomacromolecules* **2009**, *10*, 1976–1985. [CrossRef]
1249. Pan, J.; Han, X.; Niu, W.; Cameron, R.E. A model for biodegradation of composite materials made of polyesters and tricalcium phosphates. *Biomaterials* **2011**, *32*, 2248–2255. [CrossRef]
1250. Barrett, C.E.; Cameron, R.E. X-ray microtomographic analysis of α-tricalcium phosphate-poly(lactic-co-glycolic) acid nanocomposite degradation. *Polymer* **2014**, *55*, 4041–4049. [CrossRef]
1251. Ahlfeld, T.; Lode, A.; Placht, A.M.; Fecht, T.; Wolfram, T.; Grom, S.; Hoess, A.; Vater, C.; Bräuer, C.; Heinemann, S.; et al. A comparative analysis of 3D printed scaffolds consisting of poly(lactic-co-glycolic) acid and different bioactive mineral fillers: Aspects of degradation and cytocompatibility. *Biomater. Sci.* **2023**, *11*, 5590–5604. [CrossRef]
1252. Heidemann, W.; Jeschkeit, S.; Ruffieux, K.; Fischer, J.H.; Wagner, M.; Krüger, G.; Wintermantel, E.; Gerlach, K.L. Degradation of poly(D,L)lactide implants with or without addition of calciumphosphates in vivo. *Biomaterials* **2001**, *22*, 2371–2381. [CrossRef]
1253. Adamus, A.; Jozwiakowska, J.; Wach, R.A.; Suarez-Sandoval, D.; Ruffieux, K.; Rosiak, J.M. In vitro degradation of β-tricalcium phosphate reinforced poly(L-lactic acid). *Mater. Sci. Forum* **2012**, *714*, 283–290. [CrossRef]
1254. Ahola, N.; Veiranto, M.; Rich, J.; Efimov, A.; Hannula, M.; Seppälä, J.; Kellomäki, M. Hydrolytic degradation of composites of poly(L-lactide-co-ε-caprolactone) 70/30 and β-tricalcium phosphate. *J. Biomater. Appl.* **2013**, *28*, 529–543. [CrossRef]
1255. Dorozhkin, S.V. Inorganic chemistry of the dissolution phenomenon: The dissolution mechanism of calcium apatites at the atomic (ionic) level. *Comments Inorg. Chem.* **1999**, *20*, 285–299. [CrossRef]
1256. Dorozhkin, S.V. Dissolution mechanism of calcium apatites in acids: A review of literature. *World J. Methodol.* **2012**, *2*, 1–17. [CrossRef]
1257. Davison, N.L.; Barrère-de Groot, F.; Grijpma, D.W. Degradation of biomaterials. In *Tissue Engineering*, 2nd ed.; Van Blitterswijk, C.A., de Boer, J., Eds.; Academic Press: Cambridge, MA, USA, 2014; Chapter 6; pp. 177–215.
1258. Tajvar, S.; Hadjizadeh, A.; Samandari, S.S. Scaffold degradation in bone tissue engineering: An overview. *Int. Biodeter. Biodegr.* **2023**, *180*, 105599. [CrossRef]
1259. Furukawa, T.; Matsusue, Y.; Yasunaga, T.; Shikinami, Y.; Okuno, M.; Nakamura, T. Biodegradation behavior of ultra-high strength hydroxyapatite/poly(L-lactide) composite rods for internal fixation of bone fractures. *Biomaterials* **2000**, *21*, 889–898. [CrossRef]
1260. Furukawa, T.; Matsusue, Y.; Yasunaga, T.; Nakagawa, Y.; Okada, Y.; Shikinami, Y.; Okuno, M.; Nakamura, T. Histomorphometric study on high-strength hydroxyapatite/poly(L-lactide) composite rods for internal fixation of bone fractures. *J. Biomed. Mater. Res.* **2000**, *50*, 410–419. [CrossRef]
1261. Yasunaga, T.; Matsusue, Y.; Furukawa, T.; Shikinami, Y.; Okuno, M.; Nakamura, T. Bonding behaviour of ultrahigh strength unsintered hydroxyapatite particles/poly(L-lactide) composites to surface of tibial cortex in rabbits. *J. Biomed. Mater. Res.* **1999**, *47*, 412–419. [CrossRef]
1262. Habraken, W.J.E.M.; Liao, H.B.; Zhang, Z.; Wolke, J.G.C.; Grijpma, D.W.; Mikos, A.G.; Feijen, J.; Jansen, J.A. In vivo degradation of calcium phosphate cement incorporated into biodegradable microspheres. *Acta Biomater.* **2010**, *6*, 2200–2211. [CrossRef]
1263. Ngiam, M.; Liao, S.; Patil, A.J.; Cheng, Z.; Chan, C.K.; Ramakrishna, S. The fabrication of nano-hydroxyapatite on PLGA and PLGA/collagen nanofibrous composite scaffolds and their effects in osteoblastic behavior for bone tissue engineering. *Bone* **2009**, *45*, 4–16.
1264. Hasegawa, S.; Ishii, S.; Tamura, J.; Furukawa, T.; Neo, M.; Matsusue, Y.; Shikinami, Y.; Okuno, M.; Nakamura, T. A 5–7 year in vivo study of high-strength hydroxyapatite/poly(L-lactide) composite rods for the internal fixation of bone fractures. *Biomaterials* **2006**, *27*, 1327–1332.
1265. Alambiaga-Caravaca, A.M.; López-Castellano, A.; Chou, Y.F.; Luzi, A.; Núñez, J.M.; Banerjee, A.; Sancho, M.d.M.J.; Sauro, S. Release kinetics of monomers from dental composites containing fluoride-doped calcium phosphates. *Pharmaceutics* **2023**, *15*, 1948. [CrossRef]
1266. Moreno-Gomez, I. *A Phenomenological Mathematical Modelling Framework for the Degradation of Bioresorbable Composites*; Springer Theses; Springer: Cham, Switzerland, 2019; p. 368.

1267. Dalfino, S.; Savadori, P.; Piazzoni, M.; Connelly, S.T.; Giannì, A.B.; del Fabbro, M.; Tartaglia, G.M.; Moroni, L. Regeneration of critical-sized mandibular defects using 3D-printed composite scaffolds: A quantitative evaluation of new bone formation in in vivo studies. *Adv. Healthc. Mater.* **2023**, *12*, 2300128. [CrossRef]
1268. Niu, Y.; Chen, L.; Wu, T. Recent advances in bioengineering bone revascularization based on composite materials comprising hydroxyapatite. *Int. J. Mol. Sci.* **2023**, *24*, 12492. [CrossRef]
1269. Mo, X.; Zhang, D.; Liu, K.; Zhao, X.; Li, X.; Wang, W. Nano-hydroxyapatite composite scaffolds loaded with bioactive factors and drugs for bone tissue engineering. *Int. J. Mol. Sci.* **2023**, *24*, 1291. [CrossRef]
1270. Sivakumar, P.M.; Yetisgin, A.A.; Demir, E.; Sahin, S.B.; Cetinel, S. Polysaccharide-bioceramic composites for bone tissue engineering: A review. *Int. J. Biol. Macromol.* **2023**, *250*, 126237. [CrossRef]
1271. Osakue, A.S.; Martina, M.; Luvuyo, T. Calcium phosphate bonded wood and fiber composite panels: Production and optimization of panel properties. *Holzforschung* **2017**, *71*, 725–732. [CrossRef]
1272. Chen, F.F.; Zhu, Y.J.; Xiong, Z.C.; Dong, L.Y.; Chen, F.; Lu, B.Q.; Yang, R.L. Hydroxyapatite nanowire-based all-weather flexible electrically conductive paper with superhydrophobic and flame-retardant properties. *ACS Appl. Mater. Interfaces* **2017**, *9*, 39534–39548. [CrossRef]
1273. Guo, W.; Wang, X.; Zhang, P.; Liu, J.; Song, L.; Hu, Y. Nano-fibrillated cellulose-hydroxyapatite based composite foams with excellent fire resistance. *Carbohyd. Polym.* **2018**, *195*, 71–78. [CrossRef]
1274. Zhang, Z.; Wang, X.; Wang, H.; Zhao, J. Removal of Pb(II) from aqueous solution using hydroxyapatite/calcium silicate hydrate (HAP/C-S-H) composite adsorbent prepared by a phosphate recovery process. *Chem. Eng. J.* **2018**, *344*, 53–61. [CrossRef]
1275. Wang, Y.; Liang, D.; Liu, F.; Zhang, W.; Di, X.; Wang, C. A polyethylene glycol/hydroxyapatite composite phase change material for thermal energy storage. *Appl. Therm. Eng.* **2017**, *113*, 1475–1482. [CrossRef]
1276. Ion, R.M.; Nyokong, T.; Nwahara, N.; Suica-Bunghez, I.R.; Iancu, L.; Teodorescu, S.; Dulama, I.D.; Stirbescu, R.M.; Gheboianu, A.; Grigorescu, R.M. Wood preservation with gold hydroxyapatite system. *Herit. Sci.* **2018**, *6*, 37. [CrossRef]
1277. Chen, F.; Zhang, J.; Li, N.; Zhang, C.; Ji, B.; Hu, L.; Zhao, T.; Wang, Z.; Zhang, S. Heat insulating, fire retardant and flexible inorganic nanocomposite paper. *Mater. Des.* **2018**, *144*, 281–289. [CrossRef]
1278. Yang, R.L.; Zhu, Y.J.; Chen, F.F.; Qin, D.D.; Xiong, Z.C. Recyclable, fire-resistant, superhydrophobic and magnetic paper based on ultralong hydroxyapatite nanowires for continuous oil/water separation and oil collection. *ACS Sustain. Chem. Eng.* **2018**, *6*, 10140–10150. [CrossRef]
1279. Fischer, D.; Parks, S.C.; Mannhart, J. Bio-inspired synthetic ivory as a sustainable material for piano keys. *Sustainability* **2019**, *11*, 6538. [CrossRef]
1280. Saroja, A.P.V.K.; Kumar, A.R.; Moharana, B.C.; Kamaraj, M.; Ramaprabhu, S. Design of porous calcium phosphate based gel polymer electrolyte for quasi-solid state sodium ion battery. *J. Electroanal. Chem.* **2020**, *859*, 113864. [CrossRef]
1281. Lv, J.; Chen, Z.; Li, X. Calcium phosphate paints for full-daytime subambient radiative cooling. *ACS Appl. Energy Mater.* **2022**, *5*, 4117–4124. [CrossRef]
1282. Niranjana, L.S.; Mathankumar, M.; Karthikkumar, D.; Ranjithkumar, R.; Chandar, S.B.; Wong, L.S.; Djearamane, S. Characterization of calcium phosphate chitosan nanocomposite as plant growth promoter. *J. Exp. Biol. Agr. Sci.* **2022**, *10*, 567–574. [CrossRef]
1283. Waghmare, P.G.; Narwade, V.N.; Naik, K.B.; Kutte, V.D.; Bogle, K.A.; Mahabole, M.P. CuO/HAp composites: Excellent dielectric materials. *Mater. Today Proc.* **2023**, *72*, 2681–2686. [CrossRef]
1284. Guo, W.; Chen, Y.; Cui, L.; Xu, N.; Wang, M.; Sun, Y.; Yan, Y. Nano-hydroxyapatite/carbon nanotube: An excellent anode modifying material for improving the power output and diclofenac sodium removal of microbial fuel cells. *Bioelectrochemistry* **2023**, *154*, 108523. [CrossRef]
1285. Zhou, W.; Zhou, X.; Song, W.; Wang, C.; Zhang, H.; Huang, X. Removal of benzohydroxamic acid from aqueous solutions using multi-walled carbon nanotubes/iron-doped hydroxyapatite composites: Synthesis, adsorption performance and characteristics. *J. Environ. Chem. Eng.* **2023**, *11*, 111259. [CrossRef]
1286. Luu, T.T.; Huynh, N.D.; Kim, H.; Lin, Z.H.; Choi, D. Highly stretchable hydroxyapatite bionanocomposite for high-performance triboelectric nanogenerators. *Nanoscale* **2023**, *15*, 14205–14214. [CrossRef]
1287. Bongio, M.; van den Beucken, J.J.J.P.; Leeuwenburgh, S.C.G.; Jansen, J.A. Development of bone substitute materials: From 'biocompatible' to 'instructive'. *J. Mater. Chem.* **2010**, *20*, 8747–8759. [CrossRef]
1288. George, S.M.; Nayak, C.; Singh, I.; Balani, K. Multifunctional hydroxyapatite composites for orthopedic applications: A review. *ACS Biomater. Sci. Eng.* **2022**, *8*, 3162–3186. [CrossRef]
1289. Meyers, M.A.; Lin, A.Y.M.; Seki, Y.; Chen, P.Y.; Kad, B.K.; Bodde, S. Structural biological composites: An overview. *JOM* **2006**, *58*, 36–43. [CrossRef]
1290. Polo-Corrales, L.; Latorre-Esteves, M.; Ramirez-Vick, J.E. Scaffold design for bone regeneration. *J. Nanosci. Nanotechnol.* **2014**, *14*, 15–56. [CrossRef]
1291. Kumar, A.; Kargozar, S.; Baino, F.; Han, S.S. Additive manufacturing methods for producing hydroxyapatite and hydroxyapatite-based composite scaffolds: A review. *Front. Mater.* **2019**, *6*, 313. [CrossRef]
1292. Jagadeeshanayaka, N.; Awasthi, S.; Jambagi, S.C.; Srivastava, C. Bioactive surface modifications through thermally sprayed hydroxyapatite composite coatings: A review of selective reinforcements. *Biomater. Sci.* **2022**, *10*, 2484–2523. [CrossRef]

1293. Fattah-Alhosseini, A.; Chaharmahali, R.; Alizad, S.; Kaseem, M. Corrosion behavior of composite coatings containing hydroxyapatite particles on Mg alloys by plasma electrolytic oxidation: A review. *J. Magnes. Alloy* **2023**, *11*, 2999–3011. [CrossRef]
1294. Liu, F.; Wang, Y.; Cao, J.; Chen, J.; Luo, T.; Zhou, C.; Tang, Y.; Xie, H. A simple method for fabricating polymer/ceramic functionally graded material scaffold. *Ceram. Int.* **2024**, *50*, 14497–14512. [CrossRef]
1295. Joo, S.; Gwon, Y.; Kim, S.; Park, S.; Kim, J.; Hong, S. Piezoelectrically and topographically engineered scaffolds for accelerating bone regeneration. *ACS Appl. Mater. Interfaces* **2024**, *16*, 1999–2011. [CrossRef]
1296. Mouriño, V.; Cattalini, J.P.; Roether, J.A.; Dubey, P.; Roy, I.; Boccaccini, A.R. Composite polymer-bioceramic scaffolds with drug delivery capability for bone tissue engineering. *Expert Opin. Drug Deliv.* **2013**, *10*, 1353–1365. [CrossRef]
1297. Shi, J.; Dai, W.; Gupta, A.; Zhang, B.; Wu, Z.; Zhang, Y.; Pan, L.; Wang, L. Frontiers of hydroxyapatite composites in bionic bone tissue engineering. *Materials* **2022**, *15*, 8475. [CrossRef]

Disclaimer/Publisher's Note: The statements, opinions and data contained in all publications are solely those of the individual author(s) and contributor(s) and not of MDPI and/or the editor(s). MDPI and/or the editor(s) disclaim responsibility for any injury to people or property resulting from any ideas, methods, instructions or products referred to in the content.